frontiers | Research Topics

Insights in aquatic microbiology 2023

Edited by
Michael Rappe and Jin Zhou

Published in
Frontiers in Microbiology
Frontiers in Marine Science

ISSN 1664-8714
ISBN 978-2-8325-5561-3
DOI 10.3389/978-2-8325-5561-3

About Frontiers

Frontiers is more than just an open access publisher of scholarly articles: it is a pioneering approach to the world of academia, radically improving the way scholarly research is managed. The grand vision of Frontiers is a world where all people have an equal opportunity to seek, share and generate knowledge. Frontiers provides immediate and permanent online open access to all its publications, but this alone is not enough to realize our grand goals.

Frontiers journal series

The Frontiers journal series is a multi-tier and interdisciplinary set of open-access, online journals, promising a paradigm shift from the current review, selection and dissemination processes in academic publishing. All Frontiers journals are driven by researchers for researchers; therefore, they constitute a service to the scholarly community. At the same time, the *Frontiers journal series* operates on a revolutionary invention, the tiered publishing system, initially addressing specific communities of scholars, and gradually climbing up to broader public understanding, thus serving the interests of the lay society, too.

Dedication to quality

Each Frontiers article is a landmark of the highest quality, thanks to genuinely collaborative interactions between authors and review editors, who include some of the world's best academicians. Research must be certified by peers before entering a stream of knowledge that may eventually reach the public - and shape society; therefore, Frontiers only applies the most rigorous and unbiased reviews. Frontiers revolutionizes research publishing by freely delivering the most outstanding research, evaluated with no bias from both the academic and social point of view. By applying the most advanced information technologies, Frontiers is catapulting scholarly publishing into a new generation.

What are Frontiers Research Topics?

Frontiers Research Topics are very popular trademarks of the *Frontiers journals series*: they are collections of at least ten articles, all centered on a particular subject. With their unique mix of varied contributions from Original Research to Review Articles, Frontiers Research Topics unify the most influential researchers, the latest key findings and historical advances in a hot research area.

Find out more on how to host your own Frontiers Research Topic or contribute to one as an author by contacting the Frontiers editorial office: frontiersin.org/about/contact

Insights in aquatic microbiology: 2023

Topic editors

Michael Rappe — University of Hawaii at Manoa, United States

Jin Zhou — Tsinghua University, China

Citation

Rappe, M., Zhou, J., eds. (2024). *Insights in aquatic microbiology: 2023*. Lausanne: Frontiers Media SA. doi: 10.3389/978-2-8325-5561-3

Table of contents

frontiers | Frontiers in Microbiology

TYPE Editorial
PUBLISHED 03 October 2024
DOI 10.3389/fmicb.2024.1496983

OPEN ACCESS

EDITED AND REVIEWED BY
Eva Sintes,
Spanish Institute of Oceanography (IEO), Spain

*CORRESPONDENCE
Jin Zhou
zhou.jin@sz.tsinghua.edu.cn

RECEIVED 16 September 2024
ACCEPTED 23 September 2024
PUBLISHED 03 October 2024

CITATION
Zhou J and Rappe M (2024) Editorial: Insights in aquatic microbiology: 2023. *Front. Microbiol.* 15:1496983. doi: 10.3389/fmicb.2024.1496983

Editorial: Insights in aquatic microbiology: 2023

Jin Zhou[1]* and Michael Rappe[2]

[1]Shenzhen Public Platform for Screening and Application of Marine Microbial Resources, Institute for Ocean Engineering, Shenzhen International Graduate School, Tsinghua University, Shenzhen, China, [2]Marine Biology, Hawai'i Institute of Marine Biology, SOEST, University of Hawai'i at Mānoa, Kāne'ohe, HI, United States

KEYWORDS

microorganisms, marine, freshwater, aquatic microbiology, editorial

Editorial on the Research Topic
Insights in aquatic microbiology: 2023

Aquatic microbiology is a multifaceted and rapidly expanding field investigating the intricate interactions and complex dynamics of microorganisms within diverse aquatic ecosystems. This field covers a wide range of aquatic environments, from the vast expanses of the world's oceans to the serene depths of lakes, the winding currents of rivers, and the numerous other water bodies that sustain life on Earth. By studying these microbial communities, aquatic microbiologists seek to elucidate their roles in nutrient cycling, energy flow, and the overall health of the planet's aquatic systems. The section on Aquatic Microbiology, featured in the journal *Frontiers in Microbiology* and *Frontiers in Marine Science*, has emerged as a prominent publication in the field, providing leading research and insights into aquatic microbiology (Figure 1). A search on the Web of Science for the terms "aquatic" (all fields) AND "microbiology" (all fields) for the year 2023 identified 321 publications, with a notable 25.9% appearing in this specific section (Figure 1A). These publications covered several Web of Science categories, contributing to general microbiology, biotechnology, applied microbiology, and environmental sciences (Figure 1B). Aquatic microorganisms are a focal point of research, particularly in fields such as biogeochemical cycling, material metabolism, pollutant degradation, ecological restoration, and public health. Gaining a comprehensive understanding of their roles and behaviors in these contexts is essential for advancing scientific knowledge and effectively addressing environmental challenges.

In recent years, there have been significant new insights and discoveries in this field. The publications included in the current Research Topic, "*Insights in aquatic microbiology: 2023*," cover a broad range of subjects that advance our understanding of this field. They address the following aspects in both fresh- and salt-water environment:

In freshwater ecosystem:

1. Bakenhus et al. (A domesticated photoautotrophic microbial community as a biofilm model system for analyzing the influence of plastic surfaces on invertebrate grazers in limnic environments) developed a standardized approach to investigate the impacts of plastic-associated biofilms on trophic interactions and biogeochemical cycles within three freshwater aquatic ecosystems. Utilizing this model system, we are now equipped to more profoundly comprehend how plastic pollution might alter the properties of biofilms, consequently affecting the health and functionality of aquatic ecosystems.

2. Peng et al. (Insight into diversity change, variability and co-occurrence patterns of phytoplankton assemblage in headwater streams: a study of the Xijiang River basin, South China) presented a comprehensive analysis of phytoplankton diversity in headwater streams across the Xijiang River basin, revealing a significant decrease in diversity with increasing altitude. The research highlights the "isolated island" effect of high altitudes on phytoplankton assemblages, characterized by reduced homogeneous selection and increased dispersal limitation. These findings are crucial for understanding the impact of environmental gradients on aquatic biodiversity and the potential consequences of climate change on these ecosystems.
3. Zhang et al. (Response of the microbial community structure to the environmental factors during the extreme flood season in Poyang Lake, the largest freshwater lake in China) investigated the response of microbial community structures to environmental factors during the extreme flood season in Poyang Lake. The experimental results demonstrated significant differences in bacterial communities between waterbody and sediment and revealed the abundance of genes related to human pathogens. This study contributes to understanding the health risks linked to flood events and supports the development of effective freshwater lake management and conservation strategies.

In saltwater ecosystem:

1. Lee et al. (Grazing impact of the calanoid copepods *Acartia* spp. on the toxic dinoflagellate *Alexandrium pseudogonyaulax* in the western coastal waters of Korea) found that the ingestion rates of the copepod *Acartia* spp. on the harmful algae *Alexandrium pseudogonyaulax* increased with higher prey concentrations, suggesting that copepods may play a role in mitigating algal blooms. The findings illustrate the ecological significance of copepods in controlling toxic dinoflagellates and enhance our understanding of marine planktonic food webs.
2. Rey Redondo et al. (Genomic characterization and ecological distribution of *Mantoniella tinhauana*: a novel Mamiellophycean green alga from the Western Pacific) identified a novel marine alga, *Mantoniella tinhauana*, in the Western Pacific, marking a significant advancement in marine biology. Their genomic sequencing and analysis solidify the alga's status as a distinct species and elucidate its global distribution. This study enhances our understanding of marine microbial diversity and distribution while offering new molecular insights into their roles in marine ecosystems.
3. Shan et al. (An abrupt regime shift of bacterioplankton community from weak to strong thermal pollution in a subtropical bay) revealed a dramatic shift in the bacterioplankton community structure within a subtropical bay, triggered by thermal pollution from a nuclear power plant. These findings indicate a critical ecological transition and suggest that we need to monitor and mitigate the environmental impacts of industrial activities, especially in the context of rising global temperatures.
4. Ugarelli et al. (Microbiomes of *Thalassia testudinum* throughout the Atlantic Ocean, Caribbean Sea, and Gulf of Mexico are influenced by site and region while maintaining a core microbiome) revealed a resilient core microbiome within *Thalassia testudinum*. Despite vast geographical spans, the seagrass maintains a stable microbial community structure, shaped by local environmental factors. These findings hold significant implications for the conservation and management of seagrass beds, particularly in the context of global change, offering us new tools for monitoring and preserving the health of these critical ecosystems.
5. Walker et al. (Above and below-ground bacterial communities shift in seagrass beds with warmer temperatures) investigated the impact of warmer temperatures on seagrass and its associated microbial communities in Lake Macquarie, Australia. The research examined the potential for temperature-induced changes in seagrass ecosystems, emphasizing the importance of understanding microbial responses to climate change for the conservation of these vital habitats. It provides critical insights into how climate change, particularly ocean warming, could alter the delicate balance of seagrass ecosystems.
6. Yang et al. (Unraveling the important role of comammox Nitrospira to nitrification in the coastal aquaculture system) highlighted the critical role of comammox Nitrospira in nitrification processes within coastal aquaculture systems. Their comprehensive assessment of nitrifying communities in fish ponds with different feeding levels deepens our knowledge of microbial dynamics in aquaculture and offers strategic insights for sustainable nitrogen management and water quality control.

These publications in this section provide new insights into the stability and resilience of microbial ecosystems in aquatic systems, water quality management, nitrogen cycling, and the protection and restoration of ecosystems, thereby advancing the field of aquatic microbiology. They enhance our understanding of microbial community dynamics and highlight the critical role of microorganisms in maintaining the health and functionality of fresh- or salt-water environments. As research in aquatic microbiology progresses rapidly, it is crucial to adopt new technologies to improve research capabilities. Developing and utilizing technologies such as artificial intelligence and machine learning will facilitate the analysis of complex ecological data, allowing for more precise identification of changes in microbial communities and their impacts on water quality, ultimately leading to a deeper understanding and enhanced predictive capabilities. Additionally, fostering innovative scientific thinking and interdisciplinary collaboration is important. By encouraging novel research approaches and focusing on real-world problems, we can move beyond traditional studies. Strengthening collaboration among disciplines such as ecology, microbiology, hydrology, and environmental science will provide a more comprehensive analysis and resolution of issues within aquatic ecosystems. Finally, developing science-based management policies and promoting public education are essential. Updating water quality management policies and

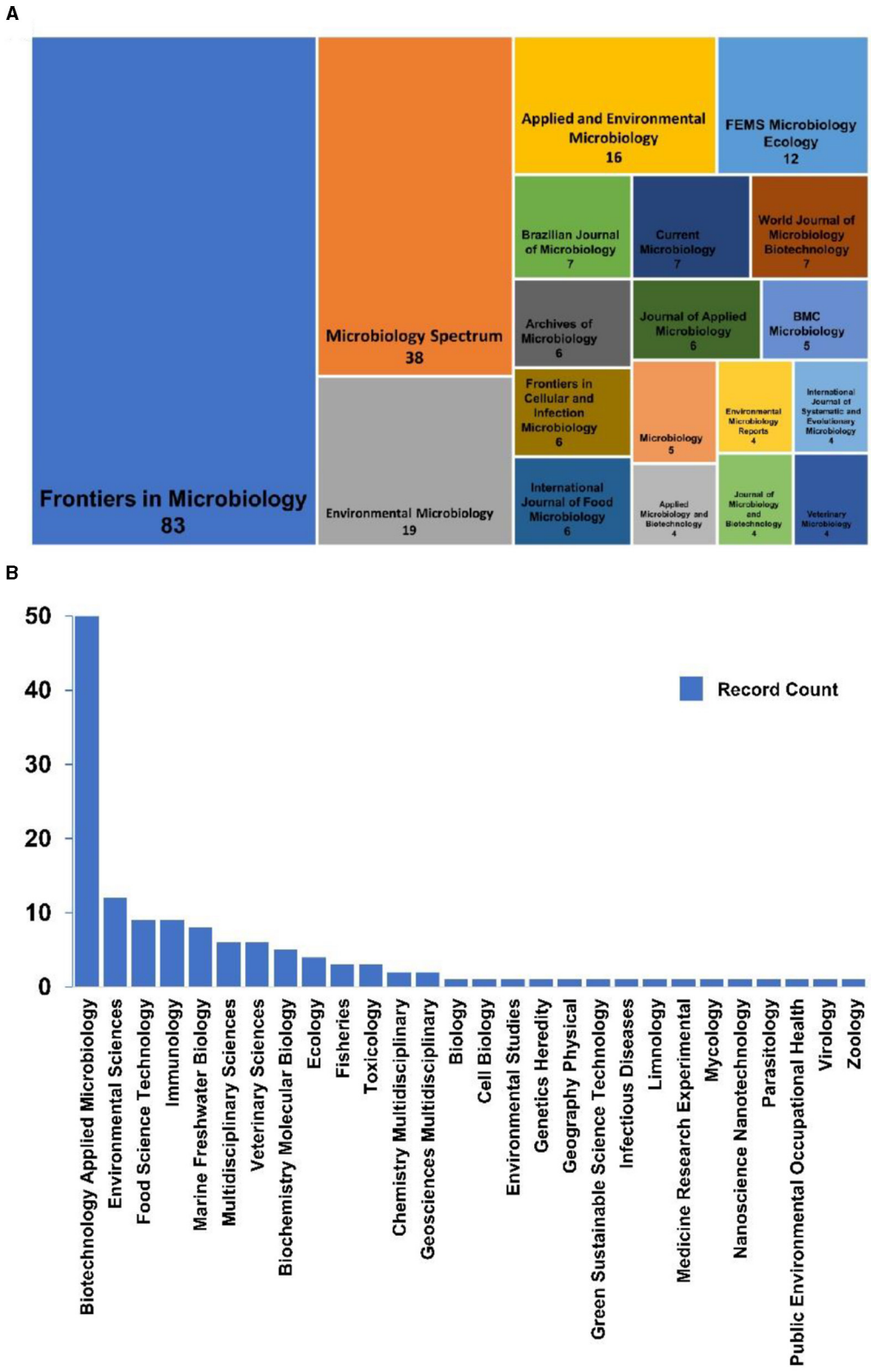

FIGURE 1
Titles and corresponding number of publications in journals that publish papers on the topic of Aquatic Microbiology during 2023 **(A)**. Information on the number of publications categorized under different topics within the search for Aquatic Microbiology **(B)**. These data have been obtained from the Web of Science.

ecological protection measures based on the latest research ensures they are grounded in scientific evidence. Moreover, increasing public awareness about the importance of microorganisms in maintaining aquatic health will foster greater public support and involvement in water protection efforts. Through these strategies, we can better understand and manage the role of aquatic microbiology in ecosystem dynamics, optimize water quality management, and promote the sustainable development of ecosystems.

Author contributions

JZ: Data curation, Funding acquisition, Writing – original draft, Writing – review & editing. MR: Conceptualization, Validation, Visualization, Writing – review & editing.

Funding

The author(s) declare financial support was received for the research, authorship, and/or publication of this article. This work was supported by the NSFC (41976126), Shenzhen Science and Technology Program (KCXFZ20230731093402005 and SGDX20220530111204028), and Innovation Team Project for Guangdong's Universities (2023KCXTD052).

Conflict of interest

The authors declare that the research was conducted in the absence of any commercial or financial relationships that could be construed as a potential conflict of interest.

The author(s) declared that they were an editorial board member of Frontiers, at the time of submission. This had no impact on the peer review process and the final decision.

Publisher's note

frontiers | Frontiers in Microbiology

TYPE Original Research
PUBLISHED 16 November 2023
DOI 10.3389/fmicb.2023.1238913

OPEN ACCESS

EDITED BY
Michael Rappe,
University of Hawaii at Manoa, United States

REVIEWED BY
Vineet Kumar,
Central University of Rajasthan, India
Xianhua Liu,
Tianjin University, China
Michael Rappe,
University of Hawaii at Manoa, United States

*CORRESPONDENCE
Bodo Philipp
✉ bodo.philipp@uni-muenster.de

†These authors have contributed equally to this work and share first authorship

RECEIVED 12 June 2023
ACCEPTED 03 November 2023
PUBLISHED 16 November 2023

CITATION
Bakenhus I, Jongsma R, Michler-Kozma D, Hölscher L, Gabel F, Holert J and Philipp B (2023) A domesticated photoautotrophic microbial community as a biofilm model system for analyzing the influence of plastic surfaces on invertebrate grazers in limnic environments. *Front. Microbiol.* 14:1238913. doi: 10.3389/fmicb.2023.1238913

A domesticated photoautotrophic microbial community as a biofilm model system for analyzing the influence of plastic surfaces on invertebrate grazers in limnic environments

Insa Bakenhus[1†], Rense Jongsma[1†], Diana Michler-Kozma[2], Lea Hölscher[1], Friederike Gabel[2], Johannes Holert[1] and Bodo Philipp[1,3*]

[1]Institute for Molecular Microbiology and Biotechnology, Universität Münster, Münster, Germany, [2]Institute for Landscape Ecology, Universität Münster, Münster, Germany, [3]Fraunhofer-Institut für Molekulare und Angewandte Ökologie IME, Umweltmikrobiologie, Schmallenberg, Germany

The environmental fate of plastic particles in water bodies is influenced by microbial biofilm formation. Invertebrate grazers may be affected when foraging biofilms on plastics compared to biofilms on natural substrata but the mechanistic basis for these effects is unknown. For analyzing these effects in ecotoxicological assays stable and reproducible biofilm communities are required that are related to the environmental site of interest. Here, a defined biofilm community was established and used to perform grazing experiments with a freshwater snail. For this, snippets of different plastic materials were incubated in the photic zone of three different freshwater sites. Amplicon sequencing of biofilms formed on these snippets showed that the site of incubation and not the plastic material dominated the microbial community composition. From these biofilms, individual microbial strains as well as photoautotrophic consortia were isolated; these consortia consisted of heterotrophic bacteria that were apparently nourished by microalga. While biofilms formed by defined dual cultures of a microalga and an Alphaproteobacterium were not accepted by the snail *P. fontinalis*, a photoautotrophic consortium (Co_3) sustained growth and metabolism of this grazer. Amplicon sequencing revealed that consortium Co_3, which could be stably maintained on solid medium under photoautotrophic conditions, reproducibly formed biofilms of a defined composition on three different plastic materials and on glass surfaces. In conclusion, our study shows that the generation of domesticated photoautotrophic microbial communities is a valid novel approach for establishing laboratory ecotoxicological assays with higher environmental relevance than those based on defined microbiota.

KEYWORDS

plastic pollution, photoautotrophic biofilms, grazing, bacteria-microalgae interactions, ecotoxicological test system

Introduction

Water pollution by plastic is a global issue with largely unknown effects on biota (Dris et al., 2020; Stubbins et al., 2021). When plastic enters aquatic systems it will quickly be colonized by microorganisms. Biofilm formation is, thus, an inevitable process and will influence the further environmental fate of plastic particles in water bodies. Biofilms can influence the sinking of plastic particles to sediments as well as their physiological effects on aquatic animals (Wright et al., 2020; Leiser et al., 2021; Okeke et al., 2022). As biofilms are a substrate for grazing animals in aquatic systems plastic surfaces might impact the grazers' physiology. An example study for this analyzed the physiology of the snail *Radix balthica* exposed to natural biofilms that had been formed in freshwater (Vosshage et al., 2018; Michler-Kozma et al., 2022). There, the grazing experiments revealed lower biofilm consumption and lower growth rates when the biofilms had been formed on plastic surfaces compared to glass surfaces.

Generally, there are several potential mechanisms by which biofilms formed on plastic may affect invertebrate grazers in a negative way. First, there might be direct toxic effects. Grazing may lead to abrasion of micro- or nanoplastic particles that may be toxic for the forager; additionally, microorganisms in the biofilms can mobilize plastic additives with toxic effects (Fauser et al., 2022; Ockenden et al., 2022). As plastic is known to adsorb chemicals from the water such toxic effects may also arise from exogenous compounds (Yu et al., 2021; Cássio et al., 2022). Additives or adsorbed chemicals may also influence the food quality of biofilms for grazers. Many invertebrate grazers rely on sterols (Shamsuzzama et al., 2020) which are mainly be derived from eukaryotic algae in the photic zone. If microplastic should adsorb alga-inhibiting herbicides the food quality of biofilms might be reduced (Carles et al., 2021; Castro-Castellon et al., 2022). By this mechanism, biofilms on plastic may indirectly contribute to effects of pesticides in aquatic foodwebs (Konschak et al., 2021; Sánchez-Bayo, 2021). The food quality of a biofilm might also be affected if plastic surfaces would be selectively colonized by microorganisms with low food quality. However, to our knowledge, such a selective colonization cannot generally be confirmed far since microbial communities of biofilms on plastic surfaces do not obviously differ from those on natural surfaces (Oberbeckmann et al., 2021). However, low abundancies of plastic-specific OTUs were detected in a large analysis of marine biofilms on plastic (Scales et al., 2021) but this seems to be restricted to the beginning of biofilm formation as plastic surfaces are being masked by biofilms with time. Additionally, nutrient availability may influence the structure of biofilm communities on plastic (Song et al., 2023).

The criteria that apply for ecotoxicological effects for grazers do also apply for microplastic-ingesting biota in a similar way (Alfonso et al., 2023). In this respect, laboratory investigations on ecotoxicological effects of (micro) plastic on aquatic organisms would generally be more meaningful if the plastic is colonized by a biofilm.

Appropriate model systems for ecotoxicological assays should, thus, comprise defined plastic, defined grazers and a defined biofilm. However, while plastic material and grazers can easily be standardized the creation of a defined biofilm is challenging. Standardized laboratory biofilms are mainly designed for testing antimicrobial activity such as antifouling materials and are mainly based on mono-species (Japanese Standards Association, 2010; ASTM International, 2020). *In-situ* biofilm generation can be largely influenced by abiotic conditions; even when these are constant significant variations in biomass content and community structure between replicates cannot be excluded. A reliable determination of key parameters such as C:N ratio or lipid content requires invasive methods that deprive the opportunity of using such biofilms for grazing experiments later.

For reproducible ecotoxicological assays with (micro) plastic synthetic biofilm communities there is the need of defined microorganisms exhibiting reproducible biofilm formation on plastic surfaces. Appropriate microbes for such a defined synthetic biofilm for grazing studies should fulfil certain requirements. First, they should originate from an ecologically relevant habitat. The photic zone would be feasible because many plastic materials are floating and many surface waters which are prone to littering are shallow (ranging, e.g., from puddles via ditches to park ponds). Second, the organisms should be maintainable as mono-cultures on solid media and be able to form biofilms when transferred to liquid medium in which surfaces for biofilm formation are offered. Apart from plastic surfaces they should also form comparable biofilms on a non-plastic reference material such as glass. Third, the envisaged defined synthetic biofilm communities should be stable which could best be achieved if the community members are interdependent. Fourth, the synthetic biofilm community must be accepted by grazers and sustain their growth and reproduction. Considering the sterol auxotrophy of many invertebrates the biofilm communities should contain eukaryotic microorganisms because only few prokaryotes can synthesize sterols (Wei et al., 2016).

Thus, the goal of our study was to obtain microorganisms that show the desired properties under laboratory conditions for establishing a defined community for grazing studies with the freshwater snail *Physa fontinalis*. We focused on limnic systems which have been less explored than marine systems (Latva et al., 2022) but are an important input for marine environments via rivers. We designed a selective strategy to retrieve microorganisms that fulfil the aforementioned requirements. First, *in-situ* enrichments for microorganisms colonizing plastic surfaces were set up in photic zone of water bodies close to dams where flow velocity is low which might enhance colonization (Watkins et al., 2019) and facilitates the installation of devices for biofilm formation. Second, these colonized plastic surfaces were brought to the lab and used as inoculum for selecting microbial communities that colonized a pristine plastic surface under photoautotrophic conditions. The respective microbes forming such a community must be able to detach from a surface and colonize a new one repeatedly. Photoautotrophic condition ensure that microalgae are present that nourish heterotrophic bacteria which is typical for limnic microbial biofilm communities in the photic zone (Gubelit and Grossart, 2020). From these photoautotrophic communities individual strains of microalgae and bacteria should be isolated that can be recombined as communities for producing reproducible biofilms on different plastic materials and glass for grazing studies for addressing the aforementioned goals of this study.

Materials and methods

In situ incubation setup and sampling

For *in-situ* incubation, research-grade polymer foils made of low-density polyethylene (PE), polyethylene terephthalate (PET) or

polystyrene (PS) were used (Goodfellow, Hamburg, DE). Foils were cut into 4 mm × 4 mm × 0.125 mm square snippets using an ethanol-sterilized wire binder (Pavo Sales B.V., Oss, NL) as described previously (Leiser et al., 2021). As containers for the incubation, stainless steel tea strainers (5 cm diameter, Contacto Bander GmbH, Erkrath, DE) were heat-sterilized (200°C, 4 h) and subsequently filled with 100 polymer snippets of a single polymer type. Incubation of the polymer snippets lasted 5 weeks from September 12th to October 17th, 2018, at three different sites: *Ems* river (51°57′06.7″ N, 7°59′56.4″ E), Lake *Emssee* (51°57′11.9″ N, 8°00′08.9″ E) and the *Rieselfelder*, an interconnected system of shallow reservoirs which were inundated by a waste water treatment plant effluent (52°01′23.4″ N, 7°39′33.8″ E). The containers were mounted to foamed polystyrene lifting bodies to a depth of about 30 cm in the respective water columns (Supplementary Figure S1). The incubations were weekly sampled by detaching one container per polymer type for measuring chlorophyll fluorescence and biofilm biomass on the snippets (see below). At each sampling site, a sterilized brush was used to remove biomass adhering on the outside of the residual containments for enabling continued sunlight penetration. For transport to the laboratory, the containments were stored at 4°C in heat-sterilized glass beakers. Prior to further processing, snippets were washed three times using sterile phosphate buffered saline (PBS, pH 7.4). After 5 weeks the *in-situ* incubation was stopped and a fraction of the snippets was used for isolating bacteria (see below). To determine the microbial community of the biofilms, additional 15 particles per plastic material and site were pooled and stored at −78°C until further processing for DNA isolation (see below).

Biofilm-biomass quantification

Biofilm-biomass quantification was performed using crystal-violet staining with protocol modifications adapted from Christensen et al. (1985), Stepanović et al. (2000, 2007) and Arias-Andres et al. (2018). After washing three times with PBS, snippets were transferred to a 24-well microplate with one particle per well. After biofilm fixation at 60°C for 1 h, 0.5 to 1 ml crystal violet (0.3% *w*/*v*) per particle was added (until they were completely submerged) with subsequent incubation on a rocker shaker for 15 min at room temperature. After removal of the crystal violet solution, particles were washed four times with $H_2O_{Millipore}$. Residual supernatants were removed and 1 ml 33% (*v*/*v*) acetic acid was added. After 20–25 min incubation at 120 rpm, 900 µl of supernatants were transferred into new 24-well microplates for measuring absorption at 595 nm with covered lid using a *Tecan® GENios™ microplate reader* (Tecan Group AG, Männedorf, CH).

Fluorometric chlorophyll determination

Chlorophyll autofluorescence was measured with the *ChemiDoc™ imager* (Bio Rad Laboratories, Hercules, USA). As excitation light source, *Green Epi Fluorescence* with a wavelength of approximately 550 nm was used (Zecher et al., 2015). Fluorescence emission was detected using the *695/55* filter. Exposure times were manually adjusted to avoid signal overmodulation. Fluorescence intensities were calculated using *Image Lab™* Version 4.1 (Bio-Rad Laboratories) and normalized to area and exposure time.

DNA extraction and sequencing

For analysing microbial communities analysis of biofilms from *in-situ* incubations and from enriched photoautotrophic consortia, DNA was extracted with the DNA Power Soil Pro Kit (Qiagen, Hilden, DE). Biofilm-covered plastic snippets were transferred into PowerBead Pro Tubes containing 800 µl solution CD1 and shaken horizontally in a vortex adapter for 1 h. After addition of 25 µl proteinase K (22 mg/ml) and incubation at 37°C for 1 h the extraction was continued according to the manufacturer's instructions. Library preparation, sequencing and data analysis were performed by Microsynth AG (Belgach, Switzerland). Extracted DNA was submitted to two-step PCR amplification of the V4-V5 region of the bacterial 16S rRNA gene, using the primer pair 515F-Y and 926R (Parada et al., 2016). PCR-products were sequenced using a v2 500 cycle kit on the Illumina MiSeq platform. Raw data was submitted to the European Nucleotide Archive (ENA) database and were assigned the Project ID PRJEB45856. For determination of relative abundances of bacterial phyla we performed standard statistical analysis and bioinformatics including the program *R* (R Core Team, 2018).

Isolation of bacteria from *in-situ* grown biofilms

For isolation of bacteria from *in-situ* grown biofilm, 15 washed snippets of each polymer type were pooled in 2 ml microcentrifuge tubes with 10 sterile glass beads (2.7 mm diameter, Carl Roth GmbH + Co. KG, Karlsruhe, DE). After adding 1 ml of sterile PBS, the tube was vortexed at low speed for 30 s. The resulting supernatant was diluted and plated on solid medium B (Jagmann et al., 2010) supplemented with 0.1% (*v*/*v*) 7-vitamins solution (Pfennig, 1978), 0.01 mM ATP (Bruns et al., 2003) and triple concentrated mixed carbon sources (Cho and Giovannoni, 2004). From these plates, colonies with different morphologies were selected for purifying bacterial strains by repeated transfers on YPG-agar medium [0.075% (*w*/*v*) yeast extract, 0.05% (*w*/*v*) peptone, 0.075% (*w*/*v*) D-glucose, 1.2% (*w*/*v*) Bacto™ Agar (Becton Dickinson GmbH, Heidelberg, DE); adapted from Bruns et al. (2003)]. All cultivation steps were performed at room temperature.

Enrichment of algal-bacterial consortia and isolation of microorganisms therefrom

For enrichment and cultivation of photoautotrophic algal-bacterial consortia from *in-situ* grown PE biofilms, modified Diatom Medium (DM; pH 6.75/HCl; adapted from Cohn and Pickett-Heaps, 1988 and Cohn et al., 2003) was used in which soil extract, $FeSO_4$ and $MnCl_2$ was replaced by 0.1% (*v*/*v*) f/2 trace element solution (Guillard and Ryther, 1962). After autoclaving, 0.1 mM $NaHCO_3$ and DM vitamin solution were added to the medium. For enrichment cultures, 15 washed PE snippets were pooled in a 2 ml microcentrifuge tube with 10 sterile glass beads (see above) in 1 ml of sterile PBS and vortexed at low speed for 30 s (Supplementary Figure S2). After removal of the supernatant, the snippets were washed three times in PBS. Single snippets were then used to inoculate 1 ml of DM in a 24-well microplate containing a sterile pristine PE snippet. These

microtiter plates were incubated for 12 days at 21°C with 180 rpm in a light incubator (Phytobiochamber Model EGCS 701, EQUiTEC; light source: Lumilux Warmwhite, Osram, DE; photon flux density: approx. 90 µE m^{-2} s^{-1}; light/dark cycle: 14: 10 h). For transferring the enrichment cultures, 20 µl of the suspended fraction were used to inoculate 980 µl DM containing two pristine PE snippets in a microtiter plate. After 12 days of incubation, when the pristine PE snippets were covered with a chlorophyll-containing biofilm, this transfer procedure was repeated. After a total of three transfers, six biofilm-covered polymer particles were streaked onto solid DM and cultivated in the light incubator. The resulting photoautotrophic algal-bacterial consortia were re-plated onto new solid DM every 1 to 2 weeks.

For isolation of heterotrophic bacteria from algal-bacterial consortia, cell material from the consortia was streaked onto solid medium B supplemented with 2 mM of each D-glucose, *N*-acetyl-D-glucosamine and sodium glycolate (MB3G). Plates were incubated in the dark. For isolation of photoautotrophic microalgae from consortia, cell material was streaked onto solid DM and transferred with weekly changing antibiotics [in chronological order: 260 µg/ml disodium carbenicillin and 60 µg/ml monosodium ampicillin, 50 µg/ml streptomycin sulfate, 10 µg/ml gentamycin sulfate, 50 µg/ml kanamycin sulfate; adapted from Cottrell and Suttle (1993)]. Plates were incubated in the light as described above for the enrichment cultures. Axenity of the algal isolates was tested by 4′,6-diamidino-2-phenylindole (DAPI) staining and by cultivation on MB3G in the dark. The resulting axenic algal isolates were re-plated onto new solid DM with 260 µg/ml disodium carbenicillin and 60 µg/ml monosodium ampicillin every 2 to 4 weeks for maintenance.

Identification of microorganisms

For taxonomical classification of isolated bacterial strains, DNA was isolated with the *Gentra Puregene Yeast/Bact. Kit* (Qiagen, Hilden, DE) according to the manufacturer's instructions. Purified genomic DNA was amplified using the primer pair *16S_27_fw* (5'-AGAGTTTGATCATGGCTCA-3′) and *16S_1492_rev* (5'-TACGGTTACCTTGTTACGACTT-3′, adapted from Weisburg et al., 1991). PCR-amplified DNA was purified with the *GeneJET PCR Purification Kit* (Thermo Fisher Scientific, Waltham, USA) and sequenced by Eurofins Genomics (Ebersberg, DE) with the *Mix2Seq Kit*.

For taxonomical classification of isolated algal strains, DNA isolation was performed according to the protocol described by Jagielski et al. (2017). For cell lysis, glass beads (d: 400–600 µm; Sigma Aldrich, St. Louis, USA), Mikro-Dismembrator S (Sartorius AG, Göttingen, DE), 300 µl of 5 M NaCl and 240 µl CTAB buffer were used. After adding the phenol/chloroform/isoamylalcohol solution, additional 10 s vortexing and subsequent centrifuging at 16,699 × *g* for 1 min were implemented.

After DNA precipitation, centrifugation was performed with 18,407 × *g*. Purified DNA was PCR-amplified using the primer pairs CHLORO_fw (5′-TGGCCTATCTTGTTGGTCTGC-3′)/CHLORO_rev (5′-GAATCAACCTGACAAGGCAAC-3′; Gumbi et al., 2017), ITS1_fw (5′-AGGAGAAGTCGTAACAAGGT-3′)/ITS4_rev (5′-TCCTCCGCTTATTGATATGC-3′; Hadi et al., 2016), rbcL_192_fw (5′-GGTACTTGGACAACWGTWTGGAC-3′)/rbcL_657_rev (5′-GAAACGGTCTCKCCARCGCAT-3′; Hadi et al., 2016), rbcL_375_fw (5′-TTTGGTTTCAAAGCIYTWCGTGC-3′)/rbcL_1089_rev (5′-ATACCACGRCTACGRTCTTT-3′; Hadi et al., 2016), tufA_fw (5′-TGAAACAGAAMAWCGTCATTATGC-3′)/tufA_rev (5′-CCTTCNCGAATMGCRAAWCGC-3′; Hall et al., 2010), tufA_50_fw (5′-TGGATGGTGCTATTYTAGTTG-3′)/tufA_870_rv (5′-ATAGTGTCRCCTGGCATAGC-3′; Hall et al., 2010). PCR-amplified DNA was purified and sequenced as described above.

For phylogenetic affiliation analysis, the BLASTn suite search tool (Altschul et al., 1990) was used.

Growth experiments with photoautotrophic consortia

Growth experiments with photoautotrophic consortia were performed for re-colonization experiments and for grazing experiments. In both cases, pre-cultures were set up by resuspending cell material from consortia growing on solid DM in liquid DM and incubated for 7 days.

For the re-colonization experiments, the photoautotrophic consortia Co_1 to Co_6 were used. Pre-cultures were inoculated from agar plates in 20 ml DM in 100 ml Erlenmeyer flasks at 175 rpm and 21°C in the light incubator (EQUiTEC). For main cultures, 800 µl DM were inoculated with 200 µl pre-culture in 24-well plates (*Thermo Scientific™ Nunc™ Cell-Culture Treated Multidishes* [Thermo Fisher Scientific Inc., Waltham, USA]) containing PE, PET or PS snippets, which had prior been sterilized by bathing in in ethanol (70% v/v) for 15 min followed by drying and 5 min UV-irradiation in a laminar-flow sterile bench before use. After 7 days incubation, chlorophyll fluorescence and biofilm biomass on the snippets were determined as described above.

Cultivation of consortium Co_3 for grazing experiments

For grazing experiments, consortium, Co_3 was used. Pre-cultures were grown in 125 ml DM in 500 ml Erlenmeyer flasks without shaking at room temperature and daylight. As biofilm surfaces, slides of 2.5 cm × 8 cm were cut from PE-, PET- and PS foils (Goodfellow, thickness: 0.125 mm), which were roughened on one side using 60 grid sandpaper. Before use, polymer slides were sterilized in 70% (*v*/*v*) ethanol for 30 min, washed in sterile H_2O_{demin} and stored in sterile H_2O_{demin} at 4°C. As control material, fully frosted glass microscope slides were used which had prior been rinsed with H_2O_{demin} and autoclaved. Before inoculation of main cultures, pre-cultures were washed via centrifugation of 50 ml at 6,000 rpm for 30 min. Supernatants were carefully discarded, and pellets were resuspended in sterile DM-medium to a volume with a chlorophyll concentration of 1 µg/ml using the corresponding chlorophyll fluorescence intensities determined for the diatom *Phaeodactylum tricornutum* as described by Zecher et al. (2015).

For the main cultures, in which biofilm formation should occur, four square petri dishes per material type were filled with 50 ml of the washed cell suspension. In each petri dish, four polymer or glass slides were placed with the rough side facing upwards. The petri dishes were incubated for 7 days at room temperature and daylight. Biofilm

formation was evaluated via chlorophyll fluorescence as described above. For analysing shifts in the bacterial community compositions via amplicon sequencing, cell material was isolated from Co_3 on solid DM media from three transfers (January 2020, August 2020, and March 2021), 7-day-old biofilms on different plastic types and from the respective surrounding supernatants before grazing started. DNA-extraction and 16S rDNA amplicon sequencing were performed as described above. To confirm that the isolated algae Alg_3.1 was originally present in Co_3 its 18S rRNA sequence was aligned against the R2 mate samples of the amplicon sequencing data of Co_3 from the three transfers using bowtie2 using the "sensitive-local" algorithm (version 2.5.1, https://github.com/BenLangmead/bowtie2).

Grazing experiments

Plastic and glass slides with biofilms of Co_3, which were produced in the growth experiments described above, were placed in 1,000 ml glass beakers with 500 ml synthetically reconstituted surface freshwater (Osterauer et al., 2010) and 4 individuals of the gastropod *Physa fontinalis*. Snails obtained from a commercial distributor for aquarist supplies, who kept the snails in quarantine had a length of 3.8 ± 0.5 mm (mean ± standard deviation). The slides were replaced every 3 ½ days with slides from the same batch stored at 4°C in the dark. Experiments lasted for 3 weeks in a climate-controlled room at 20°C with a 16:8 h cycle. The physiological parameters of *P. fontinalis* were determined in weekly intervals, including: size measured by a digital caliper as well as a digital microscope (VHX-5000, Keyence Corp.), mortality, faeces dry mass and the numbers of eggs and egg packages. Biofilms were analysed by measuring chlorophyll fluorescence before and after the grazing experiments.

Results

Composition of *in-situ* biofilm communities is dominated by the incubation site and not by the plastic material

The microplastic snippets of all three materials (PE, PET, PS) were colonized with chlorophyll-containing biofilms over time on all three incubation sites (Figure 1). The chlorophyll intensities were generally lower with the *Emssee* and *Rieselfelder* samples compared to the *Ems* samples. Microscopic examination revealed the presence of microalgae (various diatoms and *Chlorella*- and *Chlamydomonas*-like morphotypes) and of prokaryotic cells (not shown).

From all three incubation sites, strains of heterotrophic bacteria could be isolated by direct plating of sheared biofilm material (Supplementary Table S1). Most isolated strains belonged to the Alpha-, Beta- and Gammaproteobacteria including genera of characteristic freshwater bacteria such as *Gemmobacter*, *Mitsuaria*, and *Aeromonas*, respectively. Typical freshwater Bacteroidetes, such as *Flavobacterium* spp., could also be isolated.

The cultivation-independent analysis of the biofilm communities exhibited a much greater diversity than the cultivation analysis (Figure 2). While Alpha-, Beta- and Gammaproteobacteria and Bacteroidetes were also found to be abundant, the amplicon sequencing revealed a large proportion of *Planctomycetia* that were not retrieved by cultivation (Figure 2B). Furthermore, the *Rieselfelder* samples contained a large percentage of members of the genus *Nitrospira*, which were not detected in the biofilms from the other incubation sites. Statistical analysis of the cultivation-independent analysis showed that the bacterial communities clustered according to

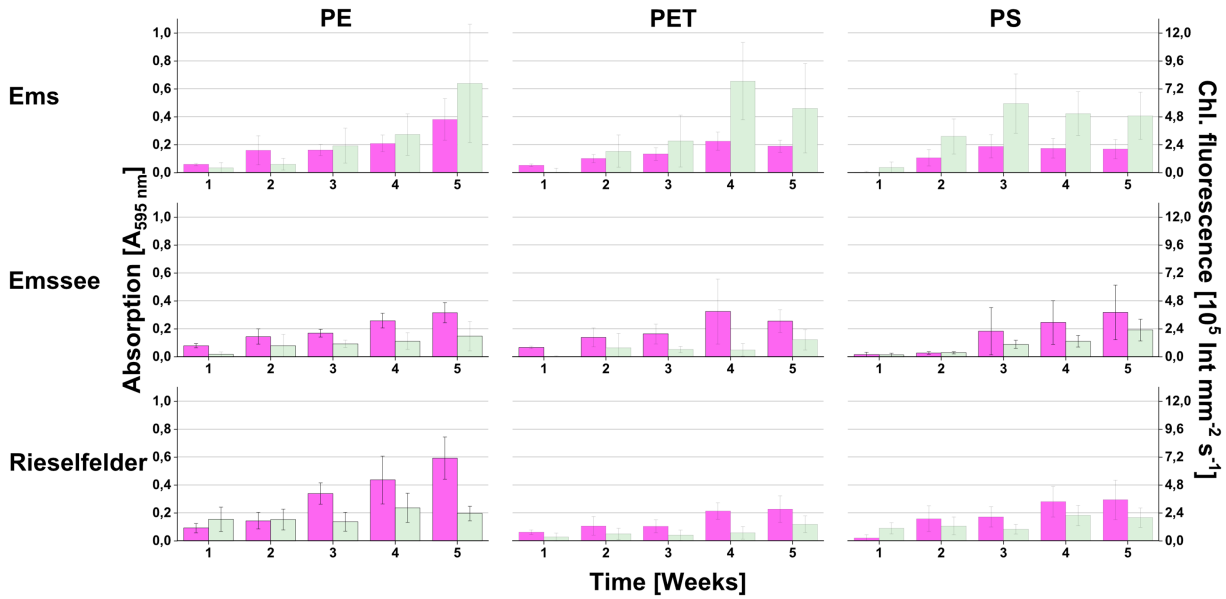

FIGURE 1
Colonization of plastic snippets during the in the *in-situ*-incubation at three different freshwater sites (*Ems*, *Emssee*, and *Rieselfelder*). At each sampling event, individual snippets were first used for measuring chlorophyll fluorescence (green bars) before they were used for measuring biofilm biomass with crystal violet (magenta bars). Error bars indicate standard deviation (n = 12).

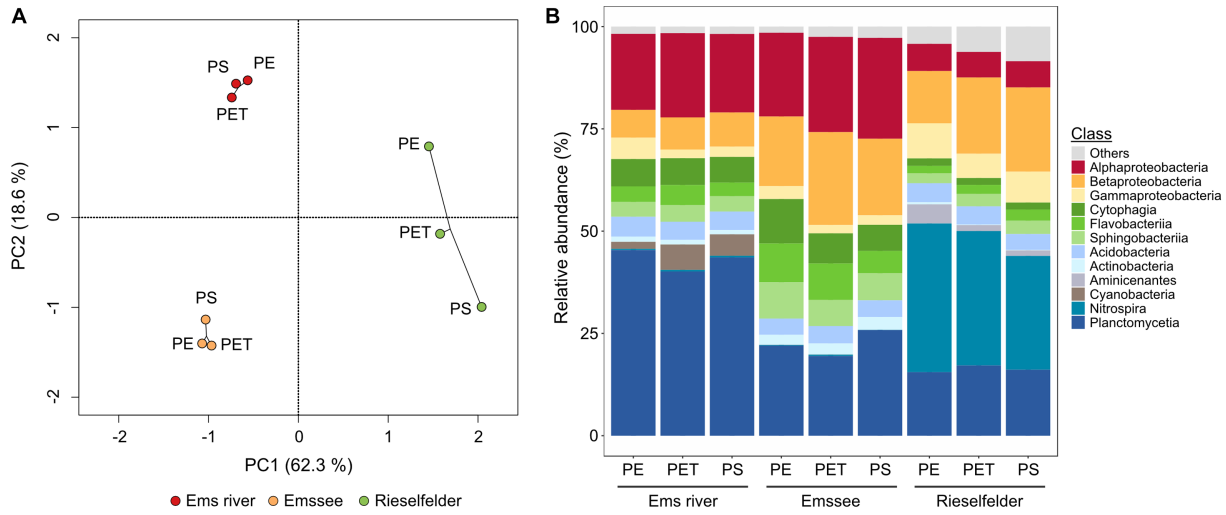

FIGURE 2
Analysis of biofilm communities on plastic snippets from *in-situ* incubations via amplicon-sequencing of genes for the 16S rRNA on the class level. **(A)** Statistical evaluation via principle-component analysis (PCA); **(B)** Relative abundances. The analysis was performed with 15 plastic snippets per polymer and location after 5 weeks of incubation at the indicated locations. Classes with <1% abundance in all samples are summarized as "others".

the incubation sites rather than the plastic material, on which the biofilm had formed (Figure 2A).

Selection for biofilm-forming photosynthetic communities results in stable photoautotrophic consortia maintainable on solid media

For isolating microorganisms from these *in-situ* enrichments that could be used for producing defined biofilms for grazing experiments we set up laboratory enrichments under photoautotrophic conditions in the next step.

These laboratory enrichments were inoculated with plastic snippets from which loosely attached microorganisms had been detached by gentle shearing forces (Supplementary Figure S2). In the following, we selected for microorganisms that were able to colonize pristine plastic snippets under photoautotrophic conditions. We restricted the enrichment to PE snippets because biofilms on this material showed the highest biofilm-biomass in the *in-situ* incubations (Figure 1). This procedure led to the enrichment of communities that reproducibly re-colonized PE-surfaces. After 3 transfers, plastic snippets with biofilms were used to inoculate solid media. By this procedure, we obtained photoautotrophic microbial communities that could be maintained on agar plates by regular transfer about every fortnight since November 2018. In total, we enriched six consortia: two originating from *Rieselfelder* (Co_1 and Co_2) and four from *Ems* river PE-particles (Co_3 to Co_6; Figure 3A). In comparison to *in-situ* grown biofilms the consortia had originated from, the bacterial communities within the consortia displayed a smaller diversity (Figure 3B). The phylum of Planctomycetes, which exhibited large proportions in the *in-situ* grown biofilms (Figure 2B) was only represented in Co_6 and Co_2 at low abundances. The phylum of *Nitrospira* was not present in the algal-bacterial consortia derived from the *Rieselfelder* while it was abundant in the *in-situ* sample. Cyanobacteria, represented in comparably small abundances within *in-situ* grown biofilms in the *Ems* river, dominated the algal-bacterial consortia Co_4 and Co_5, derived from PE biofilms grown in the *Ems* river. In Co_3 and Co_1, we also observed the yet uncultivated candidate phylum WPS-2. The presence of microalgae in the consortia was verified by microscopy (not shown).

Consortium Co_3 efficiently re-colonizes plastic surfaces

For investigating whether the consortia were able to re-colonize plastic surfaces from liquid culture after being maintained on agar plates and for identifying the consortium with the highest biofilm production, re-colonization experiments were performed with all three plastic polymers (PE, PET and PS) originally used in the *in situ* incubation (Figure 4). The consortia showed large differences in biofilm formation when exposed to plastic surfaces. Co_3, which was derived from a biofilm on PE snippets from the *Ems* river, showed the highest chlorophyll fluorescence values and highest biofilm biomass. While all consortia showed at least some biofilm biomass, there was no chlorophyll fluorescence detected in Co_1 and 5, and also only low values in other consortia.

For further characterizing the composition and stability of Co_3, we repeatedly submitted it to amplicon sequencing. These analyses showed a reduction of the diversity on class and genus levels with time. The candidate genus WPS-2 disappeared within about 8 months while members of genera with cultivated representatives remained (Figure 5A).

Biofilms formed by a defined dual-species culture are not accepted by the grazer

As Co_3 should contain microorganisms capable of re-colonizing a plastic surface from a culture with suspended cells, we isolated algal and

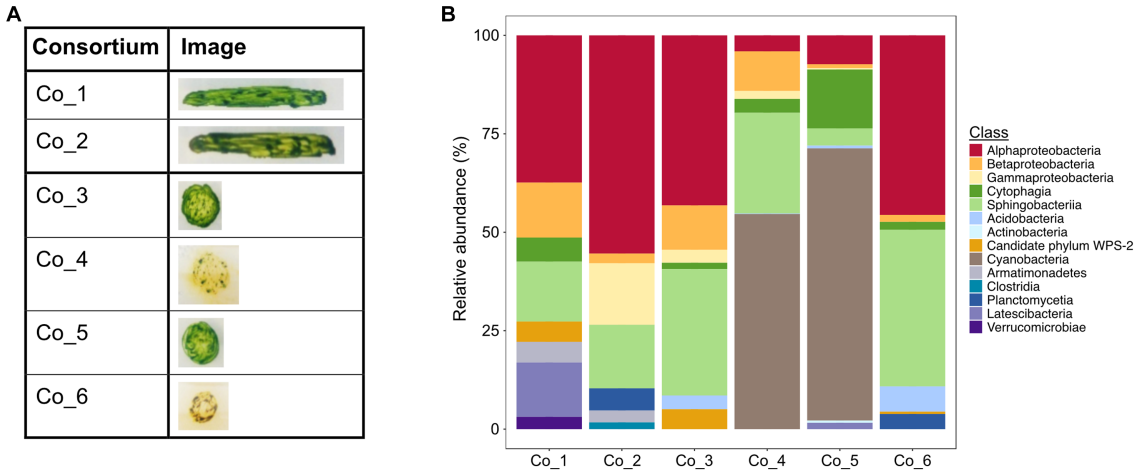

FIGURE 3
Photoautotrophic consortia enriched from *in-situ* incubations. **(A)** Macroscopic photographs of consortia on solid medium; **(B)** Analysis of consortia via amplicon-sequencing of genes for the 16S rRNA on the class level.

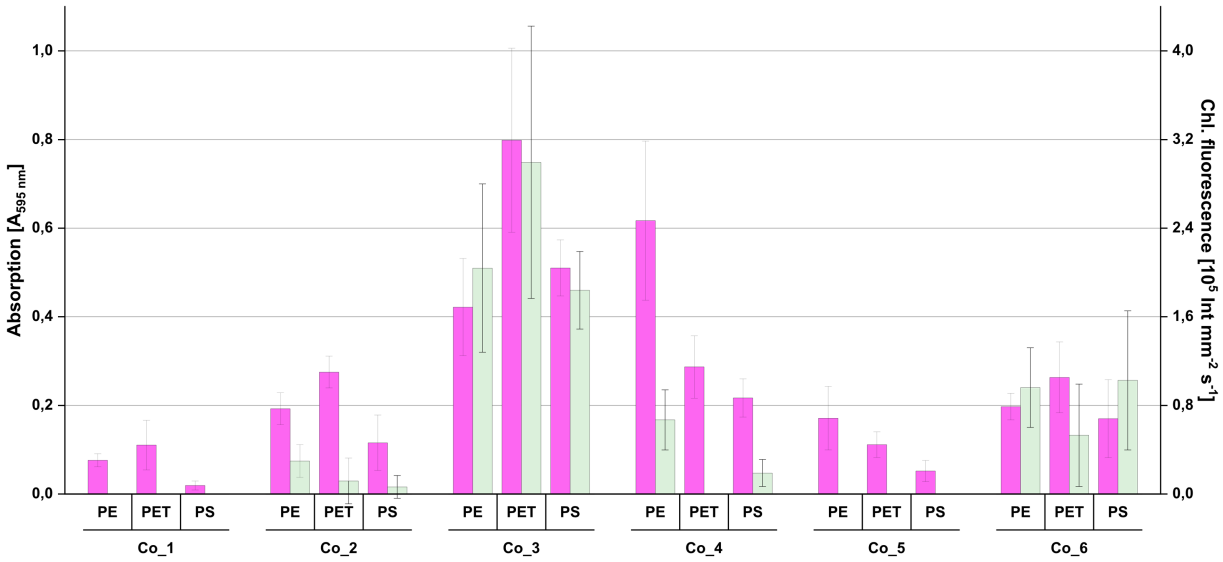

FIGURE 4
Re-colonization of plastic surfaces by the individual photoautotrophic consortia shown in Figure 3. Individual plastic surfaces were first used for measuring chlorophyll fluorescence (green bars) before they were used for measuring biofilm biomass with crystal violet (magenta bars). Error bars indicate standard deviation (n = 8).

bacterial strains from this consortium. For this, cell material from the consortia plates were transferred to solid media and growth conditions that favor the growth of axenic microalgae and heterotrophic bacteria, respectively. The procedure for obtaining axenic microalgae led to the isolation of strain Alg_3.1, which was classified as *Chlamydomonas* sp. Alignment of the 18S rRNA of the isolate to the amplicon sequencing data from Co_3 confirmed that Alg_3.1 was present in the original Co_3 consortium and in the transfers on solid DM medium (alignment rates of 4.40, 2.78, and 6.42% in January 2020, August 2020, and March 2021, respectively). The procedure for obtaining heterotrophic bacteria, which was also applied to the other consortia, led to the isolation of several strains of Alphaproteobacteria of the genus *Gemmobacter* and Betaproteobacteria of the genus *Acidovorax* (Supplementary Table S2). Apart from further proteobacterial strains, a member of the genus *Flectobacillus* (Bacteroidetes) was isolated. Pre-test with a number of these bacterial strains in co-culture with *Chlamydomonas* sp. strain Alg_3.1 revealed biofilm formation of several isolates in co-culture with *Chlamydomonas* sp. Alg_3.1 on PET (not shown). For further colonization experiments, *Gemmobacter* sp. strain O was then chosen because it showed reliable biofilm formation on different plastic surfaces. Biofilm formation and algal growth could be largely reduced when co-cultures were supplied with succinate as growth substrate for the bacterium indicating that biofilm formation was optimal when the co-culture relied on photoautotrophic conditions (Supplementary Figure S3). However, these dual-species biofilms were not grazed by our model invertebrate *Physa fontinalis* (not shown).

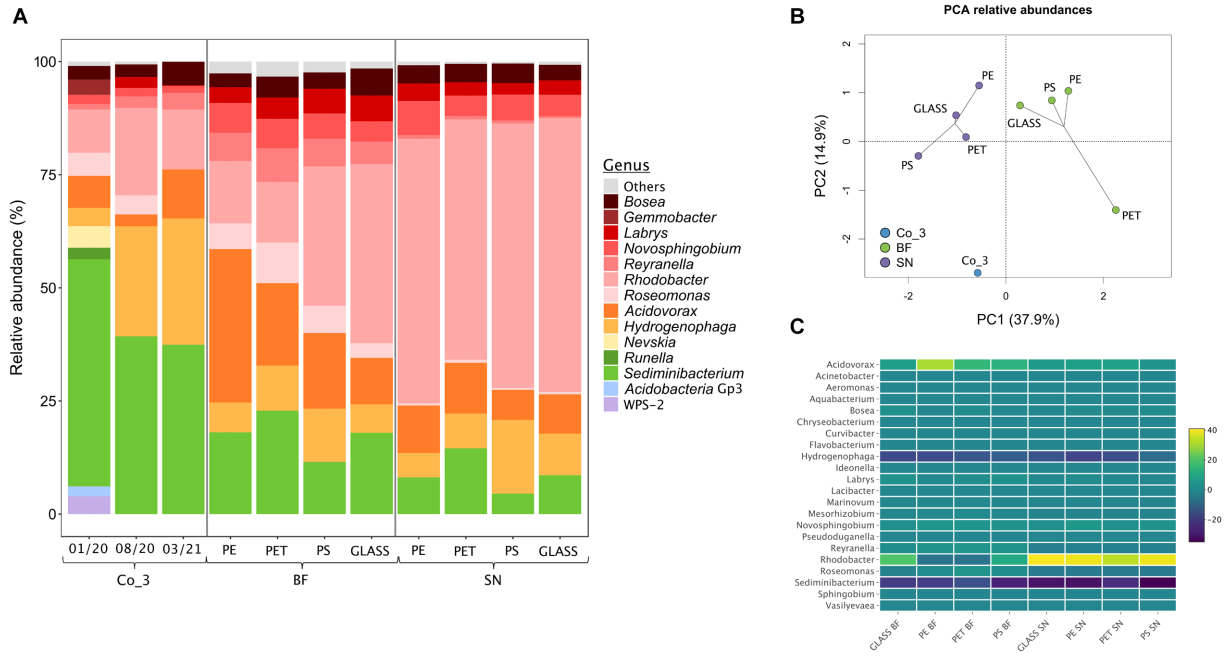

FIGURE 5
Analysis of the photoautotrophic consortium Co_3 via amplicon-sequencing of genes for the 16S rRNA on the genus level. **(A)** From left to right: relative abundancies of genera in Co_3 after maintenance on solid diatom medium for 2, 10 and 16 months after initial isolation; abundancies during a growth experiment for providing biofilms for a grazing experiment: the community composition of the consortium on solid diatom medium directly before inoculating the growth experiment (Co_3 08/20) was compared to the composition of the biofilm fraction (BF) and of the supernatant (SN) for each material. Genera with <2% abundance in all samples are summarized as "others"; **(B)** Statistical evaluation via principle-component analysis (PCA); **(C)** Heat map displaying the relative abundances within biofilm and the supernatant relative to the consortium Co_3 (08/20) on solid medium on the genus level. For each material, 3 replicates were used from which the extracted DNA was pooled.

TABLE 1 **Performance of the freshwater snail *Physa fontinalis* during grazing on biofilms formed by the photoautotrophic consortium Co_3 on different surfaces.**

Parameter	Glass (m ± stdev)	PE (m ± stdev)	PET (m ± stdev)	PS (m ± stdev)
Snail growth	0.02 ± 0.03	0.03 ± 0.06	0.05 ± 0.05	0.05 ± 0.07
Reproduction	2.13 ± 1.36	1.63 ± 1.60	1.25 ± 1.16	2 ± 2.62
Faeces mass	4.64 ± 1.17	2.56 ± 1.42	1.74 ± 0.27	1.89 ± 0.36

Growth rates (mm per snail per week), reproduction (number of eggs per snail per week) and faeces mass (mg per snail per week) were followed for 3 weeks. +/− indicates standard deviation ($n = 96$).

Consortium Co_3 forms reproducibly biofilms on different materials that are grazed by *P. fontinalis*

Due to the stability of the community composition together with the recolonization capacity biofilms of Co_3 were tested as a substrate for the grazer *P. fontinalis*. For this, we set up biofilm experiments with Co_3 by offering three types of plastic (PE, PET, PS) and glass as surfaces as control. These experiments showed that Co_3 reproducibly formed biofilms for the test period of 8 weeks (Supplementary Figure S4). During this time, *P. fontinalis* showed growth and activity for a period of 3 weeks (Table 1). Snails grazed on the biofilms leading to small but continuous growth rates, reproduction and faeces excretion. There were no significant differences in snail performance among the different substrates.

For further assessing the suitability of using Co_3 as model community we analyzed the community composition directly before the snails were added. Statistical analysis of the communities within the biofilm and the suspended fraction by amplicon sequencing revealed that the composition clustered according to the individual suspended and biofilm fractions rather than according to surface material (Figures 5A,B) as was also previously observed in the *in-situ* incubations. A heat-map analysis of the community structure indicated that the largest difference to the stock consortium of Co_3 on solid medium was the strong reduction of *Sediminibacterium* sp. and *Hydrogenophaga* sp.in the biofilm and the suspended fraction as well as a strong increase of *Rhodobacter* sp. in all suspended fractions (Figure 5C).

Discussion

Studies on the ecotoxicity of (micro) plastics on aquatic organisms should consider the influence of biofilms. However, biofilms are difficult to standardize, and there is demand on obtaining reproducible biofilm

systems that have ecological relevance. In this study, we established a stable photoautotrophic microbial consortium that reproducibly formed biofilms on different surfaces which could be used as food for the grazing snail *Physa fontinalis*. This consortium Co_3 originated from the photic zone of the *Ems* river and consisted of a *Chlamydomonas* strain and about 20 species of heterotrophic bacteria of which members of the genera *Roseomonas* (Alphaproteobacteria), *Hydrogenophaga* (Betaproteobacteria) and *Sediminibactrium* (Chitinophagaceae) were dominating community members.

Initially, we aimed at establishing a defined co-culture that can be recombined on demand from mono-cultures of photoautotrophic microalgae and heterotrophic bacteria isolated from biofilms on plastic from the photic zones of dams and reservoirs. Such defined dual cultures of individually maintainable strains that formed reliably biofilms could indeed be established but were, unfortunately, not accepted by the grazer. Based on the unexpected finding that enriched photoautotrophic consortia could be stably propagated on solid media we obtained the consortium Co_3 that showed reproducible biofilm formation on different plastic materials and could also serve as food for the grazing snail *P. fontinalis*. Importantly, Co_3 also formed biofilms on glass which offers an opportunity to analyze plastic-specific effects of this model biofilm (Wright et al., 2020).

Functional and genetic analyses of consortium Co_3 during a grazing experiment showed that it could effectively nourish *P. fontinalis* while its community structure changed only moderately in the quantity but not in the quality of its individual members. Thus, Co_3 showed a stable phenotype and genotype irrespective of the localization of cells (planktonic or in the biofilm) and of the surface material. Based on this stability and considering a broader biological definition of domestication as (Purugganan, 2022) we propose the term domesticated community for our biofilm model community.

The community structures of the *in-situ* enrichments were apparently not influenced by the plastic material but rather by the conditions at the incubation site which is also observed with biofilms on plastic in marine sites (Oberbeckmann et al., 2021). In this respect, the large proportion of *Nitrospira* in the biofilms from the Rieselfelder site, which was not observed for the other incubation sites, might have been influenced by the outflow of a large municipal sewage treatment plant in *Münster-Coerde* nearby. In the six consortia obtained by the subsequent laboratory enrichment growth of the heterotrophic bacteria relied on cross-feeding of exudates from the photoautotrophic microalgae. However, analysis of the six consortia showed that our selection for photoautotrophic growth and surface adhesion can have different outcomes regarding the structure of the communities and their ability to colonize plastics. The follow-up assay for re-colonization of surfaces from the planktonic phase after being inoculated from solid medium was therefore crucial for identifying a community with the desired prerequisites outlined in the introduction.

Within continued cultivation on solid media, the diversity of Co_3 was reduced which might have a variety of reasons ranging from adverse abiotic conditions (higher temperatures etc.) to interruption of nutrient transfer (Overmann et al., 2017). Remarkably, however, bacteria of the so-far uncultured candidate phylum WPS-2 could be propagated in the first cultures of Co_3 on solid media indicating that the domestication of such photoautotrophic microbial communities might be a way of increasing the cultivability of environmental bacteria. As bacteria of the candidate phylum WPS-2 are believed to use organic substrates that may also be exudated by algae (Sheremet et al., 2020) they might have been out-competed by other taxa which used the same substrates.

Compared to Co_3 on agar plates, the abundance of *Sediminibacterium* sp. and of *Hydrogenophaga* sp. decreased in both the biofilm and the suspended fractions in the grazing experiment while the abundance of *Rhodobacter* sp. increased (Figures 5A,C). This could indicate that *Sediminibacterium* sp. and *Hydrogenophaga* sp. were more important when the community is growing at a moist surface-liquid interface compared to the submerged situation where *Rhodobacter* sp. might have important functions. In agreement with preferred growth in biofilms, a *Sediminibacterium* strain showed upregulation of stress-related proteins in planktonic cells compared to aggregated cells (Ayarza et al., 2015).

Besides the obvious cross feeding of exudates interactions between photoautotrophic microalgae and heterotrophic bacteria can be very diverse as evidenced from natural communities (Amin et al., 2012) as well as synthetic communities for both marine (Deng et al., 2022) and limnic conditions (Lamprecht et al., 2022). We do not know the basis for the stability of Co_3 but the stable maintenance of the bacterial members suggests that bacteria are likely to support growth of the algae in a specific way.

In many natural assemblages of this type, heterotrophic bacteria feed vitamin B12 to the algae (Amin et al., 2012) but this was most probably not essential because the *Chlamydomonas* sp. from Co_3 grew also axenically without bacteria. Other metabolic interactions by which algae-associated bacteria may support growth of their photoautotrophic community member could be the degradation of organic nitrogen compounds such as methylamines and glycine betaine to ammonium that can be used by the algae. This property is apparently frequent among marine algae-associated members of the *Rhodobacteraceae* family (Zecher et al., 2020). In this respect, the repeated isolation of *Gemmobacter* spp. which is described as a common freshwater microalgae-associated bacterium of this family (Zhang et al., 2020) and is also capable of methylamine-utilization (Kröber et al., 2021) might suggest ammonium cross-feeding from bacteria to the algae is involved in our communities as well. Interestingly, Co_3 grew with monomethylamine as sole nitrogen source in liquid culture (not shown). Furthermore, metabolic interactions between microalgae and their associated bacteria might stimulate biofilm formation itself as it was also observed in other cases and can rely on a multitude of factors (Grossart et al., 2006; Windler et al., 2015).

In our study with Co_3 and *P. fontinalis*, we did not observe an influence on the fitness of the snails indicating under these conditions no harmful additives were mobilized or leached from the plastic material. This might partly be due to the fact that we did not use weathered plastics from which additives and adsorbed chemicals might leach more easily (Rummel et al., 2019; Luo et al., 2023).

As a main conclusion, our results show that domesticated communities might be a very promising approach for standardizing mixed-species biofilms for ecologically relevant ecotoxicological assays. It is compellingly easy for obtaining and maintaining a model community, at least for a defined series of experiments. While our domesticated community was genetically and phenotypically stable in the described timeframe (and it still is) it would certainly be even better to have a completely defined consortium that can be synthetically rearranged from individual stock cultures on demand, especially for exchange between labs and for certifiable protocols. In this respect, we tried to isolate the main representatives of Co_3 but

failed to do so thus far (not shown). This may indicate that metabolic interdependencies of the community members are relatively strong and that the underlying nutritional requirements are difficult to reconstitute in mono-cultures.

Data availability statement

The datasets presented in this study can be found in online repositories. The names of the repository/repositories and accession number (s) can be found at: https://www.ebi.ac.uk/ena, PRJEB45856.

Author contributions

IB conceptualized, performed, and evaluated the amplicon sequencing and contributed to the writing of manuscript together with RJ and BP. RJ conceptualized, performed, and evaluated all cultivation-based experiments and supported amplicon sequencing. Contributions of IB and RJ were equal. DM-K performed the grazing experiments. LH performed the isolation of algae and the re-colonization experiment. FG conceptualized and managed the project and supported writing the of manuscript. JH supported the evaluation of amplicon sequencing and writing of the manuscript. BP conceptualized and managed the project and wrote the manuscript. All authors contributed to the article and approved the submitted version.

Funding

The author (s) declare financial support was received for the research, authorship, and/or publication of this article. This research was supported by the BMBF project MikroPlaTaS (02WPL1448A) and by the Masterprogramm NRW 2020.

Acknowledgments

We thank Kirsten Heuer for excellent technical support with maintaining the consortia. Rebekka Lülf and Anna Hübenthal are acknowledged for support with isolating bacterial strains.

Conflict of interest

The authors declare that the research was conducted in the absence of any commercial or financial relationships that could be construed as a potential conflict of interest.

Publisher's note

All claims expressed in this article are solely those of the authors and do not necessarily represent those of their affiliated organizations, or those of the publisher, the editors and the reviewers. Any product that may be evaluated in this article, or claim that may be made by its manufacturer, is not guaranteed or endorsed by the publisher.

Supplementary material

The Supplementary material for this article can be found online at: https://www.frontiersin.org/articles/10.3389/fmicb.2023.1238913/full#supplementary-material

References

Alfonso, M. B., Lindsay, D. J., Arias, A. H., Nakano, H., Jandang, S., and Isobe, A. (2023). Zooplankton as a suitable tool for microplastic research. *Sci. Total Environ.* 905:167329. doi: 10.1016/j.scitotenv.2023.167329

Altschul, S. F., Gish, W., Miller, W., Myers, E. W., and Lipman, D. J. (1990). Basic local alignment search tool. *J. Mol. Biol.* 215, 403–410. doi: 10.1016/S0022-2836(05)80360-2

Amin, S. A., Parker, M. S., and Armbrust, E. V. (2012). Interactions between diatoms and bacteria. *Microbiol. Mol. Biol. Rev.* 76, 667–684. doi: 10.1128/MMBR.00007-12

Arias-Andres, M., Kettner, M. T., Miki, T., and Grossart, H. P. (2018). Microplastics: new substrates for heterotrophic activity contribute to altering organic matter cycles in aquatic ecosystems. *Sci. Total Environ.* 635, 1152–1159. doi: 10.1016/j.scitotenv.2018.04.199

ASTM International (2020). *ASTM E2149-20, standard test method for determining the antimicrobial activity of antimicrobial agents under dynamic contact conditions*.

Ayarza, J. M., Mazzella, M. A., and Erijman, L. (2015). Expression of stress-related proteins in *Sediminibacterium* sp. growing under planktonic conditions. *J. Basic Microbiol.* 55, 1134–1140. doi: 10.1002/jobm.201400725

Bruns, A., Nübel, U., Cypionka, H., and Overmann, J. (2003). Effect of signal compounds and incubation conditions on the culturability of freshwater bacterioplankton. *Appl. Environ. Microbiol.* 69, 1980–1989. doi: 10.1128/AEM.69.4.1980-1989.2003

Carles, L., Wullschleger, S., Joss, A., Eggen, R. I. L., Schirmer, K., Schuwirth, N., et al. (2021). Impact of wastewater on the microbial diversity of periphyton and its tolerance to micropollutants in an engineered flow-through channel system. *Water Res.* 203:117486. doi: 10.1016/j.watres.2021.117486

Cássio, F., Batista, D., and Pradhan, A. (2022). Plastic interactions with pollutants and consequences to aquatic ecosystems: what we know and what we do not know. *Biomol. Ther.* 12:798. doi: 10.3390/biom12060798

Castro-Castellon, A. T., Horton, A. A., Hughes, J. M. R., Rampley, C., Jeffers, E. S., Bussi, G., et al. (2022). Ecotoxicity of microplastics to freshwater biota: considering exposure and hazard across trophic levels. *Sci. Total Environ.* 816:151638. doi: 10.1016/j.scitotenv.2021.151638

Cho, J. C., and Giovannoni, S. J. (2004). Cultivation and growth characteristics of a diverse group of oligotrophic marine Gammaproteobacteria. *Appl. Environ. Microbiol.* 70, 432–440. doi: 10.1128/AEM.70.1.432-440.2004

Christensen, G. D., Simpson, W. A., Younger, J. J., Baddour, L. M., Barrett, F. F., Melton, D. M., et al. (1985). Adherence of coagulase-negative staphylococci to plastic tissue culture plates: a quantitative model for the adherence of staphylococci to medical devices. *J. Clin. Microbiol.* 22, 996–1006. doi: 10.1128/jcm.22.6.996-1006.1985

Cohn, S. A., Farrell, J. F., Munro, J. D., Ragland, R. L., Weitzell, R. E. Jr., and Wibisono, B. L. (2003). The effect of temperature and mixed species composition on diatom motility and adhesion. *Diatom Res.* 18, 225–243. doi: 10.1080/0269249X.2003.9705589

Cohn, S. A., and Pickett-Heaps, J. D. (1988). The effects of colchicine and dinitrophenol on the in vivo rates of anaphase a and B in the diatom *Surirella*. *Eur. J. Cell Biol.* 46, 523–530. PMID: 3181168.

Cottrell, M. T., and Suttle, C. A. (1993). Production of axenic cultures of *Micromonas pusilla* (Prasinophyceae) using antibiotic. *J. Phycol.* 29, 385–387. doi: 10.1111/j.0022-3646.1993.00385.x

Deng, Y., Mauri, M., Vallet, M., Staudinger, M., Allen, R. J., and Pohnert, G. (2022). Dynamic diatom-Bacteria consortia in synthetic plankton communities. *Appl. Environ. Microbiol.* 88:e0161922. doi: 10.1128/aem.01619-22

Dris, R., Agarwal, S., and Laforsch, C. (2020). Plastics: from a success story to an environmental problem and a global challenge. *Global Chall.* 4:2000026. doi: 10.1002/gch2.202000026

Fauser, P., Vorkamp, K., and Strand, J. (2022). Residual additives in marine microplastics and their risk assessment - a critical review. *Mar. Pollut. Bull.* 177:113467. doi: 10.1016/j.marpolbul.2022.113467

Grossart, H. P., Czub, G., and Simon, M. (2006). Algae-bacteria interactions and their effects on aggregation and organic matter flux in the sea. *Environ. Microbiol.* 8, 1074–1084. doi: 10.1111/j.1462-2920.2006.00999.x

Gubelit, Y. I., and Grossart, H. P. (2020). New methods, new concepts: what can be applied to freshwater periphyton? *Front. Microbiol.* 11:1275. doi: 10.3389/fmicb.2020.01275

Guillard, R. R. L., and Ryther, J. H. (1962). Studies of marine planktonic diatoms. I. *Cyclotella nana* Hustedt, and *Detonula confervacea* (Cleve) gran. *Can. J. Microbiol.* 8, 229–239. doi: 10.1139/m62-029

Gumbi, S. T., Majeke, B. M., Olaniran, A. O., and Mutanda, T. (2017). Isolation, identification and high-throughput screening of neutral lipid producing indigenous microalgae from south African aquatic habitats. *Appl. Biochem. Biotechnol.* 182, 382–399. doi: 10.1007/s12010-016-2333-z

Hadi, S. I. I. A., Santana, H., Brunale, P. P. M., Gomes, T. G., Oliveira, M. D., Matthiensen, A., et al. (2016). DNA barcoding green microalgae isolated from neotropical inland waters. *PLoS One* 11:e0149284. doi: 10.1371/journal.pone.0149284

Hall, J. D., Fučíková, K., Lo, C., Lewis, L. A., and Karol, K. G. (2010). An assessment of proposed DNA barcodes in freshwater green algae. *Cryptogam. Algol.* 31:529.

Jagielski, T., Gawor, J., Bakuła, Z., Zuchniewicz, K., Żak, I., and Gromadka, R. (2017). An optimized method for high quality DNA extraction from microalga *Prototheca wickerhamii* for genome sequencing. *Plant Methods* 13:77. doi: 10.1186/s13007-017-0228-9

Jagmann, N., Brachvogel, H. P., and Philipp, B. (2010). Parasitic growth of *Pseudomonas aeruginosa* in co-culture with the chitinolytic bacterium *Aeromonas hydrophila*. *Environ. Microbiol.* 12, 1787–1802. doi: 10.1111/j.1462-2920.2010.02271.x

Japanese Standards Association (2010). Antibacterial products - test for antibacterial activity and efficacy. JIS Z 2801, 2010-12-20.

Konschak, M., Zubrod, J. P., Duque Acosta, T. S., Bouchez, A., Kroll, A., Feckler, A., et al. (2021). Herbicide-induced shifts in the periphyton community composition indirectly affect feeding activity and physiology of the gastropod grazer *Physella acuta*. *Environ. Sci. Technol.* 55, 14699–14709. doi: 10.1021/acs.est.1c01819

Kröber, E., Cunningham, M. R., Peixoto, J., Spurgin, L., Wischer, D., Kruger, R., et al. (2021). Comparative genomics analyses indicate differential methylated amine utilization trait within members of the genus Gemmobacter. *Environ. Microbiol. Rep.* 13, 195–208. doi: 10.1111/1758-2229.12927

Lamprecht, O., Wagner, B., Derlon, N., and Tlili, A. (2022). Synthetic periphyton as a model system to understand species dynamics in complex microbial freshwater communities. *NPJ Biofilms Microbio.* 8:61. doi: 10.1038/s41522-022-00322-y

Latva, M., Dedman, C. J., Wright, R. J., Polin, M., and Christie-Oleza, J. A. (2022). Microbial pioneers of plastic colonisation in coastal seawaters. *Mar. Pollut. Bull.* 179:113701. doi: 10.1016/j.marpolbul.2022.113701

Leiser, R., Jongsma, R., Bakenhus, I., Möckel, R., Philipp, B., Neu, T. R., et al. (2021). Interaction of cyanobacteria with calcium facilitates the sedimentation of microplastics in a eutrophic reservoir. *Water Res.* 189:116582. doi: 10.1016/j.watres.2020.116582

Luo, H., Tu, C., He, D., Zhang, A., Sun, J., Li, J., et al. (2023). Interactions between microplastics and contaminants: a review focusing on the effect of aging process. *Sci. Total Environ.* 899:165615. doi: 10.1016/j.scitotenv.2023.165615

Michler-Kozma, D. N., Neu, T. R., and Gabel, F. (2022). Environmental conditions affect the food quality of plastic associated biofilms for the benthic grazer *Physa fontinalis*. *Sci. Total Environ.* 816:151663. doi: 10.1016/j.scitotenv.2021.151663

Oberbeckmann, S., Bartosik, D., Huang, S., Werner, J., Hirschfeld, C., Wibberg, D., et al. (2021). Genomic and proteomic profiles of biofilms on microplastics are decoupled from artificial surface properties. *Environ. Microbiol.* 23, 3099–3115. doi: 10.1111/1462-2920.15531

Ockenden, A., Northcott, G. L., Tremblay, L. A., and Simon, K. S. (2022). Disentangling the influence of microplastics and their chemical additives on a model detritivore system. *Environ. Pollut.* 307:119558. doi: 10.1016/j.envpol.2022.119558

Okeke, E. S., Ezeorba, T. P. C., Chen, Y., Mao, G., Feng, W., and Wu, X. (2022). Ecotoxicological and health implications of microplastic-associated biofilms: a recent review and prospect for turning the hazards into benefits. *Environ. Sci. Pollut. Res. Int.* 29, 70611–70634. doi: 10.1007/s11356-022-22612-w

Osterauer, R., Marschner, L., Betz, O., Gerberding, M., Sawasdee, B., Cloetens, P., et al. (2010). Turning snails into slugs: induced body plan changes and formation of an internal shell. *Evol. Dev.* 12, 474–483. doi: 10.1111/j.1525-142X.2010.00433.x

Overmann, J., Abt, B., and Sikorski, J. (2017). Present and future of culturing Bacteria. *Annu. Rev. Microbiol.* 71, 711–730. doi: 10.1146/annurev-micro-090816-093449

Parada, A. E., Needham, D. M., and Fuhrman, J. A. (2016). Every base matters: assessing small subunit rRNA primers for marine microbiomes with mock communities, time series and global field samples. *Environ. Microbiol.* 18, 1403–1414. doi: 10.1111/1462-2920.13023

Pfennig, N. (1978). *Rhodocyclus purpureus* gen. Nov. and sp. nov., a ring-shaped, vitamin B12-requiring member of the family *Rhodospirillaceae*. *Int. J. Syst. Bacteriol.* 28, 283–288. doi: 10.1099/00207713-28-2-283

Purugganan, M. D. (2022). What is domestication? *Trends Ecol. Evol.* 37, 663–671. doi: 10.1016/j.tree.2022.04.006

R Core Team (2018). R: A language and environment for statistical computing. R Foundation 782 for Statistical Computing, Vienna, Austria. Available at: https://www.R-project.org/ (Accessed June 12, 2023).

Rummel, C. D., Escher, B. I., Sandblom, O., Plassmann, M. M., Arp, H. P. H., Mac Leod, M., et al. (2019). Effects of Leachates from UV-weathered microplastic in cell-based bioassays. *Environ. Sci. Technol.* 53, 9214–9223. doi: 10.1021/acs.est.9b02400

Sánchez-Bayo, F. (2021). Indirect effect of pesticides on insects and other arthropods. *Toxics* 9:177. doi: 10.3390/toxics9080177

Scales, B. S., Cable, R. N., Duhaime, M. B., Gerdts, G., Fischer, F., Fischer, D., et al. (2021). Cross-hemisphere study reveals geographically ubiquitous, plastic-specific Bacteria emerging from the rare and unexplored biosphere. *mSphere* 6:e0085120. doi: 10.1128/mSphere.00851-20

Shamsuzzama, L. R., Trabelcy, B., Langier Goncalves, I., Gerchman, Y., and Sapir, A. (2020). Metabolic reconfiguration in *C. elegans* suggests a pathway for widespread sterol Auxotrophy in the animal kingdom. *Curr. Biol.* 30, 3031–3038.e7. doi: 10.1016/j.cub.2020.05.070

Sheremet, A., Jones, G. M., Jarett, J., Bowers, R. M., Bedard, I., Culham, C., et al. (2020). Ecological and genomic analyses of candidate phylum WPS-2 bacteria in an unvegetated soil. *Environ. Microbiol.* 22, 3143–3157. doi: 10.1111/1462-2920.15054

Song, X., Ding, J., Tian, W., Xu, H., Zou, H., and Wang, Z. (2023). Effects of plastisphere on phosphorus availability in freshwater system: critical roles of polymer type and colonizing habitat. *Sci. Total Environ.* 870:161990. doi: 10.1016/j.scitotenv.2023.161990

Stepanović, S., Vuković, D., Dakić, I., Savić, B., and Švabić-Vlahović, M. (2000). A modified microtiter-plate test for quantification of staphylococcal biofilm formation. *J. Microbiol. Methods* 40, 175–179. doi: 10.1016/s0167-7012(00)00122-6

Stepanović, S., Vuković, D., Hola, V., Di Bonaventura, G., Djukić, S., Ćirković, I., et al. (2007). Quantification of biofilm in microtiter plates: overview of testing conditions and practical recommendations for assessment of biofilm production by staphylococci. *APMIS* 115, 891–899. doi: 10.1111/j.1600-0463.2007.apm_630.x

Stubbins, A., Law, K. L., Muñoz, S. E., Bianchi, T. S., and Zhu, L. (2021). Plastics in the earth system. *Science* 373, 51–55. doi: 10.1126/science.abb0354

Vosshage, A. T. L., Neu, T. R., and Gabel, F. (2018). Plastic alters biofilm quality as food resource of the freshwater gastropod Radix balthica. *Environ. Sci. Technol.* 52, 11387–11393. doi: 10.1021/acs.est.8b02470

Wang, Q., Garrity, G. M., Tiedje, J. M., and Cole, J. R. (2007). Naive Bayesian classifier for rapid assignment of rRNA sequences into the new bacterial taxonomy. *Appl. Environ. Microbiol.* 73, 5261–5267. doi: 10.1128/AEM.00062-07

Watkins, L., McGrattan, S., Sullivan, P. J., and Walter, M. T. (2019). The effect of dams on river transport of microplastic pollution. *Sci. Total Environ.* 664, 834–840. doi: 10.1016/j.scitotenv.2019.02.028

Wei, J. H., Yin, X., and Welander, P. V. (2016). Sterol synthesis in diverse Bacteria. *Front. Microbiol.* 7:990. doi: 10.3389/fmicb.2016.00990

Weisburg, W. G., Barns, S. M., Pelletier, D. A., and Lane, D. J. (1991). 16S ribosomal DNA amplification for phylogenetic study. *J. Bacteriol.* 173, 697–703. doi: 10.1128/jb.173.2.697-703.1991

Windler, M., Leinweber, K., Bartulos, C. R., Philipp, B., and Kroth, P. G. (2015). Biofilm and capsule formation of the diatom *Achnanthidium minutissimum* are affected by a bacterium. *J. Phycol.* 51, 343–355. doi: 10.1111/jpy.12280

Wright, R. J., Erni-Cassola, G., Zadjelovic, V., Latva, M., and Christie-Oleza, J. A. (2020). Marine plastic debris: a new surface for microbial colonization. *Environ. Sci. Technol.* 54, 11657–11672. doi: 10.1021/acs.est.0c02305

Yu, Y., Mo, W. Y., and Luukkonen, T. (2021). Adsorption behaviour and interaction of organic micropollutants with nano and microplastics - a review. *Sci. Total Environ.* 797:149140. doi: 10.1016/j.scitotenv.2021.149140

Zecher, K., Hayes, K. R., and Philipp, B. (2020). Evidence of Interdomain ammonium cross-feeding from methylamine- and Glycine betaine-degrading *Rhodobacteraceae* to diatoms as a widespread interaction in the marine Phycosphere. *Front. Microbiol.* 11:533894. doi: 10.3389/fmicb.2020.533894

Zecher, K., Jagmann, N., Seemann, P., and Philipp, B. (2015). An efficient screening method for the isolation of heterotrophic bacteria influencing growth of diatoms under photoautotrophic conditions. *J. Microbiol. Methods* 119, 154–162. doi: 10.1016/j.mimet.2015.10.016

Zhang, Y., Zuo, J., Salimova, A., Li, A., Li, L., and Li, D. (2020). Phytoplankton distribution characteristics and its relationship with bacterioplankton in Dianchi Lake. *Environ. Sci. Pollut. Res.* 27, 40592–40603. doi: 10.1007/s11356-020-10033-6

frontiers | Frontiers in Microbiology

TYPE Original Research
PUBLISHED 23 February 2024
DOI 10.3389/fmicb.2024.1357797

OPEN ACCESS

EDITED BY
Jin Zhou,
Tsinghua University, China

REVIEWED BY
Annette Koenders,
Edith Cowan University, Australia
Ulisse Cardini,
Anton Dohrn Zoological Station Naples, Italy

*CORRESPONDENCE
Ulrich Stingl
✉ ustingl@ufl.edu

RECEIVED 18 December 2023
ACCEPTED 29 January 2024
PUBLISHED 23 February 2024

CITATION
Ugarelli K, Campbell JE, Rhoades OK, Munson CJ, Altieri AH, Douglass JG, Heck KL Jr, Paul VJ, Barry SC, Christ L, Fourqurean JW, Frazer TK, Linhardt ST, Martin CW, McDonald AM, Main VA, Manuel SA, Marco-Méndez C, Reynolds LK, Rodriguez A, Rodriguez Bravo LM, Sawall Y, Smith K, Wied WL, Choi CJ and Stingl U (2024) Microbiomes of *Thalassia testudinum* throughout the Atlantic Ocean, Caribbean Sea, and Gulf of Mexico are influenced by site and region while maintaining a core microbiome. *Front. Microbiol.* 15:1357797. doi: 10.3389/fmicb.2024.1357797

Microbiomes of *Thalassia testudinum* throughout the Atlantic Ocean, Caribbean Sea, and Gulf of Mexico are influenced by site and region while maintaining a core microbiome

Kelly Ugarelli[1], Justin E. Campbell[2,3], O. Kennedy Rhoades[2,3,4], Calvin J. Munson[2,5], Andrew H. Altieri[6,7], James G. Douglass[8], Kenneth L. Heck Jr.[9], Valerie J. Paul[3], Savanna C. Barry[10], Lindsey Christ[11], James W. Fourqurean[2], Thomas K. Frazer[12], Samantha T. Linhardt[9], Charles W. Martin[9,10], Ashley M. McDonald[3,10,13], Vivienne A. Main[3,11], Sarah A. Manuel[14], Candela Marco-Méndez[9,15], Laura K. Reynolds[16], Alex Rodriguez[9], Lucia M. Rodriguez Bravo[17], Yvonne Sawall[18], Khalil Smith[3,14], William L. Wied[2,3], Chang Jae Choi[1] and Ulrich Stingl[1]*

[1]Department of Microbiology and Cell Science, Ft. Lauderdale Research and Education Center, University of Florida, Davie, FL, United States, [2]Department of Biological Sciences, Institute of Environment, Coastlines and Oceans Division, Florida International University, Miami, FL, United States, [3]Smithsonian Marine Station, Fort Pierce, FL, United States, [4]Institute for the Oceans and Fisheries, University of British Columbia, Vancouver, BC, Canada, [5]Department of Ecology and Evolutionary Biology, University of California, Santa Cruz, Santa Cruz, CA, United States, [6]Department of Environmental Engineering Sciences, University of Florida, Gainesville, FL, United States, [7]Smithsonian Tropical Research Institute, Panama City, Panama, [8]The Water School, Florida Gulf Coast University, Fort Myers, FL, United States, [9]Dauphin Island Sea Lab, University of South Alabama, Dauphin Island, AL, United States, [10]University of Florida, Institute of Food and Agricultural Sciences Nature Coast Biological Station, University of Florida, Cedar Key, FL, United States, [11]International Field Studies, Inc., Andros, Bahamas, [12]College of Marine Science, University of South Florida, St. Petersburg, FL, United States, [13]Soil and Water Sciences Department, University of Florida, Gainesville, FL, United States, [14]Department of Environment and Natural Resources, Government of Bermuda, Hamilton Parish, Bermuda, [15]Center for Advanced Studies of Blanes (Spanish National Research Council), Girona, Spain, [16]Soil, Water and Ecosystem Sciences Department, University of Florida, Gainesville, FL, United States, [17]King Abdullah University of Science and Technology, Thuwal, Saudi Arabia, [18]Bermuda Institute of Ocean Sciences (BIOS), St. George's, Bermuda

Plant microbiomes are known to serve several important functions for their host, and it is therefore important to understand their composition as well as the factors that may influence these microbial communities. The microbiome of *Thalassia testudinum* has only recently been explored, and studies to-date have primarily focused on characterizing the microbiome of plants in a single region. Here, we present the first characterization of the composition of the microbial communities of *T. testudinum* across a wide geographical range spanning three distinct regions with varying physicochemical conditions. We collected samples of leaves, roots, sediment, and water from six sites throughout the Atlantic Ocean, Caribbean Sea, and the Gulf of Mexico. We then analyzed these samples using 16S rRNA amplicon sequencing. We found that site and region can influence the microbial communities of *T. testudinum*, while maintaining a plant-associated core microbiome. A comprehensive comparison

of available microbial community data from *T. testudinum* studies determined a core microbiome composed of 14 ASVs that consisted mostly of the family Rhodobacteraceae. The most abundant genera in the microbial communities included organisms with possible plant-beneficial functions, like plant-growth promoting taxa, disease suppressing taxa, and nitrogen fixers.

KEYWORDS

***Thalassia*, seagrass microbiome, amplicon sequencing, Caribbean, seagrass beds, seagrass, core microbiome**

Introduction

Seagrass meadows form ecologically important ecosystems that are at risk due to environmental change (Waycott et al., 2009). They provide food and habitat for marine animals, along with other benefits such as water quality improvement and carbon sequestration (reviewed in Dewsbury et al., 2016). However, many meadows are threatened by various environmental stressors, such as hypersalinity, hypoxia, high temperatures, eutrophication, and disease (Koch et al., 2007a; Barry et al., 2017; Bishop et al., 2017; Ugarelli et al., 2017). Nevertheless, some species exhibit a surprising capacity for resilience (Unsworth et al., 2015). For example, *Thalassia testudinum,* or turtlegrass, one of the most prominent seagrasses in the Caribbean, shows a remarkable ability to adapt to varying sediment conditions and levels of sediment anoxia (Koch et al., 2007b). Furthermore, *T. testudinum* can also adapt to prolonged nutrient stress by changing their metabolism and lipid profile (Koelmel et al., 2019), as well as their photosynthetic efficiency and biomass partitioning (Fourqurean et al., 1992; Lee and Dunton, 2000; Barry et al., 2017).

Distinct microbial communities live on and within the leaves, rhizomes, and roots of seagrasses, and provide distinct benefits to the plant (reviewed in Ugarelli et al., 2017), possibly contributing to physiological stress responses and overall resilience. Oftentimes, stressors that affect seagrasses also affect their microbiome. In *Thalassia* spp., increasing inorganic nitrogen (N) can lead to changes in the microbial communities of the rhizosphere (Zhou et al., 2021), while changes in temperature, light (Vogel et al., 2021b), water depth, and salinity (Vogel et al., 2020) can affect the phyllosphere communities. Microbial communities vary among leaf, root, sediment, and water samples (Cúcio et al., 2016; Fahimipour et al., 2017; Rotini et al., 2017; Crump et al., 2018; Hurtado-McCormick et al., 2019; Banister et al., 2021), potentially due to the distinct micro-environments and the biogeochemical processes occurring at each. For instance, the leaves release dissolved organic carbon and oxygen (Wetzel and Penhale, 1979; Borum et al., 2006) along with other exudates that may select for different microbes compared to seawater communities. The root system also releases dissolved organic carbon and oxygen (Wetzel and Penhale, 1979; Borum et al., 2006) which is especially "selective" in anoxic sediments and alters the redox conditions which influences the microbial community composition (reviewed in Ugarelli et al., 2017). Some of the most common taxa present in the microbiome of seagrasses include nitrogen fixers (reviewed in Ugarelli et al., 2017), sulfate-reducers (some of which can fix nitrogen; Küsel et al., 1999), and sulfide-oxidizers (Ettinger et al., 2017; Martin et al., 2019), all of which can be considered part of a core microbiome and provide benefits to the seagrass host.

A core microbiome can be defined as microbial taxa that are present across multiple samples of the same host species. The way core microbiomes are defined differs across studies, depending on the requirements for inclusion of taxa (i.e., both presence and abundance vs. only presence; Shade and Handelsman, 2012). In some cases, researchers consider the core microbiome to be functional rather than taxonomic, meaning that functional roles can be fulfilled by taxa of different species (e.g., any N-fixer could be considered part of the core microbiome, as long as N fixation is found in all samples of the host species reviewed in Lemanceau et al., 2017; Jones et al., 2019; Neu et al., 2021). In several seagrass studies, despite the differences in microbial community compositions at different locations, indications of core microbiomes exist. The core microbiome in these studies is generally defined as microbes that are present in most samples and is usually classified to family level (Cúcio et al., 2016; Roth-Schulze et al., 2016; Bengtsson et al., 2017; Hurtado-McCormick et al., 2019; Banister et al., 2021; Rotini et al., 2023).

Studies show that the leaf communities resemble the water communities for certain seagrass species, like *Zostera marina* (Fahimipour et al., 2017) and *Halophila stipulacea* (Conte et al., 2021b); however, this is not generally the case in other species like *Halophila ovalis* and *Posidonia australis* (Roth-Schulze et al., 2016), nor *T. testudinum* (Ugarelli et al., 2019; Vogel et al., 2020), where the leaf communities differ distinctly from the water communities. Other species of seagrasses, like *Posidonia oceanica*, have been shown to both have distinct leaf microbial communities from the water communities (Kohn et al., 2020), or similar leaf and water communities (Conte et al., 2021b) depending on the study. Seagrasses are a polyphyletic group of plants (Les et al., 1997), and the differing physiology of each species may be in part responsible for the composition of their microbiomes (Conte et al., 2021b). Not only do microbial communities differ among sample types, but also among sites (Mvungi and Mamboya, 2012; Cúcio et al., 2016; Bengtsson et al., 2017; Banister et al., 2021) that differ in environmental conditions. Moreover, microbial communities have also been shown to vary temporally based on seasons (Korlević et al., 2021) and even time of day (Rotini et al., 2020, reviewed in Conte et al., 2021a). Water temperature, depth, salinity, and phosphate concentrations have all been shown to influence the

microbial communities of *T. testudinum* (Vogel et al., 2020, 2021a). Other environmental factors such as pH (Hassenrück et al., 2015; Banister et al., 2021) and nutrient enhancement via fertilization influence the microbiome of other seagrass species (Wang L. et al., 2020), but these relationships are poorly understood for *T. testudinum*. Furthermore, no comparisons have been made of the microbiome of *T. testudinum* across broader spatial scales (within or across regions, which here we define as distinct bodies of water). Given the breadth of environmental variability of marine water bodies at larger geographic scales, these studies would enhance our understanding of the core microbiome of this seagrass species as well its influence on the physiological responses of *T. testudinum* to environmental conditions. There is only one large scale study available on the seagrass microbiome and it focuses on the leaves, roots, sediment, and water samples of *Z. marina* meadows throughout the world (Fahimipour et al., 2017). They found that the microbiome differs by site and sample type, and they found evidence of a core microbiome, at least in the roots. No such study is available for other seagrass species.

Here, we investigate the compositional microbiome of *T. testudinum* at six sites across three regions that cover a large portion of its geographic range (Phillips and Meñez, 1988): Andros (Bahamas) and Riddell's Bay (Bermuda) in the Atlantic Ocean; Carrie Bow Cay (Belize) and Bocas del Toro (Panama) in the Caribbean Sea; and two sites in Florida, USA (Crystal River and St. Joseph Bay) in the Gulf of Mexico (Figure 1). The objective of this study was to determine whether the microbial communities of *T. testudinum* across a large geographical range differ by site and region, and through comparisons with other studies, to determine if *T. testudinum* exhibits evidence of a leaf core microbiome and what organisms it comprises.

Methods

Site description and sampling methods

Samples of water, sediment, leaves and roots were collected, in that order, from a single seagrass meadow at each of six distinct sites distributed across the Gulf of Mexico and Greater Caribbean: Andros (Bahamas); Carrie Bow Cay (Belize); Riddell's Bay (Bermuda); Crystal River (FL USA); Bocas del Toro (Panama); St. Joseph Bay (FL, USA; Figure 1). These sites were a subset of a larger seagrass network (Campbell et al., 2024), and were collected between the late summer and early fall of 2018. The meadow within each site was selected by adhering to a standardized set of criteria: (1) depth (<3 m); (2) plant community composition (turtlegrass, >50% relative abundance); (3) meadow dimensions (minimum 25 m × 25 m); (4) low wave energy/storm exposure. These sites also represent a range of different sediment types: Andros (Bahamas), Carrie Bow Cay (Belize), and Riddell's Bay (Bermuda) all have high-carbonate sediments, Crystal River (FL, USA) has intermediate-carbonate sediment, Bocas del Toro (Panama) contains mixed carbonate-siliciclastic sediment, and St. Joseph Bay (FL, USA) has siliciclastic, or low-carbonate sediment (as identified in Fourqurean et al., 2023). Each site contained a grid of 50 experimental seagrass plots (each 0.25 m^2) dominated by *T. testudinum*. From these 50 plots, we sampled 10 plots at each site. Five were unmanipulated controls, while the other five received fertilizer amendments via the addition of 300 g of Osmocote (NPK 14-14-14). One of our original goals was to examine the effects of nutrient enrichment on the seagrass microbiome; however, the effectiveness of enrichment (particularly for N) was variable on the plants across our specific subset of sites from the network, and consequently, nutrient treatment did not exhibit any detectable effects on the microbial community composition, except for the alpha diversity of the roots in only one site (Bermuda; Supplementary Table S1). Thus, we grouped both the enriched and unenriched plots within a site to broadly examine regional variation in the seagrass microbiome.

For the seagrass microbial community analysis, a single, healthy-appearing *T. testudinum* shoot (extracted from the base of the shoot and inclusive of a small amount of rhizome) was harvested from the perimeter of each plot, rinsed with seawater to remove loosely attached sediment, and placed in a clean Ziplock bag. In the lab, 3 cm were cut from the basal portion of the epiphyte-free rank 2 leaf (second youngest leaf) with sterile scissors, and three root pieces were also collected with sterile plastic forceps. Adjacent to the location of the harvested shoot, a sterile syringe barrel was used to collect 2.5 ml of sediment from the surface. Three 750 µl samples of water were also collected from the surface per site with a sterile syringe barrel. All samples, including the 750 µl of water, were placed in tubes containing Xpedition Lysis/Stabilization Solution (ZYMO Research) to stabilize DNA until processing.

DNA extractions, amplification, and sequencing

The Zymo Quick-DNA Fecal/Soil Microbe Microprep Kit (ZYMO Research) was used for DNA extraction. Once the DNA was extracted, samples were sent for Illumina MiSeq sequencing of the V4 region of the 16S rRNA gene. Illumina paired-end sequencing was done at the Environmental Sample Preparation and Sequencing Facility at Argonne National Laboratory (Chicago, IL, USA). DNA quantities were standardized by concentrating, diluting, and changing the sample volume to achieve normalization prior to sequencing. Primer set 515F-806R with adapters and barcodes for multiplexing were used. PCRs were run in 25 µl reactions: 9.5 µl of MO BIO PCR Water (Qiagen, Germantown, MD, USA), 12.5 µl of QuantaBio's AccuStart II PCR ToughMix (Quantabio, Beverly, MA, USA; 2 × concentration, 1 × final), 1 µl of forward primer (5 µM concentration, 200 pM final), 1 µl Golay barcode tagged reverse primer (5 µM concentration, 200 pM final), and 1 µl of template DNA. PCR conditions were as follows: initial denaturation at 94°C for 3 min, followed by 35 cycles of 94°C for 45 s, 50°C for 60 s, and 72°C for 90 s, and a final extension of 72°C for 10 min. After amplicons were quantified with PicoGreen (Invitrogen, Eugene, OR, USA) using a plate reader (Infinite® 200 PRO, Tecan, Männedorf, Switzerland), samples were pooled in equimolar amounts and cleaned using AMPure XP Beads (Beckman Coulter, Indianapolis, IN, USA). A Qubit fluorometer (Qubit, Invitrogen, Eugene, OR, USA) was used to quantify the clean sample pool, which was then diluted to 2 nM, denatured,

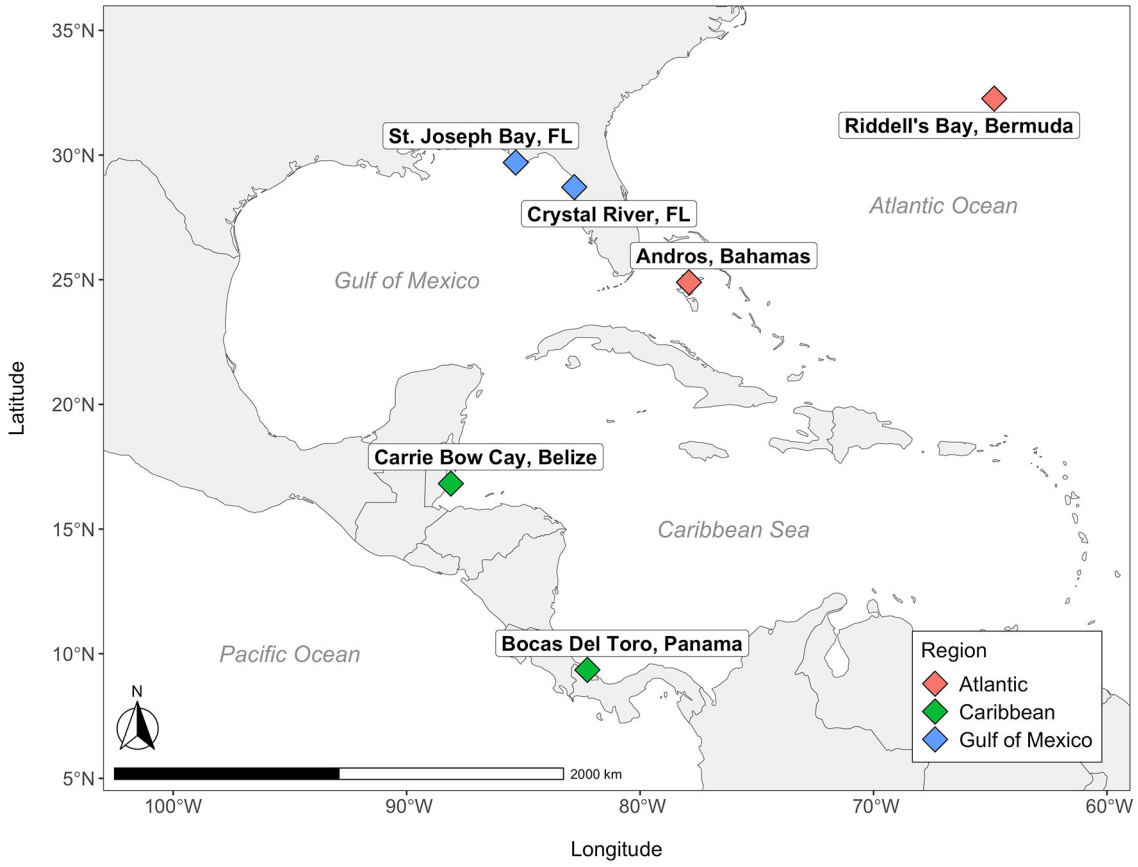

FIGURE 1
Map of seagrass sites. Colors correspond to various regions across the Western Atlantic.

and diluted to 6.75 pM with 10% Phix spiked for Illumina MiSeq sequencing.

Sequence processing

QIIME2 (v 2018.4.0; Bolyen et al., 2019) was used to demultiplex Illumina sequences, and R (v 4.2.1; R Core Team, 2013a) to run DADA2 (Callahan et al., 2016) to process the sequences and assign taxonomy using the SILVA release 132 database (Yilmaz et al., 2014). Amplicon Sequence Variants (99% ASVs) classified as "mitochondria" or "chloroplast" were filtered out of the data using the phyloseq package (McMurdie and Holmes, 2013) in R (v 4.2.1). ASVs with less than two counts in 25% of the samples were removed from the dataset as well. For the core microbiome study with multiple datasets, QIIME2 (v 2022.8) was used for classification using the SILVA release 132 database (Yilmaz et al., 2014). Raw sequences produced in this study are available at the NCBI Sequence Read Archive (accession number PRJNA1019313.

Multi-study data processing

Prior studies that analyzed amplicon sequencing data generated from the same primer set (515F-806R) and that were of similar lengths (~250 bp) were combined with the amplicon sequencing data from this study for the analysis of the core microbiome of *T. testudinum*. Only studies on the *T. testudinum* leaf communities matched our criteria. These studies included Vogel et al. (2020, 2021a,b) and Rodríguez-Barreras et al. (2021). It is also important to note that three studies by Vogel et al. (2020, 2021a,b), used swabs to examine the microbial community of the leaf surface rather than the whole leaf, which might bias the results. The sites included for the comparisons are the six sites of the current study, Taylor Creek and Round Island in the Indian River Lagoon near Ft. Pierce, Florida, USA (Vogel et al., 2021a,b), Apalachee, Florida, USA (Vogel et al., 2020), and Cerro Gordo (Vega Baja, Puerto Rico), Isla de Cabra (Cataño, Puerto Rico), and Mar Azul (Luquillo, Puerto Rico; Rodríguez-Barreras et al., 2021).

Raw sequencing data from the selected studies were downloaded from the SRA archives (PRJNA691349, ERR4556266, ERR4556184, and ERR4556221). The sequence reads for the selected studies were already merged; thus, this study's paired-end reads were merged prior to combining all reads into a single file

for processing. Briefly, the paired-end reads were merged using USEARCH v.11.0.667 (Edgar, 2010). The reads were merged if a ≥50 bp overlap was present, with a maximum of 5% mismatch. Reads with a maximum error rate of >0.001 or shorter than 200 bp were discarded. Primer sequences were trimmed using Cutadapt v.1.13 (Martin, 2011). The quality of the reads was assessed using FastQC v.0.11.8 (Andrews, 2010) and low-quality sequence ends were trimmed at a Phred quality (*Q*) threshold of 25 using a 10 bp sliding window in Sickle 1.33 (Joshi and Fass, 2011). After the removal of single sequence reads (using USEARCH), ASVs were identified using the UNOISE3 algorithm implemented in USEARCH with the default parameters, and an ASV table was generated using the otutab command. Taxonomy for the multi-study data was assigned using the Qiime2 qiime feature-classifier classify-sklearn command. Mitochondria and chloroplasts were filtered out of the dataset using the qiime taxa filter-table command. R (v 4.2.1; R Core Team, 2013a) was then used for further data analysis. The R packages microbiome (Lahti et al., 2017) and phyloseq (McMurdie and Holmes, 2013) were used to extract the core microbiome from the multi-study data set. Previous studies have defined core microbiomes as being present in 50%−100% of the samples, and as low as 30% (Neu et al., 2021). We considered ASVs that had at least two counts in at least 80% of the samples to form the core microbiome to avoid the excluding low abundance taxa, taking into account the wide range that spans between most of the sampling sites.

Data analysis and visualization

R packages phyloseq (McMurdie and Holmes, 2013), ggplot2 (Wickham, 2009), vegan (Oksanen et al., 2018), stats (R Core Team, 2013b), pvclust (Suzuki and Shimodaira, 2006), qiime2R (Bisanz, 2018), tidyverse (Wickham et al., 2019), ape (Paradis and Schliep, 2019), viridis (Garnier et al., 2023), and ggordiplots (Quensen, 2020) were used for data visualization and microbial community analysis and statistics.

After removing outliers from the datasets, permutational multivariate analysis of variance (PERMANOVA) with 9,999 permutations was used to determine significant differences in the alpha-diversity among sites and region using the Chao1 and Shannon diversity metrics (Soriano-Lerma et al., 2020; Aires et al., 2021). Hierarchical clustering of the Euclidean distance matrices was used for analysis of the beta-diversity among the different sample types. Weighted Unifrac Distance Matrices were used for comparisons by sample type through ordination plots. A PERMANOVA analysis of the Bray-Curtis, Euclidean, Jaccard, Unifrac and Weighted Unifrac distance matrices was performed to determine whether there were significant differences in beta diversity by site or region. Factors were neither nested nor crossed as we were interested in the effects of sites and region alone.

To compare the taxonomic composition of microbial communities among sample types, the relative abundance of the top 20 genera were plotted with R (v 4.2.1). ASVs labeled "NA" were filtered out before determining the top 20 most abundant genera but were still considered for relative abundance calculations. The tax_glom function in phyloseq (McMurdie and Holmes, 2013) was used to combine all ASVs by assigned genus and then plotted with the plot_bar function in phyloseq. JMP pro (16.1.0, JMP®) was used for statistical analysis of the relative abundance of each of the top 20 genera by site ($n = 6$) using an analysis of variance (ANOVA) followed by a *post-hoc* Tukey's honest significant difference test ($\alpha = 0.05$) and Bonferroni-adjusted *p*-values to correct for multiple genera.

TABLE 1 PERMANOVA of Chao1 and Shannon diversity indices to compare alpha diversity of microbial communities by sites and region.

Sample-type	Site		Region	
	Chao1	Shannon	Chao1	Shannon
Leaf	0.130	**0.004****	0.143	**0.011***
Root	**0.006****	0.261	**0.002***	**0.045***
Sediment	**0.001****	**0.002****	0.367	0.062
Water	**0.001****	0.092	**0.001****	**0.006***

Bold values and asterisks indicate significant differences.
*$p < 0.05$.
**$p < 0.01$.

Results

Alpha diversity

Shannon diversity indices of leaves and sediment microbial communities differed significantly by site (Table 1). Shannon diversity indices of the leaves, root, and water communities also varied significantly by region. Chao1 diversity of the roots, sediment, and water differed significantly by site, and varied significantly by region for the roots and water (Table 1).

The highest alpha diversity was found in the sediment (average ± standard deviation for Chao1 634.45 ± 149.67 and for Shannon 5.56 ± 0.38; Figure 2). The alpha diversity of the microbial communities of the roots was the second highest (Chao1 398.97 ± 155.56; Shannon 4.71 ± 0.78) followed by the water samples (Chao1 173.61 ± 71.62; Shannon 3.76 ± 0.588) and finally the leaves (Chao1 112.58 ± 97.11; Shannon 3.75 ± 0.77; Figure 2).

Beta diversity

Hierarchical clustering analysis suggested that the microbial communities clustered according to sample type (leaf, root, sediment, water; Supplementary Figure S1). Root and sediment communities always clustered more closely, suggesting more similarities in their microbial communities (Supplementary Figure S1). Leaves and water samples clustered more closely to each other at four of the six sites, while at Crystal River (FL, USA) and Bocas del Toro (Panama), leaves and water samples occurred in different branches in the cluster dendrograms, suggesting fewer similarities in their microbial communities compared to those clustering in the same branches (Supplementary Figure S1).

The beta diversity of the microbial communities of all sample types differed significantly by region and site, with the exception of

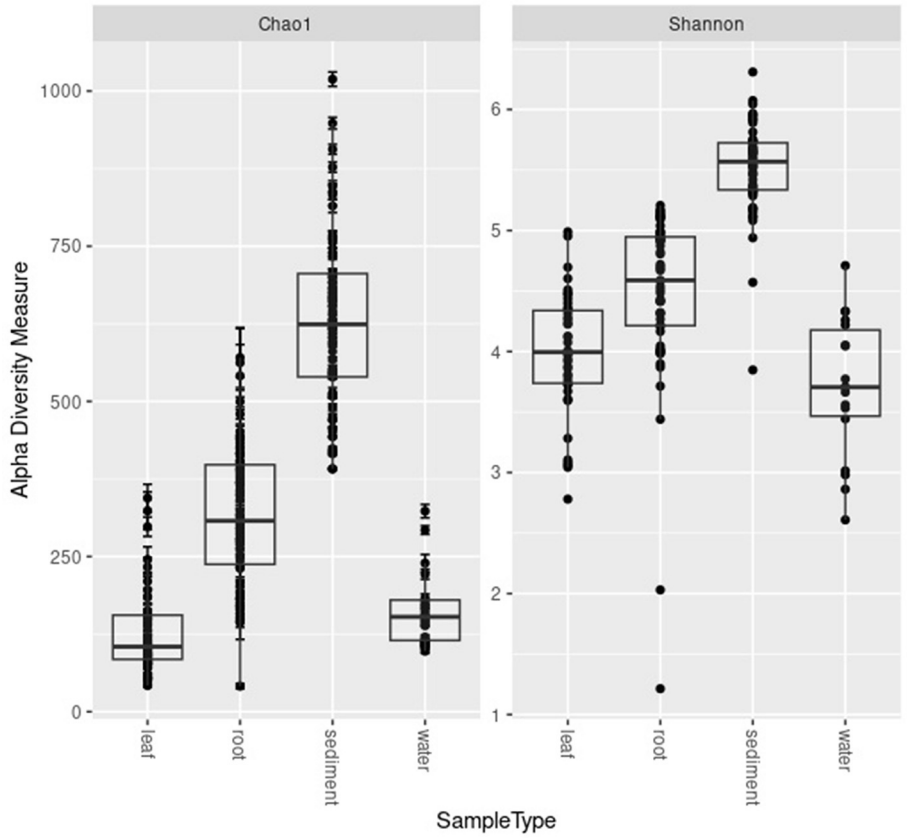

FIGURE 2
Boxplots of Chao1 and Shannon diversity metrics for the microbial communities of the leaves, roots, sediment, and water samples.

water samples, which did not significantly differ by site (Table 2). Using the Weighted Unifrac Distance metric to visualize clustering based on similarities, the sediment and water communities cluster more distinctly by region as compared with plant-associated sample types, with Crystal River (FL, USA) and St. Joseph Bay (FL, USA) being the most distinct, while the remaining sites cluster more closely together (Figure 3). The differences in sediment communities might be driven by region (Gulf of Mexico vs. Atlantic and Caribbean; Figure 3C) as well as site. The water communities seem to cluster mostly by region (Figure 3D) and the Gulf of Mexico water samples were the most distinct, while Caribbean Sea and Atlantic Ocean samples were more similar, but still mostly cluster separately (Figure 3D).

When comparing the Weighted Unifrac distance of the leaves and roots, no clear, distinct clustering by region is apparent as samples mostly cluster together, with slight distinctions by site (Figures 3A, B). Despite differing significantly in several beta diversity metrics (Bray-Curtis, Euclidean, Jaccard, Unifrac, and Weighted Unifrac; Table 2), the clustering from the Weighted Unifrac distance metric suggests that some similarity still occurs among the microbial communities of all sites when considering both the presence and the abundance of taxa in the leaves and in the roots, suggesting a core microbiome is present.

Multi-study community analysis and core microbiome

The Weighted Unifrac distance metric of the leaf communities of all included studies (Vogel et al., 2020, 2021a,b; Rodríguez-Barreras et al., 2021) were similar in most field collected samples, with the exception of the Apalachee, Florida samples (Vogel et al., 2020), which form a distinct cluster (Figure 4). The study on *T. testudinum* plants that were transplanted into aquaria from the Indian River Lagoon are separated into two clusters: one that is closely similar to the microbiome of most field collected samples and one that forms a more distinct cluster (Vogel et al., 2021a). It is possible that the former are the samples that were taken after 10 days of acclimation, while the latter are the ones taken at the end of the 30-day experiment, resulting in an altered surface microbiome (Vogel et al., 2021a).

There were 14 ASVs that comprised the core microbiome (Supplementary Table S2). Three of these were classified to genus level, including *Labrenzia, Rhodovulum, Methylotenera*, and one was classified to species: *Hirschia maritima*. The remaining ASVs were only classified to family level: Rhodobacteraceae (eight ASVs), Halieaceae, and Hyphomonadaceae (two ASVs; Supplementary Table S2). All core microbiome ASVs were present in all studies except for four ASV (belonging to the

TABLE 2 PERMANOVA results for the comparison of the Bray-Curtis, Euclidean, and Jaccard beta diversity metrics of the microbial communities of the leaves, roots, sediment, and water samples.

Sample type	Bray-Curtis	Euclidean	Unifrac	Weighted unifrac	Jaccard
Site					
Leaf	0.0001***	0.0001***	0.0001***	0.0001***	0.0001***
Root	0.0001***	0.0001***	0.0001***	0.0001***	0.0001***
Sediment	0.0001***	0.0001***	0.0001***	0.0001***	0.0001***
Water	0.0001***	0.085****	0.0001***	0.0001***	0.0001***
Region					
Leaf	0.0001***	0.0005***	0.0001***	0.0001***	0.0001***
Root	0.0001***	0.0001***	0.0001***	0.0001***	0.0001***
Sediment	0.0001***	0.0001***	0.0001***	0.0001***	0.0001***
Water	0.0001***	0.0124*	0.0002***	0.0001***	0.0001***

*$p < 0.05$.
***$p < 0.001$.
****$p < 0.1$.

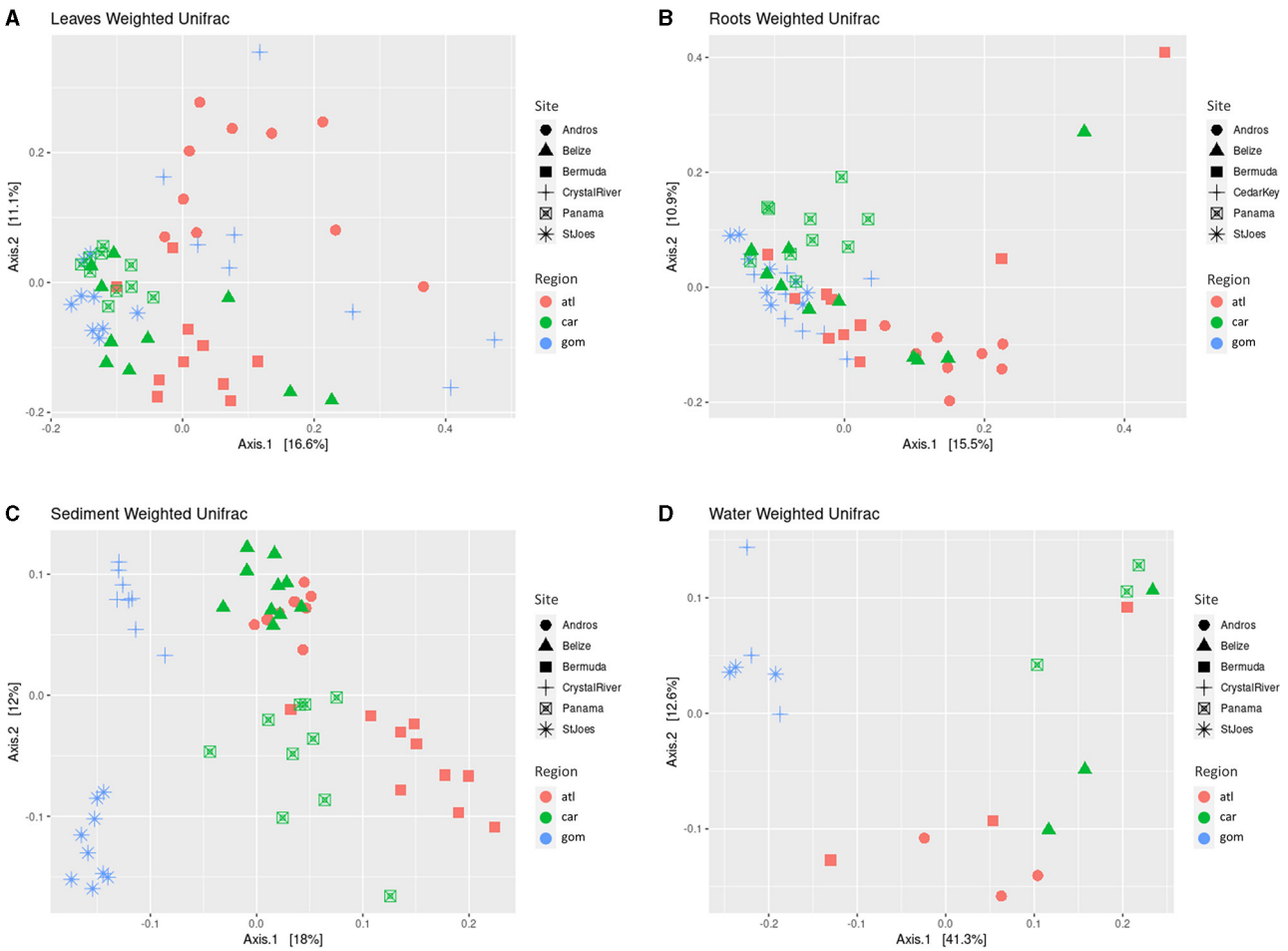

FIGURE 3
Principal coordinate analysis (PCoA) of weighted Unifrac distance matrices of the microbial communities of the leaves **(A)**, roots **(B)**, sediments **(C)**, and water samples **(D)**. Shapes depict sites. Colors indicate region. atl, Atlantic Ocean; car, Caribbean Sea; gom, Gulf of Mexico. Belize, Carrie Bow Cay (Belize); Bermuda, Riddell's Bay (Bermuda); Panama, Bocas del Toro (Panama); StJoes, St. Joseph Bay (FL, USA).

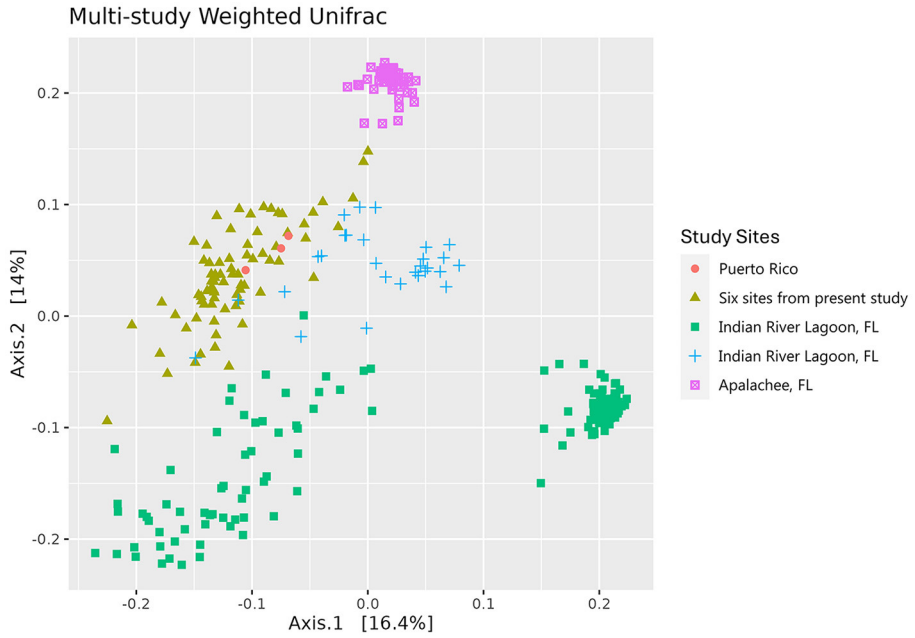

FIGURE 4
Principal coordinate analysis (PCoA) of the weighted Unifrac distance matrices of the microbial communities of the leaves of *Thalassia testudinum* from multiple studies. Colors and shapes indicate the sites covered by different studies: peach circles = Puerto Rico (Rodríguez-Barreras et al., 2021), mustard triangles = Andros, St. Joseph Bay, Crystal River, Riddell's Bay, Bocas del Toro, Carrie Bow Cay (present study), green squares = Indian River Lagoon, FL (Vogel et al., 2021a), blue crosses = Indian River Lagoon, FL (Vogel et al., 2021b), magenta square saltires = Apalachee, FL (Vogel et al., 2020).

family Rhodobacteraceae) that were absent in Rodríguez-Barreras et al. (2021) (Zotu152, Zotu16, Zotu343, Zotu99). ASV Zotu78 had the highest average relative abundance (0.4%−8.7%) within the core microbiome, while Zotu343 had the lowest (0–0.58%, Supplementary Table S2). In general, most ASVs in the core microbiome belong to the family Rhodobacteraceae (eight ASVs), while a few belong to Hyphomonadaceae (three ASVs). The remaining taxa of the core microbiome only had one ASV in the families Stappiaceae, Halieaceae, and Methylophilaceae. The sequences for these ASVs are available in the Supplementary material.

Abundant taxa

The relative abundance of the top 20 genera per sample type (leaves, roots, sediment, and water) are shown in Figure 4. Several genera were abundant in more than one sample type, including *Delftia* in all sample types; *Vibrio* in the leaves and water; *Desulfatiglans, Desulfatitalea, Desulfococcus, Desulfosarcina, Sediminispirochaeta, SEEP-SRB1, Spirochaeta 2, Subgroup 23,* and *Sva0081* in the roots and sediment; and *Herbasipillum* in the sediment and water (Figure 5, Supplementary Tables S3–S6). The most abundant genera seem to be present in most samples within each sample type and have differential prevalence among the sites.

Leaves

The leaf communities were similar among sites, with 13 of the top 20 genera present in all sites, except for seven genera: *Celeribacter* [absent in Carrie Bow Cay (Belize) and Bocas del Toro (Panama)], *Lentilitoribacter* [absent in Andros (Bahamas) and Crystal River (FL, USA)], *Pelagibacterium* [absent in Bocas del Toro (Panama)], *Rivularia_PCC-7116* [absent in Riddell's Bay (Bermuda), Crystal River (FL, USA), Bocas del Toro (Panama), and St. Joseph Bay (FL, USA)], and *OM27_clade*, *Thalassobius,* and *Tropicibacter* [absent in Crystal River (FL, USA); Figure 5A, Supplementary Table S3]. Several genera were significantly more abundant in certain sites: *Candidatus* Endobugula in Carrie Bow Cay (Belize), Bocas del Toro (Panama), and St. Joseph Bay (FL, USA; $p = 0.002$); *Celericabter* and *Lentilitoribacter* in Riddell's Bay (Bermuda; $p = 0.004$ and $p = 0.018$, respectively); *Marinagarivorans* in Bocas del Toro (Panama; $p = 0.002$); *Methylotenera* and *OM27_clade* in St. Joseph Bay (FL, USA; $p = 0.002$ for both), and *Oceanicella* in Andros (Bahamas; $p = 0.046$). The remaining genera had no significant differences in their relative abundance by site.

Roots

The root communities were similar with most of the top 20 genera present in all sites except for *Thalassospira*, which was only present in Carrie Bow Cay (Belize) and St. Joseph Bay (FL, USA; Figure 5B, Supplementary Table S4). Seven of the 20 genera differed significantly in their relative abundance between sites.

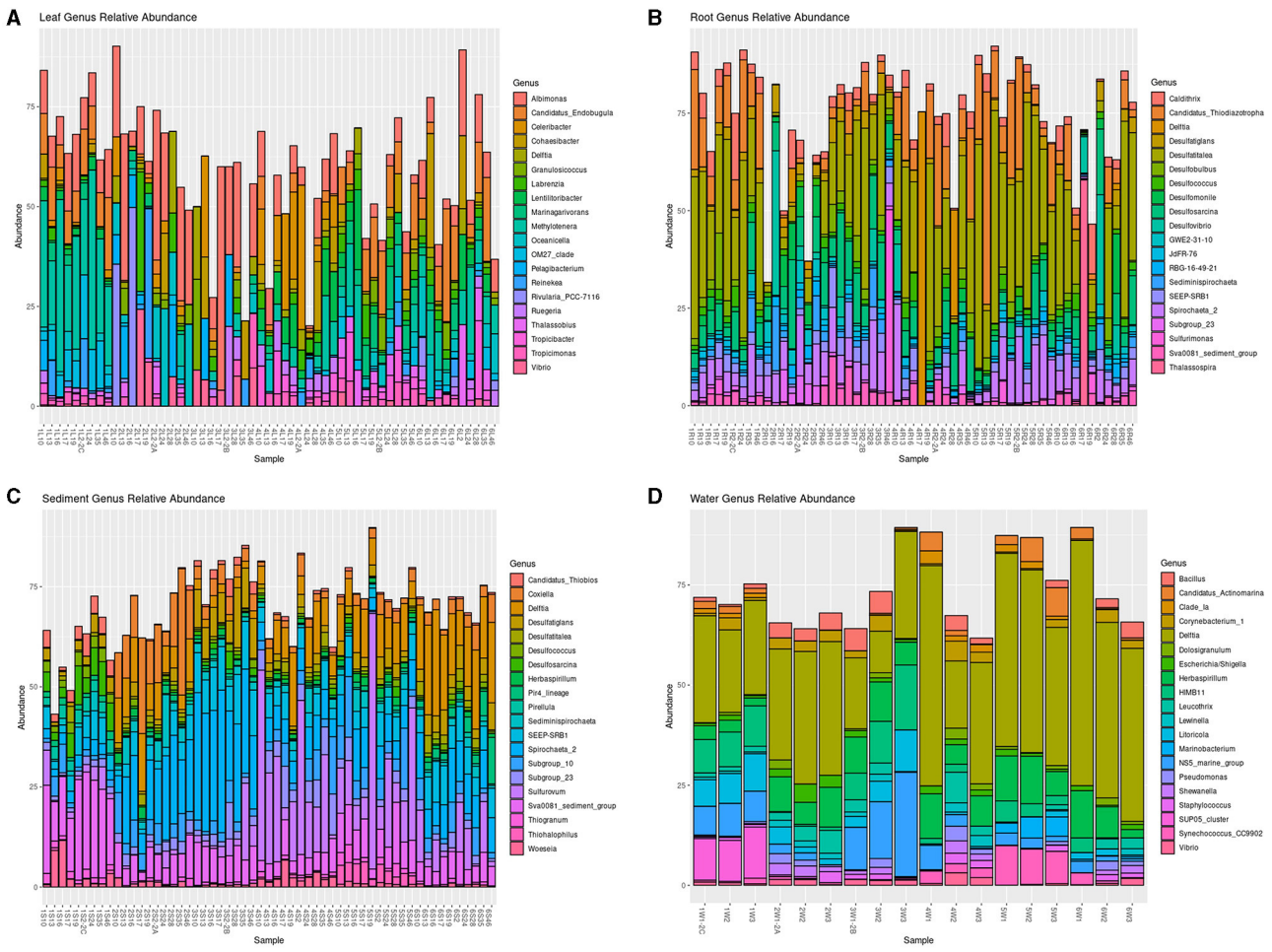

FIGURE 5
Top 20 most abundant taxa of the microbial communities of the leaves **(A)**, roots **(B)**, sediment **(C)**, and water **(D)** samples. Genera labeled NA were filtered out of dataset. Sample names that start with 1 are St. Joseph Bay, 2 Andros, 3 Crystal River, 4 Riddell's Bay, 5 Bocas del Toro, and 6 Carrie Bow Cay.

Candidatus Thiodiazotropha was significantly more abundant in Bocas del Toro (Panama) than in the other sites ($p = 0.016$); *Desulfatitalea* was significantly more abundant in Bocas del Toro (Panama) and St. Joseph Bay (FL, USA; $p = 0.01$); *GWE2-31-10, RBG-16-49-21,* and *Subgroup_23* were significantly more abundant in Andros (Bahamas; $p = 0.024$, $p = 0.002$, and $p = 0.002$, respectively); *SEEP-SRB1* and *Sva0081_sediment_group* were significantly more abundant in Crystal River (FL, USA; $p = 0.002$, for both; Supplementary Table S4).

Sediment

All top 20 genera except for one genus, *Thiohalophilus* (absent in Crystal River), were present in all sites (Figure 5C; Supplementary Table S5). All but two genera, *Sediminispirochaeta* and *Subgroup_10*, differed significantly in their abundance by site (Supplementary Table S5). *Candidatus*_Thiobios is significantly more abundant in St. Joseph Bay (FL, USA), followed by Crystal River (FL, USA; $p = 0.002$); *Coxiella* in Andros (Bahamas; $p = 0.002$); *Delftia* in Carrie Bow Cay (Belize), followed by Andros (Bahamas), Riddell's Bay (Bermuda) and Bocas del Toro (Panama; $p = 0.002$); *Desulfococcus* and *Desulfosarcina* in St. Joseph Bay (FL, USA; $p = 0.002$ for both); *Herbaspirillum, Thiogranum,* and *Thiohalophilus* in Bocas del Toro (Panama; $p = 0.002$ for all); *Pir4_lineage* in Belize ($p = 0.002$); *Pirellula, Sva0081_sediment_group,* and *Woeseia* in St. Joseph Bay (FL, USA; $p = 0.002$); *SEEP-SRB1* and *Spirochaeta_2* in Crystal River (FL, USA; $p = 0.002$ for both); *Subgroup_23* and *Sulfurovum* in Riddell's Bay (Bermuda; $p = 0.002$ and $p = 0.008$, respectively; Supplementary Table S5).

Water

Water communities were similar between sites with 16 of the top 20 genera present in all sites. *Candidatus*_Actinomarina and *Clade_Ia* were absent in Andros (Bahamas); *Marinobacterium* was absent in Andros (Bahamas), Riddell's Bay (Bermuda), and St. Joseph Bay (FL, USA); and *SUP05_cluster* was only present in Crystal River (FL, USA; Figure 5D; Supplementary Table S6). Seven of the top 20 genera differed significantly by site: *Clade_Ia* was

significantly more abundant in Riddell's Bay (Bermuda) and Bocas del Toro (Panama; $p = 0.008$); *HIMB11* and *NS5_marine_group* in Crystal River (FL, USA; $p = 0.006$ and $p = 0.026$, respectively); *Litoricola* and *SUP05_cluster* in St. Joseph Bay (FL, USA; $p = 0.028$ and $p = 0.002$, respectively); and *Marinobacterium* and *Synechococcus_CC9902* in Bocas del Toro (Panama; $p = 0.002$ for both; Supplementary Table S6).

Discussion

Microbial communities by site and region

The microbial communities of *T. testudinum* in this study differ by sample type (water, sediment, leaves, roots) with high similarities between sediment and roots and partially between the leaves and the water samples. Significant differences in the microbial communities between sites, both in alpha and beta diversity, were also observed. Several studies on various seagrass species corroborate these results (Cúcio et al., 2016; Fahimipour et al., 2017; Rotini et al., 2017; Crump et al., 2018; Hurtado-McCormick et al., 2019; Ugarelli et al., 2019). Our data also indicate that the microbial communities differ by region (i.e., Atlantic Ocean, Caribbean Sea, or Gulf of Mexico), with alpha and beta diversities differing significantly for all sample types; however, the weighted Unifrac distances of the leaf and root communities do not show distinct clustering, suggesting that the plant-associated microbial communities of *T. testudinum* share some, although not statistically significant similarities between regions (Figure 3; Tables 1, 2). This further suggests that a core microbiome is present at least in the leaves and root samples. Water and sediment samples show more apparent clustering by region, suggesting a clearer distinction in the microbial communities of the surrounding environments. Interestingly, sediment communities were impacted by region only under the Shannon diversity metric (i.e., richness and evenness) and not the Chao1 metric (i.e., richness), suggesting that species evenness, rather than richness, is driving the differences in the sediment microbial communities (Table 1). The significant differences in the microbial communities between regions is likely due to the diverse physicochemical parameters at each location (e.g., pH, salinities, nutrient levels of the water and sediment), which have been shown to affect the communities of seagrasses in other studies (Hassenrück et al., 2015; Vogel et al., 2020, 2021a; Wang L. et al., 2020; Banister et al., 2021). Furthermore, evidence suggests that the microbial communities of seagrasses can differ temporally by season (Korlević et al., 2021) as well as time of day (Rotini et al., 2020; reviewed in Conte et al., 2021a). Because the samples collected from each site at each region were not collected on the same day nor at exactly the same time of day, we cannot exclude that the differences in the microbiomes can also be due to temporal variations.

Previous studies have shown that sediment lithology can influence the microbial communities of sediments throughout various aquatic systems, including marine (Hoshino et al., 2020), deep Arctic (Kanzog and Ramette, 2009), rivers (Wang et al., 2016), and lagoons (Obi et al., 2016; Aldeguer-Riquelme et al., 2022), possibly due to the composition of organic matter. In seagrass meadows, several factors were shown to significantly impact the microbial communities of the sediments, including carbon (C) to N ratios as well as a combination of total inorganic C, total organic C, dissolved oxygen, pH, and seagrass density (*Z. marina,* Ettinger et al., 2017), in addition to location, plant nutrient composition, sediment composition (e.g., moderate-fine sandy soil and silt-sandy soil), and sediment grain size (*T. hemprichii*, *Enhalus acoroides*, or a mix of both) (Zhang et al., 2020, 2022). Despite their importance in determining the microbial communities of sediments in seagrass meadows, few studies have evaluated the impact of sediment parameters on seagrass-associated microbiomes. In the present study, there were three sites with high carbonate sediment, and one site for the intermediate carbonate, mixed carbonate, and low carbonate (siliciclastic) sediment types. Although the sample size was not large enough to examine the effects of sediment type on the microbial communities of *T. testudinum*, it is also possible that this factor played a role in shaping the microbial communities (Supplementary Figure S2). More sampling sites for each sediment type would provide a better scope of the effects of sediment composition on the *T. testudinum* microbiome.

Core microbiome across regions and studies

To date, the only large-scale study on the microbiome associated with the leaves, roots, sediment, and water samples reports on *Z. marina* meadows; this study covers most of its geographical range, which is more extensive than the range of *T. testudinum* (Fahimipour et al., 2017). No such study is available for other seagrass species. Fahimipour et al. (2017) found that the microbiome differed by site and sample type, and they found evidence of a core microbiome, at least on the roots. The authors also found more distinct differences in their leaf communities and that the communities of the leaves were similar to that of the water. This is not generally the case in other species like *H. ovalis* and *P. australis* (Roth-Schulze et al., 2016), nor *T. testudinum* (Ugarelli et al., 2019; Vogel et al., 2020), where the leaf communities differ clearly from the water communities. This indicates a strong distinction between the microbiome composition of the two seagrass species, where it seems that *T. testudinum* has a more defined leaf-associated core microbiome in most of its geographical range. Aires et al. (2021) also suggests a more distinct core microbiome in *T. testudinum* compared to *H. stipulacea* and *H. wrightii* in the Caribbean Sea.

In the present study, while the microbial communities of all sample types differed significantly, Weighted Unifrac PCoA plots show some similarities in microbial community compositions of the leaves and roots across regions (Figure 3). This indicates that, although the microbial communities significantly differ between sites in presence-absence and abundances, a core microbiome composed of similar taxa is likely still present in *T. testudinum* plants across the three regions. Indications of core microbiomes have also been found in other seagrass studies on various species (Cúcio et al., 2016; Bengtsson et al., 2017; Hurtado-McCormick et al., 2019; Vogel et al., 2020), and it has been suggested that seagrasses might actually select for a core microbiome (Roth-Schulze et al., 2016; Kardish and Stachowicz, 2021). The concept

of the core microbiome ties in with the holobiont concept, which suggests that plants and their microbial communities act as one functional unit to ensure the survival of the whole system (Lemanceau et al., 2017; Jones et al., 2019). For example, in *Agarophyton* seaweed, surface metabolites were shown to deter pathogens while attracting microbes with a potential to protect against disease, i.e., host and microbes work together to prevent disease, ultimately benefiting the holobiont (Saha and Weinberger, 2019). The core microbiome is usually defined as microbial taxa that are present in the microbial communities of several members of the same species and are not necessarily abundant (Lundberg et al., 2012; Neu et al., 2021). In general, studies have defined core microbiomes as being present in 50%−100% of the samples, and as low as 30% (Neu et al., 2021). However, most studies require OTUs to be present in 100% of the samples, which can risk the exclusion of low-abundance taxa that can be of importance (Neu et al., 2021). For our purposes, we defined the leaf core microbiome as taxa that were present in at least 80% of the samples to avoid the exclusion of low abundance taxa, especially because of the wide range that spans between most of the sampling sites. It is debated whether core microbiomes are functional, meaning different taxa serve the same function in the community across different plants of the same species, or taxonomical, meaning the same taxa are present to serve the same function in plants of the same species (Lemanceau et al., 2017; Jones et al., 2019; Neu et al., 2021). In this study, it seems likely that the core microbiome of *T. testudinum* across the Caribbean might be in part taxonomical as well as functional.

The results of this study are unique in that they suggest similarities in the microbial communities of plant associated microbes at the genus level throughout a wide geographical range of *T. testudinum* that includes sites that are thousands of kilometers apart, while other studies usually focus on shorter ranges (e.g., Vogel et al., 2020, 2021b; Aires et al., 2021). Combining the amplicon data that is available from *T. testudinum* studies allows a better investigation of the plant associated core microbiome of *T. testudinum*. After combining our amplicon data with amplicon data that are similar in sequence length and were generated with the same primers used in this study (Vogel et al., 2020, 2021a,b; Rodríguez-Barreras et al., 2021), we found strong similarities in field collected *T. testudinum* leaf microbiomes, suggesting a leaf core microbiome exists in *T. testudinum*. This is important because it suggests that *T. testudinum* houses a core microbiome that is widespread throughout most of its geographical range, and possibly even all of its range, at least in the phyllosphere communities.

The multi-study core microbiome consisted of 14 ASVs, which is within the range of prior core microbiome studies [21 ASVs in Vogel et al., 2020 (*T. testudinum*), six ASVs in Hurtado-McCormick et al., 2019 (*Z. muelleri*), and 14 ASVs in Bengtsson et al., 2017 (*Z. marina*)] but at a much wider geographical span than previous studies. Out of the 14 core ASVs, 8 ASVs are in the family Rhodobacteraceae, which is known to produce secondary metabolites that have antimicrobial, quorum sensing, and iron chelating functions (Henriksen et al., 2022). This family also contains purple non-sulfur bacteria and has members that are involved with the biogeochemical cycles of sulfur and carbon (Pujalte et al., 2014). Rhodobacteraceae have also been found in other seagrass species as part of the core microbiome, such as *T. hemprichii* (Rotini et al., 2020), *Z. muelleri* (Hurtado-McCormick et al., 2020), and *Z. marina* (Bengtsson et al., 2017). In the core microbiome of *T. testudinum*, we also found three ASVs in the family Hyphomonadaceae. This family is composed of prosthecate bacteria that produce a polysaccharide-based adhesin that allows for primary colonization of surfaces and biofilm formation (Abraham and Rohde, 2014; Oberbeckmann et al., 2018). Hyphomonadaceae were found as part of the core microbiome of the leaves of *T. hemprichii* (Rotini et al., 2020). The core microbiome also included one ASV in the family Stappiaceae, one in Halieaceae, and one in Methylophilaceae. Certain genera within Stappiaceae, such as *Stappia*, can oxidize carbon monoxide (Weber and King, 2007), and the family has been found associated with *H. stipulaceae* roots (Conte et al., 2023). Halieaceae have been previously found in *Cymodocea nodosa* sediments (Markovski et al., 2022), but not on the leaves. This family includes genera involved with photoheterotrophy (Spring et al., 2015). Finally, Methylophilaceae was also found as part of the leaf core microbiome of *Z. marina* (Bengtsson et al., 2017; Adamczyk et al., 2022), and are known as methylotrophs, capable of using methanol and methylamine as energy sources (Doronina et al., 2014).

Although this study was able to compare the leaf microbiome data from four previous studies, several other *T. testudinum* leaf and root microbiome data exist, but the methods employed for sampling and data processing differed from this study and were therefore not included in the multi-study core microbiome analysis. Without standardized sampling and data processing methods, proper data comparisons are difficult. Furthermore, to have a better scope of the composition of the core microbiome of *T. testudinum*, more sampling locations should be included for the leaves and similar studies should also be performed on the roots when more comparable data is available. With a more defined core microbiome, these studies can later lead to investigating the functions that the core microbiome serves on *T. testudinum* and possibly ways to monitor the health of seagrass meadows.

Abundant taxa include genera with potentially beneficial functions for the host

In general, several genera with potentially important functions were abundant in the microbiome of *T. testudinum* throughout all our sampling locations. Nitrogen fixers such as *Delftia* (Agafonova et al., 2017) were found in all sample types. Other N-fixers were found only in certain sample types, such as *Candidatus* Thiodiazotropha (Petersen et al., 2016) in the roots, *Herbaspirillum* (Ureta et al., 1995), in the water and sediment samples, and *Desulfatitalea* (Rolando et al., 2022) in the roots and sediment. *Candidatus* Thiodiazotropha not only fixes N but can also oxidize sulfur (Rolando et al., 2022). In other seagrass species, such as *H. ovalis*, *Candidatus* Thiodiazotropha was associated with stressed plant roots (Martin et al., 2019) and this genus is also commonly found in lucinid bivalves that are associated with seagrasses (König et al., 2016). Interestingly, our findings show that *Candidatus* Thiodiazotropha was significantly less abundant

on the roots of Andros (Bahamas), where the leaf N:P ratios were significantly higher than the other sites (Fourqurean et al., 2023; Supplementary Table S4). It is possible that this genus is less prevalent at this site because the plants have more nitrogen relative to phosphorus (P) in their leaves and likely more P-limited relative to other sites. A similar case might be true for *Desulfatitalea,* which is both an N fixer and a sulfate reducer (Higashioka et al., 2013; Rolando et al., 2022) and was significantly less abundant in the roots of Andros (Bahamas) compared to the roots of Bocas del Toro (Panama) and St. Joseph Bay (FL, USA), and relatively less abundant than the remaining sites (Supplementary Table S4). This genus was found in the roots of *T. testudinum* in previous studies (Aires et al., 2021), and in other seagrasses and saltwater plants, such as *H. wrightii* and *H. stipulacea* (Aires et al., 2021), and *Spartina alterniflora* (Rolando et al., 2022).

Other abundant taxa with potential benefits for *T. testudinum* include *Delftia*, which can promote plant growth, antagonize pathogens, and fix N (Agafonova et al., 2017), and was present in all sample types (Figure 5). *Labrenzia* displayed antimicrobial activity against bacteria and fungi (Amiri Moghaddam et al., 2018; Raj Sharma et al., 2019), can form biofilms (Zaynab et al., 2021), and was present in the leaves of all the sites. *Celeribacter*, which is known to contain genes for import and export of C, N, P, and sulfur (S) (Wang X. et al., 2020) and potentially provides some of these nutrients to the plant, was present in the leaves of all sites, except for the Caribbean Sea sites (Supplementary Table S3). *Celeribacter* was previously detected in *H. stipulacea* and *T. testudinum* (Aires et al., 2021) as well. *Candidatus* Endobugula was most abundant in the leaves of the Caribbean Sea sites and in St. Joseph Bay (FL, USA) (Supplementary Table S3), and, in bryozoans, are known to produce bryostatins and polyketides, which have been shown to chemically deter fish from eating their larvae (Davidson et al., 2001; Lim and Haygood, 2004; Lopanik et al., 2004). *Ruegeria* was also prevalent in the leaves of all sites and has previously been associated with possibly producing probiotics for coral (Kitamura et al., 2021), containing algicidal properties (Riclea et al., 2012), and has previously been found in seagrasses (Weidner et al., 2000). In the root samples, *JdFR-76* has been correlated with suppression of root rot disease in oil palms (Goh et al., 2020), and possibly can also aids in disease suppression for *T. testudinum*. Several sulfur oxidizers were also present in the roots of *T. testudinum* including *Candidatus* Thiodiazotropha, *Spirochaeta 2* (Dubinina et al., 2011), and *Sulfurimonas*, which has been linked with seagrass rhizospheres in *Enhaulus acoroides* (Zhang et al., 2022). Sulfur oxidizers can potentially help seagrasses withstand sulfide, which is toxic to plants, by oxidizing it to sulfate (reviewed in Ugarelli et al., 2017).

Within the top 20 most abundant taxa, there were also taxa that can be associated with diseases in marine flora and fauna, and possible common human pathogenic genera in the water samples. In the leaves, some of these genera include *Cohaesibacter,* associated with stony coral tissue loss disease (Rosales et al., 2020), *Granulosicoccus*, associated with black/purple tissue in *Z. muelleri* (Hurtado-McCormick et al., 2020), and *Thalassobius*, associated with lobster epizootic shell disease (Quinn et al., 2012). In the roots, *SEEP-SRB1* and *Desulfomonile* have been previously linked to stressed *H. ovalis* roots (Martin et al., 2020) and are known as sulfate reducers. Other sulfate reducers found in the roots of *T. testudinum* include *Desulfatiglans* (Galushko and Kuever, 2019), *Desulfobulbus* (Higashioka et al., 2013), *Desulfococcus* (Bridge et al., 1999), *Desulfosarcina* (Kleindienst et al., 2014), and *Desulfovibrio* (Price et al., 2014). The water samples contained taxa that can be associated with human pathogens, including *Corynebacterium, Escherichia/Shigella,* and *Staphylococcus*. Further information on the possible functions and/or interesting facts of the top 20 most abundant taxa can be found in Supplementary Table S7.

Conclusion

In conclusion, this study shows that *T. testudinum* microbiomes significantly differ across a large geographical range by site and region, and that potentially beneficial taxa are present in their microbiomes. Most importantly, this study shows that *T. testudinum* shares a leaf core microbiome that is present, not only in these six sites and three regions, but also in other studies that included sites in Taylor Creek and Round Island in the Indian River Lagoon near Ft. Pierce, Florida, USA (Vogel et al., 2021a,b), Apalachee, Florida, USA (Vogel et al., 2020), and Cerro Gordo in Vega Baja, Puerto Rico, Isla de Cabra in Cataño, Puerto Rico, and Mar Azul in Luquillo, Puerto Rico (Rodríguez-Barreras et al., 2021). Knowing the composition of the core microbiome of *T. testudinum* can provide us with a tool that we can use to monitor seagrass health by determining patterns of changes in the core microbiome composition of stressed vs. healthy plants.

Data availability statement

The data presented in the study were deposited in the NCBI Sequence Read Archive repository, accession number PRJNA1019313.

Author contributions

KU: Writing – review & editing, Data curation, Formal analysis, Visualization, Writing – original draft. JC: Writing – review & editing, Conceptualization, Funding acquisition, Methodology, Resources, Supervision. OR: Resources, Writing – review & editing. CJM: Resources, Writing – review & editing. AA: Resources, Writing – review & editing. JD: Resources, Writing – review & editing. KH: Resources, Writing – review & editing. VP: Resources, Writing – review & editing. SB: Resources, Writing – review & editing. LC: Resources, Writing – review & editing. JF: Resources, Writing – review & editing. TF: Writing – review & editing. SL: Writing – review & editing, Resources. CWM: Resources, Writing – review & editing. AM: Resources, Writing – review & editing. VM: Resources, Writing – review & editing. SM: Resources, Writing – review & editing. CM-M: Resources, Writing – review & editing. LKR: Resources, Writing – review & editing, Supervision. AR: Resources, Writing – review & editing. LMR: Resources, Writing – review & editing. YS: Resources, Writing – review & editing. KS: Resources, Writing – review & editing. WW: Resources, Writing – review & editing. CC: Investigation, Methodology, Visualization, Writing – review & editing, Data curation, Formal

analysis. US: Writing – review & editing, Conceptualization, Project administration, Resources, Supervision.

Funding

The author(s) declare financial support was received for the research, authorship, and/or publication of this article. This work was supported by the US National Science Foundation (OCE-1737247 to JC, AA, and VP, OCE-2019022 to JC, OCE-1737144 to KH, and OCE-1737116 to JD).

Acknowledgments

This work would not have been possible without the support of numerous technicians, students and volunteers who assisted in the field work associated with this project. Aaron John, Anna Safryghin, Jade Reinhart, Kasia Malinowski, Laura Woodlee, Matthew Speegle, Michael England, Sam Glew, and Trinitti Leon at the Andros site. Scott Alford, Theresa Gruninger, Audrey Looby, Cayla Sullivan, Sawyer Downey, Whitney Scheffel, Jamila Roth, and Tim Jones at the Crystal River site. This work was conducted under the following permits: at Belize under permit #0004-18 issued by the Belize Fisheries Department; at Panama under permit #s SE/AP-23-17 and SE/AO-1-19 issued by the Ministerio de Ambiente de la Republica de Panama; at Andros by permits issued by the Bahamas National Trust and the Bahamas Environment, Science and Technology Commission. This is contribution #1686 from the Coastlines and Oceans Division of the Institute of Environment at Florida International University.

Conflict of interest

LC and VM were employed by International Field Studies, Inc.

The remaining authors declare that the research was conducted in the absence of any commercial or financial relationships that could be construed as a potential conflict of interest.

The author(s) declared that they were an editorial board member of Frontiers, at the time of submission. This had no impact on the peer review process and the final decision.

Publisher's note

Supplementary material

The Supplementary Material for this article can be found online at: https://www.frontiersin.org/articles/10.3389/fmicb.2024.1357797/full#supplementary-material

SUPPLEMENTARY FIGURE S1
Cluster Dendrogram of the Euclidean distance matrices of the microbial communities of the leaf, root, sediment, and water samples of each site. Sediment is orange, roots are brown, water is blue, and leaves are green.

SUPPLEMENTARY FIGURE S2
Principal coordinate analysis (PCoA) of weighted Unifrac distance matrices of the microbial communities of the leaves **(A)**, roots **(B)**, sediments **(C)** and water samples **(D)**. Shapes depict sites. Colors indicate sediment-type. atl, Atlantic Ocean; car, Caribbean Sea; gom, Gulf of Mexico. H-carb, high carbonate; I-carb, intermediate carbonate; L-carb_sil, low carbonate (siliciclastic); M-carbsil, mixed carbonate siliciclastic.

SUPPLEMENTARY TABLE S1
PERMANOVA of both alpha (Shannon and Chao1) and beta (Bray-Curtis and Euclidean) diversity indices to compare the microbial community composition between enriched and non-enriched plots at each site.

SUPPLEMENTARY TABLE S2
Relative abundance and taxonomic data of ASVs that compose the core microbiome of *T. testudinum* across several studies.

SUPPLEMENTARY TABLE S3
ANOVA results of the relative abundance of the Top 20 most abundant leaf genera by site, with Bonferroni corrected *p*-values, followed by *post-hoc* Tukey's HSD.

SUPPLEMENTARY TABLE S4
ANOVA results of the relative abundance of the Top 20 most abundant root genera by site, with Bonferroni corrected *p*-values, followed by *post-hoc* Tukey's HSD.

SUPPLEMENTARY TABLE S5
ANOVA results of the relative abundance of the Top 20 most abundant sediment genera by site, with Bonferroni corrected *p*-values, followed by *post-hoc* Tukey's HSD.

SUPPLEMENTARY TABLE S6
ANOVA results of the relative abundance of the Top 20 most abundant water genera by site, with Bonferroni corrected *p*-values, followed by *post-hoc* Tukey's HSD.

SUPPLEMENTARY TABLE S7
Top 20 most abundant genera by sample type with a list of possible functions and/or interesting facts relating to seagrasses, marine flora or fauna, or other plant systems.

References

Abraham, W.-R., and Rohde, M. (2014). "The family Hyphomonadaceae BT," in *The Prokaryotes: Alphaproteobacteria and Betaproteobacteria*, eds E. Rosenberg, E. F. DeLong, S. Lory, E. Stackebrandt, and F. Thompson (Berlin, Heidelberg: Springer Berlin Heidelberg), 283–299. doi: 10.1007/978-3-642-30197-1_260

Adamczyk, E. M., O'Connor, M. I., and Parfrey, L. W. (2022). Seagrass (*Zostera marina*) transplant experiment reveals core microbiota and resistance to environmental change. *Mol. Ecol.* 31, 5107–5123. doi: 10.1111/mec.16641

Agafonova, N. V., Doronina, N. V., Kaparullina, E. N., Fedorov, D. N., Gafarov, A. B., Sazonova, O. I., et al. (2017). A novel *Delftia* plant symbiont capable of autotrophic methylotrophy. *Microbiology* 86, 96–105. doi: 10.1134/S0026261717010039

Aires, T., Stuij, T. M., Muyzer, G., Serrão, E. A., and Engelen, A. H. (2021). Characterization and comparison of bacterial communities of an invasive and two native caribbean seagrass species sheds light on the possible influence

of the microbiome on invasive mechanisms. *Front. Microbiol.* 12:653998. doi: 10.3389/fmicb.2021.653998

Aldeguer-Riquelme, B., Rubio-Portillo, E., Álvarez-Rogel, J., Giménez-Casalduero, F., Otero, X. L., Belando, M.-D., et al. (2022). Factors structuring microbial communities in highly impacted coastal marine sediments (Mar Menor lagoon, SE Spain). *Front. Microbiol.* 13:937683. doi: 10.3389/fmicb.2022.937683

Amiri Moghaddam, J., Dávila-Céspedes, A., Kehraus, S., Crüsemann, M., Köse, M., Müller, C. E., et al. (2018). Cyclopropane-containing fatty acids from the marine bacterium *Labrenzia* sp. 011 with antimicrobial and GPR84 activity. *Mar. Drugs* 16:369. doi: 10.3390/md16100369

Andrews, S. (2010). *FastQC: A Quality Control Tool for High Throughput Sequence Data.* V 0.11.8. Available online at: http://www.bioinformatics.babraham.ac.uk/projects/fastqc/

Banister, R. B., Schwarz, M. T., Fine, M., Ritchie, K. B., and Muller, E. M. (2021). Instability and stasis among the microbiome of seagrass leaves, roots and rhizomes, and nearby sediments within a natural ph gradient. *Microb. Ecol.* 84, 703–716. doi: 10.1007/s00248-021-01867-9

Barry, S. C., Jacoby, C. A., and Frazer, T. K. (2017). Environmental influences on growth and morphology of *Thalassia testudinum*. *Mar. Ecol. Prog. Ser.* 570, 57–70. doi: 10.3354/meps12112

Bengtsson, M. M., Bühler, A., Brauer, A., Dahlke, S., Schubert, H., and Blindow, I. (2017). Eelgrass leaf surface microbiomes are locally variable and highly correlated with epibiotic eukaryotes. *Front. Microbiol.* 8:1312. doi: 10.3389/fmicb.2017.01312

Bisanz, J. E. (2018). *qiime2R: Importing QIIME2 Artifacts and Associated Data into R Sessions.* V 0.99.6. Available online at: https://github.com/jbisanz/qiime2R

Bishop, N., DL, M., and Ross, C. (2017). Effects of multi-stress exposure on the infection dynamics of a *Labyrinthula* sp.-turtle grass pathosystem. *Mar. Ecol. Prog. Ser.* 581, 119–133. doi: 10.3354/meps12318

Bolyen, E., Rideout, J. R., Dillon, M. R., Bokulich, N. A., Abnet, C. C., Al-Ghalith, G. A., et al. (2019). Reproducible, interactive, scalable and extensible microbiome data science using QIIME 2. *Nat. Biotechnol.* 37, 852–857. doi: 10.1038/s41587-019-0209-9

Borum, J., Sand-Jensen, K., Binzer, T., Pedersen, O., and Greve, T. M. (2006). "Oxygen movement in seagrasses BT," in *Seagrasses: Biology, Ecologyand Conservation*, eds A. W. D. Larkum, R. J. Orth, and C. M. Duarte (Dordrecht: Springer Netherlands), 255–270. doi: 10.1007/978-1-4020-2983-7_10

Bridge, T. A. M., White, C., and Gadd, G. M. (1999). Extracellular metal-binding activity of the sulphate-reducing bacterium *Desulfococcus multivorans*. *Microbiology* 145, 2987–2995. doi: 10.1099/00221287-145-10-2987

Callahan, B. J., McMurdie, P. J., Rosen, M. J., Han, A. W., Johnson, A. J. A., and Holmes, S. P. (2016). DADA2: high-resolution sample inference from Illumina amplicon data. *Nat. Methods* 13:581. doi: 10.1038/nmeth.3869

Campbell, J. E., Rhoades, O. K., Munson, C. J., Altieri, A. H., Douglass, J. G., and Heck, K. L. (2024). Herbivore effects increase with latitude across the extent of a foundational seagrass. *Nat. Ecol. Evol.* doi: 10.1038/s41559-024-02336-5

Conte, C., Apostolaki, E. T., Vizzini, S., and Migliore, L. (2023). A tight interaction between the native seagrass *Cymodocea nodosa* and the exotic *Halophila stipulacea* in the aegean sea highlights seagrass holobiont variations. *Plants* 12:350. doi: 10.3390/plants12020350

Conte, C., Rotini, A., Manfra, L., D'Andrea, M. M., Winters, G., and Migliore, L. (2021a). The seagrass holobiont: what we know and what we still need to disclose for its possible use as an ecological indicator. *Water* 13:406. doi: 10.3390/w13040406

Conte, C., Rotini, A., Winters, G., Vasquez, M. I., Piazza, G., Kletou, D., et al. (2021b). Elective affinities or random choice within the seagrass holobiont? The case of the native *Posidonia oceanica* (L.) Delile and the exotic *Halophila stipulacea* (Forssk.) Asch. from the same site (Limassol, Cyprus). *Aquat. Bot.* 174:103420. doi: 10.1016/j.aquabot.2021.103420

Crump, B. C., Wojahn, J. M., Tomas, F., and Mueller, R. S. (2018). Metatranscriptomics and amplicon sequencing reveal mutualisms in seagrass microbiomes. *Front. Microbiol.* 9:388. doi: 10.3389/fmicb.2018.00388

Cúcio, C., Engelen, A. H., Costa, R., and Muyzer, G. (2016). Rhizosphere microbiomes of European seagrasses are selected by the plant, but are not species specific. *Front. Microbiol.* 7:1–15. doi: 10.3389/fmicb.2016.00440

Davidson, S. K., Allen, S. W., Lim, G. E., Anderson, C. M., and Haygood, M. G. (2001). Evidence for the biosynthesis of bryostatins by the bacterial symbiont "*Candidatus* endobugula sertula" of the Bryozoan *Bugula neritina*. *Appl. Environ. Microbiol.* 67, 4531–4537. doi: 10.1128/AEM.67.10.4531-4537.2001

Dewsbury, B. M., Bhat, M., and Fourqurean, J. W. (2016). A review of seagrass economic valuations: gaps and progress in valuation approaches. *Ecosyst. Serv.* 18, 68–77. doi: 10.1016/j.ecoser.2016.02.010

Doronina, N., Kaparullina, E., and Trotsenko, Y. (2014). "The family Methylophilaceae BT," in *The Prokaryotes: Alphaproteobacteria and Betaproteobacteria*, eds E. Rosenberg, E. F. DeLong, S. Lory, E. Stackebrandt, and F. Thompson (Berlin: Springer Berlin Heidelberg), 869–880. doi: 10.1007/978-3-642-30197-1_243

Dubinina, G., Grabovich, M., Leshcheva, N., Rainey, F. A., and Gavrish, E. (2011). *Spirochaeta perfilievii* sp. nov., an oxygen-tolerant, sulfide-oxidizing, sulfur- and thiosulfate-reducing spirochaete isolated from a saline spring. *Int. J. Syst. Evol. Microbiol.* 61. 110–117. doi: 10.1099/ijs.0.018333-0

Edgar, R. C. (2010). Search and clustering orders of magnitude faster than BLAST. *Bioinformatics* 26, 2460–2461. doi: 10.1093/bioinformatics/btq461

Ettinger, C. L., Voerman, S. E., Lang, J. M., Stachowicz, J. J., and Eisen, J. A. (2017). Microbial communities in sediment from *Zostera marina* patches, but not the *Z. marina* leaf or root microbiomes, vary in relation to distance from patch edge. *PeerJ* 5:e3246. doi: 10.7717/peerj.3246

Fahimipour, A. K., Kardish, M. R., Lang, J. M., Green, J. L., Eisen, J. A., and Stachowicz, J. J. (2017). Global-scale structure of the eelgrass microbiome. *Appl. Environ. Microbiol.* 83:e03391-16. doi: 10.1128/AEM.03391-16

Fourqurean, J. W., Campbell, J. E., Rhoades, O. K., Munson, C. J., Krause, J. R., Altieri, A. H., et al. (2023). Seagrass abundance predicts surficial soil organic carbon stocks across the range of *Thalassia testudinum* in the Western North Atlantic. *Estuaries Coasts* 46, 1280–1301. doi: 10.1007/s12237-023-01210-0

Fourqurean, J. W., Zieman, J. C., and Powell, G. V. N. (1992). Phosphorus limitation of primary production in Florida Bay: evidence from C:N:P ratios of the dominant seagrass *Thalassia testudinum*. *Limnol. Oceanogr.* 37, 162–171. doi: 10.4319/lo.1992.37.1.0162

Galushko, A., and Kuever, J. (2019). "Desulfatiglans," in *Bergey's Manual of Systematics of Archaea and Bacteria*, eds M. E. Trujillo, S. Dedysh, P. DeVos, B. Hedlund, P. Kämpfer, F. A. Rainey and W. B. Whitman (Berlin: Springer), 1–4. doi: 10.1002/9781118960608.gbm01679

Garnier, S., Ross, N., Rudis, R., Camargo, P. A., Sciaini, M., and Scherer, C. (2023). *viridis(Lite) - Colorblind-Friendly Color Maps for R.* V 0.4.2. doi: 10.5281/zenodo.4678327

Goh, Y. K., Zoqratt, M. Z., Goh, Y. K., Ayub, Q., and Ting, A. S. (2020). Determining soil microbial communities and their influence on *Ganoderma* disease incidences in oil palm (*Elaeis guineensis*) via high-throughput sequencing. *Biology* 9:424. doi: 10.3390/biology9120424

Hassenrück, C., Hofmann, L. C., Bischof, K., and Ramette, A. (2015). Seagrass biofilm communities at a naturally CO2-rich vent. *Environ. Microbiol. Rep.* 7, 516–525. doi: 10.1111/1758-2229.12282

Henriksen, N. N. S. E., Lindqvist, L. L., Wibowo, M., Sonnenschein, E. C., Bentzon-Tilia, M., and Gram, L. (2022). Role is in the eye of the beholder—the multiple functions of the antibacterial compound tropodithietic acid produced by marine Rhodobacteraceae. *FEMS Microbiol. Rev.* 46:fuac007. doi: 10.1093/femsre/fuac007

Higashioka, Y., Kojima, H., Watanabe, M., and Fukui, M. (2013). *Desulfatitalea tepidiphila* gen. nov., sp. nov., a sulfate-reducing bacterium isolated from tidal flat sediment. *Int. J. Syst. Evol. Microbiol.* 63, 761–765. doi: 10.1099/ijs.0.043356-0

Hoshino, T., Doi, H., Uramoto, G.-I., Wörmer, L., Adhikari Rishi, R., Xiao, N., et al. (2020). Global diversity of microbial communities in marine sediment. *Proc. Natl. Acad. Sci.* 117, 27587–27597. doi: 10.1073/pnas.1919139117

Hurtado-McCormick, V., Kahlke, T., Krix, D., Larkum, A., Ralph, P. J., and Seymour, J. R. (2020). Seagrass leaf reddening alters the microbiome of *Zostera muelleri*. *Mar. Ecol. Prog. Ser.* 646, 29–44. doi: 10.3354/meps13409

Hurtado-McCormick, V., Kahlke, T., Petrou, K., Jeffries, T., Ralph, P. J., and Seymour, J. R. (2019). Regional and microenvironmental scale characterization of the *Zostera muelleri* seagrass microbiome. *Front. Microbiol.* 10:1011. doi: 10.3389/fmicb.2019.01011

JMP®. *Version 16.1.0.* Cary, NC: SAS Institute Inc., 1989–2023.

Jones, P., Garcia, B. J., Furches, A., Tuskan, G. A., and Jacobson, D. (2019). Plant host-associated mechanisms for microbial selection. *Front. Plant Sci.* 10:862. doi: 10.3389/fpls.2019.00862

Joshi, N. A., and Fass, J. N. (2011). *Sickle: A Sliding-Window, Adaptive, Quality-Based Trimming Tool for FastQ Files.* V 1.33. Available online at: https://github.com/najoshi/sickle

Kanzog, C., and Ramette, A. (2009). Microbial colonisation of artificial and deep-sea sediments in the Arctic Ocean. *Mar. Ecol.* 30, 391–404. doi: 10.1111/j.1439-0485.2009.00290.x

Kardish, M. R., and Stachowicz, J. J. (2021). More than a stick in the mud: eelgrass leaf and root bacterial communities are distinct from those on physical mimics. *bioRxiv*. doi: 10.1101/2021.05.31.446483

Kitamura, R., Miura, N., Ito, M., Takagi, T., Yamashiro, H., Nishikawa, Y., et al. (2021). Specific detection of coral-associated *Ruegeria*, a potential probiotic bacterium, in corals and subtropical seawater. *Mar. Biotechnol.* 23, 576–589. doi: 10.1007/s10126-021-10047-2

Kleindienst, S., Herbst, F.-A., Stagars, M., von Netzer, F., von Bergen, M., Seifert, J., et al. (2014). Diverse sulfate-reducing bacteria of the *Desulfosarcina/Desulfococcus* clade are the key alkane degraders at marine seeps. *ISME J.* 8, 2029–2044. doi: 10.1038/ismej.2014.51

Koch, M. S., Schopmeyer, S., Kyhn-Hansen, C., and Madden, C. J. (2007b). Synergistic effects of high temperature and sulfide on tropical seagrass. *J. Exp. Mar. Bio. Ecol.* 341, 91–101. doi: 10.1016/j.jembe.2006.10.004

Koch, M. S., Schopmeyer, S. A., Holmer, M., Madden, C. J., and Kyhn-Hansen, C. (2007a). *Thalassia testudinum* response to the interactive stressors hypersalinity, sulfide and hypoxia. *Aquat. Bot.* 87, 104–110. doi: 10.1016/j.aquabot.2007.03.004

Koelmel, J. P., Campbell, J. E., Guingab-Cagmat, J., Meke, L., Garrett, T. J., and Stingl, U. (2019). Re-modeling of foliar membrane lipids in a seagrass allows for growth in phosphorus deplete conditions. *PLoS ONE* 14:e0218690. doi: 10.1371/journal.pone.0218690

Kohn, T., Rast, P., Kallscheuer, N., Wiegand, S., Boedeker, C., Jetten, M. S. M., et al. (2020). The microbiome of *Posidonia oceanica* seagrass leaves can be dominated by planctomycetes. *Front. Microbiol.* 11:1458. doi: 10.3389/fmicb.2020.01458

König, S., Gros, O., Heiden, S. E., Hinzke, T., Thürmer, A., Poehlein, A., et al. (2016). Nitrogen fixation in a chemoautotrophic lucinid symbiosis. *Nat. Microbiol.* 2:16193. doi: 10.1038/nmicrobiol.2016.193

Korlević, M., Markovski, M., Zhao, Z., Herndl, G. J., and Najdek, M. (2021). Seasonal dynamics of epiphytic microbial communities on marine macrophyte surfaces. *Front. Microbiol.* 12:671342. doi: 10.3389/fmicb.2021.671342

Küsel, K., Pinkart, H. C., Drake, H. L., and Devereux, R. (1999). Acetogenic and sulfate-reducing bacteria inhabiting the rhizoplane and deep cortex cells of the sea grass *Halodule wrightii*. *Appl. Environ. Microbiol.* 65, 5117–5123. doi: 10.1128/AEM.65.11.5117-5123.1999

Lahti, L., Shetty, S., et al. (2017). *Tools for Microbiome Analysis in R.* V 1.23.1. Available at: http://microbiome.github.com/microbiome

Lee, K.-S., and Dunton, K. H. (2000). Effects of nitrogen enrichment on biomass allocation, growth, and leaf morphology of the seagrass *Thalassia testudinum*. *Mar. Ecol. Prog. Ser.* 196, 39–48. doi: 10.3354/meps196039

Lemanceau, P., Blouin, M., Muller, D., and Moënne-Loccoz, Y. (2017). Let the core microbiota be functional. *Trends Plant Sci.* 22, 583–595. doi: 10.1016/j.tplants.2017.04.008

Les, D. H., Cleland, M. A., and Waycott, M. (1997). Phylogenetic studies in Alismatidae, II: evolution of marine angiosperms (seagrasses) and hydrophily. *Syst. Bot.* 22, 443–463. doi: 10.2307/2419820

Lim, G. E., and Haygood, M. G. (2004). "*Candidatus* Endobugula glebosa," a specific bacterial symbiont of the marine bryozoan *Bugula simplex*. *Appl. Environ. Microbiol.* 70, 4921–4929. doi: 10.1128/AEM.70.8.4921-4929.2004

Lopanik, N., Lindquist, N., and Targett, N. (2004). Potent cytotoxins produced by a microbial symbiont protect host larvae from predation. *Oecologia* 139, 131–139. doi: 10.1007/s00442-004-1487-5

Lundberg, D. S., Lebeis, S. L., Paredes, S. H., Yourstone, S., Gehring, J., Malfatti, S., et al. (2012). Defining the core *Arabidopsis thaliana* root microbiome. *Nature* 488, 86–90. doi: 10.1038/nature11237

Markovski, M., Najdek, M., Herndl, G. J., and Korlević, M. (2022). Compositional stability of sediment microbial communities during a seagrass meadow decline. *Front. Mar. Sci.* 9:966070. doi: 10.3389/fmars.2022.966070

Martin, B. C., Alarcon, M. S., Gleeson, D., Middleton, J. A., Fraser, M. W., Ryan, M. H., et al. (2020). Root microbiomes as indicators of seagrass health. *FEMS Microbiol. Ecol.* 96:fiz201. doi: 10.1093/femsec/fiz201

Martin, B. C., Bougoure, J., Ryan, M. H., Bennett, W. W., Colmer, T. D., Joyce, N. K., et al. (2019). Oxygen loss from seagrass roots coincides with colonisation of sulphide-oxidising cable bacteria and reduces sulphide stress. *ISME J.* 13, 707–719. doi: 10.1038/s41396-018-0308-5

Martin, M. (2011). Cutadapt removes adapter sequences from high-throughput sequencing reads. *EMBnet J.* 17. doi: 10.14806/ej.17.1.200

McMurdie, P. J., and Holmes, S. (2013). phyloseq: an R package for reproducible interactive analysis and graphics of microbiome census data. *PLoS ONE* 8:e61217. doi: 10.1371/journal.pone.0061217

Mvungi, E. F., and Mamboya, F. A. (2012). Photosynthetic performance, epiphyte biomass and nutrient content of two seagrass species in two areas with different level of nutrients along the Dar es Salaam coast. *African J. Mar. Sci.* 34, 323–330. doi: 10.2989/1814232X.2012.709957

Neu, A. T., Allen, E. E., and Roy, K. (2021). Defining and quantifying the core microbiome: challenges and prospects. *Proc. Natl. Acad. Sci.* 118:e2104429118. doi: 10.1073/pnas.2104429118

Oberbeckmann, S., Kreikemeyer, B., and Labrenz, M. (2018). Environmental factors support the formation of specific bacterial assemblages on microplastics. *Front. Microbiol.* 8:2709. doi: 10.3389/fmicb.2017.02709

Obi, C. C., Adebusoye, S. A., Ugoji, E. O., Ilori, M. O., Amund, O. O., and Hickey, W. J. (2016). Microbial communities in sediments of lagos lagoon, nigeria: elucidation of community structure and potential impacts of contamination by municipal and industrial wastes. *Front. Microbiol.* 7:1213. doi: 10.3389/fmicb.2016.01213

Oksanen, J., Blanchet, F., Guillaume Friendly, M., Kindt, R., Legendre, P., McGlinn, D., et al. (2018). *vegan: Community Ecology Package.* V 2.6-4. Available online at: http://cran.rproject.org/package=vegan

Paradis, E., and Schliep, K. (2019). ape 5.0: an environment for modern phylogenetics and evolutionary analyses in R. *Bioinformatics* 35, 526–528. doi: 10.1093/bioinformatics/bty633

Petersen, J. M., Kemper, A., Gruber-Vodicka, H., Cardini, U., van der Geest, M., Kleiner, M., et al. (2016). Chemosynthetic symbionts of marine invertebrate animals are capable of nitrogen fixation. *Nat. Microbiol.* 2:16195. doi: 10.1038/nmicrobiol.2016.195

Phillips, R. C., and Meñez, E. G. (1988). Seagrasses. *Smithson. Contrib. Mar. Sci.* 34:69.

Price, M. N., Ray, J., Wetmore, K. M., Kuehl, J. V., Bauer, S., Deutschbauer, A. M., et al. (2014). The genetic basis of energy conservation in the sulfate-reducing bacterium *Desulfovibrio alaskensis* G20. *Front. Microbiol.* 5:577. doi: 10.3389/fmicb.2014.00577

Pujalte, M. J., Lucena, T., Ruvira, M. A., Arahal, D. R., and Macián, M. C. (2014). "The family Rhodobacteraceae BT," in *The Prokaryotes: Alphaproteobacteria and Betaproteobacteria*, eds E. Rosenberg, E. F. DeLong, S. Lory, E. Stackebrandt, and F. Thompson (Berlin: Springer Berlin Heidelberg), 439–512. doi: 10.1007/978-3-642-30197-1_377

Quensen, J., Simpson, G., and Oksanen, J. (2024). *ggordiplots: Make 'ggplot2' Versions of Vegan's Ordiplots.* V 0.4.1. Available online at: https://github.com/jfq3/ggordiplots

Quinn, R. A., Metzler, A., Smolowitz, R. M., Tlusty, M., and Chistoserdov, A. Y. (2012). Exposures of *Homarus americanus* shell to three bacteria isolated from naturally occurring epizootic shell disease lesions. *J. Shellfish Res.* 31, 485–493. doi: 10.2983/035.031.0208

R Core Team (2013a). *R: A Language and Environment for Statistical Computing.* V 4.2.1. Available online at: http://www.r-project.org/

R Core Team (2013b). *The R Stats Package.* V 4.2.1. Available online at: http://www.rproject.org/

Raj Sharma, A., Zhou, T., Harunari, E., Oku, N., Trianto, A., and Igarashi, Y. (2019). Labrenzbactin from a coral-associated bacterium *Labrenzia* sp. *J. Antibiot.* 72, 634–639. doi: 10.1038/s41429-019-0192-x

Riclea, R., Gleitzmann, J., Bruns, H., Junker, C., Schulz, B., and Dickschat, J. S. (2012). Algicidal lactones from the marine *Roseobacter* clade bacterium *Ruegeria pomeroyi*. *Beilstein J. Org. Chem.* 8, 941–950. doi: 10.3762/bjoc.8.106

Rodríguez-Barreras, R., Tosado-Rodríguez, E. L., and Godoy-Vitorino, F. (2021). Trophic niches reflect compositional differences in microbiota among Caribbean sea urchins. *PeerJ* 9:e12084. doi: 10.7717/peerj.12084

Rolando, J. L., Kolton, M., Song, T., and Kostka, J. E. (2022). The core root microbiome of *Spartina alterniflora* is predominated by sulfur-oxidizing and sulfate-reducing bacteria in Georgia salt marshes, USA. *Microbiome* 10:37. doi: 10.1186/s40168-021-01187-7

Rosales, S. M., Clark, A. S., Huebner, L. K., Ruzicka, R. R., and Muller, E. M. (2020). *Rhodobacterales* and *Rhizobiales* are associated with stony coral tissue loss disease and its suspected sources of transmission. *Front. Microbiol.* 11:681. doi: 10.3389/fmicb.2020.00681

Roth-Schulze, A. J., Zozaya-Valdés, E., Steinberg, P. D., and Thomas, T. (2016). Partitioning of functional and taxonomic diversity in surface-associated microbial communities. *Environ. Microbiol.* 18, 4391–4402. doi: 10.1111/1462-2920.13325

Rotini, A., Conte, C., Seveso, D., Montano, S., Galli, P., Vai, M., et al. (2020). Daily variation of the associated microbial community and the Hsp60 expression in the Maldivian seagrass *Thalassia hemprichii*. *J. Sea Res.* 156:101835. doi: 10.1016/j.seares.2019.101835

Rotini, A., Conte, C., Winters, G., Vasquez, M. I., and Migliore, L. (2023). Undisturbed Posidonia oceanica meadows maintain the epiphytic bacterial community in different environments. *Environ. Sci. Pollut. Res.* 30, 95464–95474. doi: 10.1007/s11356-023-28968-x

Rotini, A., Mejia, A. Y., Costa, R., Migliore, L., and Winters, G. (2017). Ecophysiological plasticity and bacteriome shift in the seagrass *Halophila stipulacea* along a depth gradient in the Northern Red Sea. *Front. Plant Sci.* 7:2015. doi: 10.3389/fpls.2016.02015

Saha, M., and Weinberger, F. (2019). Microbial "gardening" by a seaweed holobiont: surface metabolites attract protective and deter pathogenic epibacterial settlement. *J. Ecol.* 107, 2255–2265. doi: 10.1111/1365-2745.13193

Shade, A., and Handelsman, J. (2012). Beyond the Venn diagram: the hunt for a core microbiome. *Environ. Microbiol.* 14, 4–12. doi: 10.1111/j.1462-2920.2011.02585.x

Soriano-Lerma, A., Pérez-Carrasco, V., Sánchez-Marañón, M., Ortiz-González, M., Sánchez-Martín, V., Gijón, J., et al. (2020). Influence of 16S rRNA target region on the outcome of microbiome studies in soil and saliva samples. *Sci. Rep.* 10:13637. doi: 10.1038/s41598-020-70141-8

Spring, S., Scheuner, C., Göker, M., and Klenk, H.-P. (2015). A taxonomic framework for emerging groups of ecologically important marine gammaproteobacteria based on the reconstruction of evolutionary relationships using genome-scale data. *Front. Microbiol.* 6:281. doi: 10.3389/fmicb.2015.00281

Suzuki, R., and Shimodaira, H. (2006). Pvclust: an R package for assessing the uncertainty in hierarchical clustering. *Bioinformatics* 22, 1540–1542. doi: 10.1093/bioinformatics/btl117

Ugarelli, K., Chakrabarti, S., Laas, P., and Stingl, U. (2017). The seagrass holobiont and its microbiome. *Microorganism* 5. doi: 10.3390/microorganisms5040081

Ugarelli, K., Laas, P., and Stingl, U. (2019). The microbial communities of leaves and roots associated with turtle grass (*Thalassia testudinum*) and manatee grass (*Syringodium filliforme*) are distinct from seawater and sediment communities, but are similar between species and sampling Si. *Microorganisms* 7. doi: 10.3390/microorganisms7010004

Unsworth, R. K. F., Collier, C. J., Waycott, M., Mckenzie, L. J., and Cullen-Unsworth, L. C. (2015). A framework for the resilience of seagrass ecosystems. *Mar. Pollut. Bull.* 100, 34–46. doi: 10.1016/j.marpolbul.2015.08.016

Ureta, A., Alvarez, B., Ramón, A., Vera, M. A., and Martinez-Drets, G. (1995). Indentification of *Acetobacter diazotrophicus*, *Herbaspirillum seropedicae* and *Herbaspirillum rubrisubalbicans* using biochemical and genetic criteria. *Plant Soil* 172, 271–277. doi: 10.1007/BF00011329

Vogel, M. A., Mason, O. U., and Miller, T. E. (2020). Host and environmental determinants of microbial community structure in the marine phyllosphere. *PLoS ONE* 15:e0235441. doi: 10.1371/journal.pone.0235441

Vogel, M. A., Mason, O. U., and Miller, T. E. (2021a). Composition of seagrass phyllosphere microbial communities suggests rapid environmental regulation of community structure. *FEMS Microbiol. Ecol.* 97:fiab013. doi: 10.1093/femsec/fiab013

Vogel, M. A., Mason, O. U., and Miller, T. E. (2021b). Environmental stressors alter the composition of seagrass phyllosphere microbial communities. *Clim. Chang. Ecol.* 2:100042. doi: 10.1016/j.ecochg.2021.100042

Wang, L., Tomas, F., and Mueller, R. S. (2020). Nutrient enrichment increases size of *Zostera marina* shoots and enriches for sulfur and nitrogen cycling bacteria in root-associated microbiomes. *FEMS Microbiol. Ecol.* 96:fiaa129. doi: 10.1093/femsec/fiaa129

Wang, X., Yu, M., Wang, L., Lin, H., Li, B., Xue, C.-X., et al. (2020). Comparative genomic and metabolic analysis of manganese-oxidizing mechanisms in *Celeribacter manganoxidans* DY25T: its adaptation to the environment of polymetallic nodules. *Genomics* 112, 2080–2091. doi: 10.1016/j.ygeno.2019.12.002

Wang, Z., Su, Y., Zhang, Y., Guo, H., Meng, D., and Wang, Y. (2016). Ecology-types determine physicochemical properties and microbial communities of sediments obtained along the Songhua River. *Biochem. Syst. Ecol.* 66, 312–318. doi: 10.1016/j.bse.2016.04.008

Waycott, M., Duarte, C. M., Carruthers, T. J. B., Orth, R. J., Dennison, W. C., Olyarnik, S., et al. (2009). Accelerating loss of seagrasses across the globe threatens coastal ecosystems. *Proc. Natl. Acad. Sci. U. S. A.* 106, 12377–12381. doi: 10.1073/pnas.0905620106

Weber, C. F., and King, G. M. (2007). Physiological, ecological, and phylogenetic characterization of *Stappia*, a marine CO-oxidizing bacterial genus. *Appl. Environ. Microbiol.* 73, 1266–1276. doi: 10.1128/AEM.01724-06

Weidner, S., Arnold, W., Stackebrandt, E., and Pühler, A. (2000). Phylogenetic analysis of bacterial communities associated with leaves of the seagrass *Halophila stipulacea* by a culture-independent small-subunit rRNA gene approach. *Microb. Ecol.* 39, 22–31. doi: 10.1007/s002489900194

Wetzel, R. G., and Penhale, P. A. (1979). Transport of carbon and excretion of dissolved organic carbon by leaves and roots/rhizomes in seagrasses and their epiphytes. *Aquat. Bot.* 6, 149–158. doi: 10.1016/0304-3770(79)90058-5

Wickham, H. (2009). ggplot2: elegant graphics for data analysis. *J. Stat. Softw.* 35, 65–88. doi: 10.1007/978-0-387-98141-3

Wickham, H., Averick, M., Bryan, J., Chang, W., McGowan, L. D., François, R., et al. (2019). Welcome to the {tidyverse}. *J. Open Source Softw.* 4:1686. doi: 10.21105/joss.01686

Yilmaz, P., Parfrey, L. W., Yarza, P., Gerken, J., Pruesse, E., Quast, C., et al. (2014). The SILVA and "all-species living tree project (LTP)" taxonomic frameworks. *Nucleic Acids Res.* 42, D643–D648. doi: 10.1093/nar/gkt1209

Zaynab, M., Chen, H., Chen, Y., Ouyang, L., Yang, X., Hu, Z., et al. (2021). Signs of biofilm formation in the genome of *Labrenzia* sp. PO1. *Saudi J. Biol. Sci.* 28, 1900–1912. doi: 10.1016/j.sjbs.2020.12.041

Zhang, X., Liu, S., Jiang, Z., Wu, Y., and Huang, X. (2022). Gradient of microbial communities around seagrass roots was mediated by sediment grain size. *Ecosphere* 13:e3942. doi: 10.1002/ecs2.3942

Zhang, X., Zhao, C., Yu, S., Jiang, Z., Liu, S., Wu, Y., et al. (2020). Rhizosphere microbial community structure is selected by habitat but not plant species in two tropical seagrass beds. *Front. Microbiol.* 11:161. doi: 10.3389/fmicb.2020.00161

Zhou, W., Dong, J., Ding, D., Long, L., Suo, A., Lin, X., et al. (2021). Rhizosphere microbiome dynamics in tropical seagrass under short-term inorganic nitrogen fertilization. *Environ. Sci. Pollut. Res.* 28, 19021–19033. doi: 10.1007/s11356-020-12048-5

frontiers | Frontiers in Microbiology

TYPE Original Research
PUBLISHED 03 April 2024
DOI 10.3389/fmicb.2024.1362968

OPEN ACCESS

EDITED BY
Jin Zhou,
Tsinghua University, China

REVIEWED BY
Hong Wei Yu,
Chinese Academy of Sciences (CAS), China
Shuangshuang Li,
Hebei University of Engineering, China
Yuying Li,
Nanyang Normal University, China

*CORRESPONDENCE
Dawen Zhang
✉ zdw3296@163.com

RECEIVED 29 December 2023
ACCEPTED 13 February 2024
PUBLISHED 03 April 2024

CITATION
Zhang L, Yuan L, Xiang J, Liao Q, Zhang D and Liu J (2024) Response of the microbial community structure to the environmental factors during the extreme flood season in Poyang Lake, the largest freshwater lake in China.
Front. Microbiol. 15:1362968.
doi: 10.3389/fmicb.2024.1362968

Response of the microbial community structure to the environmental factors during the extreme flood season in Poyang Lake, the largest freshwater lake in China

Li Zhang[1], Lijuan Yuan[1], Jianjun Xiang[1], Qiegen Liao[1], Dawen Zhang[1]*and Jutao Liu[2]

[1]Institute of Quality & Safety and Standards of Agricultural Products Research, Jiangxi Academy of Agricultural Sciences, Nanchang, Jiangxi, China, [2]Jiangxi Provincial Institute of Water Sciences, Nanchang, Jiangxi, China

Background: Poyang Lake is the largest freshwater lake in China, and there are several studies on the composition and diversity of bacteria in Poyang Lake, while few quantitative studies were carried out on the response of the bacterial community to environmental factors during the extreme flood season in Poyang Lake.

Methods: The connected-lake heterogeneity of bacterial community composition (BCC) was investigated in Poyang Lake during the flood season in 2020. Illumina high-throughput sequencing technology was used in this study.

Results: The bacterial community structure in the water was different from that in the sediment of Poyang Lake during extreme flood seasons. The bacterial diversity in water was much lower than that in sediment. In the water column, the dominant phyla were *Actinobacteriota*, while the composition of bacteria in sediment was more complex than that in water, and the dominant phyla in sediment were *Proteobacteria, Chloroflexi, Acidobacteriota*, and *Actinobacteriota*. The bacterial diversity in the water of Poyang Lake showed seasonal dynamics, while no seasonal variation of bacterial communities in sediment was observed. The bacterial community structure in the sediment from the two bays and channel areas of Poyang Lake can be distinguished from each other. The microbial diversity in sediment gradually increased from the Sancha Bay to the Zhouxi Bay and then to the channel, but the total nitrogen (TN) concentration in sediment (STN) and the total phosphorus (TP) concentration in sediment (STP) showed opposite trends. This might be due to the anthropogenic disturbances from the extreme flood. The bacterial community structure in, water column was significantly correlated with WT, NH4-N, STP, SOM, Chl a, DO, TP, and Eh, while the bacterial community structure in sediment was significantly correlated with SOM and STP.

Conclusion: The bacterial community structure in water was greatly different from that in sediment in Poyang Lake during extreme flood seasons. The bacterial community structure in the water column was not only sensitive to the geochemical characteristics of the water but also affected by some nutrient concentrations in the sediment. During the wet seasons, bacterial diversity was only affected by SOM and STP.

KEYWORDS

Poyang Lake, bacterial diversity, extreme flood season, environmental factors, microbial community

1 Introduction

It is well known that bacteria play an important role as the major primary producers in the freshwater lake ecosystem (Newton et al., 2011). The bacterial community characteristics in water and sediment can potentially indicate the health of the freshwater ecosystem due to their basic biochemical cycling position in lake systems (Lindström and Östman, 2011). Therefore, a comprehensive understanding of the bacterial diversity and distribution characteristics in freshwater lake ecosystems is meaningful for better management and the maintenance of the lake's ecological environment.

Poyang Lake is the largest freshwater lake in China and is the most important wintering site for the East Asian and Australian Flyways. The hydrological conditions in Poyang Lake are quite different than those in disconnected lakes. Poyang Lake has rapidly changing terrain and complex hydrodynamics, which have then formed its unique natural geographical landscape. The water level of Poyang Lake changes drastically throughout the year, with 8.7–22 m. Due to the strong disturbance of natural and human activities, natural and anthropogenic inputs of nutrients and xenobiotics in Poyang Lake have also consistently increased (Ni et al., 2020). The trophic level index (TLI) of Poyang Lake had increased from 46.08 to 56.38 and achieved the light eutropher level (Liu et al., 2023). Therefore, the health threat to the Poyang Lake ecosystem is becoming increasingly serious.

There have been several studies on the composition and diversity of bacteria in Poyang Lake, and many have focused on the relationships between bacterial communities and the physicochemical properties of the lake (Ding et al., 2015; Ren et al., 2019). The bacterial distribution in lakes is affected by many physicochemical factors, including water temperature (WT), oxygen concentration, light intensity, illuminant time, seasonal variation, and the degree and type of water pollution (Adams et al., 2015; Felfödi, 2020; Zhang et al., 2020). Shallow groundwater samples in the Poyang Lake basin showed that the bacterial community structure of high-nitrate groundwater is different from that of low-nitrate groundwater (Dong et al., 2019). The spatial distribution patterns of bacterial community composition (BCC) in the surface sediments from the main basins and mouths of major rivers that discharge into the Poyang Lake varied largely among sampling sites (Kou et al., 2016). The anthropogenic disturbances also have significant impacts on the composition and metabolic function of the bacterial community (Jin et al., 2019). Water level fluctuations had significant impacts on the bacterial communities of Poyang Lake. The bacterial communities are taxonomically sensitive in the dry season while more functionally sensitive in the wet season (Ren et al., 2019). It is widely recognized that water and sediment are both indispensable components of a lake, and the habitats are interactional and interdependent in the aquatic environment. Frequent resuspension and deposition of materials (e.g., bacteria) in the water column and sediment were observed in the lake (Qian et al., 2018). There have been many studies that examined the bacterial communities in the water and sediment of Poyang Lake (Dong et al., 2019; Jin et al., 2019; Sun et al., 2020; Guo et al., 2023). For example, Guo et al. (2023) studied the influence of sediment-to-soil conversion on microbial composition and stability in Poyang Lake in December. Sun et al. (2020) examined the bacterial diversities and community compositions in freshwater and sediment niches and explored the relationship between environmental parameters and the diversity and structure of bacterial communities in Poyang Lake, but this study was focused on the entrance area of five tributaries of Poyang Lake. In addition, there has been no study on the bacterial communities and the response of the bacterial communities to environmental factors when the extreme flood occurred in Poyang Lake. Moreover, the bacterial community from the water and sediment of Poyang Lake and the correlation between the bacterial community and the water and sediment need to be extensively studied (Ding et al., 2015; Kou et al., 2016; Ren et al., 2019; Sun et al., 2020).

However, with global warming, the frequency and intensity of extreme precipitation events have increased. In 2020, rainfall in the Yangtze River basin will reach 1441.5 mm, 22% more than usual and the most since 1961 (Chen, 2020; Huang et al., 2021). Under the influence of heavy rain in the middle and lower reaches of the Yangtze River, Poyang Lake experienced a large-scale flood. The water level when we sampled in July was 21.74 m (measured at Xingzi Station, an iconic hydrological station on Poyang Lake), which was at the historic high level of Poyang Lake (Liao et al., 2021). Thus, the aims of the present study are to (1) analyze the bacterial diversity comprehensively and (2) evaluate the effects of environmental factors on the bacterial community in Poyang Lake ecosystems during the extreme flood season.

2 Materials and methods

2.1 Study site description and sample collection

Poyang Lake (28°52′21″–29°06′46″N, 116°10′24″–116°23′50″E) is located in the middle and lower reaches of the Yangtze River, northern Jiangxi Province, China (Figure 1). It is the largest freshwater lake and Yangtze-connected lake in China, with a storage capacity of 2.95 billion m^3. Each year, approximately 1.457×10^{11} m^3 of water from Poyang Lake flows into the Yangtze River, which accounts for approximately 15.6% of the Yangtze River's water volume.

The water and sediment samples were collected from June to October 2020 in Poyang Lake, when the water level (measured at Xingzi Station, an iconic hydrological station on Poyang Lake) was from 16.16 to 21.74 m. A total of 10 sample sites were set. Sites 1, 2, 3,

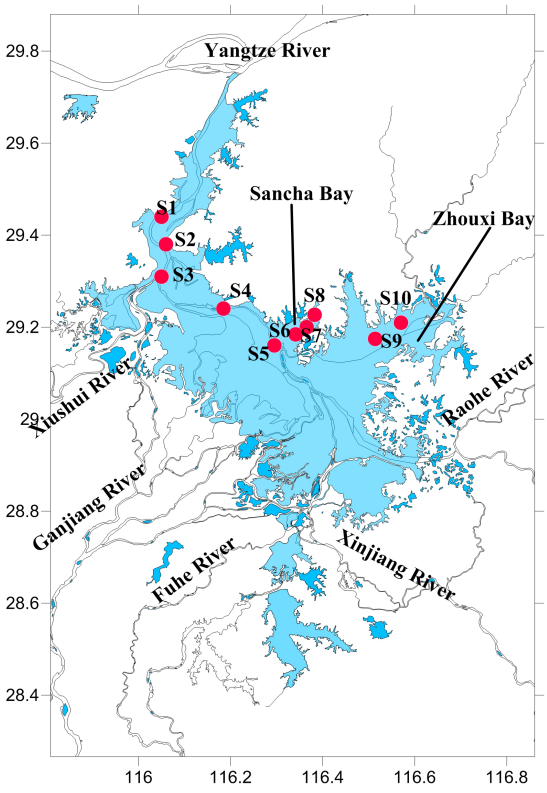

FIGURE 1
The map of Poyang Lake with sampling stations.

4, and 5 were set in the channel area, where there is always water throughout the year. Sites 6, 7, and 8 were set in the Sancha Bay, which was a closed branch and not connected with other rivers, and the water depth (WD) was too low to get to this area by boat during the dry season. Sites 9 and 10 were located near the Zhouxi Bay, where a branch of the lake was connected to the inflow mouth of a river (Figure 1).

Water samples at each site were collected from surface water (top 50 cm) with a 5-L Schindler sampler. In total, 300 mL of water samples from each site were filtered through a 0.2 μm polycarbonate membrane filter (Whatman, United Kingdom). The filter membranes were immediately frozen in liquid nitrogen and then stored at −80°C in the laboratory until DNA extraction. Sediment samples were collected simultaneously from the same sites (top 5 cm) with an Ekman grabber. A total of 10 g of sediment samples were collected in sterile self-sealed tubes and stored as the same as the filter membranes before. Duplicate water and sediment samples were collected to measure physical and chemical parameters.

2.2 Physicochemical parameters of water and sediment

2.2.1 Water

In the field, WT, pH, oxidation–reduction potential (Eh), conductivity (CO), and dissolved oxygen (DO) were determined using a five-star portable multi-parameter measuring instrument (Orion, CO, USA). Transparency (TR) was measured by a Secchi disk, and the WD was measured using a digital ultrasonic echo sounder (Umwelt and Wissenschafts Technik, Mondsee, Austria). Chlorophyll a (Chl *a*) and chlorophyll b (Chl *b*) were analyzed according to the Chinese Water Resources Industry Standard (SL 88–2012) (Department of Water and Soil Conservation, 2012). Chemical oxygen demand (COD_{Mn}), total nitrogen (TN), total dissolved nitrogen (DTN), total phosphorus (TP), total dissolved phosphorus (DTP), ammonium (NH_4), nitrite (NO_2), and nitrate (NO_3) contents in the water sample were analyzed according to the American Public Health Association (1998). Phycocyanin (PC) in the water sample was analyzed according to the method of Zhang et al. (2013).

2.2.2 Sediment

Total nitrogen concentration in sediment (STN), total phosphorus concentration in sediment (STP), and organic matter in sediment (SOM) were analyzed according to the method of Jin and Tu (1990).

2.2.2.1 DNA extraction and PCR amplification

DNA extraction and PCR amplification were analyzed according to the methods of He et al. (2017). Genomic DNA was isolated from samples with the PowerWater DNA Isolation Kit (Mo Bio Laboratories, Solana Beach, CA, USA) according to the manufacturer's instructions. Extracted genomic DNA was detected by 1% agarose gel electrophoresis. An aliquot of 10 ng purified DNA template from each sample was amplified in a 50 μL reaction system with the following conditions: 1 cycle of 95°C for 3 min followed by 30 cycles of denaturation at 95°C for 30 s, annealing at 55°C for 30 s, extension at 72°C for 45 s, and a final extension at 72°C for 10 min. The primer pairs 338F (5′-ACTCCTACGGGAGGCAGCAG-3′) and 806R (5′-GGACTACHVGGGTWTCTAAT-3′) were used for the 16S rRNA amplification (Xu et al., 2016). PCR was carried out on a GeneAmp 9700 PCR system (Applied Biosystems, Foster City, CA, USA). The PCR-amplified products were visualized on agarose gels (2% gel electrophoresis) and purified with a DNA gel extraction kit (Axygen Biosciences, Union City, CA, USA). PCR products were quantified using the QuantiFluor™-ST fluorometer quantitative system (Promega Biotech, Beijing, China) and mixed with the appropriate proportion based on sequencing requirements. Sequencing was conducted by Majorbio Bio-Pharm Technology Co., Ltd., Shanghai, China, using an Illumina MiSeq platform (Illumina, San Diego, CA, USA).

2.3 Processing of Illumina sequencing data

Before analysis, raw FASTQ files were demultiplexed and quality-filtered using the software package Quantitative Insight into Microbial Ecology (QIIME, version 1.9.1). The overlapped paired-end sequences were assembled with FLASH. Bacterial reads were truncated at any site receiving an average quality score of <20 over a 50 bp sliding window, discarding the truncated reads that were shorter than 50 bp. Any read containing one or more ambiguous base calls ("N") was discarded. In addition, the truncated reads of <80% (of the raw read length) of consecutive high-quality base calls were discarded. Only sequences that overlapped longer than 10 bp were assembled according to their overlap sequence. Unique sequences were clustered into operational taxonomic units (OTUs), defined as having at least 97% similarity. Taxonomic assignment on the OTUs was performed

using the ribosomal database project (RDP) classifier (version 2.2)[1] against the SILVA (Release132)[2] ribosomal RNA gene database with a minimum confidence threshold of 0.7. Sequences representing chloroplasts and mitochondria were filtered out. Shared and unique OTUs were graphically represented in Venn diagrams as described in Chen and Boutros (2011).

2.4 Statistical analyses

Sobs richness estimates, Shannon's diversity index values, Shannon's evenness index values, and the Good's coverage were calculated in MOTHUR for total, and the evaluation index is used in the OTU at a similar level of 97% (0.97). The unweighted pair-group method with arithmetic mean (UPGMA) was selected for beta diversity to capture phylogenetic distance while not taking relative abundance into consideration. UniFrac distance metrics analysis was performed using OTUs for each sample, and principal coordinate analysis (PCoA) and hierarchical clustering analysis were computed using QIIME software (Version 1.9.1)[3] with unweighted_uniFrac distance. PCoA was conducted based on RDP classifier results from MOTHUR, OTUs, and weighted UniFrac. Linear discriminant analysis (LDA) effect size (LEfSe) was used to elucidate the differences among bacterial taxa. The LDA score of ≥4 was considered to be an important contributor to the model. The relationship between environmental variables and the bacterial communities in Poyang Lake was analyzed by redundancy analysis (RDA)/canonical correlation analysis (CCA). Redundant variables were eliminated by functions of envfit (permu = 999) and vif.cca. The comparison of predicted functional profiles between water and sediment habitats was examined by using FAPROTAX based on raw OTU tables. It was defined as significant when the Welch *t*-test yielded a value of p of <0.05. The shifts in the relative abundance of bacterial phyla were displayed by a heat map, which was modeled with a vegan package in R. The Spearman correlation coefficients of the top 20 abundant bacterial phyla and environmental factors were calculated and displayed on the heat map.

3 Results

3.1 Physicochemical variables

Significant fluctuations in the physicochemical properties were observed in each sample site from June to October 2020, while there were obvious differences between different sampling sites during the same time as well. The results of physicochemical parameters in water and sediment samples are shown in Table 1. In the water column, the values of TR, pH, Eh, WT, CO, DO, suspended substance (SS), TN, DTN, TP, DTP, NO_3-N, NO_2-N, NH_4-N, PO_4-P, COD_{Mn}, Chl *a*, Chl *b*, and PC ranged from 50 to 150 cm, 7.38 to 8.80, 134.90 to 437.30 mV, 19.08 to 34.10°C, 0.07 to 0.14 ms/cm, 3.62 to 12.88 mg/L, 0.80 to 38.50 mg/L, 0.92 to 2.84 mg/L, 0.80 to 1.87 mg/L, 0.03 to 0.19 mg/L, 0.01 to 0.11 mg/L, 0.19 to 1.10 mg/L, 0.00 to 0.07 mg/L, 0.15 to 0.62 mg/L, 1.00 to 21.00 μg/L, 2.12 to 4.57 mg/L, 3.64 to 61.75 μg/L, 0.02 to 50.91 μg/L, and 14.29 to 489.60 μg/L, respectively, and with the average values of 93.76 cm, 8.02, 252.65 mV, 26.71°C, 0.10 ms/cm, 7.83 mg/L, 9.84 mg/L, 1.42 mg/L, 1.18 mg/L, 0.08 mg/L, 0.05 mg/L,0.53 mg/L, 0.01 mg/L,0.32 mg/L, 7.10 μg/L, 2.99 mg/L, 34.53 μg/L, 18.28 μg/L, and 64.22 μg/L, respectively. In sediment, the contents of STN, STP, and SOM ranged from 1.49 to 11.56 mg/kg, 0.13 to 1.41 mg/kg, and 2.44 to 10.76 g/100 g, respectively, with mean values of 5.01 mg/kg, 0.78 mg/kg, and 6.04 g/100 g, respectively.

TABLE 1 Physicochemical parameters in water and sediment samples collected from Poyang Lake.

Parameters	Mean	Maximum	Minimum
Transparency (cm)	93.76	150.00	50.00
pH	8.02	8.80	7.38
Eh (mV)	252.65	437.30	134.90
Water temperature (°C)	26.71	34.10	19.08
Conductivity (ms/cm)	0.10	0.14	0.07
DO (mg/L)	7.83	12.88	3.62
SS(mg/L)	9.84	38.50	0.80
TN(mg/L)	1.42	2.84	0.92
DTN(mg/L)	1.18	1.87	0.80
TP(mg/L)	0.08	0.19	0.03
DTP(mg/L)	0.05	0.11	0.01
NO_3-N(mg/L)	0.53	1.10	0.19
NO_2-N(mg/L)	0.01	0.07	0.00
NH_4-N(mg/L)	0.32	0.62	0.15
PO_4-P(μg/L)	7.10	21.00	1.00
COD_{Mn}(mg/L)	2.99	4.57	2.12
Chl *a*(μg/L)	34.53	61.75	3.64
Chl *b*(μg/L)	18.28	50.91	0.02
PC (μg/L)	64.22	489.60	14.29
STN (mg/kg)	5.01	11.56	1.49
STP(mg/kg)	0.78	1.41	0.13
SOM(g/100 g)	6.04	10.76	2.44

3.2 Diversity of bacterial communities in water and sediment samples

Sequencing data were successfully generated from 34 water samples and 49 sediment samples. DNA from all water samples in July was not successfully extracted. A total of 3,810,287 16S rRNA sequence tags were generated through pyrosequencing, with an average read length of approximately 416 bp that ranged in size from 202 to 534 bp and clustered into 17,465 OTUs at a 97% nucleotide similarity level. The microbial diversity in sediment (16,380 OTUs) was higher than that in water (6,682 OTUs) samples; meanwhile, unique species accounted for 16.24% of all 6,682 OTUs in water and 65.83% of all 16,380 OTUs in sediment, and the number of shared OTUs between water and sediment was 5,597 (Figure 2). All data were

1 http://sourceforge.net/projects/rdp-classifier/

2 http://www.arb-silva.de

3 http://qiime.org/install/index.html

normalized to the smallest sequence tag, and then the data were reanalyzed to show a normal distribution of variances (Table 2).

In the water column, the dominant phyla (relative abundance>2%) were *Actinobacteriota* (33.45%), followed by *Cyanobacteria* (29.73%), *Proteobacteria* (22.01%), *Bacteroidota* (4.02%), and *Chloroflexi* (3.06%), making up 91.91% of the total OTUs (Figure 3). During the survey period, *Actinobacteriota* peaked in September, while *Cyanobacteria* peaked in June, and *Proteobacteria* changed indistinguishably. The composition of bacteria in sediment was more complex than in water. *Proteobacteria* (17.63%), *Actinobacteriota* (14.73%), *Chloroflexi* (14.63%), and *Acidobacteriota* (14.49%) occupied the first concentration gradient in sediment, with a total content of 61.48%. *Nitrospirota* (4.59%), *Bacteroidota* (4.04%), *Myxococcota* (3.67%), *Desulfobacterota* (3.49%), *MBNT15* (3.22%), *Gemmatimonadota* (2.50%), *Sva0485* (2.20%), and *Firmicutes* (2.11%) were close behind, with a total content of 25.82% (Figure 3).

Comparing relative abundances of these dominant phyla between the water column and sediment, *Actinobacteriota* (33.45% vs. 14.73%, $p < 0.001$) and *Cyanobacteria* (29.73% vs. 1.48%, $p < 0.001$) had a significantly higher relative abundance in water than in sediment, while *Chloroflexi* (3.06% vs. 14.63%, $p < 0.001$), *Acidobacteriota* (0.72% vs. 14.49%, $p < 0.001$), *Nitrospirota* (0.078% vs. 4.59%, $p < 0.001$), *Myxococcota* (0.19% vs. 3.67%, $p < 0.001$), *Desulfobacterota* (0.14% vs. 3.49%, $p < 0.001$), *MBNT15* (0.032% vs. 3.22%, $p < 0.001$),

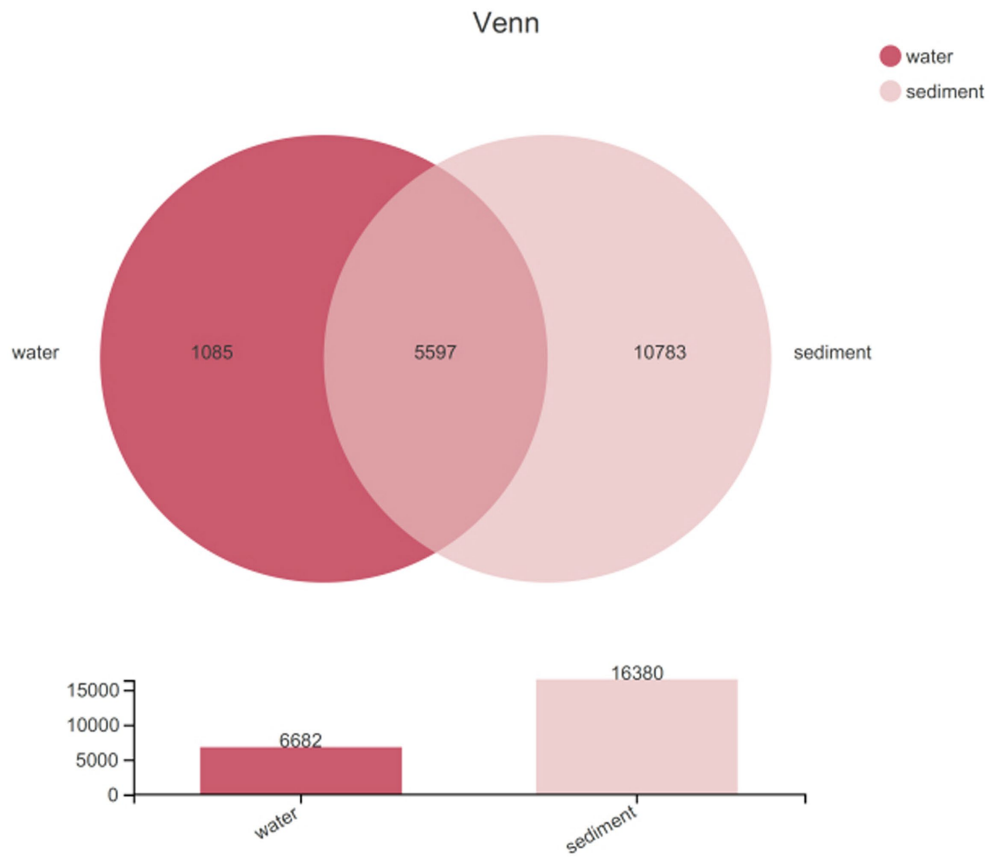

FIGURE 2
A Venn diagram showing the unique and shared OTUs in water column and sediment.

TABLE 2 Normalized summary of sequence library, OTUs, and bacterial diversity indices of water column samples and sediment samples from Poyang Lake.

		Nseqs	OTUs	Chao	Shannon	Simpson	Coverage
Sediment	Mean	47941.24	3929.88	5685.09	6.77	0.0058	0.950
	Maximum	84887.00	6045.00	7660.80	7.46	0.0409	0.989
	Minimum	34303.00	1794.00	2207.11	4.80	0.0018	0.904
Water	Mean	42975.47	1043.53	1276.93	4.28	0.0518	0.992
	Maximum	56,596	2,146	2282.87	5.18	0.103	0.999
	Minimum	33,714	471	503.36	3.42	0.0224	0.983

Firmicutes (0.75% vs. 2.11%, $p < 0.001$), *Gemmatimonadota* (0.28% vs. 2.50%, $p < 0.001$), and *Sva 0485* (0.03% vs. 2.20%, $p < 0.001$) had a significantly lower relative abundance in water samples (Wilcoxon rank-sum test) (Figure 4).

The LEfSe method identified a suite of specialized bacterial taxa enriched in the water column and sediment, respectively (Figure 5). Based on the bacteria abundance at the phylum level, partitioning around medoids (PAM) analysis was performed to cluster the microflora at the phylum level (Figure 5, Jensen–Shannon distance). The result showed that the water column and sediment have their own unique bacterial types (Figure 6). The water samples belonged to the *Proteobacteria* type, while the sediment samples belonged to the *Actinobacteriota* type.

To assess changes in the diversity of bacterial communities with each sample, hierarchical cluster analysis was performed (Figure 7A). The resulting dendrograms revealed apparent differences between water and sediment. The samples from water niches clustered closely together, while the samples from sediment formed the other group. Water samples from the same month were clustered closely together. On the whole, sediment samples from 10 sites were separated into three groups: the channel areas group (namely sites 1–5), the Lake Bay group (sites 6–8), and the Zhouxi Bay group (sites 9 and 10). The same

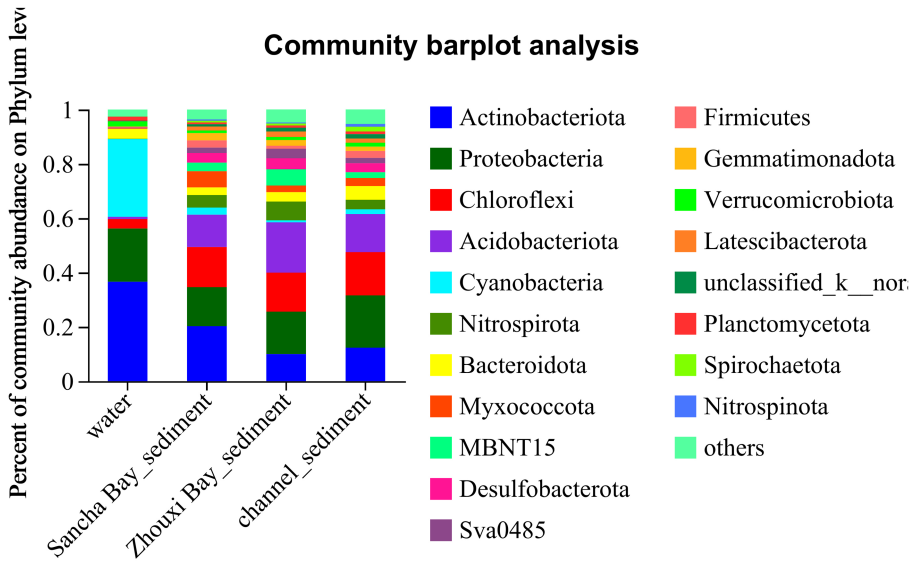

FIGURE 3
The distribution of microbial community for water and sediment from the Sancha Bay, the Zhouxi Bay, and channel areas on the phylum level.

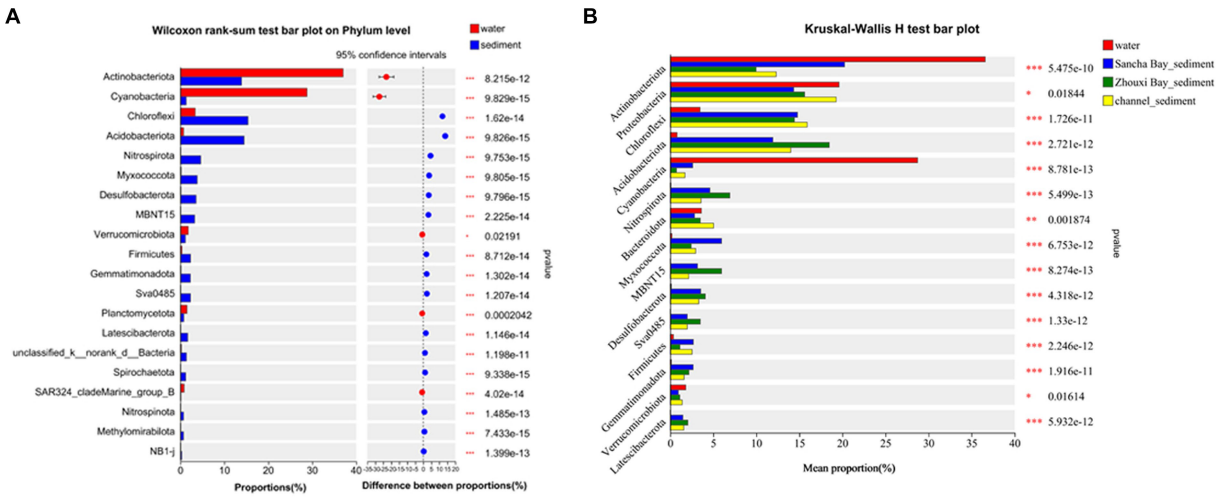

FIGURE 4
Wilcoxon rank-sum test bar plot on phylum level showing the significant differences between water and sediment **(A)**, Kruskal–Wallis H-test bar plot at the phylum level showing the significant differences among water and sediment from the Sancha Bay, the Zhouxi Bay, and channel **(B)**. Positive differences in mean relative abundance indicate the bacterium is overrepresented on sediment **(A)**, while negative differences indicate greater abundance in water **(A)**. $*p < 0.05$; $**p < 0.01$; $***p < 0.001$.

10.3389/fmicb.2024.1362968

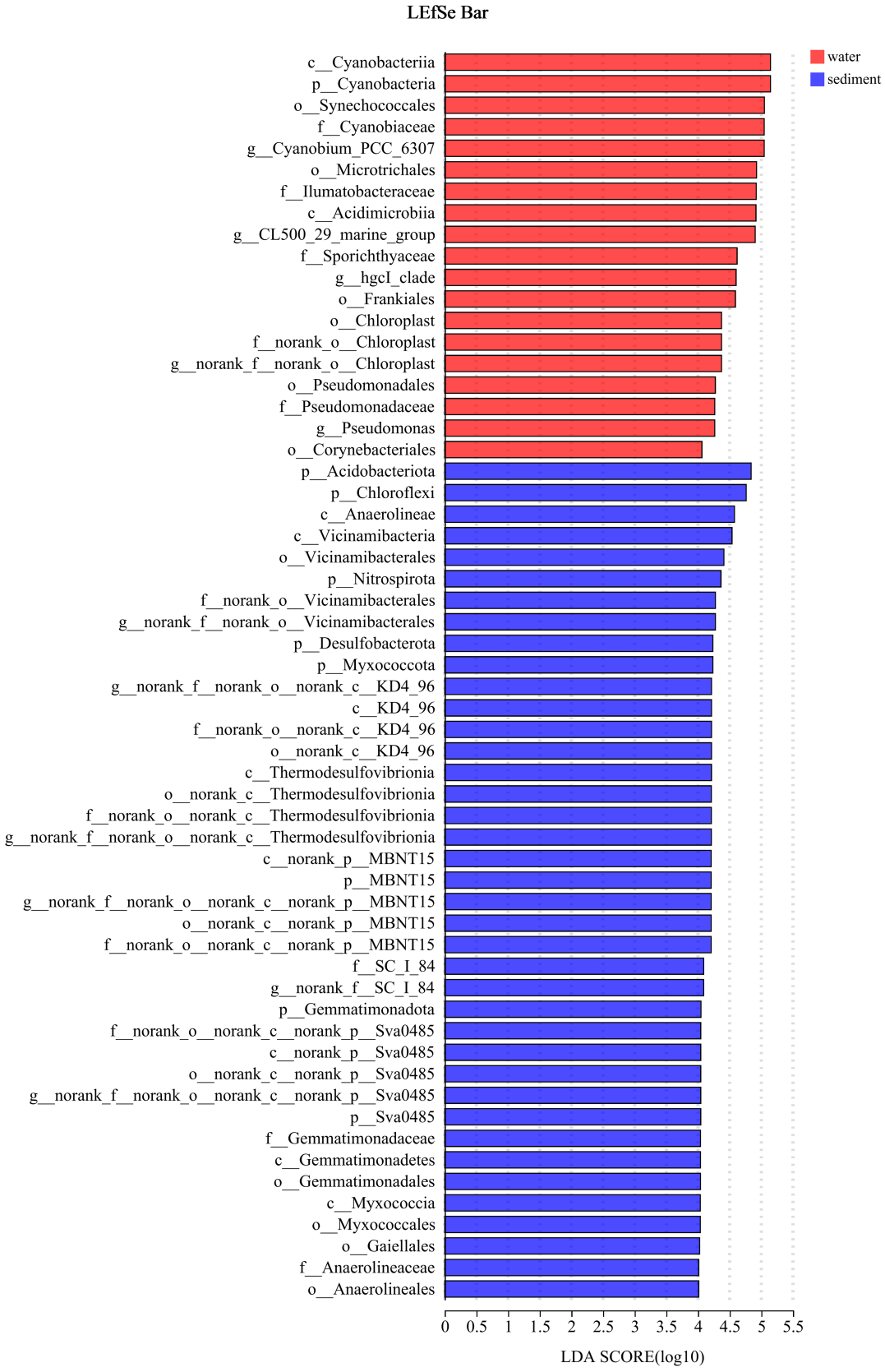

FIGURE 5
Indicator bacteria with LDA scores of 4 or greater in bacterial communities (phylogenetic levels from phylum to genus associated with water and sediment). Different colored regions represent different constituents (red, water; blue, sediment).

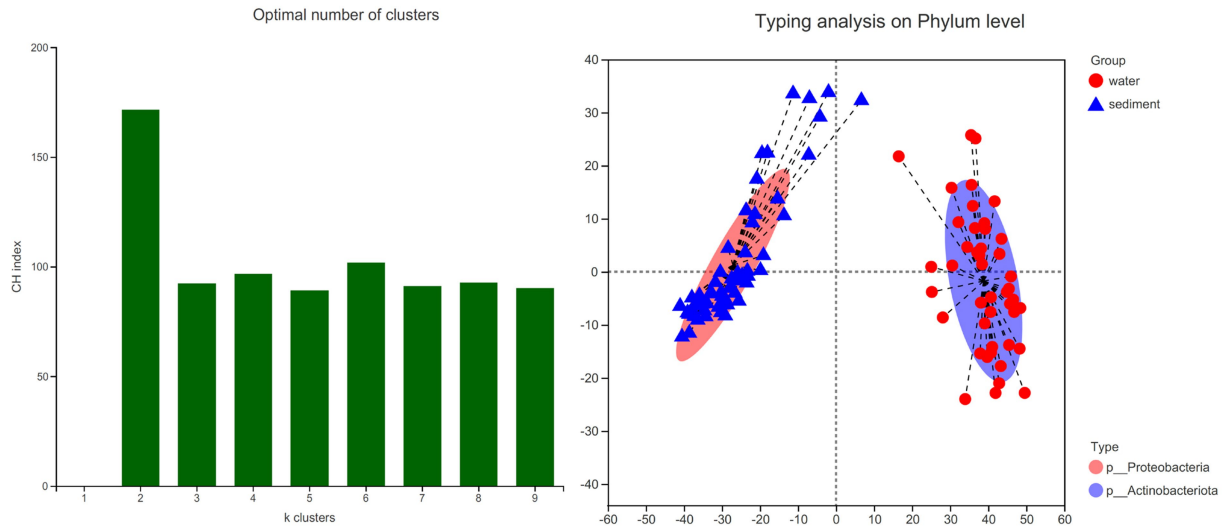

FIGURE 6
Bacterial type analysis for water and sediment using Jensen–Shannon distance. The left panel shows that the data are most naturally separated into two clusters by the PAM method. The *x*-axis shows the cluster number; the *y*-axis shows the CH index, a measure of cluster separation. The right panel shows the clustering of the first two principal components. The data indicates that water column bacteria belong to the Proteobacteria type, while sediment bacteria belong to the Actinobacteriota type.

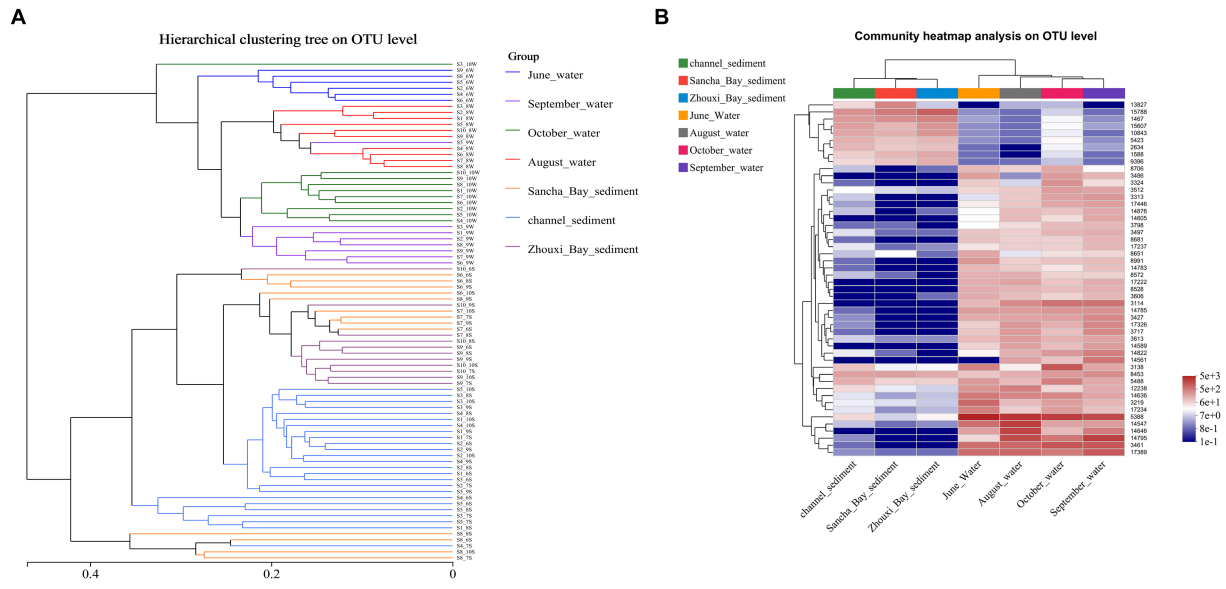

FIGURE 7
Comparison of water and sediment bacterial communities. **(A)** Hierarchical cluster analysis results based on Bray–Curtis at the OTU level. Unweighted pair-group method with arithmetic mean (UPGMA) analysis of bacterial community structure based on the 16S rRNA gene amplicon sequencing data. **(B)** The heat map showed the relative abundance of the bacterial OTU in water and sediment samples.

group clustering results were also shown in the community heat map analysis (Figure 7B).

The bacterial α-diversity indices of Poyang Lake were much lower in water than that in the sediment (Table 2). Welch's *t*-test showed an extremely significant difference in alpha diversity between water and sediment samples ($p < 0.001$) (Figures 8A–D). There were significant differences in OTU richness (Sobs) among the sediment from the Sancha Bay, the Zhouxi Bay, and the channel sites. However, no significant difference in the Shannon index was found between the sediment from the Sancha Bay and the Zhouxi Bay. The difference in the Shannon index between the Sancha Bay and the channel area was greater than that between the Zhouxi Bay and the channel area (Figures 8E–H). There were significant differences in the Shannon index among the water from different months except for June and September (Figures 8I–L).

Principal coordinates analysis results revealed that the significant differences in bacterial communities between the water column and the sediment were with the first two principal component scores,

10.3389/fmicb.2024.1362968

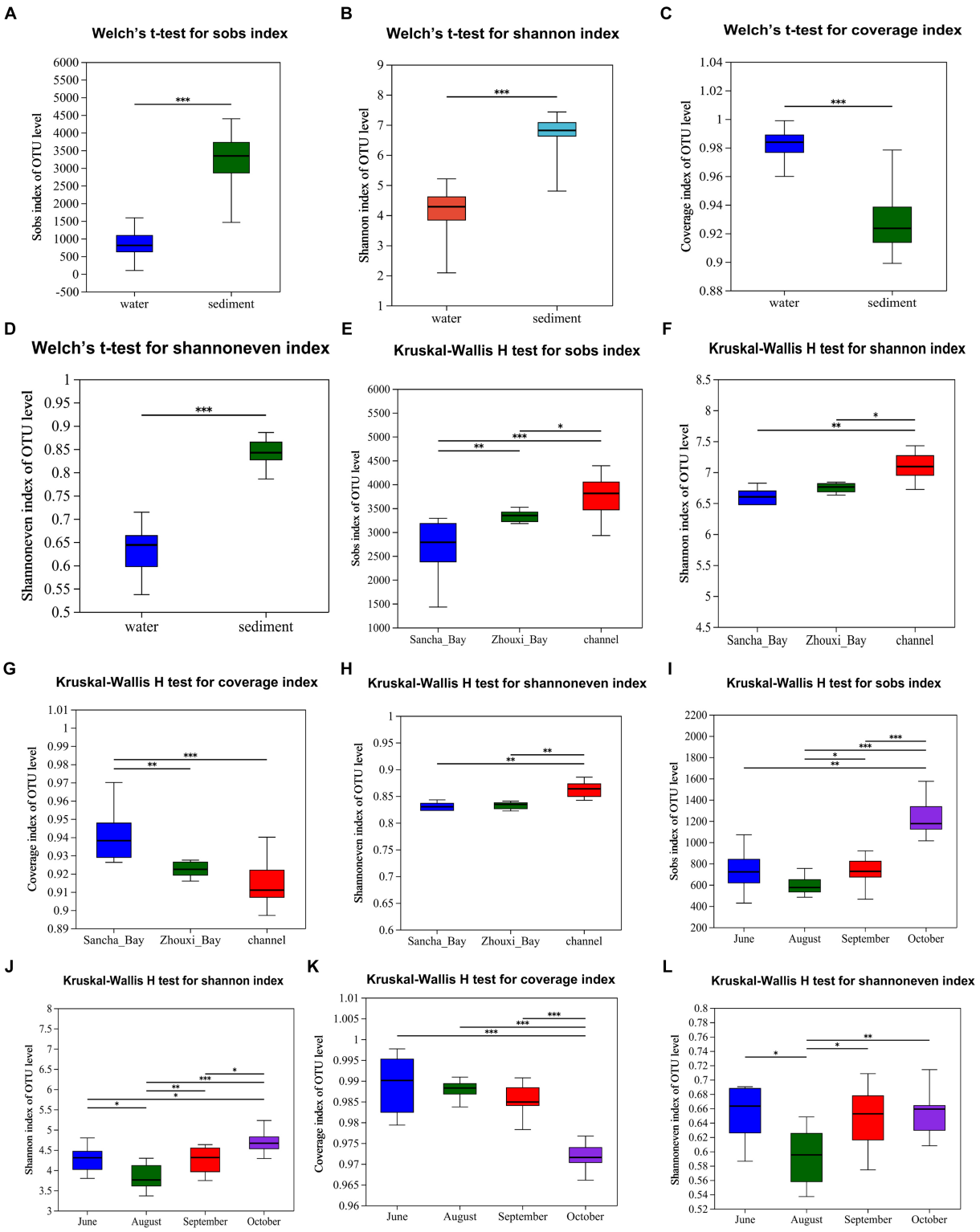

FIGURE 8
Alpha diversity (Sobs, Shannon, Coverage, and Shannoneven) of bacterial communities in the water column and sediment (**A–D**, Welch's t-test), Lake Bay sediment, channel sediment (**E–H**, Kruskal–Wallis H-test), and water from different seasons **(I–L)**. *$p < 0.05$, **$p < 0.01$, ***$p < 0.0001$.

which accounted for 34.67 and 5.30% of the total variations ($R = 0.9871$, $p = 0.001$) (Figure 9A). The water samples from different months also had obvious different bacterial communities with the first two principal component scores, which accounted for 7.74 and 15.26% of the total variations ($R = 0.7518$, $p = 0.001$) (Figure 9B), while no seasonal variation of bacterial communities in sediment was observed (Figure 9C). Obvious differences in bacterial communities in sediment among two lake bays and channel areas were found [with the first two

10.3389/fmicb.2024.1362968

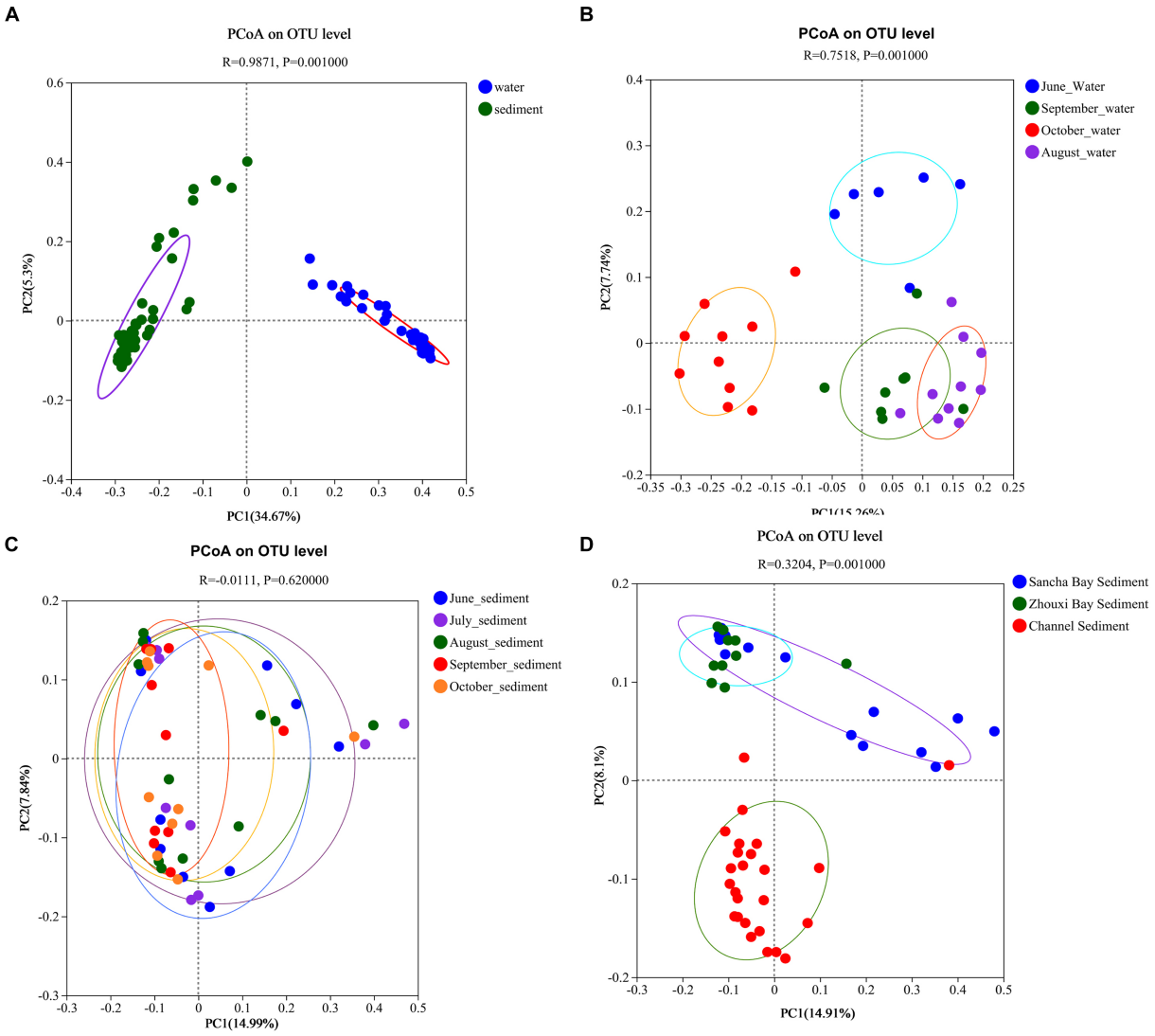

FIGURE 9
Principal coordinate analysis based on unweighted UniFrac distances between water and sediment **(A)**, among water from different months **(B)**, among sediment from different months **(C)**, and among sediment from different areas **(D)** of Poyang Lake.

principal component scores accounting for 8.10 and 14.91% of the total variations ($R = 0.3204$, $p = 0.001$)] (Figure 9D).

3.3 Putative function profiles of microbial communities

The predicted functional groups were revealed using FAPROTAX, and a total of 74 functional groups were obtained in Poyang Lake. Among them, chemoheterotrophy, aerobic chemoheterotrophy, phototrophy, photoautotrophy, cyanobacteria, oxygenic photoautotrophy, animal parasites or symbionts, human pathogens pneumonia, hydrocarbon degradation, methylotrophy, chloroplasts, methanotrophy, fermentation, nitrogen fixation, and aromatic compound degradation were the most abundant groups in both habitats (Figure 10). By using Welch *t*-test, the functional groups of chemoheterotrophy (sediment 19.77% vs. water 9.75%, $p < 0.001$), aerobic chemoheterotrophy (11.30% vs. 7.56%, $p < 0.001$), animal parasites or symbionts (9.66% vs. 2.52%, $p < 0.001$), human pathogens all (9.54% vs. 2.41%, $p < 0.001$), human pathogens pneumonia (9.12% vs. 1.78%, $p < 0.001$), hydrocarbon degradation (4.12% vs. 1.43%, $p < 0.001$), methylotrophy (4.05% vs. 0.98%, $p < 0.001$), methanotrophy (3.70% vs. 0.77%, $p < 0.001$), fermentation (3.72% vs. 0.69%, $p < 0.001$), nitrogen fixation (3.28% vs. 0.79%, $p < 0.001$), and aromatic compound degradation (2.81% vs. 0.87%, $p < 0.001$) were significantly enriched in sediment, while the mean proportions of phototrophy (water 14.96% vs. sediment 2.09%, $p < 0.001$), photoautotrophy (14.77% vs. 1.90%, $p < 0.001$), cyanobacteria (14.75% vs. 1.87%, $p < 0.001$), oxygenic photoautotrophy (14.75% vs. 1.87%, $p < 0.001$), and chloroplasts (3.36% vs. 1.42%, $p < 0.001$) were significantly higher in water (Figure 10).

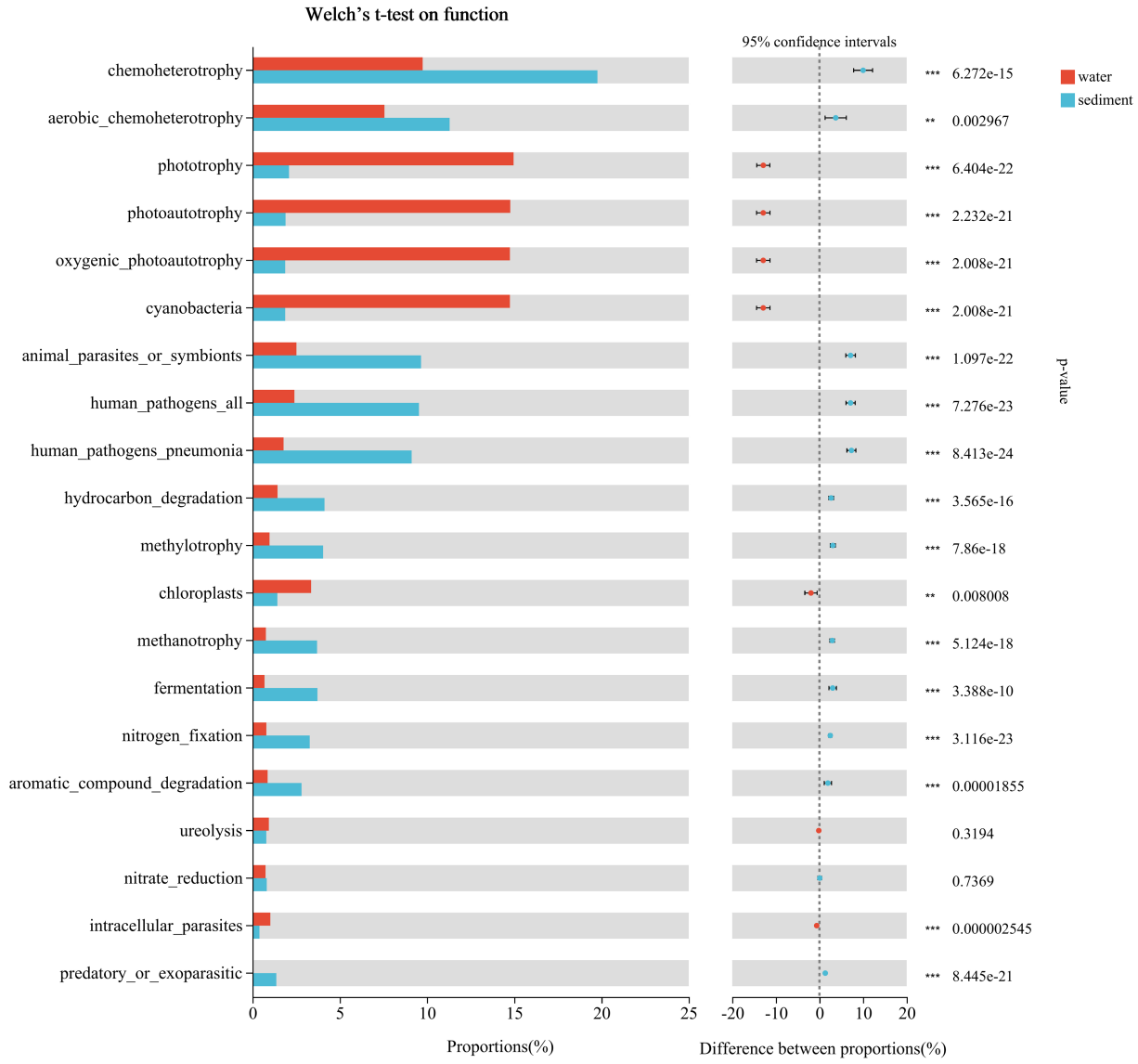

FIGURE 10
Putative function profiles of microbial communities in the water column and sediment from Poyang Lake.

3.4 Correlation between bacterial community structure and environmental parameters

Environmental factors were selected by the functions envfit (permu = 999) and vif.cca, and environmental factors with a value of p of >0.05 or vif>10 were removed from the following analysis. The vif values of NO_3-N, Chl *b*, and STN were higher than 10 and then were removed. An RDA/CCA was conducted to reveal the effect of environmental factors on the microbial community structures in water and sediment. After the removal of the redundant variables, 12 environmental factors were chosen for RDA/CCA, including WT, Eh, CO, DO, DTN, TP, NO_2-N, NH_4-N, Chl *a*, COD_{Mn}, SOM, and STP. In all the examined environmental factors, WT (p = 0.001), NH_4-N (p = 0.001), STP (p = 0.002), SOM (p = 0.001), Chl *a* (p = 0.002), DO (p = 0.003), TP (p = 0.029), and Eh (p = 0.04) were significantly correlated with the water microbial community structure in water (Figure 11A), while SOM (p = 0.001) and STP (p = 0.041) were important factors that significantly correlated with the microbial community structures in sediment (Figure 11B).

For more details, the relationship between bacterial phyla and environmental factors was demonstrated by a correlation heat map (Figure 11). In water samples (Figure 12A), *Acidobacteria* showed an extremely significant positive correlation with SOM, STP, and Chl *a*, and an extremely significant negative correlation with NH_4-N and DTN. *Cyanobacteria* showed an extremely significant positive correlation with COD_{Mn} and NH_4-N and an extremely negative correlation with Chl *a*. *Chloroflexi* demonstrated an extremely negative correlation with WT, a negative correlation with DTN and NH_4-N, a positive correlation with DO, and a significant correlation

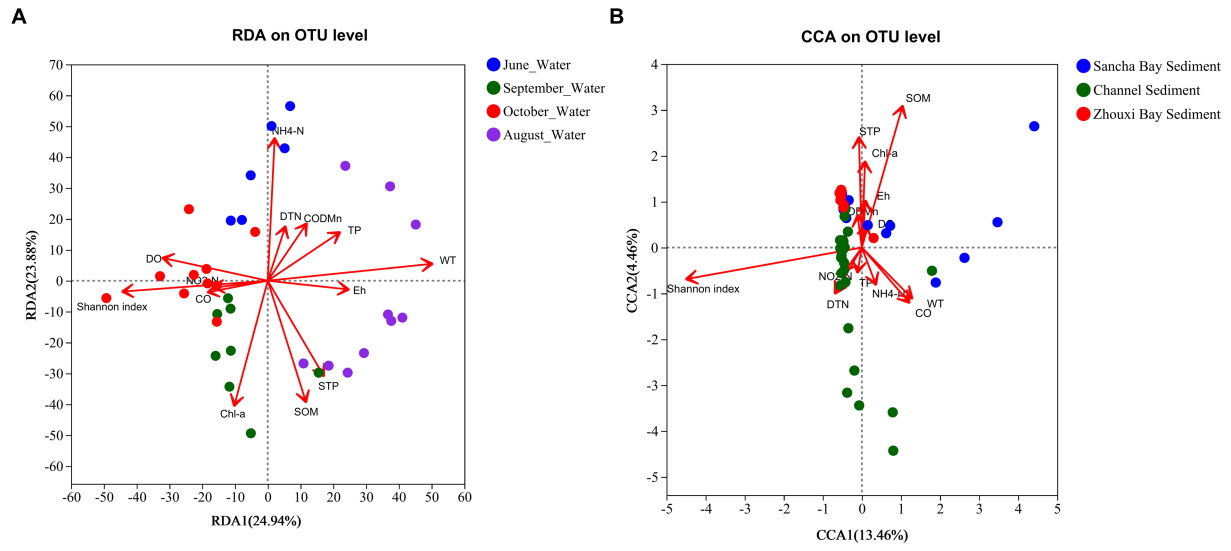

FIGURE 11
CCA/RDA analysis to show correlations between the bacterial communities and environmental factors in water **(A)** and sediment **(B)** samples from Poyang Lake.

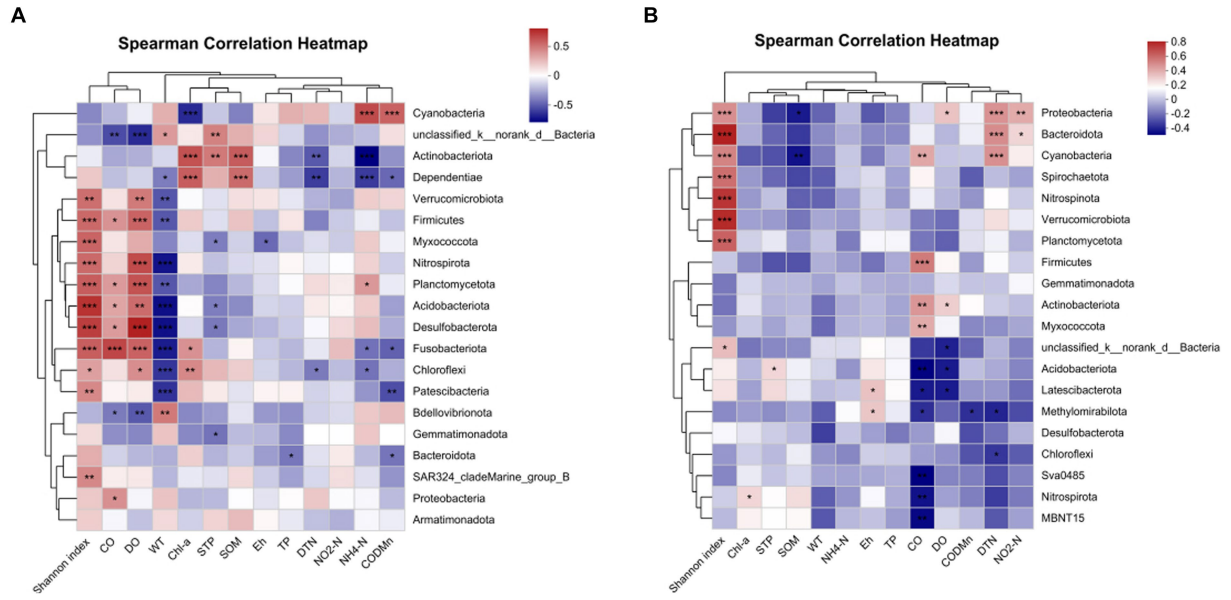

FIGURE 12
Correlation heat map of the top 20 phyla in water **(A)** sediment **(B)** and environmental factors. *X* and *Y* axes are environmental factors and phyla. R in different colors to show the right side of the legend is the color range of different *R* values. The value of 0.01 < Pnd environmental factors. X and <Pnd environmental factors. *X* and *Y* axes are environmental factors. **P* < 0.05, ***P* < 0.01, ****P* < 0.0001.

with Chl *a*. However, there were quite different correlations in sediment samples. In sediment, *Actinobacteria* was significantly positively correlated with CO and DO, while *Acidobacteriota* was extremely significantly negatively correlated with CO and DO and had a significant positive correlation with STP (Figure 12B). In addition, *Chloroflexi* demonstrated a negative correlation with DTN, and *Proteobacteria* was extremely significantly positively correlated with DTN, significantly positively correlated with NO_2-N and DO, and significantly negatively correlated with SOM (Figure 12B).

4 Discussion

4.1 Diversity of bacterial communities in water and sediment

In the present study, bacterial DNA in water samples collected from all the sampling sites in July was not extracted successfully. This might be due to the water level fluctuation. Previous studies reported that the water quality of Poyang Lake was the best in

summer (Wu et al., 2017), and the water level has a net positive effect on water quality through the dilution of environmental parameters, including the bacteria in the water (Ren et al., 2019). The water level at the time we sampled in July was 21.74 m (measured at Xingzi Station, an iconic hydrological station on Poyang Lake), which was at the historic high level of Poyang Lake (Liao and Kang, 2021). Because of the dilution, the amount of bacterial DNA in the 300 mL of water sample in July was not sufficient for the determination of bacterial diversity.

It is well known that *Proteobacteria* and *Actinobacteria* were most abundantly distributed in surface water and sediment in Poyang Lake (Dong et al., 2019; Ren et al., 2019; Zhao et al., 2020; Guo et al., 2023) and other lakes (Eiler et al., 2012; Mohiuddin et al., 2017). In the present study, the most abundant taxon in surface water during the extreme flood season was *Actinobacteriota* (33.45%), followed by *Cyanobacteria* (29.73%) and *Proteobacteria* (22.01%). While the composition of bacteria in sediment was more complex than in water, *Proteobacteria* (17.63%), *Actinobacteriota* (14.73%), *Chloroflexi* (14.63%), and *Acidobacteriota* (14.49%) occupied 60.78%. Previous studies highlighted that the different abundances of *Proteobacteria* and *Actinobacteria* in freshwater systems may be a result of different hydrological conditions, and the moderate variation in the properties of the water would not decrease their predominance (Warnecke et al., 2004; Zhao et al., 2020). According to our results, the extremely high water level (Xingzi Station: 21.74 m) did not decrease the predominance of these two groups in Poyang Lake. In the present study, the content of Cyanobacteria in water was much higher than that in sediment, which was 29.73% vs. 1.484% ($p < 0.001$). This was consistent with the finding of another research (Guo et al., 2023), which highlighted that Poyang Lake had a higher abundance of Cyanobacteria in water than that in sediment. In addition, our study also found that Cyanobacteria content was significantly different among the different sampling months ($p < 0.001$), Because of the significant correlations between Cyanobacteria biomass in water and the level of water eutrophication during the period of cyanobacterial blooms (Zhu et al., 2019), more attention must paid to the water quality of Poyang Lake (Qi et al., 2018; Zhang et al., 2021).

The distribution of TLI-PY in the whole Poyang Lake was relatively uniform (Qi, 2017), and the development of the bacterioplankton community composition in the euphotic layer showed a cyclical temporal pattern in freshwater ecosystems (Salmaso et al., 2017). In the present study, the bacterial diversity in the water of Poyang Lake during the extreme flood season showed clear temporal differentiation, while spatial differentiation was not pronounced. Such a phenomenon existed not only in these freshwaters but also in seawater (Meziti et al., 2015). In the present study, the bacterial community structure in the sediment showed obvious regionalism, and the sediment bacterial community structure from the Lake Bay and the channel area can be distinguished from each other, especially the phylum of *Proteobacteria*, *Acidobacteriota*, *Actinobacteriota*, *Nitrospirota*, and *Bacteroidota*. Similar results were reported in other lakes, which showed that the bacterial abundance and community structure of the lake sediment showed spatial heterogeneity in accordance with variations (Ding et al., 2015; Kou et al., 2016). In the present study, the Shannon index showed that there was no significant difference in bacterial diversity between the Sancha Bay and the Zhouxi Bay sediments, and this might be due to the geographical proximity of the Sancha Bay and the Zhouxi Bay areas, and the similarity of agricultural and fishing environments between these two lake bays (Zeng et al., 2023), and then the continuous heavy rain had caused a large amount of surrounding sediment to enter the lake.

In the present study, the difference in microbial diversity in sediment between the Sancha Bay and the channel was significantly higher than that between the Zhouxi Bay and the channel, and the microbial diversity gradually increased from the Sancha Bay to the Zhouxi Bay and then to the channel, but STN and STP concentrations showed opposite trends. This might be due to the anthropogenic disturbances from the extreme flood. Jin et al. (2019) reported that both physicochemical and microbiological parameters are indicated by anthropogenic disturbances in Poyang Lake, and N and P contents were not the main factors affecting bacteria abundance in the sediments of Poyang Lake (Guo et al., 2023). In addition, the exchange frequency of water flow (Adams et al., 2015) and depth (Zemskaya et al., 2020) have an impact on the bacterial structure in lakes.

Generally, the bacterial community and diversity in sediment are significantly higher than that in water. In the present study, the bacterial α-diversity indices of Poyang Lake were much lower in the water than that in the sediment. Similar results were found in Poyang Lake, and the habitat's characteristics play an important role in microbiome formation (Sun et al., 2020; Guo et al., 2023).

4.2 Putative function profiles of microbial communities

In the present study, the most abundant groups in sediment and water were chemoheterotrophy, aerobic chemoheterotrophy, phototrophy, photoautotrophy, cyanobacteria, oxygenic photoautotrophy, animal parasites or symbionts, human pathogens pneumonia, hydrocarbon degradation, methylotrophy, chloroplasts, methanotrophy, fermentation, nitrogen fixation, and aromatic compound degradation. Compared to previous studies in Poyang Lake (Zhao et al., 2020), the abundance of genes related to human pathogens in our study is much higher. Zhao et al. (2020) reported that the major functions were chemoheterotrophy, phototrophy, photoautotrophy, cyanobacterial, oxygenic photoautotrophy, aerobic chemoheterotrophy, methylotrophy, and methanol oxidation, while functions such as animal parasites or symbionts, human pathogens all, hydrocarbon degradation, nitrification, and fermentation had a much lower presentation. However, the mean proportions of animal parasites or symbionts, human pathogens all, and human pathogen pneumonia in sediment were 9.66, 9.54, and 9.12%, respectively, and in water were 2.52, 2.41, and 1.78, respectively. This might be due to the flood water, which brought a high amount of pollutants (including pathogens) into Poyang Lake and posed a risk to human health. Since the possible origins of the water pathogens in the freshwater system include point sources (e.g., industrial wastewater and urban sewage) and non-point sources (e.g., land-based runoff containing wild and domestic animal excreta, leaking sewage, and agricultural effluent) (Pachepsky et al., 2011; Wan et al., 2022), large amounts of the above pollutants can enter lakes with surface runoff during heavy rainfall.

4.3 Microbial variation in the environment

Previous studies highlighted that the characteristics of BCC in water and sediment confirmed the significant correlations between bacterial diversity and levels of nutrients (Zhu et al., 2019; Guo et al.,

2023). C, N, and P are recognized as key variables in microbial ecology due to their effects on the growth of certain bacteria in water and sediment (Zhang et al., 2020). In Poyang Lake, the nutrient concentrations in the water showed dramatic seasonal patterns (Ren et al., 2019), while the sediment nutrients showed obvious region and ecological niche distribution (Kou et al., 2016; Sun et al., 2020). This directly affected the bacterial community structure in both water and sediment. N, P, and other nutrients in the lake sediment are the endogenous load of the nutritive state of the lake. In the present study, the water bacterial diversity was not only correlated with the nutrient elements such as N and P in the water but also significantly correlated with the total P content in the sediment. This result might be due to the fact that the N, P, and other nutrients in the sediment will be released back into the water column under the mutual influence of various conditions (Cheng et al., 2020).

In the present study, during this extreme flood season, WT, NH_4-N, SOM, Chl a, STP, and TP were significantly correlated with water microbial community structure, while SOM and STP were significantly correlated with sediment microbial community structure. That is to say that the bacterial community structure in the water column was not only sensitive to the geochemical characteristics of the water (WT, NH_4-N, Chl *a*, and TP) but also affected by the nutrients in the sediment (SOM and STP). Lindström et al. (2005) and Lindström and Östman (2011) highlighted that temperature, pH, lake water retention time, and local conditions were closely related to BCC. In one terminal reservoir (Miyun Reservoir) of the South-to-North Water Diversion Project, the WT was positively correlated with the dominant bacteria; the total dissolved solids, TP, DO, and TN were the other factors that affected the structure and distribution of the water microbial community (Qu et al., 2018). In other water bodies, the relationship between microbial community diversity and WT was significantly correlated with each other (Chalifour et al., 2021). PH was also an important factor affecting bacterial diversity in many other habitats (Wang et al., 2016; Qian et al., 2018). However, in the present study, the pH values of water had little effect on the bacterial community. This might be due to the small change in the pH value (8.11 ± 0.36) in the water of Poyang Lake during the extreme flood season.

5 Conclusion

We revealed microbial structure and functions in Poyang Lake during the extreme flood season. Our study demonstrated that the bacterial community structure in water was greatly different from that in sediment in Poyang Lake during extreme flood seasons, and the dominant phyla in the water column were *Actinobacteriota, Cyanobacteria*, and *Proteobacteria,* while in sediment, the dominant phyla were *Proteobacteria*, *Actinobacteriota*, *Chloroflexi*, and *Acidobacteriota*. The bacterial community structure in the water column was affected not only by geochemical characteristics but also by the STP concentration in the sediment, and the bacterial diversity in the sediment was influenced by SOM and STP contents. In addition, the abundance of genes related to human pathogens in Poyang Lake was found, and the flood water with a high amount of pollutants is the main reason.

Data availability statement

The original contributions presented in the study are included in the article/Supplementary material, further inquiries can be directed to the corresponding author/s.

Author contributions

LZ: Conceptualization, Data curation, Formal analysis, Investigation, Methodology, Writing – original draft. LY: Formal analysis, Investigation, Writing – original draft. JX: Formal analysis, Writing – original draft. QL: Investigation, Writing – review & editing. DZ: Conceptualization, Data curation, Funding acquisition, Investigation, Supervision, Writing – original draft, Writing – review & editing. JL: Investigation, Writing – review & editing.

Funding

The author(s) declare financial support was received for the research, authorship, and/or publication of this article. This study was financially supported by the National Natural Science Foundations of China (Grant nos. 31960266, 31360133, and 42161016) and the Science and Technology Project of Jiangxi Province (Grant nos. 20213AAG01012 and 20212BCD43002).

Acknowledgments

We would like to express our heartfelt appreciation to He Liu for providing fieldwork support. Special thanks are due to the Lake Poyang Laboratory for Wetland Ecosystem Research (PLWER) for providing the foundation for the experiment.

Conflict of interest

The authors declare that the research was conducted in the absence of any commercial or financial relationships that could be construed as a potential conflict of interest.

Publisher's note

Supplementary material

The Supplementary material for this article can be found online at: https://www.frontiersin.org/articles/10.3389/fmicb.2024.1362968/full#supplementary-material

References

Adams, H. E., Crump, B. C., and Kling, G. W. (2015). Isolating the effects of storm events on arctic aquatic bacteria: temperature, nutrients, and community composition as controls on bacterial productivity. *Front. Microbiol.* 6:250. doi: 10.3389/fmicb.2015.00250

American Public Health Association (1998). *Standard methods for the examination of water and waste water. 20th edn*. Washington: American public Health Association.

Chalifour, A., Walser, J. C., Pomati, F., and Fenner, K. (2021). Temperature, phytoplankton density and bacteria diversity drive the biotransformation of micropollutants in a lake ecosystem. *Water Res.* 202:117412. doi: 10.1016/j.watres.2021.117412

Chen, M. (2020). Characteristics and Enlightenment of Rainstorm and Flood in Yangtze River in 2020. *Yangtze River* 51, 76–81 (in Chinese). doi: 10.16232/j.cnki.1001-4179.2020.12.016

Chen, H. B., and Boutros, P. C. (2011). Venn Diagram: a package for the generation of highly-customizable Venn and Euler diagrams in R. *BMC Bioinformatics* 12:35. doi: 10.1186/1471-2105-12-35

Cheng, X. L., Huang, Y. N., Li, R., Pu, X. C., Huang, W. D., and Yuan, X. F. (2020). Impacts of water temperature on phosphorus release of sediments under flowing overlying water. *J. Contam. Hydrol.* 235:103717. doi: 10.1016/j.jconhyd.2020.103717

Department of Water and Soil Conservation (2012). *SL 88–2012 Water quality-determination of chlorophyll by spectrophotometry*. Beijing: Chinese Water Conservancy and Hydropower Press.

Ding, X., Peng, X. J., Jin, B. S., Xiao, M., Chen, J. K., Li, B., et al. (2015). Spatial distribution of bacterial communities driven by multiple environmental factors in a beach wetland of the largest freshwater lake in China. *Front. Microbiol.* 6:129. doi: 10.3389/fmicb.2015.00129

Dong, Y. H., Li, J. L., Sun, Z. X., Soldatova, E., and Zan, J. J. (2019). Bacterial diversity and community structure in nitrate-contaminated shallow groundwater in the Poyang Lake basin, China. *E3S Web of Conferences* 98:01012. doi: 10.1051/e3sconf/20199801012

Eiler, A., Heinrich, F., Bertilsson, S. (2012). Coherent dynamics and association networks among lake bacterioplankton taxa. *ISME J.* 6:330–342. doi: 10.1038/ismej.2011.113

Felföldi, T. (2020). Microbial communities of soda lakes and pans in the Carpathian Basin: a review. *Biol. Futur.* 71, 393–404. doi: 10.1007/s42977-020-00034-4

Guo, J. X., Wang, X., Cao, X. F., Qi, W. X., Peng, J. F., Liu, H. J., et al. (2023). The influence of wet-to-dry season shifts on the microbial community stability and nitrogen cycle in the Poyang Lake sediment. *Sci. Total Environ.* 903:166036. doi: 10.1016/j.scitotenv.2023.16603

He, H., Chen, X. J., Hou, F. J., Wu, Y. P., and Cheng, Y. X. (2017). Bacterial and fungal community structures in Loess Plateau grasslands with different grazing intensities. *Front. Microbiol.* 8:606. doi: 10.3389/fmicb.2017.00606

Huang, Z. Y., Wang, J. Y., and Zhou, W. (2021). Characteristics Analysis of an Extreme Heavy Rain Event in the Middle Reaches of the Yangtse River from July 4 to 8 in 2020. *Torrential Rain and Disasters* 40, 333–341 (in Chinese). doi: 10.3969/j.issn.1004-9045.2021.04.001

Jin, X.C., and Tu, Q.Y. (1990). *Lake Eutrophication Survey Specification*. Beijing: Environmental Science Press, 208–230.

Jin, X., Ma, Y. T., Kong, Z. Y., Kou, W. B., Wu, L. (2019). The variation of sediment bacterial community in response to anthropogenic disturbances of Poyang Lake, China. *Wetlands* 39:S63–S73. doi: 10.1007/s13157-017-0909-1

Kou, W. B., Zhang, J., Lu, X. X., Ma, Y. T., Mou, X. Z., and Wu, L. (2016). Identification of bacterial communities in sediments of Poyang Lake, the largest freshwater lake in China. *Springer Plus* 5:401. doi: 10.1186/s40064-016-2026-7

Liao, J. Y., and Kang, S. Y. (2021). Analysis and reflection of the exceeding design standard flood in Poyang Lake Basin in 2020. *China Flood Drought Manag.* 31, 45–48 (in Chinese). doi: 10.16867/j.issn.1673-9264.2020324

Lindström, E. S., Agterveld, M. P. K., and Zwart, G. (2005). Distribution of typical freshwater bacterial groups is associated with pH, temperature, and lake water retention time. *Appl. Environ. Microbiol.* 71, 8201–8206. doi: 10.1128/AEM.71.12.8201-8206

Lindström, E. S., and Östman, Ö. (2011). The importance of dispersal for bacterial community composition and functioning. *PLoS One* 6:e25883. doi: 10.1371/journal.pone.0025883

Liu, Z. J., Wang, X. H., Jia, S. Q., and Mao, B. Y. (2023). Eutrophication causes analysis under the influencing of anthropogenic activities in China's largest fresh water lake (Poyang Lake): Evidence from hydrogeochemistry and reverse simulation methods. *J. Hydrol.* 625:130020. doi: 10.1016/j.jhydrol.2023.130020

Meziti, A., Kormas, K. A., Moustaka-Gouni, M., and Karayanni, H. (2015). Spatially uniform but temporally variable bacterioplankton in a semi-enclosed coastal area. *Syst. Appl. Microbiol.* 38, 358–367. doi: 10.1016/j.syapm.2015.04.003

Mohiuddin, M. M., Salama, Y., Schellhorn, H. E., Golding, G. B. (2017). Shotgun metagenomic sequencing reveals freshwater beach sands as reservoir of bacterial pathogens. *Water Res.* 115, 360–369. doi: 10.1016/j.watres.2017.02.057

Newton, R. J., Jones, S. E., Eiler, A., McMahon, K. D., and Bertilsson, S. (2011). A guide to the natural history of freshwater lake bacteria. *Microbiol. Mol. Biol. R.* 75, 14–49. doi: 10.1128/MMBR.00028-10

Ni, Z. K., Wang, S. R., Wu, Y., Liu, X. F., Lin, R. P., and Liu, Z. Z. (2020). Influence of exposure time on phosphorus composition and bioavailability in wetland sediments from Poyang lake, since the operation of the Three Gorges Dam. *Environ. Pollut.* 263:114591. doi: 10.1016/j.envpol.2020.114591

Pachepsky, Y., Shelton, D. R., McLain, J. E., Patel, J., and Mandrell, R. E. (2011). Irrigation waters as a source of pathogenic microorganisms in produce: a review. *Adv. Agron.* 113, 75–141. doi: 10.1016/B978-0-12-386473-4.00002-6

Qi, L.Y. (2017). *Assessment and simulation of aquatic ecosystem health in Lake Poyang*. University of Chinese Academy of Sciences: Beijing, China.

Qi, L. Y., Huang, J. C., Huang, Q., Gao, J. F., Wang, S. G., and Guo, Y. Y. (2018). Assessing aquatic ecological health for Lake Poyang, China: Part I index development. *Water* 10:943. doi: 10.3390/w10070943

Qian, G., Wang, J., Kan, J. J., Zhang, X. D., Xia, Z. Q., Zhang, X. C., et al. (2018). Diversity and distribution of anammox bacteria in water column and sediments of the Eastern Indian Ocean. *Int. Biodeterior. Biodegradation* 133, 52–62. doi: 10.1016/j.ibiod.2018.05.015

Qu, J. Q., Jia, C., Liu, Q., Li, Z., Liu, P., Yang, M., et al. (2018). Dynamics of bacterial community diversity and structure in the terminal reservoir of the south-to-north water diversion project in China. *Water* 10:709. doi: 10.3390/w10060709

Ren, Z., Qu, X. D., Zhang, M., Yu, Y., and Peng, W. Q. (2019). Distinct bacterial communities in wet and dry seasons during a seasonal water level fluctuation in the largest freshwater lake (Poyang Lake) in China. *Front. Microbiol.* 10:1167. doi: 10.3389/fmicb.2019.01167.eCollection2019

Salmaso, N., Albanese, D., Capelli, C., Boscaini, A., Pindo, M., and Donati, C. (2017). Diversity and cyclical seasonal transitions in the bacterial community in a large and deep perialpine lake. *Microb. Ecol.* 76, 125–143. doi: 10.1007/s00248-017-1120-x

Sun, R., Tu, Z. X., Fan, L., Qiao, Z. X., Liu, X. Y., Hu, S. H., et al. (2020). The correlation analyses of bacterial community composition and spatial factors between freshwater and sediment in Poyang Lake wetland by using artificial neural network (ANN) modeling. *Braz. J. Microbiol.* 51, 1191–1207. doi: 10.1007/s42770-020-00285-2

Wan, X. L., Li, J., Wang, S. Y., Fan, F., Mclaughlin, R. W., Wang, K. X., et al. (2022). Biogeographic patterns of potential pathogenic bacteria in the middle and lower reaches of the Yangtze River as well as its two adjoining lakes, China. *Front. Microbiol.* 13:972243. doi: 10.3389/fmicb.2022.972243

Wang, N. F., Zhang, T., Yang, X., Wang, S., Yu, Y., Dong, L. L., et al. (2016). Diversity and composition of bacterial community in soils and lake sediments from an arctic lake area. *Front. Microbiol.* 7:1170. doi: 10.3389/fmicb.2016.01170

Warnecke, Y. F., Amann, R., and Pernthaler, J. (2004). Actinobacterial 16S rRNA genes from freshwater habitats cluster in four distinct lineages. *Environ. Microbiol.* 6, 242–253. doi: 10.1111/j.1462-2910.2004.00561.x

Wu, Z. S., Zhang, D. W., Cai, Y. J., Wang, X. L., Zhang, L., and Chen, Y. W. (2017). Water quality assessment based on the water quality index method in Lake Poyang: The largest freshwater lake in China. *Sci. Rep.* 7:17999. doi: 10.1038/s41598-017-18285-y

Xu, N., Tan, G., Wang, H., Wang, H. Y., and Gai, X. P. (2016). Effect of biochar additions to soil on nitrogen leaching, microbial biomass and bacterial community structure. *Eur. J. Soil Biol.* 74, 1–8. doi: 10.1016/j.ejsobi.2016.02.004

Zemskaya, T. I., Cabello-Yeves, P. J., Pavlova, O. N., and Rodriguez-Valera, F. (2020). Microorganisms of Lake Baikal-the deepest and most ancient lake on earth. *Appl. Microbiol. Biotechnol.* 104, 6079–6090. doi: 10.1007/s00253-020-10660-6

Zeng, B. R., Li, Y. L., Yao, J., and Tan, Z. Q. (2023). The characteristics and evolution of structural and functional connectivity in a large catchment (Poyang Lake) during the past 30 years. *Remote Sens.* 15:3335. doi: 10.20944/preprints202305.1918.v1

Zhang, L., Fang, W. K., Li, X. C., Lu, W. X., and Li, J. (2020). Strong linkages between dissolved organic matter and the aquatic bacterial community in an urban river. *Water Res.* 184:116089. doi: 10.1016/j.watres.2020.116089

Zhang, J., Wei, Y. C., Wang, G. X., Yang, F., Cheng, C. M., and Xia, X. R. (2013). Comparison of extraction methods for phycocyanin from blooms water samples in Lake Taihu (In Chinese). *J. Lake Sci.* 25, 283–288. doi: 10.18307/2013.0216

Zhang, Y., Zhu, H. Y., Li, B., Yang, G. S., and Wan, R. G. (2021). Aquatic ecosystem health assessment of Poyang lake through extension evaluation method. *Water* 13:211. doi: 10.3390/w13020211

Zhao, M., Ma, Y. T., He, S. Y., Mou, X. Z., and Wu, L. (2020). Dynamics of bacterioplankton community structure in response to seasonal hydrological distuerbances in Poyang Lake, the largest wetland in China. *FEMS Microbiol. Ecol.* 96:fiaa 064. doi: 10.1093/femsec/fiaa064

Zhu, C. M., Zhang, J. Y., Nawaz, M. Z., Mahboob, S., Al-Ghanim, K. A., Khan, I. A., et al. (2019). Seasonal succession and spatial distribution of bacterial community structure in a eutrophic freshwater Lake, Lake Taihu. *Sci. Total Environ.* 669, 29–40. doi: 10.1016/j.scitotenv.2019.03.087

frontiers | Frontiers in Microbiology

TYPE Original Research
PUBLISHED 23 April 2024
DOI 10.3389/fmicb.2024.1355859

OPEN ACCESS

EDITED BY
Michael Rappe,
University of Hawaii at Manoa, United States

REVIEWED BY
Qiang Gao,
Qinghai University, China
Xiukun Wu,
Chinese Academy of Sciences (CAS), China
Jesper Bjerg,
Aarhus University, Denmark

*CORRESPONDENCE
Xiafei Zheng
✉ zhengxiafei@hotmail.com
Bo Wu
✉ wubo28@mail.sysu.edu.cn

RECEIVED 14 December 2023
ACCEPTED 27 March 2024
PUBLISHED 23 April 2024

CITATION
Yang X, Wu Y, Shu L, Gu H, Liu F, Ding J, Zeng J, Wang C, He Z, Xu M, Liu F, Zheng X and Wu B (2024) Unraveling the important role of comammox *Nitrospira* to nitrification in the coastal aquaculture system. *Front. Microbiol.* 15:1355859. doi: 10.3389/fmicb.2024.1355859

Unraveling the important role of comammox *Nitrospira* to nitrification in the coastal aquaculture system

Xueqin Yang[1], Yongjie Wu[2], Longfei Shu[1], Hang Gu[1], Fei Liu[1], Jijuan Ding[1], Jiaxiong Zeng[1], Cheng Wang[1], Zhili He[1,3], Meiying Xu[4], Feifei Liu[4], Xiafei Zheng[5]* and Bo Wu[1]*

[1]Southern Marine Science and Engineering Guangdong Laboratory (Zhuhai), Environmental Microbiomics Research Center, School of Environmental Science and Engineering, Sun Yat-sen University, Guangzhou, China, [2]Ministry of Ecology and Environment, South China Institute of Environmental Sciences, Guangzhou, China, [3]College of Agronomy, Hunan Agricultural University, Changsha, China, [4]State Key Laboratory of Applied Microbiology Southern China, Guangdong Institute of Microbiology, Guangdong Academy of Sciences, Guangzhou, China, [5]Ninghai Institute of Mariculture Breeding and Seed Industry, Zhejiang Wanli University, Ningbo, China

Increasing nitrogen (N) input to coastal ecosystems poses a serious environmental threat. It is important to understand the responses and feedback of N removal microbial communities, particularly nitrifiers including the newly recognized complete ammonia-oxidizers (comammox), to improve aquaculture sustainability. In this study, we conducted a holistic evaluation of the functional communities responsible for nitrification by quantifying and sequencing the key functional genes of comammox Nitrospira-amoA, AOA-amoA, AOB-amoA and Nitrospira-nxrB in fish ponds with different fish feeding levels and evaluated the contribution of nitrifiers in the nitrification process through experiments of mixing pure cultures. We found that higher fish feeding dramatically increased N-related concentration, affecting the nitrifying communities. Compared to AOA and AOB, comammox Nitrospira and NOB were more sensitive to environmental changes. Unexpectedly, we detected an equivalent abundance of comammox Nitrospira and AOB and observed an increase in the proportion of clade A in comammox Nitrospira with the increase in fish feeding. Furthermore, a simplified network and shift of keystone species from NOB to comammox Nitrospira were observed in higher fish-feeding ponds. Random forest analysis suggested that the comammox Nitrospira community played a critical role in the nitrification of eutrophic aquaculture ponds (40–70 μM). Through the additional experiment of mixing nitrifying pure cultures, we found that comammox Nitrospira is the primary contributor to the nitrification process at 200 μM ammonium. These results advance our understanding of nitrifying communities and highlight the importance of comammox Nitrospira in driving nitrification in eutrophic aquaculture systems.

KEYWORDS

nitrogen addition, nitrifying community, comammox *Nitrospira*, network, contribution to nitrification

1 Introduction

The microbially driven nitrification process, which converts ammonium to nitrate via nitrite, is a vital process of the N cycle. It is also the rate-limiting step for the N removal process (Daims et al., 2015; Kuypers et al., 2018). Newly enriched and further isolated bacteria (*Nitrospira inopinata*) were shown to possess the ability of complete ammonium oxidization to nitrate by one organism (Daims et al., 2015; van Kessel et al., 2015; Santoro, 2016; Kits et al., 2017). This type of bacteria was named complete ammonia-oxidizing (comammox) bacteria and was theoretically predicated by kinetic modeling (Costa et al., 2006). Before this, nitrification was considered a two-step process for more than one century, which was carried out by ammonia-oxidizing bacteria (AOB) or archaea (AOA) (Könneke et al., 2005) and nitrite-oxidizing bacteria (NOB), respectively (Daims et al., 2016). However, the diversity, composition, and interactions of these nitrifiers, especially the newly discovered comammox, in response to environmental changes, as well as their contribution to the nitrification process in nutrient-enriched aquaculture systems, are not yet fully understood.

The discovery of comammox raised researchers' interests on their diversity, distribution, and composition as well as their contribution to the nitrification process. To the best of our knowledge, the phylogenetic analysis showed that all known comammox bacteria were annotated as *Nitrospira* sublineage II (Daims et al., 2015; van Kessel et al., 2015; Daims et al., 2016) and were further divided into two clades, namely comammox *Nitrospira* clades A and clades B (Lawson and Lucker, 2018; Xia et al., 2018). The only isolate of comammox bacteria (*N. inopinata*) was the representative strain of clades A, which was reported to have the highest ammonia affinity than that of most AOA and AOB except the pure culture of marine AOA (*Nitrosopumilus maritimus*) (Hu and He, 2017; Kits et al., 2017). Surprisingly, no comammox *Nitrospira* have been found in the open ocean (Zhu et al., 2022). Evidence from the target enrichment of comammox *Nitrospira* in a membrane bioreactor with limiting ammonium and their predominance in biofilms of rotating biological contactor (approximately 15 μM ammonium) (Spasov et al., 2020) and rapid sand filters of drinking water treatment plants (Palomo et al., 2016; Fowler et al., 2018) further confirmed the importance of comammox *Nitrospira* to the nitrification process in those oligotrophic ecosystems.

However, a growing body of environmental research found that comammox *Nitrospira* were also widely distributed in less oligotrophic or eutrophic environments, including coastal systems (Xia et al., 2018), agricultural soils (Orellana et al., 2018), and wastewater treatments (Daims et al., 2016; Pinto et al., 2016; Bartelme et al., 2017; Wang et al., 2017; Annavajhala et al., 2018; Fowler et al., 2018). For instance, a recent study showed the abundance of comammox *Nitrospira* was much higher than canonical nitrifiers in a eutrophic lake (Chaohu lake, NH_4^+ was as high as 10 mM) and their abundance was positively related to ammonium in the paddy soils of Shaoguan and Antu (Shi et al., 2020). These results suggested that comammox *Nitrospira* may play a crucial role in nutrient-enriched environments. A previous study showed that comammox *Nitrospira* had a higher diversity than AOA or AOB (Shi et al., 2020; Spasov et al., 2020). Furthermore, comammox *Nitrospira* clade A was suggested to have a wider distribution and greater abundance compared to clade B (Fowler et al., 2018; Xia et al., 2018; Xu et al., 2020). Compared to canonical nitrifiers, clade A comammox bacteria *Ca. N. nitrificans* were positively linked to other species and served as the keystone species (Shi et al., 2020). These results suggested the diversity and niche heterogeneity of comammox *Nitrospira* may explain their ubiquity in eutrophic conditions. Due to the essential roles of nitrifiers and the hitherto under-researched role of the newly discovered comammox *Nitrospira*, it is necessary to consider all nitrifiers and a combination of their community traits (diversity, composition, interaction network, and keystone species) to better comprehend the nitrification process in eutrophic ecosystems.

In our study, we investigated the diversity and composition of the nitrifiers in aquatic ponds which were nitrogen (N) enriched environments, as N is added in the form of formulated feeds, whereas only 11–36% of the input N is converted to fish biomass (Hargreaves, 1998; Hu et al., 2012; Yuan et al., 2019). Thus, the remaining unabsorbed N which is converted into ammonium through ammonification enters into aquaculture ponds and adjacent ecosystems (Hargreaves, 1998; Hu et al., 2012; Yuan et al., 2019; Garlock et al., 2020). We selected 12 fish ponds with three replicates and divided them into two categories (small fish (SF) and large fish (LF) ponds) through different eutrophication degrees as LF ponds had higher eutrophication degrees with higher feeding amounts. We analyzed environmental variables, the abundance, composition, and diversity of comammox *Nitrospira amoA*, AOA *amoA*, AOB *amoA*, and *Nitrospira nxrB* to investigate how nitrifying communities, especially comammox *Nitrospira*, responded to different eutrophication levels. Furthermore, we used mix-culturing experiments of pure cultures (*N. inopinata*, *Nitrososphaera gargensis*, *Nitrosomonas communis,* and *N. moscoviensis*) with comparable ammonium addition to quantify their contribution to the nitrification process. We hypothesized that higher fish feeding altered the diversity, structure, and interactions of the nitrifying community, and comammox *Nitrospira* especially clade A played a crucial role in the nitrification process. This study advances our understanding of nitrifying communities, especially comammox *Nitrospira* in eutrophic conditions, and provides new insights into sustainable aquacultures.

2 Materials and methods

2.1 Site description and sampling

Aquaculture ponds were in Nansha, Guangzhou, China (22°60′97.88″N, 113°62′18.05″E) with each pond covering an area of 1.5 km^2, and the depth of water was approximately 3 m. Water and sediment samples were collected with three biological replicates in 12 ponds for a total of 72 samples on 31 May 2018. A hydrophore sampler was used to collect surface water (1 L per sample, 50 cm depth below the surface), and a Van Veen grab sampler was used to collect sediment at a depth of approximately 0–8 cm (approximately 500 g). All the samples were collected in 1 day with clear weather. Ponds were divided into six small fish (SF) ponds and six large fish ponds (LF) according to the weight of grass carp per unit volume of the pond (0.03 kg/m^2 vs. 0.06 kg/m^2) in previous studies (Zhang et al., 2020; Zheng et al., 2021). The dosage of organic fish feed per m^2 per day was approximately 5% of total fish weight. Samples were stored in a 4°C car refrigerator and transferred to the laboratory within 1 h at noon. Part of the fresh water and sediment samples were stored at 4°C for

physicochemical analysis, and the rest were stored at −80°C for microbial DNA extraction.

2.2 Physicochemical analysis

Temperature, pH, DO, and salinity of the water (approximately 50 cm below the surface water) were measured *in situ* by portable meters, which were calibrated and used according to the manufacturer's instructions (pH meter with temperature detector, SevenCompact™ pH Meter S210, Mettler-Toledo, United States; DO meter, 550A, YSI, USA; salinity meter, EUTECH SALT6+, Thermo Fisher Scientific, United States). The transparency of the water was measured *in situ* by Secchi disk. Chlorophyll a, total suspended solids (TSS), particle organic carbon (POC), dissolved organic carbon (DOC), and total organic carbon (TOC) of water were measured as previously described (Zhang et al., 2020; Zheng et al., 2021). Ammonium, nitrite, nitrate, total inorganic nitrogen (TIN), total organic nitrogen (TON), total nitrogen (TN), phosphate, total organic phosphorus (TOP), and total phosphorus (TP) were measured as previously described (Zheng et al., 2017a,b). The sediments were oven-dried at 65°C until a constant weight was reached, then sieved through a 200-mesh sieve to obtain sediment powder for the measurement of total carbon (sTC), nitrogen (sTN), and total sulfur (sTS) using an elemental analyzer (Vario TOC, Elemental, Germany). Total phosphorus (sTP), elemental sulfur (sES), and acid-volatile sulfur (sAVS) were determined as described previously (Zhang et al., 2020; Zheng et al., 2021).

2.3 Sediment microbial community DNA extraction

Microbial community DNA of 36 sediment samples (5 g of each sample) was extracted and purified by a combined protocol of the classic freeze–grind method and the DNeasy PowerSoil Kit (Qiagen, Dusseldorf, Germany) following the instructions in http://www.ou.edu/ieg/tools/protocols. The concentration and quality of extracted DNA were determined using a NanoDrop One spectrophotometer (Thermo Fisher Scientific, MA, United States) and stored at −20°C until subsequent experiments.

2.4 Quantitative real-time PCR analysis

The copy number of *amoA* genes from comammox *Nitrospira*, AOA and AOB, *nxrB* from *Nitrospira,* and 16S rRNA gene from bacterial communities were quantified by real-time quantitative PCR (qPCR) (Supplementary Table S1). Comammox *Nitrospira*, AOA and AOB *amoA*, *Nitrospira nxrB*, and 16S rRNA gene (V3 region) were obtained by using corresponding primer pairs (Supplementary Table S1) as primers and pure culture DNA as templates (*Nitrospira inopinata*, *Nitrososphaera gargensis*, *Nitrosomonas communis*, *Nitrospira moscoviensis,* and *E. coli*, respectively). The fragment of the V3 region was amplified using universal primers 338F and 536R (Xia et al., 2018). Purified PCR products were cloned into the pEASY TA vector (TransGen Biotech, Beijing, China), inserted into competent cells, and spread onto an LB plate. *E. coli* with target genes were selected to grow in a liquid LB medium, and then, plasmids were extracted as standards for quantification using the NucleoSpin Plasmid Kit (Macherey-Nagel, Düren, Germany). The concentration of plasmids was determined using Qubit 4.0 (Thermo Fisher Scientific, MA, United States). The qPCRs were run with three technical replicates in a Bio-Rad C1000 CFX96 real-time PCR system (United States). Each qPCR was prepared in a 20-μl reaction mix containing 10 μL of SYBR Green Supermix (Bio-Rad, United States), 4 μL of the suspension, 0.5 μL of each primer (10 μM), and 5 μL of ddH_2O. The thermal qPCR program was as follows: 3 min at 98°C, followed by 40 cycles of 15 s at 98°C, 30s for annealing at 46, 55, 56, 52, and 57.5°C, respectively, for five marker genes, and 30s at 72°C, and then ended with a final extension at 72°C for 10 min. The amplification efficiency was between 90 and 110%, and the correlation coefficient (r^2) of the standard curve was greater than 0.99.

2.5 PCR amplification, purification, and high-throughput sequencing

The functional maker genes of nitrifiers including comammox *Nitrospira amoA* (Ntsp-amoA 162F and Ntsp-amoA 359R) (Fowler et al., 2018), AOA *amoA* (Arch-amoA26F and Arch-amoA417R) (Park et al., 2008) and AOB *amoA* (amoA-1F and amoA-2R) (Rotthauwe et al., 1997), and *Nitrospira nxrB* (169Fand 638R) (Pester et al., 2014) were amplified using a PCR thermocycler instrument (T100, Bio-Rad, United States) (Supplementary Table S1). Although theoretically both NOB and known comammox contained *Nitrospira nxrB* gene (Annavajhala et al., 2018; Roots et al., 2019), here *Nitrospira nxrB* had approximately 10-fold higher abundance than comammox *Nitrospira amoA*. The amplification system with a total volume of 25 μL contained 12.5 μL of 2xEasyTaq SuperMix (TransGen Biotech, Beijing, China), 8.5 μL ddH_2O, 1 μL of forward and reverse primers (10 μM), and 2 μL of appropriately diluted DNA (approximately 10–50 ng/μL). The thermal program was initial denaturation at 98°C for 3 min, followed by 25 cycles of denaturation at 98°C for 15 s, annealing for 30s (46, 56, 56, and 52°C for four marker genes, respectively), and extension at 72°C for 30s and ended with a final extension at 72°C for 10 min. PCR products were purified using an AxyPrep PCR Clean-up Kit (Axygen, MA, United States). The concentration of purified PCR product was determined using the Qubit 4.0 fluorometer (Thermo Fisher Scientific, MA, United States), and the quality was checked using a LabChip GX Touch HT nucleic acid analyzer (PerkinElmer, MA, United States). Purified PCR products after the quality control were pooled at equal concentrations for sequencing using an Illumina MiSeq-PE300 or NovaSeq-PE250 system according to the manufacturer's guidelines. Raw sequence data have been submitted to NCBI Sequence Read Archives with an accession number PRJNA834749.

2.6 Sequencing data analysis

The raw data were split by their specific barcodes and then trimmed to remove sequencing primers. Sequence combination, adapter removal, length, and quality control were performed using Cutadapt (Martin, 2011) and fastp (Chen et al., 2018). Chimeras were

removed through VSEARCH (Rognes et al., 2016) by mapping to the Ribosomal Database Project (RDP) database. RDP FrameBot was used to correct frameshift errors (Wang et al., 2013), and UNOISE3 was selected to generate the zero-radius operational taxonomic units (zOTUs) table (Edgar, 2013; Edgar, 2016). zOTUs table was filtered by discarding zOTUs with an average relative abundance of lower than 1/10,000. Finally, the total sequence number was resampled to 10,999. The reference database for annotation was downloaded from FunGene Pipeline.[1] The quality before and after quality control was visualized by FastQC[2] and multiQC.[3]

2.7 Molecular ecological network analysis of nitrifiers

Networks among nitrifiers in SF and LF pond sediments were constructed to elucidate their possible interactions by molecular ecological network analysis (MENA)[4] (Deng et al., 2012) and visualized using gephi (version 0.9.2).[5] zOTUs co-occurred in more than half of the samples that were kept for network construction via the random matrix theory (RMT) method. Network topological properties and module separation were further analyzed (Deng et al., 2012). The connectivity of each node was determined based on the within-module connectivity (Zi) and among-module connectivity (Pi) (Guimera and Amaral, 2005). Nodes were further divided into four categories (module hubs, network hubs, connectors, and peripherals) with a threshold of 2.5 (Zi) and 0.62 (Pi), respectively (Shi et al., 2016).

2.8 The relative contribution of comammox *Nitrospira*, AOA, and AOB to ammonium oxidation

According to the above sequencing results, four ubiquitous monocultures were selected to represent four types of nitrifiers with *N. inopinata* as comammox, *Nitrososphaera gargensis* as AOA, *Nitrosomonas communis* as AOB, and *N. moscoviensis* as NOB. Nitrifiers were cultivated in the medium as described previously (Daims et al., 2015) with 0.2, 1, and 2 mM ammonium at 37°C. The initial total biomass in different treatments was the same (4×10^4 cells/mL). The measurement of cell density, ammonium, nitrite, and nitrate was described in our previous paper (Yang et al., 2022). Nitrate concentration was used when calculating the contribution of nitrifiers to nitrification as it is the product of nitrification. Three ammonium oxidizers were co-cultured with NOB separately [comammox+NOB (1), AOA + NOB (2), and AOB + NOB (3)]. Their maximum nitrate production rates were obtained by detecting the dynamics of nitrate concentration (μ1, μ2, and μ3). Similarly, four nitrifiers were equally mixed and co-cultured together (N4 communities), the maximum nitrate production rate (μ) and relative abundance of the nitrifiers at the endpoint were obtained (abundance of comammox *Nitrospira*: A_c; abundance of AOA: A_A; abundance of AOB: A_B; and abundance of NOB: A_N). The nitrate production rate of the N4 community in theory (μ_{theory}) was roughly calculated as $\mu_{theory} = A_c{*}\mu_1 + A_A{*}\mu_2 + A_B{*}\mu_3$. There was no difference between μ_{theory} and μ which we obtained from the N4 community. The relative contribution of nitrifiers (W_c, W_A, and W_B) in N4 to nitrification was calculated using maximum nitrate production rates of ammonium oxidizers as the weight of their relative abundance in the N4 community (e.g., $W_c = A_c {*}\mu_1/\mu_{theory}{*}100\%$) (Brooks et al., 2015).

2.9 Statistical analysis

Alpha- and beta-diversity were calculated using Qiime (version 1.9.1) (Caporaso et al., 2010). Further analyses and figure plots including the alpha- and beta-diversity indices, principal coordinates analysis (PCoA), redundancy analysis (RDA), Mantel test, and random forest were performed using R (version 4.1.0) with different packages such as ggplot2 (Ginestet, 2011), vegan (Dixon, 2003), ieggr, rfPermute[6] (Breiman, 2001) and ecodist (Goslee and Urban, 2007). The phylogenetic analysis was performed in MEGA X using the maximum-likelihood method (Kumar et al., 2018). Parametric and non-parametric tests were performed with IBM SPSS 22 (SPSS Inc., United States).

3 Results

3.1 Physicochemical properties in fish ponds

Compared to SF ponds, LF ponds had higher ammonium, nitrite, nitrate, total inorganic nitrogen (TIN), total nitrogen (TN), lower total organic nitrogen (TON), and pH with significant difference ($p < 0.05$). The differences in detailed physicochemical properties including basic water parameters, C, N, S, and P-related parameters in water and sediments of SF and LF ponds are summarized in Table 1. In total, 19 of 26 parameters showed significant ($p < 0.05$) differences between LF and SF ponds, indicating wide fluctuations of environmental conditions brought by higher N input to aquaculture ponds, and this may have an impact on the diversity and function of nitrifying communities.

3.2 The abundance of comammox *Nitrospira* and AOB are of equal magnitude

To determine the composition and predominance of sediment nitrifying communities in aquaculture ponds, we measured the abundance of comammox *Nitrospira amoA*, AOA *amoA*, AOB *amoA*, *Nitrospira nxrB*, and 16S rRNA genes by qPCR. No significant abundance difference was observed in the ratio of the total nitrifiers and total bacteria (16S rRNA) in different fish farming. In general, NOB were the most abundant nitrifiers in all fish ponds, followed by

1 http://fungene.cme.msu.edu/
2 http://www.bioinformatics.babra-ham.ac.uk/projects/fastqc/
3 https://multiqc.info/
4 http://ieg2.ou.edu/MENA/
5 https://github.com/gephi/gephi/
6 https://github.com/EricArcher/rfPermute

TABLE 1 Physicochemical properties of water and sediment in SF and LF fish ponds, which are shown as mean ± SD (standard deviation) ($n = 18$).

	Parameters	SF ponds	LF ponds
Water	Temperature (°C)	32.86 ± 1.39^a	33.68 ± 0.27^b
	pH	8.34 ± 0.52^b	7.91 ± 0.34^a
	DO (mg/L)	8.81 ± 5.96	6.34 ± 2.51
	Salinity (%)	1.39 ± 0.34	1.50 ± 0.25
	Transparency (cm)	19.70 ± 6.65^b	11.33 ± 1.81^a
	Chla (μg/L)	135.6 ± 58.0^b	88.19 ± 28.17^a
	TSS (mg/L)	19.82 ± 19.94^a	67.85 ± 13.35^b
	POC (mg/L)	33.34 ± 14.68^b	24.48 ± 2.70^a
	DOC (mg/L)	31.26 ± 7.52^b	15.60 ± 4.50^a
	TOC (mg/L)	64.59 ± 17.43^b	40.08 ± 4.56^a
	NH_4^+ (mg/L)	0.554 ± 0.303	0.722 ± 0.382
	NO_2^- (mg/L)	0.278 ± 0.317^a	0.631 ± 0.365^b
	NO_3^- (mg/L)	1.11 ± 1.48^a	4.48 ± 1.46^b
	TIN (mg/L)	1.94 ± 1.72^a	5.84 ± 1.87^b
	TON (mg/L)	4.84 ± 1.03^b	4.00 ± 0.84^a
	TN (mg/L)	6.79 ± 2.00^a	9.84 ± 1.35^b
	PO_4^- (mg/L)	0.397 ± 0.272^b	0.085 ± 0.095^a
	TOP (mg/L)	0.353 ± 0.210	0.240 ± 0.111
	TP (mg/L)	0.741 ± 0.392^b	0.324 ± 0.065^a
Sediment	sTC (%)	17.29 ± 6.56	17.20 ± 6.66
	sTOC (%)	11.73 ± 5.17	12.93 ± 5.80
	sTN (%)	1.51 ± 0.67	1.38 ± 0.62
	sTS (%)	2.82 ± 1.87^b	0.99 ± 0.37^a
	sES (mg/g)	20.23 ± 10.07^b	7.65 ± 2.85^a
	sAVS (mg/g)	437.3 ± 176.6^b	126.0 ± 35.9^a
	sTP (%)	0.142 ± 0.045^a	0.184 ± 0.060^b

Each parameter with different letters showed statistical differences ($p < 0.05$, t-test or Mann–Whitney U-test). *Fish ponds with different sizes of grass carp are abbreviated as SF and LF. Parameters determination from water included temperature, pH, dissolved oxygen (DO), salinity, transparency, chlorophyll a, total suspended solid (TSS), particle organic carbon (POC), dissolved organic carbon (DOC), total organic carbon (TOC), ammonium, nitrite, nitrate, total inorganic nitrogen (TIN), total organic nitrogen (TON), total nitrogen (TN), phosphate, total organic phosphorus (TOP), and total phosphorus (TP). Sediment properties included total carbon (sTC), total organic carbon (sTOC), total nitrogen (sTN), total sulfur (sTS), elemental sulfur (sES), acid-volatile sulfur (sAVS), and total phosphorus (sTP).

AOB, comammox *Nitrospira,* and AOA (Figure 1A). We found an unexpectedly high abundance of comammox *Nitrospira amoA* [$(2.18 \pm 0.23) \times 10^7$-$(1.37 \pm 0.21) \times 10^7$ copies/g wet sediment], which accounted for 39.44–32.23% of the ammonia oxidizer and 0.09–0.17%- of all the bacteria in the SF and LF ponds. The abundance of AOB *amoA* was from $(2.31 \pm 0.48) \times 10^7$ to $(2.30 \pm 0.18) \times 10^7$ copies/g wet sediment in the SF and LF ponds (Figure 1A and Supplementary Table S2). The abundance of comammox *Nitrospira amoA* in the SF ponds was significantly higher than in LF ponds ($p < 0.05$). The phylogenetic tree analysis revealed that sequences of comammox *Nitrospira amoA* (361 zOTUs) could be grouped into clade A (294 zOTUs) and clade B (67 zOTUs), and comammox *Nitrospira* clade A were the predominant clade in the SF (66.05%) and LF (89.41%) ponds (Supplementary Table S3).

3.3 The difference between comammox *Nitrospira* and other nitrifiers in community structure

To further understand the diversity and community structure of sediment nitrifying communities by fish farming, functional genes of comammox *Nitrospira amoA*, AOA *amoA*, AOB *amoA*, and *Nitrospira nxrB* were sequenced and analyzed. In general, α-diversity indices showed that NOB had higher diversity, followed by comammox *Nitrospira*, AOA, and AOB (Supplementary Table S4). Higher fish feeding mainly reduced the α-diversity of all nitrifying communities except comammox *Nitrospira*; they showed significantly ($p < 0.05$) higher values of observed richness and phylogenetic diversity in the LF ponds (Supplementary Table S4). For the within-beta diversity, LF pond sediments had a significantly ($p < 0.001$) lower value of the Bray–Curtis dissimilarity than that of SF pond sediments (Figure 1B; Supplementary Figure S1). In addition, the principal coordinates analysis (PCoA) revealed that higher dissimilarity of comammox *Nitrospira amoA* in the SF and LF ponds than AOA and AOB *amoA* (Figure 2), which together with the above results suggested that comammox *Nitrospira* may be more sensitive to aquaculture activities.

3.4 Comammox *Nitrospira* and NOB were more sensitive to environmental changes

We further investigated the relative importance of environmental variables in the assembly of nitrifiers in aquaculture ponds. The Mantel tests showed that all 26 environmental variables were significantly ($p < 0.05$) correlated with the comammox *Nitrospira* and NOB community structure (except salinity for comammox *Nitrospira* and NH_4^+ in pond water for both) (Figure 3). TOC and TP were the most important drivers that shaped the composition of the comammox *Nitrospira*, while TSS and nitrate mainly affected the composition of NOB. AOA communities were only significantly ($p < 0.05$) related to temperature, salinity, and DOC. AOB communities were significantly ($p < 0.05$) related to 14 out of 26 environmental conditions including sES, phosphate, TP, sTS, POC, temperature, TOC, transparency, TOP, sAVS, pH, DOC, nitrate, and TIN (Figure 3). The RDA confirmed that these significant correlations and these environmental variables explained a large proportion of the variation in the comammox *Nitrospira* community (45.81%, $p < 0.001$) and the NOB community (44.56%, $p < 0.001$). However, the RDA model only explained 22.66% ($p < 0.001$) of variations in the AOA community and 26.05% ($p < 0.001$) of variations in the AOB community (Figure 4). The linear regression analysis also showed that the richness of comammox *Nitrospira* was positively correlated with temperature, DO, nitrate, and TIN (Supplementary Figure S2). Additionally, we analyzed the correlations between dominant nitrifiers and environmental variables. Relative abundances of the dominant comammox *Nitrospira* and NOB species were significantly ($p < 0.05$) correlated with N-related parameters especially nitrate, TIN, and TN (Supplementary Tables S5, S6). However, the dominant AOA and AOB species were relatively insensitive to related N parameters and other environmental changes compared to comammox *Nitrospira* and NOB species (Supplementary Tables S7, S8). These results indicated that comammox *Nitrospira* and NOB communities were more sensitive to environmental variables than AOA and AOB.

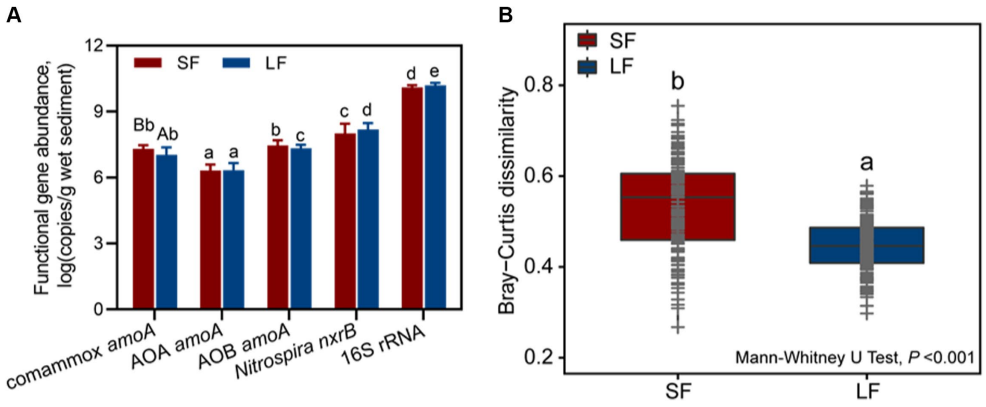

FIGURE 1
Abundance and beta diversity of nitrifiers in SF and LF ponds. **(A)** Abundances of comammox *Nitrospira amoA*, AOA *amoA*, AOB *amoA*, *Nitrospira nxrB*, and 16S rRNA genes in SF and LF pond sediments. Data are represented as mean ± SD ($n = 18$). Different capital letters mean a statistical significance ($p < 0.05$) between SF and LF pond sediments based on Student's *t*-test; different small letters mean a statistical significance ($p < 0.05$) among different functional genes within the same fish size pond sediments based on one-way ANOVA. **(B)** Beta diversity of sediment nitrifying communities in the SF and LF ponds was estimated based on Bray–Curtis distance matrixes of all 36 samples. Different letters showed statistical differences ($p < 0.001$, Mann–Whitney *U*-test).

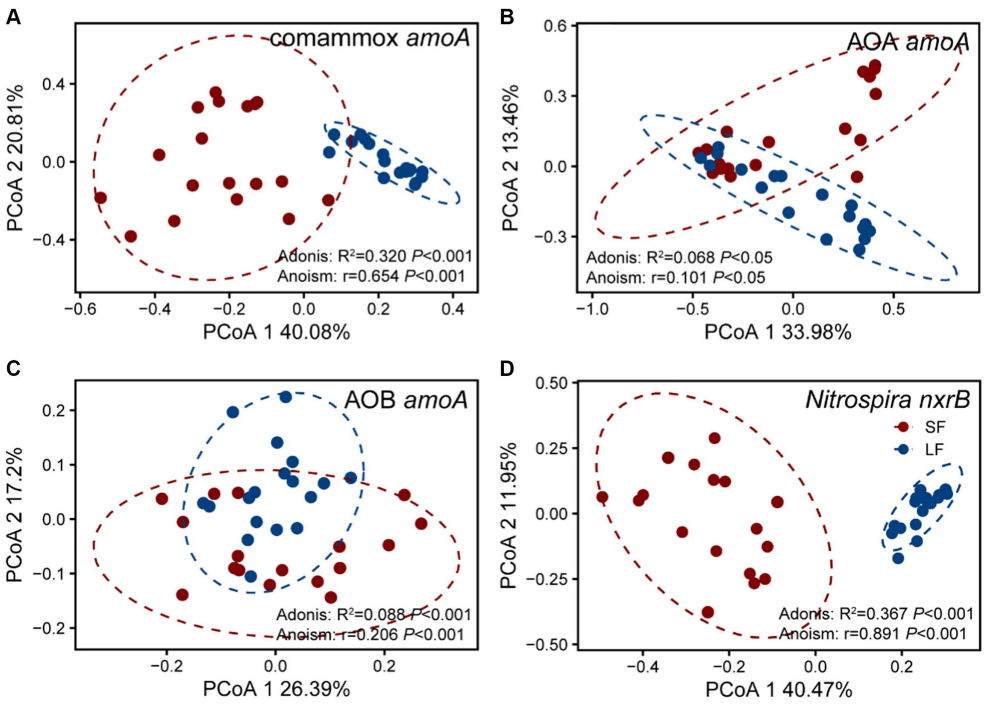

FIGURE 2
Principal co-ordinates analysis (PCoA) of four nitrifying communities in the SF and LF ponds, **(A)** AOA *amoA*, **(B)** AOB *amoA*, **(C)** Comammox *Nitrospira amoA*, and **(D)** *Nitrospira nxrB*. The samples in an ellipse showed 95% confidence within this group. The values of PCoA1 and PCoA2 labels were percentages of variations explained. Colors represent SF or LF pond sediments, respectively. The significance of dissimilarities was examined by the Adonis and Anosim tests.

3.5 High fish feeding reduced networks of potential interactions

To explore the influence of fish farming on the interactions of nitrifiers in aquaculture systems, we constructed co-occurrence networks of sediment nitrifying communities in the SF and LF ponds (Figure 5; Supplementary Figure S2). Compared to the SF ponds, we found lower total nodes, links, average degree, density, connectedness, average path distance, and centralization of stress centrality of the co-occurrence network of nitrifying communities in LF ponds (Figures 5A,B; Supplementary Table S9). The potential interactions among nitrifiers were mostly positive (>98%) in both SF and LF ponds. In addition, we observed one module hub (nxrB_94) and two connectors (nxrB_247; nxrB_1316) all derived from

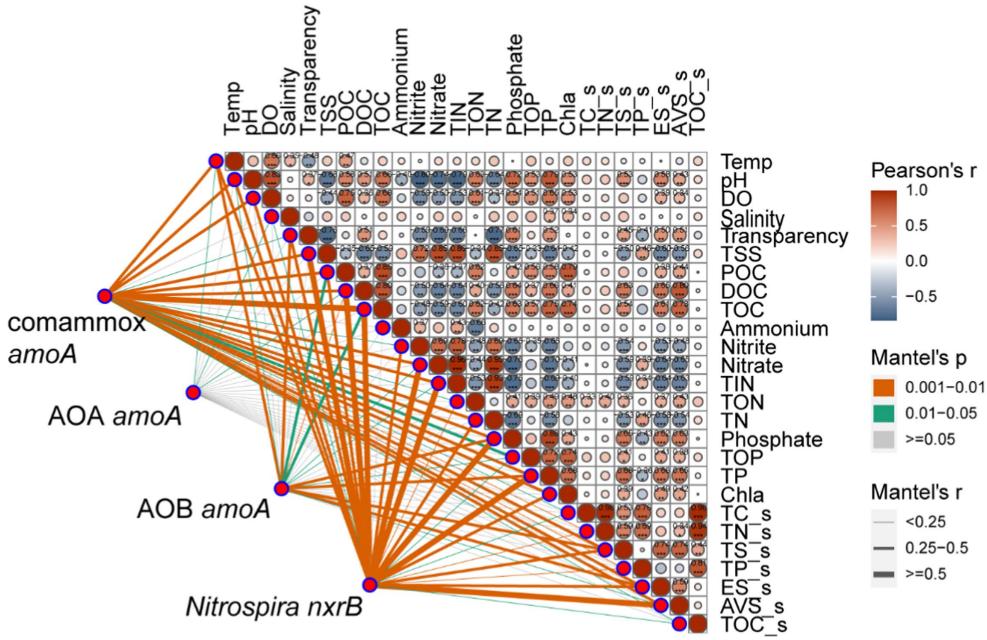

FIGURE 3
Relationships between nitrifying communities and environmental variables using the Mantel tests. The Mantel tests between nitrifiers (comammox *Nitrospira amoA*, AOA *amoA*, AOB *amoA,* and *Nitrospira nxrB*) and environmental variables in fish ponds based on Pearson's correlations.

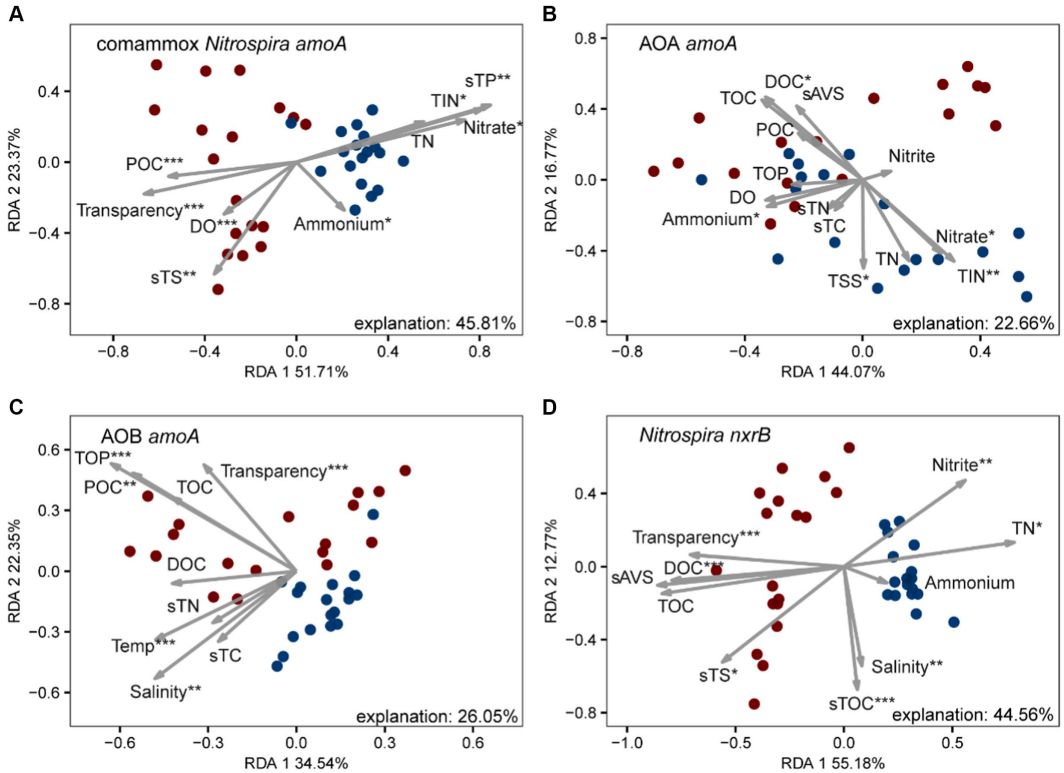

FIGURE 4
Redundancy analysis (RDA) of environmental drivers to nitrifying communities, **(A)** comammox *Nitrospira amoA*, **(B)** AOA *amoA*, **(C)** AOB *amoA*, and **(D)** *Nitrospira nxrB*. The values of RDA1 and RDA2 labels represented the percentages explained.

Nitrospira nxrB in SF ponds and four module hubs (com_29, com_57, com_103, com_134) derived from comammox *Nitrospira amoA* in LF ponds (Figure 5; Supplementary Table S10). Among those core taxa, nxrB_94 was the most abundant zOTU in the SF ponds and its relative abundance was significantly ($p < 0.05$) higher in SF pond sediments than in LF ponds (0.40% vs. 0.02%). However, the

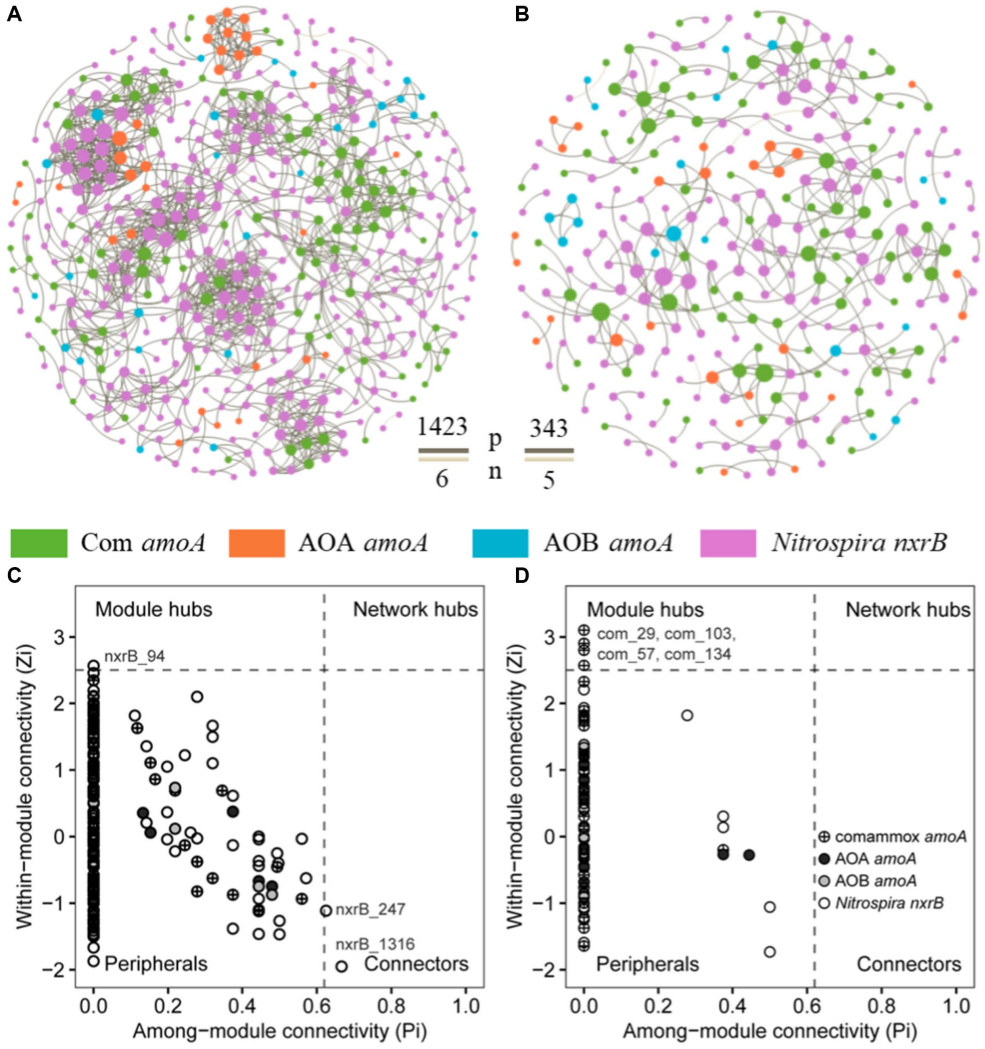

FIGURE 5
Co-occurrence networks of nitrifiers in aquaculture ponds, **(A)** SF ponds; **(B)** LF ponds, the brown and beige line between nodes showed positive and negative interactions, respectively. The network nodes in SF **(C)** and LF **(D)** ponds were separated by among-module connectivity (Pi) and within-module connectivity (Zi) within a threshold of 0.62 and 2.5 (Deng et al., 2012; Shi et al., 2016), respectively.

abundance of com_29 in the LF pond samples was significantly ($p < 0.05$) higher than in the SF samples (0.08% vs. 1.07%). In addition, com_29 had the highest relative abundance than other keystones in LF pond sediments (Supplementary Table S10). Together, a less complex co-occurrence network of nitrifiers was observed in the LF ponds, and keystone species were shifted from *Nitrospira* nxrB species in the SF ponds to comammox *Nitrospira* in LF ponds in the coastal aquaculture ecosystem.

3.6 The contribution of comammox *Nitrospira* to nitrification is unneglectable in eutrophic conditions

To estimate the potential contribution of nitrifiers to nitrification, the abundance and richness of nitrifiers and keystone species were used to predict nitrification potentials. We found that only the abundance of comammox *Nitrospira amoA* contributed to nitrification potential (24.67%) (Figure 6A) with a statistical significance ($p < 0.05$). However, both the richness of AOB *amoA* and comammox *Nitrospira amoA* contributed to nitrification potential with a statistical significance ($p < 0.05$) (Figure 6B). In addition, we assessed the contribution of core taxa to nitrification potential in fish ponds (Figure 6C). We found these core taxa explained a large proportion of nitrification potential variations. Among these core taxa, com_29 which belonged to comammox *Nitrospira* made a relatively important contribution to nitrification potential ($p < 0.05$). Moreover, we estimated the contribution of ammonium oxidizers to the nitrification process through mixed co-culture of four nitrifiers with three different ammonium supplies from 0.2 to 2 mM. We found that the relative contribution of comammox *Nitrospira* to nitrification was significantly higher than AOA and AOB under 0.2 mM ammonium ($p < 0.05$) (Figure 6D). When ammonium supply increased to 1 mM, the relative contribution of AOB and comammox was comparable (48.86% vs. 47.60%). Further increasing ammonium to 2 mM, AOB contributed to most of the nitrification (98.11%).

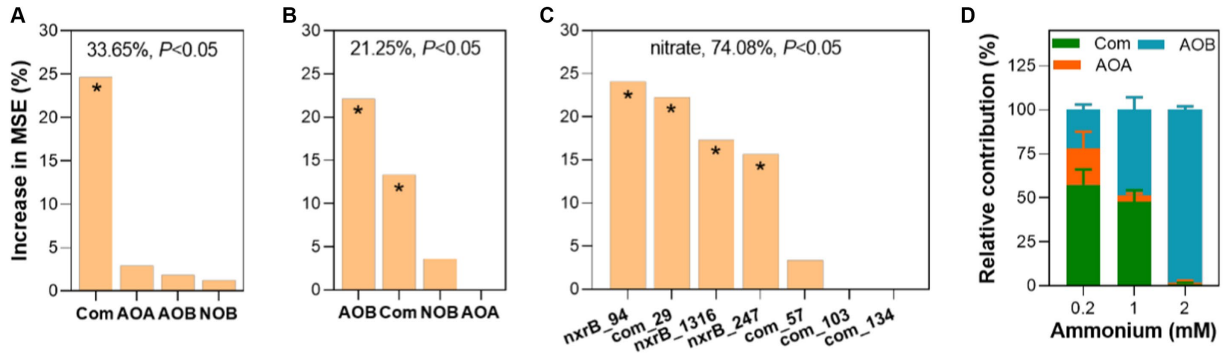

FIGURE 6
Exploring the contribution of four types of nitrifiers to nitrification. Contribution of the abundance **(A)** and richness **(B)** of four nitrifiers and keystone species **(C)** to nitrification potential analyzed by random forest. **(D)** The relative contribution of ammonium oxidizers to nitrification in synthetic nitrifying communities. The accuracy importance of measurement was computed for each tree and averaged over the forest (ntree = 1,000, nrep = 1,000). The overall explanatory degree and the significance of the models were calculated and shown. The higher importance of the predictor was reflected by a higher mean squared error (MSE). Asterisk (*) showed a statistically significant difference in the predictor ($p < 0.05$). More details can be found in the methods.

These results confirmed the significant role of comammox *Nitrospira* in the nitrification process at a rough range of ammonium in eutrophic environments.

4 Discussion

The predominance of comammox *Nitrospira* in oligotrophic environments has been studied well, while their contribution to nitrification in eutrophic environments has been poorly understood (Smith and Schindler 2009; Williams and Crutzen 2010; Deegan et al. 2012). Understanding the response of nitrifiers, especially the newly discovered comammox *Nitrospira* to eutrophic conditions, is particularly important for N removal and sustainable aquaculture as the presence of excessive nutrients in ecosystems such as aquaculture is a common issue. In this study, we found that the comammox *Nitrospira* community had higher α-diversity than that of AOB and AOA as expected. Surprisingly, we found that the abundance of comammox *Nitrospira* is equivalent to that of AOB and comammox *Nitrospira* was more sensitive to aquaculture environmental variations than other nitrifiers (AOA and AOB). They played a critical role in the interaction networks of the nitrifiers and the nitrification process in the aquaculture ecosystem and laboratory experiments of mixed-culturing nitrifiers. These results generally support our hypothesis that comammox *Nitrospira* play a major role in the nitrification process in eutrophic aquaculture ecosystems.

The abundance and diversity of comammox *Nitrospira*, AOA, AOB, and NOB responded to nutrient addition differently. In our study, we detected a high abundance of comammox *Nitrospira* which was equivalent to AOB and followed by AOA. The abundance of comammox *Nitrospira* was negatively affected by higher nutrient addition but was still at the same magnitude as AOB and positively correlated to the C/N ratio, which indicated their crucial role in the nitrification process in eutrophic aquaculture ponds. Our results were contrasting with the previous findings which showed the abundance of comammox *Nitrospira* was much lower than that of AOA or AOB in slight eutrophic agricultural soils (Guo et al., 2017; Shi et al., 2018, 2020; Wang et al., 2020; Xu et al., 2020). Their observations could be explained by the difference in substrate affinity among nitrifiers (Prosser and Nicol, 2012; Hu and He, 2017; Kits et al., 2017; Wang et al., 2020; Yue et al., 2022); specifically, comammox *Nitrospira inopinata* have the highest affinity for ammonia (0.65 μM), followed by most AOA (>5.7 μM) and most AOB (>1,000 μM). Comammox *Nitrospira* were generally considered to have a lower growth rate than AOB (Costa et al., 2006; Hu and He, 2017), while the substrate concentration here was between the ammonia affinity of comammox *Nitrospira* and AOB where they were at similar growth rate (Yang et al., 2022). However, eutrophic aquatic environments, such as wastewater treatment plants and coastal aquaculture filter systems, and agricultural soils with higher C/N ratios were shown to harbor a high abundance of comammox *Nitrospira*, which was consistent with our study (Foesel et al., 2008; Annavajhala et al., 2018; Pan et al., 2018; Li et al., 2019; Zheng et al., 2019). The ammonium concentration of our study was 40–70 μM, which was much higher than the affinity of those reported for *N. inopinata*. The high diversity and abundance of comammox *Nitrospira* in these eutrophic aquatic environments may be due to the metabolic versatility of these comammox *Nitrospira* species (Spasov et al., 2020; Xu et al., 2020; Vijayan et al., 2021). In addition, their higher α-diversity indices than canonical ammonium-oxidizers in this study hinted that besides the subtract range, environmental factors, metabolic versatility, growth yields, and biofilm formation capabilities could also affect the diversity and abundance of these newly discovered nitrifiers (Lawson and Lucker, 2018; Spasov et al., 2020). Moreover, we found the proportion of comammox *Nitrospira* clade A significantly had a greater abundance and it was increased along with nutrient addition. These results were consistent with previous findings that clade A was suggested to have a wider distribution, higher diversity, and greater abundance than clade B (Fowler et al., 2018; Shi et al., 2018; Xia et al., 2018; Xu et al., 2020; Zhu et al., 2022) due to their lower ammonia affinity of clade A for ammonia transportation (Koch et al., 2019). These results together suggested the niche heterogeneity and metabolic flexibility of comammox *Nitrospira* may guide diverse niches.

The unabsorbed N of fish feed is largely converted to ammonium through ammonification (Hargreaves, 1998; Hu et al., 2012), which not only increased the N-related parameters but also altered other

parameters, thus affecting nitrification activity and nitrifying community (Magill et al., 2000; Kraft et al., 2014; Chen et al., 2016; He et al., 2018, 2020). In this study, we found that AOA and AOB were significantly correlated with several environmental variables including pH, temperature, and salinity. However, comammox *Nitrospira* and NOB communities were sensitive to most of the environmental changes, the changes in N-related parameters could explain more variation in their communities. These results were partly consistent with previous studies that pH, temperature, salinity, and ammonium availability shaped the composition of nitrifying communities especially AOA and AOB communities in agricultural soils and coastal ecosystems (Guo et al., 2017; Xia et al., 2018; Xu et al., 2020; Zhao et al., 2021; Yue et al., 2022). It was reported that N addition altered ammonium availability by reducing pH and increasing substrate concentrations (Hallin et al., 2009; Shi et al., 2018). Furthermore, in this study, increasing temperature and DO only increased the richness of comammox *Nitrospira*, which confirmed that other environmental variables affect the diversity of this newly discovered nitrifier besides ammonium. Moreover, nitrate also positively correlated with the comammox richness while negatively correlated with NOB richness, which hinted the important role of comammox in nitrification and their higher sensitivity to the nitrifying reaction products compared to canonical nitrite oxidizer. In addition to the effect of environmental changes on microbial community assembly, these co-existed microbial species interacting with each other and forming complex microbial community networks played a profound role in various ecosystem services (Barberán et al., 2012; Tu et al., 2020; Yue et al., 2022). In this study, we found that high fish feeding decreased the complexity of nitrifying communities. This result was consistent with an investigation of nitrifying microbial communities' response to long-term fertilization of inorganic fertilization, not organic fertilization (Banerjee et al., 2016; Yue et al., 2022). It suggested nutrient addition altered the resource-related co-occurrence of microorganisms. Co-occurrence relationships also lie in metabolic connections among microbial groups. For example, co-metabolic interactions between ammonia oxidizers and NOB have been observed in co-culture experiments (Yang et al., 2022) and genome-based exploration (Pachiadaki et al., 2017). Moreover, we found a high proportion of positive interactions among nitrifiers in the fish ponds. Additionally, the interspecific interactions among nitrifiers decreased under higher nutrient input, which may result from the enough N for nitrifiers caused by the nutrient addition (ammonium inhibition) that weakens the co-metabolic interactions among nitrifiers (Yang et al., 2022).

Keystone species hold together the complex microbial interactions in the ecosystem and were suggested as the drivers of microbial structure and functioning (Banerjee et al., 2018). The shift of keystone species caused by environmental changes might alter the function of the entire ecosystem (Banerjee et al., 2018; Herren and McMahon, 2018; Yang et al., 2021). We found that keystone nodes were dramatically different between the SF and LF ponds. NOB served as keystones to maintain nitrification in the SF ponds, which was consistent with previous studies showing that *Nitrospira* NOB were the dominant and keystone species in the Pearl River estuary (Hou et al., 2018), agricultural soils, and soil microcosms (Xu et al., 2020; Xun et al. 2021). While the keystones shifted to comammox *Nitrospira* with higher fish feeding in the LF ponds, implying in addition to driving the nitrification process, comammox *Nitrospira* also contributed to the N removal process as the core connector to maintain the stability and functioning of nitrifying communities in eutrophic aquaculture habitats.

Due to the importance of nitrifiers in N cycling and N removal in various environments, their relative contribution to nitrification especially the newly discovered comammox *Nitrospira* in eutrophic conditions has drawn attention from researchers. It was well known that comammox *Nitrospira* were the dominant species that contributed most to nitrification in oligotrophic environments (Palomo et al., 2016; Roots et al., 2019). However, their contributions to nitrification in eutrophic environments were poorly understood. It was still controversial whether AOA or AOB contributed more to the nitrification process although it has been studied for decades (Jia and Conrad, 2009; Guo et al., 2017; Wang et al., 2021). The newly discovered comammox *Nitrospira* which joined the chaos complicated their contribution to the nitrification process. In our study, we used simplified mix-culturing experiments of nitrifiers to show that comammox *Nitrospira* contributed most to ammonium oxidation under a relatively eutrophic ammonium concentration (0.2 mM) and their contributions decreased significantly with the increase of ammonium supply. This result confirmed that comammox *Nitrospira* could outcompete AOB at a comparable ammonium concentration (Roots et al., 2019), hinting at their importance in less-eutrophic environments. Our result was not consistent with previous findings in eutrophic agriculture soil where AOB were the main contributor to nitrification (Jia and Conrad, 2009; Prosser and Nicol, 2012; Prosser et al., 2020). This may result from the limitations of our mixed nitrifying communities in representing complex ecosystems. We also found that close linkages between nitrification potential and the abundance of comammox *Nitrospira*, diversity of AOB and comammox *Nitrospira*, keystone species of NOB, and comammox *Nitrospira* explained a large proportion of nitrate variation in the fish ponds. These results consistently emphasized the important role of comammox *Nitrospira* in less-eutrophic coastal aquaculture.

5 Conclusion

In summary, this study showed that aquaculture activity altered the diversity, richness, abundance, and interactions of nitrifying communities. Unexpected abundant comammox *Nitrospira* were observed in the aquaculture ecosystem, and they were more sensitive to aquaculture environmental changes compared to canonical nitrifiers. Comammox *Nitrospira* species were keystones in shaping the nitrifying communities and played an important role in nitrification potential. This study fills the gap of comammox *Nitrospira* in the coastal eutrophic environment and advances our understanding of their contribution to nitrification. Future studies may focus on understanding the role of comammox *Nitrospira* in nitrifying communities, their contribution to the nitrification process, and underlying mechanisms using synthetic nitrifying communities, RNA-Seq, and ^{15}N isotope tracer.

Data availability statement

The datasets presented in this study can be found in online repositories. The names of the repository/repositories and accession

number(s) can be found at: https://www.ncbi.nlm.nih.gov/bioproject/PRJNA834749.

Author contributions

XY: Conceptualization, Data curation, Formal analysis, Methodology, Software, Validation, Visualization, Writing – original draft, Writing – review & editing. YW: Methodology, Software, Writing – review & editing. LS: Resources, Supervision, Writing – review & editing. HG: Investigation, Methodology, Software, Writing – review & editing. FL: Investigation, Methodology, Software, Writing – review & editing. JD: Investigation, Methodology, Software, Writing – review & editing. JZ: Data curation, Investigation, Writing – review & editing. CW: Resources, Writing – review & editing. ZH: Resources, Writing – review & editing. MX: Supervision, Writing – review & editing. FFL: Writing – review & editing. XZ: Data curation, Formal analysis, Funding acquisition, Investigation, Project administration, Software, Supervision, Writing – review & editing. BW: Funding acquisition, Project administration, Software, Supervision, Writing – review & editing.

Funding

The author(s) declare that financial support was received for the research, authorship, and/or publication of this article. This study was supported by the National Natural Science Foundation of China (32000070, 32102821, 52070196, 31800417, and 31770539).

Conflict of interest

The authors declare that the research was conducted in the absence of any commercial or financial relationships that could be construed as a potential conflict of interest.

Publisher's note

All claims expressed in this article are solely those of the authors and do not necessarily represent those of their affiliated organizations, or those of the publisher, the editors and the reviewers. Any product that may be evaluated in this article, or claim that may be made by its manufacturer, is not guaranteed or endorsed by the publisher.

Supplementary material

The Supplementary material for this article can be found online at: https://www.frontiersin.org/articles/10.3389/fmicb.2024.1355859/full#supplementary-material

References

Annavajhala, M. K., Kapoor, V., Santo-Domingo, J., and Chandran, K. (2018). Comammox functionality identified in diverse engineered biological wastewater treatment systems. *Environ. Sci. Technol. Lett.* 5, 110–116. doi: 10.1021/acs.estlett.7b00577

Banerjee, S., Helgason, B., Wang, L., Winsley, T., Ferrari, B. C., and Siciliano, S. D. (2016). Legacy effects of soil moisture on microbial community structure and n_2o emissions. *Soil Biol. Biochem.* 95, 40–50. doi: 10.1016/j.soilbio.2015.12.004

Banerjee, S., Schlaeppi, K., and van der Heijden, M. G. (2018). Keystone taxa as drivers of microbiome structure and functioning. *Nat. Rev. Microbiol.* 16, 567–576. doi: 10.1038/s41579-018-0024-1

Barberán, A., Bates, S. T., Casamayor, E. O., and Fierer, N. (2012). Using network analysis to explore co-occurrence patterns in soil microbial communities. *ISME J.* 6, 343–351. doi: 10.1038/ismej.2011.119

Bartelme, R. P., McLellan, S. L., and Newton, R. J. (2017). Freshwater recirculating aquaculture system operations drive biofilter bacterial community shifts around a stable nitrifying consortium of ammonia-oxidizing archaea and comammox nitrospira. *Front. Microbiol.* 8:101. doi: 10.3389/fmicb.2017.00101

Breiman, L. (2001). Random forests. *Mach. Learn.* 45, 5–32. doi: 10.1023/A:1010933404324

Brooks, J. P., Edwards, D. J., Harwich, M. D., Rivera, M. C., Fettweis, J. M., Serrano, M. G., et al. (2015). The truth about metagenomics: quantifying and counteracting bias in 16s rrna studies. *BMC Microbiol.* 15:66. doi: 10.1186/s12866-015-0351-6

Caporaso, J. G., Kuczynski, J., Stombaugh, J., Bittinger, K., Bushman, F. D., Costello, E. K., et al. (2010). Qiime allows analysis of high-throughput community sequencing data. *Nat. Methods* 7, 335–336. doi: 10.1038/nmeth.f.303

Chen, H., Gurmesa, G. A., Zhang, W., Zhu, X. M., Zheng, M. H., Mao, Q. G., et al. (2016). Nitrogen saturation in humid tropical forests after 6 years of nitrogen and phosphorus addition: hypothesis testing. *Funct. Ecol.* 30, 305–313. doi: 10.1111/1365-2435.12475

Chen, S., Zhou, Y., Chen, Y., and Gu, J. (2018). Fastp: an ultra-fast all-in-one fastq preprocessor. *Bioinformatics* 34, i884–i890. doi: 10.1093/bioinformatics/bty560

Costa, E., Perez, J., and Kreft, J. U. (2006). Why is metabolic labour divided in nitrification? *Trends Microbiol.* 14, 213–219. doi: 10.1016/j.tim.2006.03.006

Daims, H., Lebedeva, E. V., Pjevac, P., Han, P., Herbold, C., Albertsen, M., et al. (2015). Complete nitrification by nitrospira bacteria. *Nature* 528, 504–509. doi: 10.1038/nature16461

Daims, H., Luecker, S., and Wagner, M. (2016). A new perspective on microbes formerly known as nitrite-oxidizing bacteria. *Trends Microbiol.* 24, 699–712. doi: 10.1016/j.tim.2016.05.004

Deegan, L. A., Johnson, D. S., Warren, R. S., Peterson, B. J., Fleeger, J. W., Fagherazzi, S., et al. (2012). Coastal eutrophication as a driver of salt marsh loss. *Nature* 490, 388–392. doi: 10.1038/nature11533

Deng, Y., Jiang, Y. H., Yang, Y. F., He, Z. L., Feng, L., and Zhou, J. Z. (2012). Molecular ecological network analyses. *BMC Bioinformatics.* 13:113. doi: 10.1186/1471-2105-13-113

Dixon, P. (2003). Vegan, a package of r functions for community ecology. *J. Veg. Sci.* 14, 927–930. doi: 10.1111/j.1654-1103.2003.tb02228.x

Edgar, R. C. (2013). Uparse: highly accurate otu sequences from microbial amplicon reads. *Nat. Methods* 10, 996–998. doi: 10.1038/nmeth.2604

Edgar, R. C. (2016). Unoise2: improved error-correction for illumina 16s and its amplicon sequencing. *BioRxiv.*:081257

Foesel, B. U., Gieseke, A., Schwermer, C., Stief, P., Koch, L., Cytryn, E., et al. (2008). Nitrosomonas nm143-like ammonia oxidizers and *Nitrospira marina*-like nitrite oxidizers dominate the nitrifier community in a marine aquaculture biofilm. *FEMS Microbiol. Ecol.* 63, 192–204. doi: 10.1111/j.1574-6941.2007.00418.x

Fowler, S. J., Palomo, A., Dechesne, A., Mines, P. D., and Smets, B. F. (2018). Comammox nitrospira are abundant ammonia oxidizers in diverse groundwater-fed rapid sand filter communities. *Environ. Microbiol.* 20, 1002–1015. doi: 10.1111/1462-2920.14033

Garlock, T., Asche, F., Anderson, J., Bjorndal, T., Kumar, G., Lorenzen, K., et al. (2020). A global blue revolution: aquaculture growth across regions, species, and countries. *Rev Fish Sci Aquacult.* 28, 107–116. doi: 10.1080/23308249.2019.1678111

Ginestet, C. (2011). Ggplot2: elegant graphics for data analysis. *J. R. Stat. Soc. Ser. A Stat. Soc.* 174, 245–246. doi: 10.1111/j.1467-985X.2010.00676_9.x

Goslee, S. C., and Urban, D. L. (2007). The ecodist package for dissimilarity-based analysis of ecological data. *J. Stat. Softw.* 22, 1–19. doi: 10.18637/jss.v022.i07

Guimera, R., and Amaral, L. A. N. (2005). Functional cartography of complex metabolic networks. *Nature* 433, 895–900. doi: 10.1038/nature03288

Guo, J., Ling, N., Chen, H., Zhu, C., Kong, Y., Wang, M., et al. (2017). Distinct drivers of activity, abundance, diversity and composition of ammonia-oxidizers: evidence from a long-term field experiment. *Soil Biol. Biochem.* 115, 403–414. doi: 10.1016/j.soilbio.2017.09.007

Hallin, S., Jones, C. M., Schloter, M., and Philippot, L. (2009). Relationship between n-cycling communities and ecosystem functioning in a 50-year-old fertilization experiment. *ISME J.* 3, 597–605. doi: 10.1038/ismej.2008.128

Hargreaves, J. A. (1998). Nitrogen biogeochemistry of aquaculture ponds. *Aquaculture* 166, 181–212. doi: 10.1016/S0044-8486(98)00298-1

He, Q., Song, J., Zhang, W., Gao, S., Wang, H., and Yu, J. (2020). Enhanced simultaneous nitrification, denitrification and phosphorus removal through mixed carbon source by aerobic granular sludge. *J. Hazard. Mater.* 382:121043. doi: 10.1016/j.jhazmat.2019.121043

He, Q., Song, Q., Zhang, S., Zhang, W., and Wang, H. (2018). Simultaneous nitrification, denitrification and phosphorus removal in an aerobic granular sequencing batch reactor with mixed carbon sources: reactor performance, extracellular polymeric substances and microbial successions. *Chem. Eng. J.* 331, 841–849. doi: 10.1016/j.cej.2017.09.060

Herren, C. M., and McMahon, K. D. (2018). Keystone taxa predict compositional change in microbial communities. *Environ. Microbiol.* 20, 2207–2217. doi: 10.1111/1462-2920.14257

Hou, L., Xie, X., Wan, X., Kao, S.-J., Jiao, N., and Zhang, Y. (2018). Niche differentiation of ammonia and nitrite oxidizers along a salinity gradient from the pearl river estuary to the South China Sea. *Biogeosciences* 15, 5169–5187. doi: 10.5194/bg-15-5169-2018

Hu, H. W., and He, J. Z. (2017). Comammox-a newly discovered nitrification process in the terrestrial nitrogen cycle. *J. Soils Sediments* 17, 2709–2717. doi: 10.1007/s11368-017-1851-9

Hu, Z., Lee, J. W., Chandran, K., Kim, S., and Khanal, S. K. (2012). Nitrous oxide (n_2o) emission from aquaculture: A review. *Environ. Sci. Technol.* 46, 6470–6480. doi: 10.1021/es300110x

Jia, Z. J., and Conrad, R. (2009). Bacteria rather than archaea dominate microbial ammonia oxidation in an agricultural soil. *Environ. Microbiol.* 11, 1658–1671. doi: 10.1111/j.1462-2920.2009.01891.x

Kits, K. D., Sedlacek, C. J., Lebedeva, E. V., Han, P., Bulaev, A., Pjevac, P., et al. (2017). Kinetic analysis of a complete nitrifier reveals an oligotrophic lifestyle. *Nature* 549, 269–272. doi: 10.1038/nature23679

Koch, H., van Kessel, M. A. H. J., and Lucker, S. (2019). Complete nitrification: insights into the ecophysiology of comammox nitrospira. *Appl. Microbiol. Biotechnol.* 103, 177–189. doi: 10.1007/s00253-018-9486-3

Könneke, M., Bernhard, A. E., de la Torre, J. R., Walker, C. B., Waterbury, J. B., and Stahl, D. A. (2005). Isolation of an autotrophic ammonia-oxidizing marine archaeon. *Nature* 437, 543–546. doi: 10.1038/nature03911

Kraft, B., Tegetmeyer, H. E., Sharma, R., Klotz, M. G., Ferdelman, T. G., Hettich, R. L., et al. (2014). The environmental controls that govern the end product of bacterial nitrate respiration. *Science* 345, 676–679. doi: 10.1126/science.1254070

Kumar, S., Stecher, G., Li, M., Knyaz, C., and Tamura, K. (2018). Mega x: molecular evolutionary genetics analysis across computing platforms. *Mol. Biol. Evol.* 35, 1547–1549. doi: 10.1093/molbev/msy096

Kuypers, M. M. M., Marchant, H. K., and Kartal, B. (2018). The microbial nitrogen-cycling network. *Nat. Rev. Microbiol.* 16, 263–276. doi: 10.1038/nrmicro.2018.9

Lawson, C. E., and Lucker, S. (2018). Complete ammonia oxidation: an important control on nitrification in engineered ecosystems? *Curr. Opin. Biotechnol.* 50, 158–165. doi: 10.1016/j.copbio.2018.01.015

Li, C. Y., Hu, H. W., Chen, Q. L., Chen, D. L., and He, J. Z. (2019). Comammox nitrospira play an active role in nitrification of agricultural soils amended with nitrogen fertilizers. *Soil Biol. Biochem.* 138:107609. doi: 10.1016/j.soilbio.2019.107609

Magill, A. H., Aber, J. D., Berntson, G. M., McDowell, W. H., Nadelhoffer, K. J., Melillo, J. M., et al. (2000). Long-term nitrogen additions and nitrogen saturation in two temperate forests. *Ecosystems* 3, 238–253. doi: 10.1007/s100210000023

Martin, M. (2011). Cutadapt removes adapter sequences from high-throughput sequencing reads. *EMBnet J.* 17, 10–12. doi: 10.14806/ej.17.1.200

Orellana, L. H., Chee-Sanford, J. C., Sanford, R. A., Loffler, F. E., and Konstantinidis, K. T. (2018). Year-round shotgun metagenomes reveal stable microbial communities in agricultural soils and novel ammonia oxidizers responding to fertilization. *Appl. Environ. Microbiol.* 84, e01646–e01617. doi: 10.1128/AEM.01646-17

Pachiadaki, M. G., Sintes, E., Bergauer, K., Brown, J. M., Record, N. R., Swan, B. K., et al. (2017). Major role of nitrite-oxidizing bacteria in dark ocean carbon fixation. *Science* 358, 1046–1051. doi: 10.1126/science.aan8260

Palomo, A., Fowler, S. J., Gulay, A., Rasmussen, S., Sicheritz-Ponten, T., and Smets, B. F. (2016). Metagenomic analysis of rapid gravity sand filter microbial communities suggests novel physiology of nitrospira spp. *ISME J.* 10, 2569–2581. doi: 10.1038/ismej.2016.63

Pan, K. L., Gao, J. F., Fan, X. Y., Li, D. C., and Dai, H. H. (2018). The more important role of archaea than bacteria in nitrification of wastewater treatment plants in cold season despite their numerical relationships. *Water Res.* 145, 552–561. doi: 10.1016/j.watres.2018.08.066

Park, S.-J., Park, B.-J., and Rhee, S.-K. (2008). Comparative analysis of archaeal 16s rrna and amoa genes to estimate the abundance and diversity of ammonia-oxidizing archaea in marine sediments. *Extremophiles* 12, 605–615. doi: 10.1007/s00792-008-0165-7

Pester, M., Maixner, F., Berry, D., Rattei, T., Koch, H., Lucker, S., et al. (2014). Nxrb encoding the beta subunit of nitrite oxidoreductase as functional and phylogenetic marker for nitrite-oxidizing nitrospira. *Environ. Microbiol.* 16, 3055–3071. doi: 10.1111/1462-2920.12300

Pinto, A. J., Marcus, D. N., Ijaz, U. Z., Santos, Q. M. B.-D. L., Dick, G. J., and Raskin, L. (2016). Metagenomic evidence for the presence of comammox nitrospira-like bacteria in a drinking water system. *mSphere* 1, e00054–e00015. doi: 10.1128/mSphere.00054-15

Prosser, J. I., Hink, L., Gubry-Rangin, C., and Nicol, G. W. (2020). Nitrous oxide production by ammonia oxidizers: physiological diversity, niche differentiation and potential mitigation strategies. *Glob. Chang. Biol.* 26, 103–118. doi: 10.1111/gcb.14877

Prosser, J. I., and Nicol, G. W. (2012). Archaeal and bacterial ammonia-oxidisers in soil: the quest for niche specialisation and differentiation. *Trends Microbiol.* 20, 523–531. doi: 10.1016/j.tim.2012.08.001

Rognes, T., Flouri, T., Nichols, B., Quince, C., and Mahe, F. (2016). Vsearch: a versatile open source tool for metagenomics. *PeerJ* 4:e2584. doi: 10.7717/peerj.2584

Roots, P., Wang, Y., Rosenthal, A. F., Griffin, J. S., Sabba, F., Petrovich, M., et al. (2019). Comammox nitrospira are the dominant ammonia oxidizers in a mainstream low dissolved oxygen nitrification reactor. *Water Res.* 157, 396–405. doi: 10.1016/j.watres.2019.03.060

Rotthauwe, J.-H., Witzel, K.-P., and Liesack, W. (1997). The ammonia monooxygenase structural gene amoa as a functional marker: molecular fine-scale analysis of natural ammonia-oxidizing populations. *Appl. Environ. Microbiol.* 63, 4704–4712. doi: 10.1128/aem.63.12.4704-4712.1997

Santoro, A. E. (2016). The do-it-all nitrifier: the discovery of bacteria that can oxidize both ammonia and nitrite upends a long-held dogma. *Science* 351, 342–343. doi: 10.1126/science.aad9839

Shi, X. Z., Hu, H. W., Wang, J. Q., He, J. Z., Zheng, C. Y., Wan, X. H., et al. (2018). Niche separation of comammox nitrospira and canonical ammonia oxidizers in an acidic subtropical forest soil under long-term nitrogen deposition. *Soil Biol. Biochem.* 126, 114–122. doi: 10.1016/j.soilbio.2018.09.004

Shi, Y., Jiang, Y., Wang, S., Wang, X., and Zhu, G. (2020). Biogeographic distribution of comammox bacteria in diverse terrestrial habitats. *Sci. Total Environ.* 717:137257. doi: 10.1016/j.scitotenv.2020.137257

Shi, S., Nuccio, E. E., Shi, Z. J., He, Z., Zhou, J., and Firestone, M. K. (2016). The interconnected rhizosphere: high network complexity dominates rhizosphere assemblages. *Ecol. Lett.* 19, 926–936. doi: 10.1111/ele.12630

Smith, V. H., and Schindler, D. W. (2009). Eutrophication science: where do we go from here? *Trends Ecol. Evol.* 24, 201–207. doi: 10.1016/j.tree.2008.11.009

Spasov, E., Tsuji, J. M., Hug, L. A., Doxey, A. C., Sauder, L. A., Parker, W. J., et al. (2020). High functional diversity among nitrospira populations that dominate rotating biological contactor microbial communities in a municipal wastewater treatment plant. *ISME J.* 14, 1857–1872. doi: 10.1038/s41396-020-0650-2

Tu, Q., Yan, Q., Deng, Y., Michaletz, S. T., Buzzard, V., Weiser, M. D., et al. (2020). Biogeographic patterns of microbial co-occurrence ecological networks in six american forests. *Soil Biol. Biochem.* 148:107897. doi: 10.1016/j.soilbio.2020.107897

van Kessel, M. A. H. J., Speth, D. R., Albertsen, M., Nielsen, P. H., Opden Camp, H. J. M., Kartal, B., et al. (2015). Complete nitrification by a single microorganism. *Nature* 528, 555–559. doi: 10.1038/nature16459

Vijayan, A., Jayadradhan, R. K. V., Pillai, D., Geetha, P. P., Joseph, V., and Sarojini, B. S. I. (2021). Nitrospira as versatile nitrifiers: taxonomy, ecophysiology, genome characteristics, growth, and metabolic diversity. *J. Basic Microbiol.* 61, 88–109. doi: 10.1002/jobm.202000485

Wang, Y., Ma, L., Mao, Y., Jiang, X., Xia, Y., Yu, K., et al. (2017). Comammox in drinking water systems. *Water Res.* 116, 332–341. doi: 10.1016/j.watres.2017.03.042

Wang, Q., Quensen, J. F. III, Fish, J. A., Lee, T. K., Sun, Y., Tiedje, J. M., et al. (2013). Ecological patterns of nifh genes in four terrestrial climatic zones explored with targeted metagenomics using framebot, a new informatics tool. *mBio* 4:e00592-13. doi: 10.1128/mBio.00592-13

Wang, S., Wang, X., Jiang, Y., Han, C., Jetten, M. S., Schwark, L., et al. (2021). Abundance and functional importance of complete ammonia oxidizers and other nitrifiers in a riparian ecosystem. *Environ. Sci. Technol.* 55, 4573–4584. doi: 10.1021/acs.est.0c00915

Wang, X. M., Wang, S. Y., Jiang, Y. Y., Zhou, J. M., Han, C., and Zhu, G. B. (2020). Comammox bacterial abundance, activity, and contribution in agricultural rhizosphere soils. *Sci. Total Environ.* 727:138563. doi: 10.1016/j.scitotenv.2020.138563

Williams, J., and Crutzen, P. J. (2010). Nitrous oxide from aquaculture. *Nat. Geosci.* 3:143. doi: 10.1038/ngeo804

Xia, F., Wang, J.-G., Zhu, T., Zou, B., Rhee, S.-K., and Quan, Z.-X. (2018). Ubiquity and diversity of complete ammonia oxidizers (comammox). *Appl. Environ. Microbiol.* 84, e01390–e01318. doi: 10.1128/AEM.01390-18

Xu, S., Wang, B., Li, Y., Jiang, D., Zhou, Y., Ding, A., et al. (2020). Ubiquity, diversity, and activity of comammox nitrospira in agricultural soils. *Sci. Total Environ.* 706:135684. doi: 10.1016/j.scitotenv.2019.135684

Xun, W. B., Liu, Y. P., Li, W., Ren, Y., Xiong, W., Xu, Z. H., et al. (2021). Specialized metabolic functions of keystone taxa sustain soil microbiome stability. *Microbiome* 9:35. doi: 10.1186/s40168-020-00985-9

Yang, F., Chen, Q., Zhang, Q., Long, C., Jia, W., and Cheng, X. (2021). Keystone species affect the relationship between soil microbial diversity and ecosystem function under land use change in subtropical China. *Funct. Ecol.* 35, 1159–1170. doi: 10.1111/1365-2435.13769

Yang, X., Yu, X., He, Q., Deng, T., Guan, X., Lian, Y., et al. (2022). Niche differentiation among comammox (nitrospira inopinata) and other metabolically distinct nitrifiers. *Front. Microbiol.* 13:956860. doi: 10.3389/fmicb.2022.956860

Yuan, J., Xiang, J., Liu, D., Kang, H., He, T., Kim, S., et al. (2019). Rapid growth in greenhouse gas emissions from the adoption of industrial-scale aquaculture. *Nat. Clim. Chang.* 9, 318–322. doi: 10.1038/s41558-019-0425-9

Yue, H., Banerjee, S., Liu, C., Ren, Q., Zhang, W., Zhang, B., et al. (2022). Fertilizing-induced changes in the nitrifying microbiota associated with soil nitrification and crop yield. *Sci. Total Environ.* 841:156752. doi: 10.1016/j.scitotenv.2022.156752

Zhang, K., Zheng, X., He, Z., Yang, T., Shu, L., Xiao, F., et al. (2020). Fish growth enhances microbial sulfur cycling in aquaculture pond sediments. *Microb. Biotechnol.* 13, 1597–1610. doi: 10.1111/1751-7915.13622

Zhao, M. Y., Tang, X. F., Sun, D. Y., Hou, L. J., Liu, M., Zhao, Q., et al. (2021). Salinity gradients shape the nitrifier community composition in nanliu river estuary sediments and the ecophysiology of comammox nitrospira inopinata. *Sci. Total Environ.* 795:148768. doi: 10.1016/j.scitotenv.2021.148768

Zheng, X., Tang, J., Ren, G., and Wang, Y. (2017a). The effect of four microbial products on production performance and water quality in integrated culture of freshwater pearl mussel and fishes. *Aquac. Res.* 48, 4897–4909. doi: 10.1111/are.13309

Zheng, X., Tang, J., Zhang, C., Qin, J., and Wang, Y. (2017b). Bacterial composition, abundance and diversity in fish polyculture and mussel-fish integrated cultured ponds in China. *Aquac. Res.* 48, 3950–3961. doi: 10.1111/are.13221

Zheng, M. S., Wang, M. Y., Zhao, Z. R., Zhou, N., He, S. S., Liu, S. F., et al. (2019). Transcriptional activity and diversity of comammox bacteria as a previously overlooked ammonia oxidizing prokaryote in full-scale wastewater treatment plants. *Sci. Total Environ.* 656, 717–722. doi: 10.1016/j.scitotenv.2018.11.435

Zheng, X. F., Zhang, K. K., Yang, T., He, Z. L., Shu, L. F., Xiao, F. S., et al. (2021). Sediment resuspension drives protist metacommunity structure and assembly in grass carp (*Ctenopharyngodon idella*) aquaculture ponds. *Sci. Total Environ.* 764:142840. doi: 10.1016/j.scitotenv.2020.142840

Zhu, G., Wang, X., Wang, S., Yu, L., Armanbek, G., Yu, J., et al. (2022). Towards a more labor-saving way in microbial ammonium oxidation: a review on complete ammonia oxidization (comammox). *Sci. Total Environ.* 829:154590. doi: 10.1016/j.scitotenv.2022.154590

frontiers | Frontiers in Microbiology

TYPE Original Research
PUBLISHED 30 April 2024
DOI 10.3389/fmicb.2024.1395583

OPEN ACCESS

EDITED BY
Jin Zhou,
Tsinghua University, China

REVIEWED BY
Juan Ling,
Chinese Academy of Sciences (CAS), China
Keqiang Shao,
Chinese Academy of Sciences (CAS), China

*CORRESPONDENCE
Lijuan Ren
✉ lijuanren@jnu.edu.cn

RECEIVED 04 March 2024
ACCEPTED 03 April 2024
PUBLISHED 30 April 2024

CITATION
Shan Z, Chen H, Deng Y, He D and Ren L (2024) An abrupt regime shift of bacterioplankton community from weak to strong thermal pollution in a subtropical bay. *Front. Microbiol.* 15:1395583. doi: 10.3389/fmicb.2024.1395583

An abrupt regime shift of bacterioplankton community from weak to strong thermal pollution in a subtropical bay

Zhiyi Shan[1], Haiming Chen[1], Yuan Deng[1], Dan He[2] and Lijuan Ren[1]*

[1]Department of Ecology and Institute of Hydrobiology, Jinan University, Guangzhou, China, [2]Center for Evolution and Conservation Biology, Southern Marine Science and Engineering Guangdong Laboratory (Guangzhou), Guangzhou, China

Thermal pollution from the cooling system of the nuclear power plants greatly changes the environmental and the ecological conditions of the receiving marine water body, but we know little about their impact on the steady-state transition of marine bacterioplankton communities. In this study, we used high-throughput sequencing based on the 16S rRNA gene to investigate the impact of the thermal pollution on the bacterioplankton communities in a subtropical bay (the Daya Bay). We observed that thermal pollution from the cooling system of the nuclear power plant caused a pronounced thermal gradient ranging from 19.6°C to 24.12°C over the whole Daya Bay. A temperature difference of 4.5°C between the northern and southern parts of the bay led to a regime shift in the bacterioplankton community structure. In the three typical scenarios of regime shifts, the steady-state transition of bacterioplankton community structure in response to temperature increasing was more likely consistent with an abrupt regime shift rather than a smooth regime or a discontinuous regime model. Water temperature was a decisive factor on the regime shift of bacterioplankton community structure. High temperature significantly decreased bacterioplankton diversity and shifted its community compositions. *Cyanobium* and *Synechococcus* of Cyanobacteria, NS5 marine group of Bacteroidota, and *Vibrio* of Gammaproteobacteria were found that favored high temperature environments. Furthermore, the increased water temperature significantly altered the community assembly of bacterioplankton in Daya Bay, with a substantial decrease in the proportion of drift and others, and a marked increase in the proportion of homogeneous selection. In summary, we proposed that seawater temperature increasing induced by the thermal pollution resulted in an abrupt regime shift of bacterioplankton community in winter subtropical bay. Our research might broad our understanding of marine microbial ecology under future conditions of global warming.

KEYWORDS

bacterioplankton diversity, thermal pollution, regime shift, a subtropical bay, community assembly

1 Introduction

Regime shifts are present in most natural ecosystems and complex social systems (Rial et al., 2004; Schröder et al., 2005; Brock and Carpenter, 2006; Dakos et al., 2019; Hughes et al., 2019). Regime shifts in ecosystems could be regarded as a sudden change in ecosystem status where core ecosystem structures, functions and processes are fundamentally shifted at an environmental threshold (Lees et al., 2006; Dakos et al., 2019; Berdugo et al., 2020). These regime shifts are generally driven by external perturbations or the system's internal dynamics following the environmental changes (Scheffer et al., 2001; Guttal and Jayaprakash, 2007; Lu and Hedin, 2019). The external perturbations include global change such as climate warming, overexploitation, invasive species, and eutrophication in both freshwater and marine ecosystems (Hare and Mantua, 2000; Schröder et al., 2005; Andersen et al., 2009; McMahon et al., 2015; Rocha et al., 2018). In most cases, these external perturbations can suddenly tip ecosystems to an alternative stable state, and according to this, they may be early warned by warning signal of the regime shifts (Guttal and Jayaprakash, 2008; McGlathery et al., 2013; Wernberg et al., 2016; Putten et al., 2019). The existence of an abrupt change-point in ecological system is a necessary condition for warning a regime shift. There are three typical scenarios for regime shifts: smooth, abrupt, and discontinuous. Two of them, smooth and abrupt, can be reversibly in response to the change in environment, however the other one was not reversible (Andersen et al., 2009; Dakos et al., 2019). The first one is smooth pressure-status relationships (smooth regime shift). In this type of regime shifts, environmental conditions often change gradually, even linearly. Ecosystem in this state tend to change in a smooth way. The second one is threshold-like state responses (abrupt regime shift), in which the ecosystem state shifts to another state suddenly after the environmental condition exceeds a threshold. The last one is bistable systems with hysteresis (discontinuous regime shift), which the hysteresis loop linking the ecosystem state to the environmental driver results in jumps between two alternative states when the driver is first slowly increased and then decreased again (DeYoung et al., 2004; Lees et al., 2006; Su et al., 2019; Martin et al., 2020; Moi et al., 2021).

Most studies of steady-state transition are focused on marine fish (Rahman et al., 2019; Perälä et al., 2020), phytoplankton, zooplankton (Djeghri et al., 2023), sediment (Dijkstra et al., 2019), or ecosystem (Szalaj et al., 2021), but fewer research investigates bacterioplankton community. Bacterioplankton is an indispensable part of the plankton food web and plays a crucial role in the biogeochemistry cycle by regenerating nutrients and decomposing organic matter (Ruiz-González et al., 2015). The temperature optimum varies among different bacterioplankton populations, and thus water temperature is one of the main driving factors that determine the community structure of bacterioplankton (Daufresne et al., 2009; Adams et al., 2010; Ren et al., 2013, 2017). A small increase in water temperature will indirectly lead to changes in the abundance and biomass of bacterioplankton (Christoffersen et al., 2006; Özen et al., 2013). Simultaneously, environmental warming will enhance the complexity of species associations, leading to changes in the diversity, structure and function of bacterial community (Zhu et al., 2019; Zhao et al., 2020; Yuan et al., 2021). In the study of Xingyun Lake, it had been shown that water temperature was a major factor affecting plankton biomass and community succession, and meanwhile, temperature was a major force in the regime shift (Wang et al., 2010). Rosero-López and his colleague found that the increase in temperature significantly enhanced the abundance of cyanobacteria and promoted the transition of regime shifts in aquatic ecosystems (Rosero-López et al., 2022). Temperature was thus a significant environmental factor affecting the diversity, community structure and function of bacterioplankton, and it might be also a factor that promoted regime shifts of bacterioplankton community in water bodies. There may be an early warning temperature that serves as an indicator for steady state transformation (Zhang et al., 2015; Anderson et al., 2018; Rosero-López et al., 2022).

Daya Bay is a typical subtropical bay locating in the north of the South China Sea (Tang et al., 2018). Long-term thermal pollution from the cooling systems of the nuclear power plants generates a temperature gradient in the Daya Bay, making it an ideal experimental area for studying regime shift driven by seawater temperature increasing. Long-term thermal pollution can cause changes in the bacterioplankton community compositions (Niu et al., 2011; Eiler et al., 2012; Ren et al., 2019), and the increase in water temperature as an external driving force might promote the steady-state transformation of bacterial community structure. Therefore, in this study, we aimed to answer (i) whether there is a steady-state transition driven by the increase in seawater temperature caused by the long-term thermal pollution from the nuclear power plants? (ii) which of the three typical models (smooth regime shift, abrupt regime shift, and discontinuous regime shift) does the steady-state transformation of bacterial community structure match when in response to an external driving force of seawater temperature increasing? (iii) how do the diversity and structure of bacterioplankton communities change after steady-state transformation. Our research might contribute to a better understanding of marine microbial ecology under future conditions of global warming.

2 Materials and methods

2.1 Study area

Daya Bay is located in the northern South China Sea (22°30′N to 22°50′N, 114°29′E to 114°49′E) between Shenzhen and Huizhou on the south of Guangdong Province, China. The depth in the middle of the Daya bay is about 10 meters while the depth of the bay mouth is match up to 20 meters. The Daya Bay belongs to subtropical monsoon climate, with an average annual air temperature of 22°C. Our water samples were collected on December 1st (2021) when the air temperature was from 9°C to 18°C. The northeast and west of Daya Bay were mostly used for aquaculture, the north was petrochemical area, the east was tourism development zone, and the southwest was located by the Daya Bay nuclear power station which began operation with an installed capacity of 1.968 million kilowatts in 1994 and with an installed capacity of 2.172 million kilowatts in 2010 (data provided by South China Nuclear and Radiation Safety Supervision Station of the Ministry of Ecology and Environment). Thermal effluents from the two nuclear power plants cooling systems have been present in the

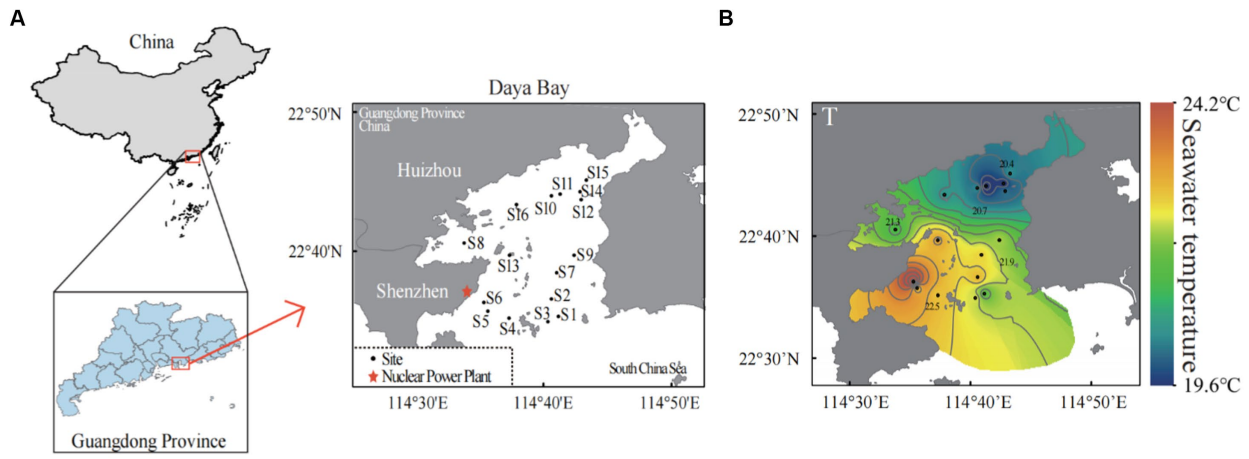

FIGURE 1
Sampling sites in the subtropical Daya Bay on the northern coast of the South China Sea. A total of 16 sites were sampled in the bay area: seven scattered sites in the north (S8, S10–S12, S14–S16), two scattered sites in the middle of the bay area (S9, S13), seven scattered sites in the south (S1–S7), and site S6 is the site near the outlet of thermal effluents from nuclear power plants **(A)**. The distributions of seawater temperature in the Daya Bay **(B)**.

Daya Bay for more than 20 years and have generated a comparatively stable temperature gradient (a temperature increase from 0 to 5°C at the sampling time).

2.2 Water sample collection and environmental determination

We totally set 16 sampling sites according to the functional area of Daya Bay. Seven sites were located in the south of the bay which were more affected by the thermal effluents from the nuclear power plants (S1–S7), and S6 was sampling site that was closest to the nuclear power plants. There were two sites in the middle of the bay (S9 and S13) and the remaining 7 sites were in the north of the bay (S8, S10–S12, S14–S16) (Figure 1A). We collected three replicates at each sampling site. The sea surface temperature, salinity, dissolved oxygen and pH were measured in each replicate site by using multi-parameter water quality analyzer (YSI 6600, Yellow Spring, OH, United States; Xu et al., 2010). In each replicate site, 5-liter surface seawater was collected by using 0.2-μm-pore-size Isopore filters (Millipore, Billerica, MA, United States). The filters were unsealed in a clean bench and stored at −80°C in refrigerator until further analyses. Another 500 mL of surface seawater in each replicate site was collected for the nutrient measurements including ammonium nitrogen (NH_4^+), nitrate nitrogen (NO_3^-), nitrite nitrogen (NO_2^-), silicate (SiO_3^{2-}) and soluble reactive phosphorus (SRP). All these nutrients were determined using a UV–visible spectrophotometer (UV2450; Shimadzu, Tokyo, Japan) according to marine monitoring specifications (General Administration of Quality Supervision, 2007).

2.3 DNA extraction and PCR amplification, high-throughput sequencing and data processing

We use PowerWater DNA isolation Kit (MoBio Laboratories, CarIsbad, CA) to extract the Genomic DNA from the biomass collected on the filters, then purify the Genomic DNA by using PowerClean DNA Clean-up Kit (MoBio Laboratories, CarIsbad, CA, United States). Using a NanoDrop 2000 spectrophotometer (Thermo Scientific, Wilmington, DE Ren et al., 2019) to quantify the DNA and determine its quality. With 60 ng DNA as template, PCR amplification was performed in the V3 and V4 hypervariable regions of bacterial 16S rRNA genes, and the amplification primers were F515(5′-GTGCCAGCMGCCGCGGTAA-3′) and R907(3′-CCGTCAATTCCTTTGAGTTT-5′). We added a unique 12-mer tag to the 5′ end of each single DNA sample for pooling multiple samples in one Illumina sequencing run. The cycling conditions of PCR reactions included 94°C for 5 min initially, soon afterwards 30 cycles of denaturation for 30 s at 94°C, 30 s at 52°C for annealing, 30 s at 72°C for extension, and 10 min at 72°C for a final extension. The PCR products were visualized on 1% agarose gels by agarose gel electrophoresis, and then used the PicoGreen dsDNA assay kit (Invitrogen Corporation, CarIsbad, CA, United States) to quantify the positive amplicons. Zymo's Genomic DNA Clean & Concentrator kit (Zymo Research Corporation, Irvine, CA, United States) were used to equally combine and purify the PCR products. Ultimately, using the Illumina HiSeq 2500 platform to sequence the amplicons.

Raw sequences based on 16S rRNA gene were processed with the mothur software package (version 1.30.0, 2013)[1] according to the MiSeq standard operating procedure (Kozich et al., 2013). To sum up, raw reads were combined, denoised, trimmed, quality-filtered, and aligned to the SILVA 16S version 138 using mothur (Quast et al., 2013). After that, the high-sequences were clustered into ASVs at a rate of 100% similarity level, meanwhile, the lineages belonging to chloroplasts, mitochondria, eukaryotes or unknown were removed. Each of the representative ASV sequences was classified using the SILVA 16S version 138 at the recommended bootstrap threshold of 80% (Wang et al., 2007). All singletons and ASVs occurring in only two samples were excluded from the ASV table in order to minimize

1 http://www.mothur.org

bias caused by sequencing depth. Finally, we obtained 4,602 ASVs in ASV table through the entire sample set. Ultimately, the minimum number of sequences in the whole sample was randomly subsampled to correct for differences in sequencing depth, and then the following metrics described below were all based on this final ASV table.

2.4 Statistical analyses

The spatial distribution of seawater temperature was visualized by using the Spatial Analyst tool and 3D Analyst tool of ArcToolbox in ArcGIS software. Bacterioplankton community structure was analyzed by performing detrended correspondence analysis (DCA) in the R package of vegan. To determine the existence of regime shift, we drew a linear fitting diagram between DCA1 values and water temperature by using ggplot2 and ggpmisc package in R (Hu et al., 2020). And the critical point estimation of regime shift was according to the linear fitting diagram between DCA1 values and water temperature by using piecewise regression analyses (Hu et al., 2020).

Subsequently, our study had done the analyses to explore the differences among the states of regime shifts. We used the vegan package of R to perform permutational multivariate analysis of variance (PERMANOVE) to test whether the states of regime shift had significant influence on bacterioplankton community structure. Columnar stacking maps about the relative abundance of bacterioplankton were conducted using GraphPad Prism 8 software. The venn plot was performed to verify the shared and unique bacterioplankton ASVs among different states of regime shifts by using the VennDiagram package in R. The redundancy analysis (RDA) was carried out to link bacterioplankton community compositions with environmental variables by using the ggvegan package in R. The relationships of the relative abundance of bacterioplankton phylum, family, and genus with temperature, as well as the relationships of the ASV richness and Shannon index with temperature was assessed by using the ordinary least square (OLS). The heatmaps were performed to show the distributions of the relative abundances of the top 25 genus/families (clades) along temperature gradients using the "pheatmap" package in R. Bacterioplankton community assembly processes were calculated by using iCAMP and treeio packages in R, and visualized by GraphPad Prism8 (Ning et al., 2020).

3 Results

3.1 The steady-state transformation of bacterioplankton community structure in response to long-term thermal pollution in the Daya Bay

In our study, the winter water temperature in Daya Bay ranged from 19.6°C to 24.12°C, and it was found being the primary environmental factor influencing the compositions of the bacterioplankton community. There were significant positive correlations between temperature and salinity/solubility reactive phosphorus (SRP) and negetive correlations between temperature and pH/NH_4^+ (Supplementary Figure S1). Due to long-term thermal pollution from the nuclear power plant, seawater temperature increased in the Daya Bay, leading to a significant temperature difference of 4.5°C between the southern and northern parts of the bay (Figure 1B).

Linear regression analysis between DCA I axis values and seawater temperature revealed that the steady-state transformation of bacterioplankton community structure in response to seawater temperature increasing aligned with abrupt regime shift of the three typical ecological steady-state transition models (smooth regime shift, abrupt regime shift, and discontinuous regime shift). Critical points were identified at 20.5°C and 22°C, resulting in three stable states: State 1 (<20.5°C), Transition State (TS, 20.5°C < and < 22°C), and State 2 (>22°C) (Figure 2A). In redundancy analysis, the RDA1 axis explained 22.2% of bacterioplankton community structure, and the RDA2 axis explained 9.22%. A significant divergence in bacterioplankton community structure was observed between State 2 and the others, while State 1 and TS also differed on the RDA2 axis (Supplementary Figure S1). Similar findings were observed in detrended correspondence analysis (DCA), showing a significant divergence in the bacterioplankton community compositions according to seawater temperature (Figure 2B).

3.2 Alpha diversity patterns of bacterioplankton according to the three states in regime shift

ASV richness index, Shannon index, Simpson index, Pielou index, Chao1 index, and ACE index all exhibited a highly significant negative correlations with temperature (Spearman correlations: $R = -0.546$, $p < 0.01$ for ASV richness index; $R = -0.674$, $p < 0.01$ for Shannon index; $R = -0.696$, $p < 0.01$ for Simpson index; $R = -0.709$, $p < 0.01$ for Pielou index; $R = -0.552$, $p < 0.01$ for Chao1 index; $R = -0.550$, $p < 0.01$ for ACE index) (Table 1). The linear regression curve and the steady-state change curve of alpha diversity indices (Shannon index and ASV Richness index) with seawater temperature fitted well. The alpha diversity of bacterioplankton communities decreased with increasing temperature, accompanied by significant changes during regime shifts (Figures 3A,B). Comparative analyses of alpha diversity indices (Shannon index and ASV Richness) among the three stable states indicated that alpha diversity in state 2 was lower than in TS, and both were lower than in state 1(Figures 3C,D). This suggested a decreasing trend in alpha diversity with increasing seawater temperature.

3.3 The shifts in bacterioplankton community compositions according to the three states of regime shifts

At the phylum level, bacterioplankton phyla with top five highest relative abundance had significant correlations with seawater temperature (Spearman correlations: $R = 0.570$, $p < 0.01$ for Actinobacteriota; $R = -0.506$, $p < 0.01$ for Alphaproteobacteria; $R = -0.748$, $p < 0.01$ for Bacteroidota; $R = 0.525$, $p < 0.01$ for Cyanobacteria; $R = -0.544$, $p < 0.01$ for Gammaproteobacteria) (Supplementary Figure S2; Supplementary Table S1). Among the transition of regime shift, a noticeable change occurred in the compositions of bacterioplankton communities. In state 2, the relative

10.3389/fmicb.2024.1395583

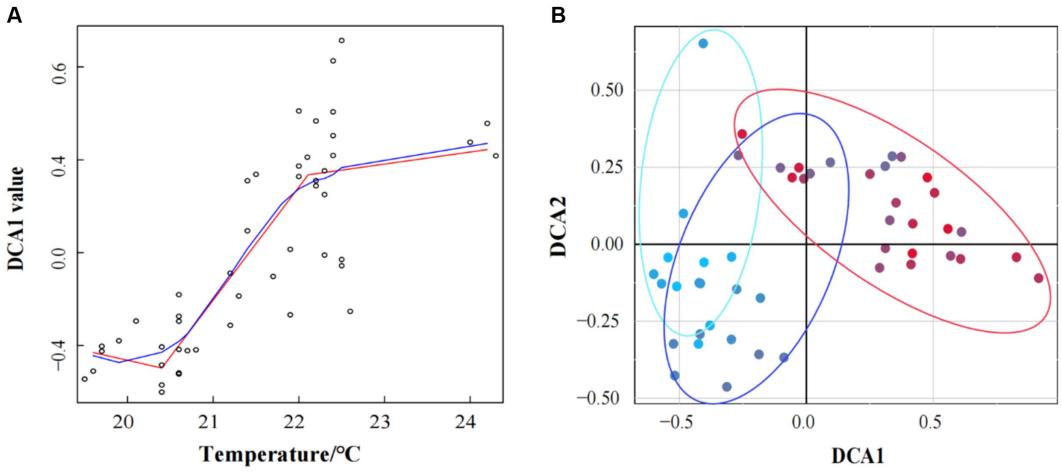

FIGURE 2
Under temperature conditions, DCA1 values exhibited a regime shift, with critical points of 20.5°C and 22°C. The blue line was a smooth fitting curve between the DCA1 value and water temperature; The red line was a segmented linear regression line that displayed the tipping point **(A)**. Detrended correspondence analysis (DCA) of bacterioplankton community structures in winter of Daya Bay. The blue circle represented samples below 20.5°C, the purple circle represented samples between 20.5°C and 22°C, and the red circle represented samples above 22°C **(B)**.

TABLE 1 **The relationships between environmental factors and the alpha diversity of bacterioplankton, including the Spearman correlation statistic's *R* values and statistical significance, determined through 9,999 permutations.**

α diversity	Environment factors	*R* value	*p* value
ASV Richness	T	−0.546	<0.01
Shannon	T	−0.674	<0.01
Simpson	T	−0.696	<0.01
Pielou	T	−0.709	<0.01
Chao1	T	−0.552	<0.01
ACE	T	−0.550	<0.01
Richness	Sal	−0.346	0.016
Shannon	Sal	−0.436	0.002
Simpson	Sal	−0.499	0.0003
Pielou	Sal	−0.472	0.001
Chao1	Sal	−0.349	0.015
ACE	Sal	−0.349	0.015

T, seawater temperature; Sal, Salinity.

abundance of Gammaproteobacteria, Bacteroidota, Planctomycetota and Alphaproteobacteria was significantly lower than in state 1. In contrast, Cyanobacteria and Actinobacteriota exhibited significantly higher relative abundance in state 2. The transition state exhibited intermediate relative abundance between state 1 and state 2 (Supplementary Figure S3). DCA analysis of the top seven phyla by relative abundance, with linear analysis of DCA I axis data and seawater temperature, showed that the trends of Actinobacteriota, Alphaproteobacteria, Bacteroidota, and Campilobacterota aligned well with abrupt regime shift of the three typical ecological steady-state transition models (Supplementary Figure S4).

Among the top 10 genus/families (clades) with the highest relative abundance, Formosa and NS4 marine group of Bacteroidota, *Halieaceae* of Gammaproteobacteria, and HIMB11 of Alphaproteobacteria exhibited significant decrease in abundance as the steady state transitioned from state 1 to state 2. In contrast, the relative abundance of NS5 marine group of Bacteroidota, *Synechococcus* of Cyanobacteria, and Candidatus *Actinomarina* of Actinobacteriota increased when the steady state transitioned from state 1 to state 2 (Figure 4). *Arcobacteraceae* of Campilobacterota, *Blastopirellula* of Planctomycetota, *Halieaceae* and Luminiphilus of Gammaproteobacteria, *Ascidiaceihabitans* of Alphaproteobacteria, and NS9 marine group, *Cryomorphaceae*, and *Fluviicola* of Bacteroidota dominated in state 1. In the transition state, the main lineages or clades were mostly composed of the bacteria UBA10353 marine group of Gammaproteobacteria, Sva0996 marine group of Actinobacteriota, NS4 marine group, and NS2b marine group of Bacteroidota, and HIMB11 and *Rhodobacteraceae* of Alphaproteobacteria. Meanwhile, *Synechococcus* and *Cyanobium* of Cyanobacteria, NS5 marine group of Bacteroidota, SAR11 clade and SAR116 clade of Alphaproteobacteria, and SAR86 clade of Gammaproteobacteria dominated in state 2 (Figure 5).

In linear regression analyses, the relative abundance of *Cyanobium* and *Synechococcus* of Cyanobacteria, NS5 marine group of Bacteroidota, and *Vibrio* of Gammaproteobacteria showed a significant positive correlation with seawater temperature. Simultaneously, the relative abundance of *Flavobacteriaceae* of Bacteroidota and *Rhodobacteraceae* of Alphaproteobacteria decreased with increasing seawater temperature. Additionally, SAR11 clade of Alphaproteobacteria, UBA10353 marine group, and SAR86 clade of Gammaproteobacteria showed a lower correlation with seawater temperature. The linear regression curves of these nine genus/families (clades) with temperature were similar, and bacterioplankton relative abundance underwent changes during their regime shifts (Supplementary Figure S6).

Based on the ASV table, a Venn diagram was constructed to show shared and unique ASVs among the three states during regime shifts. The results revealed a total of 934 shared ASVs among the three states, accounting for 20.6% of the total ASVs. State 1 had 791 unique ASVs,

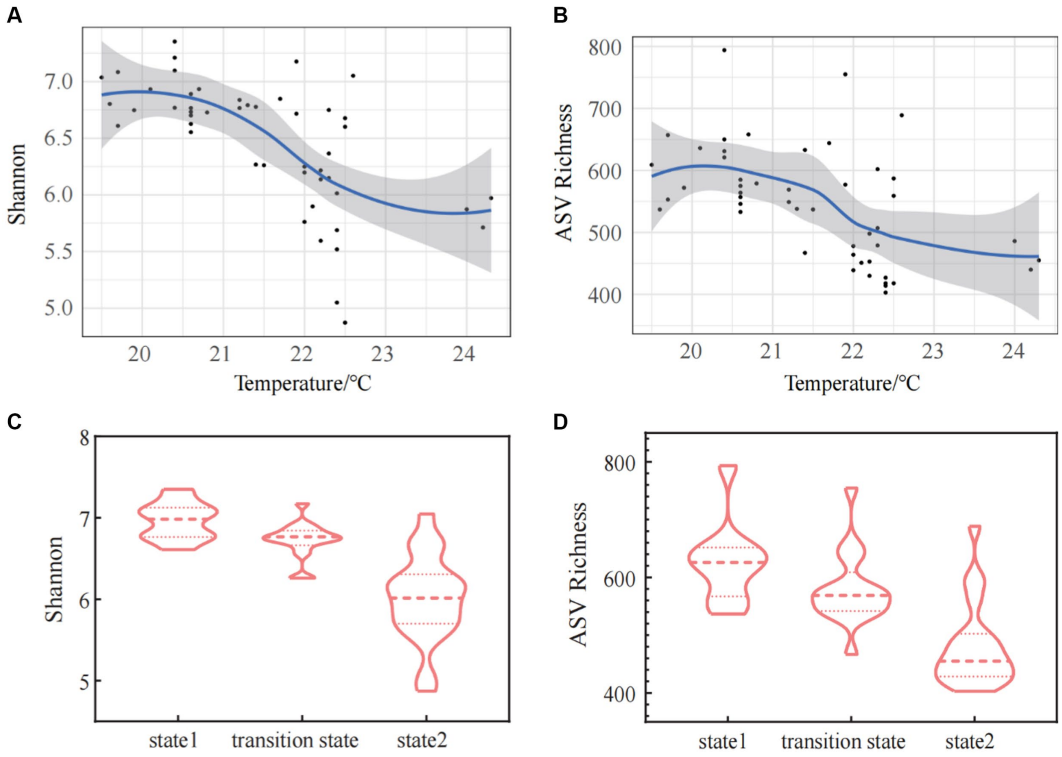

FIGURE 3
The alpha diversity [Shannon index **(A)** and ASV Richness index **(B)**] of bacterioplankton along the gradient of the water temperature. The changes of Shannon index **(C)** and ASV Richness index **(D)** in three states of the regime shift.

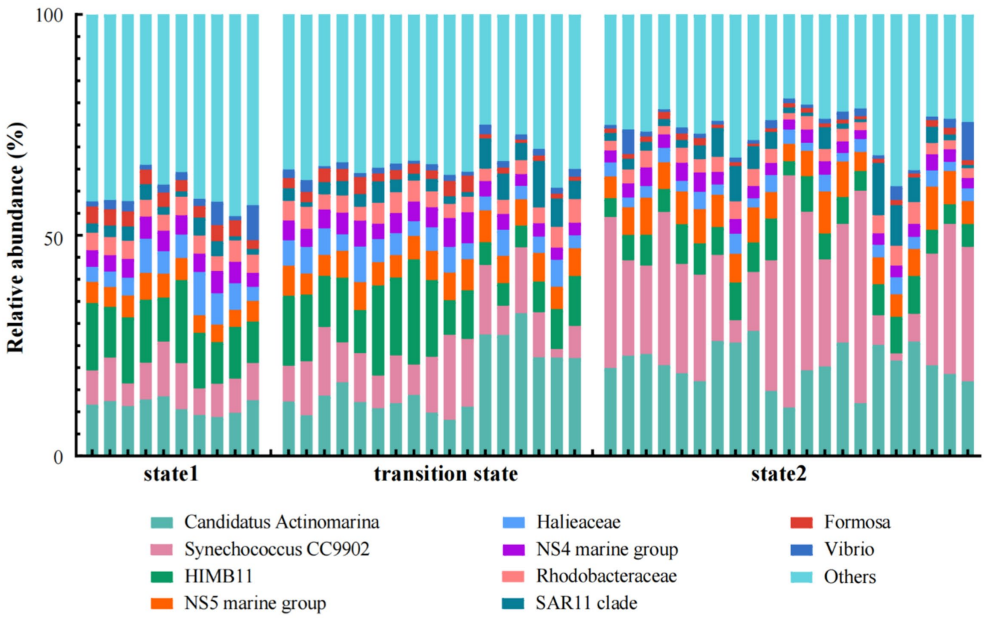

FIGURE 4
Relative abundances of the dominant bacterial taxa in the three states of regime shift which was separated by water temperature.

representing 17.5%, TS had 1,157 unique ASVs, constituting 25.6%, and state 2 had 1,048 unique ASVs, making up 23.2%. The number of unique ASVs in TS and state 2 was significantly higher than in state 1 (Supplementary Figure S5). Additionally, permutational multivariate analysis of variance showed that BCCs among the three stable states had significant differences ($p < 0.01$), and the differences of the

10.3389/fmicb.2024.1395583

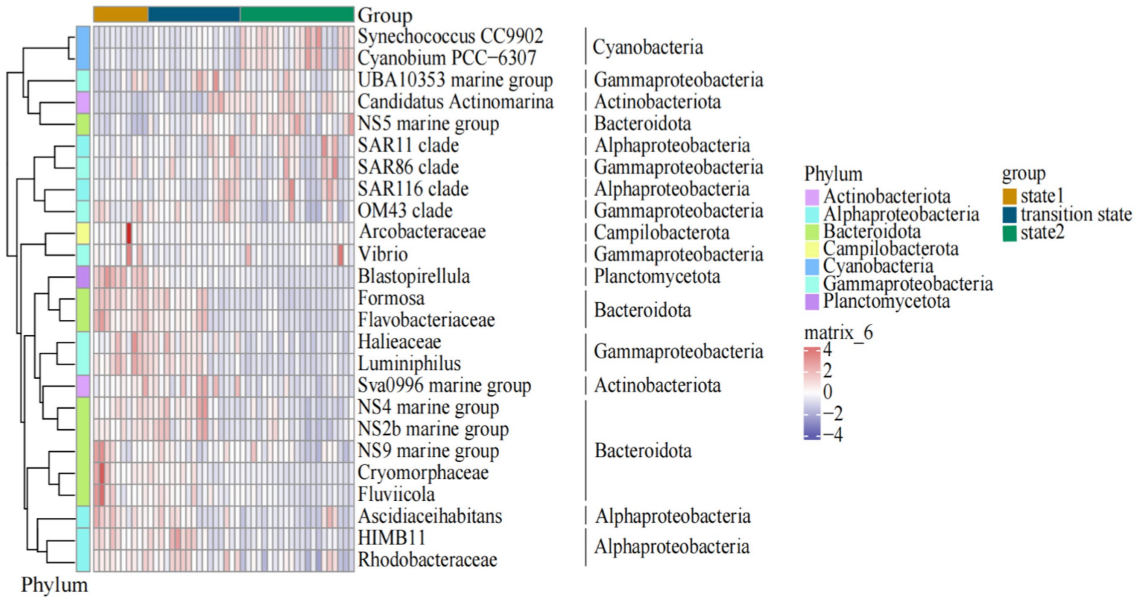

FIGURE 5
The distributions of the dominant bacterioplankton taxa along the gradient of the water temperature in the Daya Bay.

TABLE 2 Significance tests of bacterioplankton community compositions (BCCs) in three states of regime shift, respectively.

	F model	R^2	*p* value
State 1 vs. state 2	19.638	0.404	<0.001
State 1 vs. TS	3.830	0.133	0.002
State 2 vs. TS	10.277	0.222	<0.001
Overall	11.328	0.335	0.001

Permutational multivariate analysis of variance (PERMANOVA) based on Bray–Curtis dissimilarity matrices was used. $p < 0.01$. TS, transition state.

pairwise BCC comparisons among the three stable states were also highly significant ($p < 0.01$) (Table 2).

3.4 The shifts in bacterioplankton community assembly processes according to the three states in regime shift

In the three states in regime shift, the processes of the bacterioplankton community assembly (including heterogeneous selection, homogeneous selection, dispersal limitation, homogenizing dispersal, and drift and others) were dominantly characterized by homogeneous selection (74.75%), followed by drift and others (18.54%) and dispersal limitation (5.22%). While, homogenizing dispersal made a smaller contribution (1.39%), and heterogeneous selection almost had no impact (0.10%) (Figure 6A). When calculating the processes of bacterioplankton community assembly by grouping samples based on bacterioplankton regime shift driven by seawater temperature, the results revealed that homogeneous selection consistently dominated in all three states. In the transition of regime shift, the proportion of homogeneous selection increased from 58.02% in state 1 to 79.50% in TS, and reaching to 82.31% in state 2. In contrast, the relative importance of drift and others significantly decreased after the transition of regime shift, dropping from 36.56% in state 1 to below 15% in state 2. Additionally, the proportion of homogenizing dispersal in state 2 was significantly lower than in state 1 and TS (Figure 6B).

4 Discussion

The thermal effluents from two nuclear power plants in Daya Bay have been present for more than 20 years and have generated comparatively stable temperature gradients (a temperature increase from 0 to 5°C) in the whole Bay. We found the increase in seawater temperature of the bay as an external driving force caused a steady-state transition of bacterioplankton community structure. This steady-state transition more likely matched an abrupt regime shift rather than a smooth regime or a discontinuous regime model, and it caused significant changes of bacterioplankton community diversity, compositions and structure.

4.1 Temperature increasing caused by long-term thermal pollution caused an abrupt regime shift of bacterioplankton community structure in the Daya Bay

Due to Daya Bay being a semi enclosed bay, the long-term thermal effluents from the cooling systems of the Daya Bay Nuclear Power Plant, has significantly impacts on the seawater temperature in Daya Bay, resulting in a substantial temperature difference between the northern and the southern parts of the bay in winter (Figures 1A,B). Our study revealed long-term thermal effluents from nuclear power plants had a strong impact on bacterioplankton community, and beyond a certain temperature critical point, the bacterioplankton community structure underwent a regime shift. Our findings were

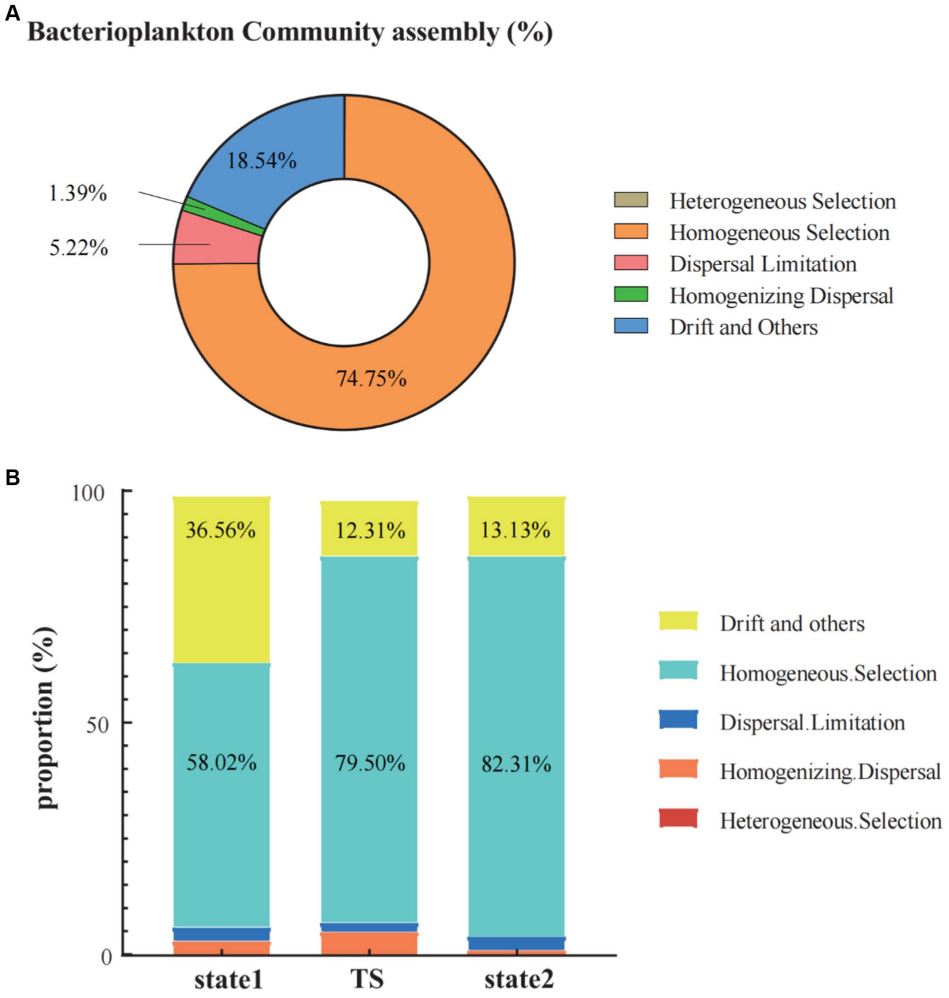

FIGURE 6
The community assembly processes in the Daya Bay included heterogeneous selection, homogeneous selection, dispersal limitation, homogenizing dispersal and the drift and other fractions **(A)**. The bar chart showed the trend of changes in the proportions of community assembly processes (heterogeneous selection, homogeneous selection, dispersal limitation, homogenizing dispersal and the drift and other) in the three states of the regime shift, respectively **(B)**.

supported by the existing research, which suggested that water temperature was one of the important environmental factors in shaping aquatic plankton communities (Wang et al., 2010; Berner et al., 2018; Rosero-López et al., 2022). For instance, in the research on the impact of water flow on benthic cyanobacteria, Rosero-López et al. (2022) found that a decrease in water flow can lead to an increase in water temperature, resulting in a significant decrease in benthic cyanobacteria biomass. Upon reaching a certain critical point, the structure and function of benthic communities underwent a sudden shift (Rosero-López et al., 2022).

Our research found that in the winter of the Daya Bay, bacterioplankton community structure underwent a significant transformation when the seawater temperature reached 20.5°C and 22°C, indicating that these temperatures were critical points for the occurrence of regime shifts in bacterioplankton community structure in the Daya Bay (Figure 2A). The study of Berner et al. (2018) on the relationship between seawater temperature and bacterial communities in the Northwest of Gotland Sea (Baltic Proper) showed that changes in temperature directly affect bacterial community composition. An increase in temperature lead to an increase in cyanobacterial biomass and a faster peak (Berner et al., 2018). Therefore, it is confirmed once again that the bacterioplankton community is highly sensitive to changes in water temperature and can produce a rapid response. Moreover, a significant temperature difference was found to easily induce a regime shift in aquatic bacterioplankton community (Wang et al., 2010; Berner et al., 2018; Rosero-López et al., 2022).

4.2 The regime shift of bacterioplankton community structure under thermal pollution decreased bacterioplankton alpha diversity

In the aquatic ecosystems, the alpha diversity of the bacterioplankton community (e.g., Shannon index, ASV Richness, etc.) was influenced by various environmental factors. As water temperature could affect the activity of microbial metabolic enzymes directly, the impact of seawater temperature on the alpha diversity of microbial communities was direct and significant (Adams et al., 2010). Especially in coastal areas, changes in water temperature have a

filtering effect on microbial communities, influencing their composition and altering their diversity (Trombetta et al., 2019; Lambert et al., 2021; Trombetta et al., 2021). Several studies had confirmed that water temperature can directly or indirectly affect the microbial diversity (Wu et al., 2019; Liu et al., 2023). Research on microorganisms in sediment from the South China Sea indicated that a decrease in temperature can lead to a reduction in bacterial diversity (Wu et al., 2019). The study of Trombetta et al. demonstrated that temperature was the primary driving force for the diversity of bacterioplankton in coastal ecosystems, and the increase in seawater temperature significantly affected the diversity of bacterioplankton communities (Trombetta et al., 2022).

Our research found a significant negative relationship between the alpha diversity of bacterioplankton community (Shannon index, ASV Richness) and the changes in water temperature in the surface seawater of Daya Bay during winter. Many studies had also demonstrated that the microbial richness decreased with increasing temperature (Rao et al., 2021; Grabowska-Grucza et al., 2022; Xing et al., 2022). The correlation analysis between bacterioplankton diversity and temperature showed that there was a significant positive correlation between bacterioplankton diversity and water temperature at 9°C to 19°C, while there was a significant negative correlation between bacterioplankton and water temperature at 19°C to 30°C (Liu et al., 2023). Similarly, in the experiment at geothermal environment, it was also demonstrated that microbial diversity was directly controlled by temperature, and the diversity of microorganisms began to show a decreasing trend at around 20°C (Sharp et al., 2014). This temperature was identified as the critical point for significant changes in the alpha diversity of bacterioplankton communities in aquatic environments. As confirmed by our research, when seawater temperature high than 20.5°C, it caused a regime shift in the alpha diversity of bacterioplankton communities. However, the alpha diversity of bacterioplankton community will not continue to decrease. Instead, it reached a new stable state around 22.5°C (state 2). The diversity change was more apparent in the transition state.

4.3 The regime shifts of bacterioplankton community structure under thermal pollution changed bacterioplankton community composition

In our study, specific bacterioplankton taxa were found in each of the three states in the regime shifts (Figures 4, 5; Supplementary Figure S3). One such taxa was *Synechococcus*, supporting previous observations that temperature was an important factor influencing *Synechococcus* distribution (Hamilton et al., 2014; Kolda et al., 2020). Our study showed that the relative abundance of *Synechococcus* in state 2 (> 22°C) was significantly higher than that in state 1 (20.5°C) and TS (from 20.5°C to 22°C) in winter seawater. It was similar to the findings in Kim et al. (2018), which indicated that relative abundance of *Synechococcus* was increased at 24°C compared to an environment temperature of 20°C. When seawater temperature ranging from 21°C to 28°C, the relative abundance of NS5 marine group increased as temperature increasing, showing a significant positive correlation with seawater temperature (Liu et al., 2022). Similarly, in our study, the relative abundance of NS5 marine group was positively correlated with temperature when it in a range of 20°C to 24°C (Supplementary Figure S6). This finding was probably because NS5 marine group preferred environments with high chlorophyll-a concentration and enriched nutrient conditions in the marine ecosystems (Lucas et al., 2015; Díez-Vives et al., 2019; Tong et al., 2021). Our study found that the relative abundance of *Flavobacteriaceae* of Bacteriodota and *Rhodobacteraceae* of Alphaproteobacteria showed significant negative correlations with increasing temperature (Supplementary Figure S6). Similar findings were shown in previous studies that an increase in water temperature can lead to a significant decrease in the richness and the relative abundance of *Flavobacteriaceae* and *Rhodobacteraceae* (Buchan et al., 2014; Gutiérrez et al., 2018). The response of these specific bacterial taxa to the increase in seawater temperature suggested that different bacterioplankton taxa tended to have different optimal temperatures, and led to a regime shift of bacterioplankton community structure under thermal pollution.

4.4 The regime shifts of bacterioplankton community structure under thermal pollution changed bacterioplankton community assembly processes

There are several community assembly processes that determined community diversity and dynamics, including heterogeneous selection (HeS), homogeneous selection (HoS), dispersal limitation (DL), homogenizing dispersal (HD), and 'drift and others' (DR) (Vellend, 2010; Vellend et al., 2014). In general, homogeneous selection was the main community assembly process (70–80%) of communities in marine surface bacterioplankton community, and stochastic processes had much weaker impact on surface water bodies (Allen et al., 2020). The community assembly process in the surface seawater of Daya Bay was similar to the findings of Allen et al. (2020), which also showed homogeneous selection being the main community assembly process in determining bacterial community assembly. Studies had also shown that moderately eutrophic bays had an inducing effect on the selectivity and stability of bacterioplankton communities, thereby enhancing community structure and deterministic processes, which typically played a more important role than stochastic processes (Dai et al., 2017; Li et al., 2020; Jiao et al., 2021; Wu et al., 2021). Our research drew the same conclusion that, as eutrophic bay, the deterministic process dominated in Daya Bay.

Water temperature was one of the key factors affecting community assembly and the most important environmental modulator for balancing stochastic and deterministic assembly processes (Allen et al., 2020; Zhu et al., 2022; Liu et al., 2023). Our research also confirmed that the impact of changes in water temperature on deterministic and stochastic processes was most evident at the critical point of 20.5°C in regime shift. Studies had confirmed that deterministic processes made a greater contribution to the community assembly of bacterioplankton in warm waters (Chen et al., 2022; Liu et al., 2023). For instance, in previous study, Chen et al. pointed out that deterministic processes dominated the community assembly when the temperature was below 30°C, and stochastic processes dominated the community assembly process when the temperature exceeded 30°C (Chen et al., 2022). In our study, the winter temperature range of seawater in Daya Bay was 19°C to 24°C, and deterministic processes dominated the community assembly of bacterioplankton from low temperature to high temperature environments. Our research also found that when the regime shift from state 1 to TS in the Daya Bay, that was, after the water temperature exceeded 20°C,

homogeneous selection increased by 30% in the community assembly, while the proportion of drift and others decreased by about 25%; When the temperature was below 20.5°C, although homogeneous selection accounts for a large proportion, the proportion of drift and others was also high. When the temperature rose to 22°C, there was no significant change in homogeneous selection and 'drift and others', but there was a significant decrease in homogenizing dispersal. The strong effect of homogeneous selection is probably because of the extremely high population growth rates of bacteria (Van der Gucht et al., 2007). Bacterioplankton can rapidly track changes in the environmental temperatures (Muylaert et al., 2002). Thus, the persistence of newly arrived bacterioplankton taxa that migrated via flowing water was more likely to be controlled by homogeneous selection than by dispersal limitation or drift. This finding was in line with a previous study conducted on grassland microbial communities in response to experimental warming (Ning et al., 2020). It showed that warming gradually enhanced homogeneous selection which is primarily imposed on Bacillales, but weakened drift in microbial community. In summary, we found high temperatures induced by thermal pollution changed the relative importance of different community assembly processes, and caused a regime shift of bacterioplankton community structure in the subtropical Daya Bay.

5 Conclusion

Our study revealed that long-term thermal pollution from the cooling system of the nuclear power plants caused a regime shift of winter bacterioplankton community structure in a subtropical bay. In the three typical scenarios of regime shifts, the steady-state transition of bacterioplankton community structure in response to temperature increasing was more likely consistent with an abrupt regime shift rather than a smooth regime or a discontinuous regime model. The regime shift caused significant changes of bacterioplankton community diversity, compositions and assembly processes. We found bacterioplankton diversity decreased significantly as regime shifts from low-temperature habitats to high-temperature environments. The proportion of homogeneous selection significantly increased, and *Cyanobium*, *Synechococcus*, NS5 marine group and *Vibrio* were found dominating in regime state of high-temperature environments. Our research might broad the understanding of the ecological impact of thermal effluents on subtropical bays.

Data availability statement

The datasets presented in this study can be found in online repositories. The names of the repository/repositories and accession number(s) can be found below: https://www.ncbi.nlm.nih.gov/, PRJNA961834.

Author contributions

ZS: Conceptualization, Data curation, Formal analysis, Investigation, Methodology, Resources, Software, Supervision, Validation, Visualization, Writing – original draft, Writing – review & editing. HC: Writing – review & editing. YD: Writing – review & editing. DH: Writing – review & editing. LR: Writing – review & editing, Conceptualization, Data curation, Funding acquisition, Methodology, Project administration, Supervision, Visualization.

Funding

The author(s) declare that financial support was received for the research, authorship, and/or publication of this article. This work was supported by National Natural Science Foundation of China (32171517) and Project of Southern Marine Science and Engineering Guangdong Laboratory (Guanzhou) (GML20220017).

Acknowledgments

We acknowledge Guibin Ma, Chuangfeng Wu, Ziyin Deng, Xueling Xiong, and Haokun Yang for assistance with experimental sampling and data analyses.

Conflict of interest

The authors declare that the research was conducted in the absence of any commercial or financial relationships that could be construed as a potential conflict of interest.

Publisher's note

Supplementary material

The Supplementary material for this article can be found online at: https://www.frontiersin.org/articles/10.3389/fmicb.2024.1395583/full#supplementary-material

References

Adams, H. E., Crump, B. C., and Kling, G. W. (2010). Temperature controls on aquatic bacterial production and community dynamics in arctic lakes and streams. *Environ. Microbiol.* 12, 1319–1333. doi: 10.1111/j.1462-2920.2010.02176.x

Allen, R., Hoffmann, L. J., Larcombe, M. J., Louisson, Z., and Summerfield, T. C. (2020). Homogeneous environmental selection dominates microbial community assembly in the oligotrophic South Pacific gyre. *Mol. Ecol.* 29, 4680–4691. doi: 10.1111/mec.15651

Andersen, T., Carstensen, J., Hernández-García, E., and Duarte, C. M. (2009). Ecological thresholds and regime shifts: approaches to identification. *Trends Ecol. Evol.* 24, 49–57. doi: 10.1016/j.tree.2008.07.014

Anderson, E. P., Jenkins, C. N., Heilpern, S., Maldonado-Ocampo, J. A., Carvajal-Vallejos, F. M., Encalada, A. C., et al. (2018). Fragmentation of Andes-to-Amazon connectivity by hydropower dams. *Sci. Adv.* 4:eaao1642. doi: 10.1126/sciadv.aao1642

Berdugo, M., Delgado-Baquerizo, M., Soliveres, S., Hernández-Clemente, R., Zhao, Y., Gaitán, J. J., et al. (2020). Global ecosystem thresholds driven by aridity. *Science* 367, 787–790. doi: 10.1126/science.aay5958

Berner, C., Bertos-Fortis, M., Pinhassi, J., and Legrand, C. (2018). Response of microbial communities to changing climate conditions during summer cyanobacterial blooms in the Baltic Sea. *Front. Microbiol.* 9:1562. doi: 10.3389/fmicb.2018.01562

Brock, W. A., and Carpenter, S. R. (2006). Variance as a leading indicator of regime shift in ecosystem services. *Ecol. Soc.* 11:9. doi: 10.5751/es-01777-110209

Buchan, A., LeCleir, G. R., Gulvik, C. A., and González, J. M. (2014). Master recyclers: features and functions of bacteria associated with phytoplankton blooms. *Nat. Rev. Microbiol.* 12, 686–698. doi: 10.1038/nrmicro3326

Chen, H., Chen, Z., Chu, X., Deng, Y., Qing, S., Sun, C., et al. (2022). Temperature mediated the balance between stochastic and deterministic processes and reoccurrence of microbial community during treating aniline wastewater. *Water Res.* 221:118741. doi: 10.1016/j.watres.2022.118741

Christoffersen, K., Andersen, N., Søndergaard, M., Liboriussen, L., and Jeppesen, E. (2006). Implications of climate-enforced temperature increases on freshwater pico- and nanoplankton populations studied in artificial ponds during 16 months. *Hydrobiologia* 560, 259–266. doi: 10.1007/s10750-005-1221-2

Dai, W., Zhang, J., Tu, Q., Deng, Y., Qiu, Q., and Xiong, J. (2017). Bacterioplankton assembly and interspecies interaction indicating increasing coastal eutrophication. *Chemosphere* 177, 317–325. doi: 10.1016/j.chemosphere.2017.03.034

Dakos, V., Matthews, B., Hendry, A. P., Levine, J., Loeuille, N., Norberg, J., et al. (2019). Ecosystem tipping points in an evolving world. *Nat. Ecol. Evol.* 3, 355–362. doi: 10.1038/s41559-019-0797-2

Daufresne, M., Lengfellner, K., and Sommer, U. (2009). Global warming benefits the small in aquatic ecosystems. *Proc. Natl. Acad. Sci. USA* 106, 12788–12793. doi: 10.1073/pnas.0902080106

DeYoung, B., Harris, R., Alheit, J., Beaugrand, G., Mantua, N., and Shannon, L. (2004). Detecting regime shifts in the ocean: data considerations. *Prog. Oceanogr.* 60, 143–164. doi: 10.1016/j.pocean.2004.02.017

Díez-Vives, C., Nielsen, S., Sánchez, P., Palenzuela, O., Ferrera, I., Sebastián, M., et al. (2019). Delineation of ecologically distinct units of marine Bacteroidetes in the northwestern Mediterranean Sea. *Mol. Ecol.* 28, 2846–2859. doi: 10.1111/mec.15068

Dijkstra, Y. M., Schuttelaars, H. M., and Schramkowski, G. P. (2019). A regime shift from low to high sediment concentrations in a tide-dominated estuary. *Geophys. Res. Lett.* 46, 4338–4345. doi: 10.1029/2019GL082302

Djeghri, N., Boyé, A., Ostle, C., and Hélaouët, P. (2023). Reinterpreting two regime shifts in North Sea plankton communities through the lens of functional traits. *Glob. Ecol. Biogeogr.* 32, 962–975. doi: 10.1111/geb.13659

Eiler, A., Heinrich, F., and Bertilsson, S. (2012). Coherent dynamics and association networks among lake bacterioplankton taxa. *ISME J.* 6, 330–342. doi: 10.1038/ismej.2011.113

General Administration of Quality Supervision. (2007). *General Administration of Quality Supervision, Inspection and Quaran tine (AQSIQ) of the People's Republic of China. The specification for marine monitoring of China. Part 4: seawater analysis. GB 173784-2007*. Beijing, China: Standards Press of China, (In Chinese.)

Grabowska-Grucza, K., Bukowska, A., Siuda, W., Chróst, R. J., and Kiersztyn, B. (2022). Impact of increasing temperature on the taxonomic and metabolic structure of bacterial communities in a global warming context. *Aquat. Microb. Ecol.* 88, 135–148. doi: 10.3354/ame01988

Gutiérrez, M. H., Narváez, D., Daneri, G., Montero, P., Pérez-Santos, I., and Pantoja, S. (2018). Linking seasonal reduction of microbial diversity to increase in winter temperature of waters of a Chilean Patagonia Fjord. *Front. Mar. Sci.* 5:277. doi: 10.3389/fmars.2018.00277

Guttal, V., and Jayaprakash, C. (2007). Impact of noise on bistable ecological systems. *Ecol. Model.* 201, 420–428. doi: 10.1016/j.ecolmodel.2006.10.005

Guttal, V., and Jayaprakash, C. (2008). Changing skewness: an early warning signal of regime shifts in ecosystems. *Ecol. Lett.* 11, 450–460. doi: 10.1111/j.1461-0248.2008.01160.x

Hamilton, T. J., Paz-Yepes, J., Morrison, R. A., Palenik, B., and Tresguerres, M. (2014). Exposure to bloom-like concentrations of two marine *Synechococcus* cyanobacteria (strains CC9311 and CC9902) differentially alters fish behaviour. *Conserv. Physiol.* 2, 1–9. doi: 10.1093/conphys/cou020

Hare, S. R., and Mantua, N. J. (2000). Empirical evidence for North Pacific regime shifts in 1977 and 1989. *Prog. Oceanogr.* 47, 103–145. doi: 10.1016/S0079-6611(00)00033-1

Hu, A., Wang, J., Sun, H., Niu, B., Si, G., Wang, J., et al. (2020). Mountain biodiversity and ecosystem functions: interplay between geology and contemporary environments. *ISME J.* 14, 931–944. doi: 10.1038/s41396-019-0574-x

Hughes, T. P., Kerry, J. T., Baird, A. H., Connolly, S. R., Chase, T. J., Dietzel, A., et al. (2019). Global warming impairs stock–recruitment dynamics of corals. *Nature* 568, 387–390. doi: 10.1038/s41586-019-1081-y

Jiao, C., Zhao, D., Huang, R., He, F., and Yu, Z. (2021). Habitats and seasons differentiate the assembly of bacterial communities along a trophic gradient of freshwater lakes. *Freshw. Biol.* 66, 1515–1529. doi: 10.1111/fwb.13735

Kim, Y., Jeon, J., Kwak, M. S., Kim, G. H., Koh, I. S., and Rho, M. (2018). Photosynthetic functions of *Synechococcus* in the ocean microbiomes of diverse salinity and seasons. *PLoS One* 13:e0190266. doi: 10.1371/journal.pone.0190266

Kolda, A., Ljubesic, Z., Gavrilovic, A., Jug-Dujakovic, J., Pikelj, K., and Kapetanovic, D. (2020). Metabarcoding cyanobacteria in coastal waters and sediment in central and southern Adriatic Sea. *Acta Bot. Croat.* 79, 157–169. doi: 10.37427/botcro-2020-021

Kozich, J. J., Westcott, S. L., Baxter, N. T., Highlander, S. K., and Schloss, P. D. (2013). Development of a dual-index sequencing strategy and curation pipeline for analyzing amplicon sequence data on the MiSeq illumina sequencing platform. *Appl. Environ. Microbiol.* 79, 5112–5120. doi: 10.1128/AEM.01043-13

Lambert, S., Lozano, J. C., Bouget, F. Y., and Galand, P. E. (2021). Seasonal marine microorganisms change neighbours under contrasting environmental conditions. *Environ. Microbiol.* 23, 2592–2604. doi: 10.1111/1462-2920.15482

Lees, K., Pitois, S., Scott, C., Frid, C., and MacKinson, S. (2006). Characterizing regime shifts in the marine environment. *Fish Fish.* 7, 104–127. doi: 10.1111/j.1467-2979.2006.00215.x

Li, N., Chen, X., Zhao, H., Tang, J., Jiang, G., Li, Z., et al. (2020). Spatial distribution and functional profile of the bacterial community in response to eutrophication in the subtropical Beibu gulf, China. *Mar. Pollut. Bull.* 161:111742. doi: 10.1016/j.marpolbul.2020.111742

Liu, A. C. H., Chang, F. H., Yang, J. W., Saito, H., Umezawa, Y., Chen, C. C., et al. (2022). Free-living marine bacterioplankton composition and diversity along the Kuroshio region. *Deep Sea Res. Part 1 Oceanogr. Res. Pap.* 183:103741. doi: 10.1016/j.dsr.2022.103741

Liu, N., Wang, B., Yang, M., Li, W., Shi, X., and Liu, C. Q. (2023). The different responses of planktonic bacteria and archaea to water temperature maintain the stability of their community diversity in dammed rivers. *Ecol. Process.* 12:25. doi: 10.1186/s13717-023-00438-9

Lu, M., and Hedin, L. O. (2019). Global plant–symbiont organization and emergence of biogeochemical cycles resolved by evolution-based trait modelling. *Nat. Ecol. Evol.* 3, 239–250. doi: 10.1038/s41559-018-0759-0

Lucas, J., Wichels, A., Teeling, H., Chafee, M., Scharfe, M., and Gerdts, G. (2015). Annual dynamics of North Sea bacterioplankton: seasonal variability superimposes short-term variation. *FEMS Microbiol. Ecol.* 91:fiv099. doi: 10.1093/femsec/fiv099

Martin, R., Schlüter, M., and Blenckner, T. (2020). The importance of transient social dynamics for restoring ecosystems beyond ecological tipping points. *Proc. Natl. Acad. Sci. USA* 117, 2717–2722. doi: 10.1073/pnas.1817154117

McGlathery, K. J., Reidenbach, M. A., D'Odorico, P., Fagherazzi, S., Pace, M. L., and Porter, J. H. (2013). Nonlinear dynamics and alternative stable states in shallow coastal systems. *Oceanography* 26, 220–231. doi: 10.5670/oceanog.2013.66

McMahon, K. W., McCarthy, M. D., Sherwood, O. A., Larsen, T., and Guilderson, T. P. (2015). Millennial-scale plankton regime shifts in the subtropical North Pacific Ocean. *Science* 350, 1530–1533. doi: 10.1126/science.aaa9942

Moi, D. A., Alves, D. C., Antiqueira, P. A. P., Thomaz, S. M., Teixeira de Mello, F., Bonecker, C. C., et al. (2021). Ecosystem shift from submerged to floating plants simplifying the food web in a tropical shallow lake. *Ecosystems* 24, 628–639. doi: 10.1007/s10021-020-00539-y

Muylaert, K., Van der Gucht, K., Vloemans, N., Meester, L. D., Gillis, M., and Vyverman, W. (2002). Relationship between bacterial community composition and bottom-up versus top-down variables in four eutrophic shallow lakes. *Appl. Environ. Microbiol.* 68, 4740–4750. doi: 10.1128/AEM.68.10.4740-4750.2002

Ning, D., Yuan, M., Wu, L., Zhang, Y., Guo, X., Zhou, X., et al. (2020). A quantitative framework reveals ecological drivers of grassland microbial community assembly in response to warming. *Nat. Commun.* 11:4717. doi: 10.1038/s41467-020-18560-z

Niu, Y., Shen, H., Chen, J., Xie, P., Yang, X., Tao, M., et al. (2011). Phytoplankton community succession shaping bacterioplankton community composition in Lake Taihu, China. *Water Res.* 45, 4169–4182. doi: 10.1016/j.watres.2011.05.022

Özen, A., Šorf, M., Trochine, C., Liboriussen, L., Beklioglu, M., Søndergaard, M., et al. (2013). Long-term effects of warming and nutrients on microbes and other plankton in mesocosms. *Freshw. Biol.* 58, 483–493. doi: 10.1111/j.1365-2427.2012.02824.x

Perälä, T., Olsen, E. M., and Hutchings, J. A. (2020). Disentangling conditional effects of multiple regime shifts on Atlantic cod productivity. *PLoS One* 15:e0347414. doi: 10.1371/journal.pone.0237414

Putten, I. V., Boschetti, F., Ling, S., and Richards, S. A. (2019). Perceptions of system-identity and regime shift for marine ecosystems. *ICES J. Mar. Sci.* 76, 1736–1747. doi: 10.1093/icesjms/fsz058

Quast, C., Pruesse, E., Yilmaz, P., Gerken, J., Schweer, T., Yarza, P., et al. (2013). The SILVA ribosomal RNA gene database project: improved data processing and web-based tools. *Nucleic Acids Res.* 41, D590–D596. doi: 10.1093/nar/gks1219

Rahman, S. M. M., Jung, H. K., Park, H. J., Park, J. M., and Lee, C. I. (2019). Synchronicity of climate driven regime shifts among the east Asian marginal sea waters and major fish species. *J. Environ. Biol.* 40, 948–961. doi: 10.22438/jeb/40/5(SI)/SI-18

Rao, M. P. N., Dong, Z. Y., Luo, Z. H., Li, M. M., Liu, B. B., Guo, S. X., et al. (2021). Physicochemical and microbial diversity analyses of Indian hot springs. *Front. Microbiol.* 12:627200. doi: 10.3389/fmicb.2021.627200

Ren, L., He, D., Chen, Z., Jeppesen, E., Lauridsen, T. L., Søndergaard, M., et al. (2017). Warming and nutrient enrichment in combination increase stochasticity and beta diversity of bacterioplankton assemblages across freshwater mesocosms. *ISME J.* 11, 613–625. doi: 10.1038/ismej.2016.159

Ren, L., He, D., Zeng, J., and Wu, Q. L. (2013). Bacterioplankton communities turn unstable and become small under increased temperature and nutrient-enriched conditions. *FEMS Microbiol. Ecol.* 84, 614–624. doi: 10.1111/1574-6941.12089

Ren, L., Song, X., He, D., Wang, J., Tan, M., Xia, X., et al. (2019). Bacterioplankton metacommunity processes across thermal gradients: weaker species sorting but stronger niche segregation in summer than in winter in a subtropical bay. *Appl. Environ. Microbiol.* 85, e02088–e02118. doi: 10.1128/AEM.02088-18

Rial, J. A., Pielke, R. A., Beniston, M., Claussen, M., Canadell, J., Cox, P., et al. (2004). Nonlinearities, feedbacks and critical thresholds within the earth's climate system. *Clim. Chang.* 65, 11–38. doi: 10.1023/B:CLIM.0000037493.89489.3f

Rocha, J. C., Peterson, G., Bodin, Ö., and Levin, S. (2018). Cascading regime shifts within and across scales. *Science* 362, 1379–1383. doi: 10.1126/science.aat7850

Rosero-López, D., Todd Walter, M., Flecker, A. S., De Bièvre, B., Osorio, R., González-Zeas, D., et al. (2022). A whole-ecosystem experiment reveals flow-induced shifts in a stream community. *Commun. Biol.* 5:420. doi: 10.1038/s42003-022-03345-5

Ruiz-González, C., Niño-García, J. P., Lapierre, J. F., and del Giorgio, P. A. (2015). The quality of organic matter shapes the functional biogeography of bacterioplankton across boreal freshwater ecosystems. *Glob. Ecol. Biogeogr.* 24, 1487–1498. doi: 10.1111/geb.12356

Scheffer, M., Carpenter, S., Foley, J. A., Folke, C., and Walker, B. (2001). Catastrophic shifts in ecosystems. *Nature* 413, 591–596. doi: 10.1038/35098000

Schröder, A., Persson, L., and De Roos, A. M. (2005). Direct experimental evidence for alternative stable states: a review. *Oikos* 110, 3–19. doi: 10.1111/j.0030-1299.2005.13962.x

Sharp, C. E., Brady, A. L., Sharp, G. H., Grasby, S. E., Stott, M. B., and Dunfield, P. F. (2014). Humboldt's spa: microbial diversity is controlled by temperature in geothermal environments. *ISME J.* 8, 1166–1174. doi: 10.1038/ismej.2013.237

Su, H., Wu, Y., Xia, W., Yang, L., Chen, J., Han, W., et al. (2019). Stoichiometric mechanisms of regime shifts in freshwater ecosystem. *Water Res.* 149, 302–310. doi: 10.1016/j.watres.2018.11.024

Szalaj, D., Silva, A., Ré, P., and Cabral, H. (2021). Detecting regime shifts in the portuguese continental shelf ecosystem within the last three decades. *Front. Mar. Sci.* 8:629130. doi: 10.3389/fmars.2021.629130

Tang, H., Ke, Z., Yan, M., Wang, W., Nie, H., Li, B., et al. (2018). Concentrations, distribution, and ecological risk assessment of heavy metals in Daya bay, China. *Water (Switzerland)* 10:80. doi: 10.3390/W10060780

Tong, F., Zhang, P., Zhang, X., and Chen, P. (2021). Impact of oyster culture on coral reef bacterioplankton community composition and function in Daya bay, China. *Aquac. Environ. Interact.* 13, 489–503. doi: 10.3354/AEI00421

Trombetta, T., Bouget, F. Y., Félix, C., Mostajir, B., and Vidussi, F. (2022). Microbial diversity in a north western Mediterranean Sea shallow coastal lagoon under contrasting water temperature conditions. *Front. Mar. Sci.* 9:858744. doi: 10.3389/fmars.2022.858744

Trombetta, T., Vidussi, F., Mas, S., Parin, D., Simier, M., and Mostajir, B. (2019). Water temperature drives phytoplankton blooms in coastal waters. *PLoS One* 14:e0214933. doi: 10.1371/journal.pone.0214933

Trombetta, T., Vidussi, F., Roques, C., Mas, S., Scotti, M., and Mostajir, B. (2021). Co-occurrence networks reveal the central role of temperature in structuring the plankton community of the Thau lagoon. *Sci. Rep.* 11:17675. doi: 10.1038/s41598-021-97173-y

Van der Gucht, K., Cottenie, K., Muylaert, K., Vloemans, N., Cousin, S., Declerck, S., et al. (2007). The power of species sorting: local factors drive bacterial community composition over a wide range of spatial scales. *Proc. Natl. Acad. Sci.* 104, 20404–20409. doi: 10.1073/pnas.070720010

Vellend, M. (2010). Conceptual synthesis in community ecology. *Q. Rev. Biol.* 85, 183–206. doi: 10.1086/652373

Vellend, M., Srivastava, D. S., Anderson, K. M., Brown, C. D., Jankowski, J. E., Kleynhans, E. J., et al. (2014). Assessing the relative importance of neutral stochasticity in ecological communities. *Oikos* 123, 1420–1430. doi: 10.1111/oik.01493

Wang, Q., Garrity, G. M., Tiedje, J. M., and Cole, J. R. (2007). Naive Bayesian classifier for rapid assignment of rRNA sequences into the new bacterial taxonomy. *Appl. Environ. Microbiol.* 73, 5261–5267. doi: 10.1128/AEM.00062-07

Wang, Y., Wang, Z., Wu, W., Hu, M., Wang, Z., Xu, A., et al. (2010). Seasonal regime shift of an alternative-state lake Xingyun, China. *Fresenius Environ. Bull.* 19, 1474–1485.

Wernberg, T., Bennett, S., Babcock, R. C., Bettignies, T. D., Cure, K., Depczynski, M., et al. (2016). Climate-driven regime shift of a temperate marine ecosystem. *Science* 353, 169–172. doi: 10.1126/science.aad8745

Wu, J., Hong, Y., Chang, X., Jiao, L., Li, Y., Liu, X., et al. (2019). Unexpectedly high diversity of anammox bacteria detected in deep-sea surface sediments of the South China Sea. *FEMS Microbiol. Ecol.* 95:fiz013. doi: 10.1093/femsec/fiz013

Wu, W., Xu, Z., Dai, M., Gan, J., and Liu, H. (2021). Homogeneous selection shapes free-living and particle-associated bacterial communities in subtropical coastal waters. *Divers. Distrib.* 27, 1904–1917. doi: 10.1111/ddi.13193

Xing, X., Xu, H., Wang, D., Yang, X., Qin, H., and Zhu, B. (2022). Nitrogen use aggravates bacterial diversity and network complexity responses to temperature. *Sci. Rep.* 12:13989. doi: 10.1038/s41598-022-15536-5

Xu, H., Paerl, H. W., Qin, B., Zhu, G., and Gaoa, G. (2010). Nitrogen and phosphorus inputs control phytoplankton growth in eutrophic Lake Taihu, China. *Limnol. Oceanogr.* 55:420–432. doi: 10.4319/lo.2010.55.1.0420

Yuan, M. M., Guo, X., Wu, L., Zhang, Y., Xiao, N., Ning, D., et al. (2021). Climate warming enhances microbial network complexity and stability. *Nat. Clim. Chang.* 11, 343–348. doi: 10.1038/s41558-021-00989-9

Zhang, M., Xu, J., and Hansson, L. A. (2015). Local environment overrides regional climate influence on regime shift in a north temperate lake. *Aquat. Ecol.* 49, 105–113. doi: 10.1007/s10452-015-9509-4

Zhao, M., Ma, Y. T., He, S. Y., Mou, X., and Wu, L. (2020). Dynamics of bacterioplankton community structure in response to seasonal hydrological disturbances in Poyang Lake, the largest wetland in China. *FEMS Microbiol. Ecol.* 96:fiaa064. doi: 10.1093/femsec/fiaa064

Zhu, J., Ma, Y., Huang, L., and Zhang, W. (2022). Homogeneous selection is not always important in bacterial community in the eutrophic enclosed bay. *Ecol. Process.* 11:27. doi: 10.1186/s13717-022-00373-1

Zhu, C., Zhang, J., Nawaz, M. Z., Mahboob, S., Al-Ghanim, K. A., Khan, I. A., et al. (2019). Seasonal succession and spatial distribution of bacterial community structure in a eutrophic freshwater Lake, Lake Taihu. *Sci. Total Environ.* 669, 29–40. doi: 10.1016/j.scitotenv.2019.03.087

frontiers | Frontiers in Microbiology

TYPE Original Research
PUBLISHED 07 May 2024
DOI 10.3389/fmicb.2024.1358574

OPEN ACCESS

EDITED BY
Jin Zhou,
Tsinghua University, China

REVIEWED BY
Shengwei Hou,
Southern University of Science and Technology, China
Sophie Charvet,
American Museum of Natural History, United States

*CORRESPONDENCE
Charmaine Cheuk Man Yung
✉ ccmyung@ust.hk

RECEIVED 20 December 2023
ACCEPTED 12 April 2024
PUBLISHED 07 May 2024

CITATION
Rey Redondo E, Xu Y and Yung CCM (2024) Genomic characterisation and ecological distribution of *Mantoniella tinhauana*: a novel Mamiellophycean green alga from the Western Pacific.
Front. Microbiol. 15:1358574.
doi: 10.3389/fmicb.2024.1358574

Genomic characterisation and ecological distribution of *Mantoniella tinhauana*: a novel Mamiellophycean green alga from the Western Pacific

Elvira Rey Redondo, Yangbing Xu and Charmaine Cheuk Man Yung*

Department of Ocean Science, The Hong Kong University of Science and Technology, Kowloon, Hong Kong SAR, China

Mamiellophyceae are dominant marine algae in much of the ocean, the most prevalent genera belonging to the order Mamiellales: *Micromonas*, *Ostreococcus* and *Bathycoccus*, whose genetics and global distributions have been extensively studied. Conversely, the genus *Mantoniella*, despite its potential ecological importance, remains relatively under-characterised. In this study, we isolated and characterised a novel species of Mamiellophyceae, *Mantoniella tinhauana*, from subtropical coastal waters in the South China Sea. Morphologically, it resembles other *Mantoniella* species; however, a comparative analysis of the 18S and ITS2 marker genes revealed its genetic distinctiveness. Furthermore, we sequenced and assembled the first genome of *Mantoniella tinhauana*, uncovering significant differences from previously studied Mamiellophyceae species. Notably, the genome lacked any detectable outlier chromosomes and exhibited numerous unique orthogroups. We explored gene groups associated with meiosis, scale and flagella formation, shedding light on species divergence, yet further investigation is warranted. To elucidate the biogeography of *Mantoniella tinhauana*, we conducted a comprehensive analysis using global metagenomic read mapping to the newly sequenced genome. Our findings indicate this species exhibits a cosmopolitan distribution with a low-level prevalence worldwide. Understanding the intricate dynamics between Mamiellophyceae and the environment is crucial for comprehending their impact on the ocean ecosystem and accurately predicting their response to forthcoming environmental changes.

KEYWORDS

biogeography, genomics, Mamiellophyceae, *Mantoniella tinhauana* sp. nov., marine algae, metagenomics

Introduction

Mamiellophyceae, an early-branching class of photosynthetic picoeukaryotes within the Chlorophyta (Marin and Melkonian, 2010), dominate various ocean regions (Wang et al., 2019; Yung et al., 2022), particularly coastal waters (Lopes dos Santos et al., 2017; Tragin and Vaulot, 2018). Among the Mamiellophyceae, the order Mamiellales, which includes the families Mamiellaceae and Bathycoccaceae, encompasses the most extensively studied marine

Mamiellophyceae genera: *Micromonas* (Mamiellaceae), *Ostreococcus* and *Bathycoccus* (Bathycoccaceae), and more recently, *Mantoniella* (Mamiellaceae).

Understanding the biogeography and diversity of Mamiellophyceae is crucial due to their important role in primary production, impact on ocean ecosystems and sensitivity to environmental disturbances (Monier et al., 2016). Distinguishing Mamiellophyceae species based on morphology alone is challenging, as evidenced by the similarities among previously identified *Mantoniella* species (Yau et al., 2020b). Therefore, molecular methods are essential for accurate species identification and unravelling the relationship between their distribution and environmental factors. Previous studies have revealed genetic adaptations and distinct ecological niches within different Mamiellophyceae clades and species (Lovejoy et al., 2007; Foulon et al., 2008; Demir-Hilton et al., 2011; Subirana et al., 2013; Hu et al., 2016; Simmons et al., 2016; Simon et al., 2017; Tragin and Vaulot, 2019). For example, *M. antarctica* (Marchant et al., 1989), *M. baffinensis* and *M. beaufortii* (Balzano et al., 2012; Yau et al., 2020b) were exclusively found in cold, polar waters, while *M. squamata* is the only named *Mantoniella* species known to have a distribution beyond polar regions (Tragin and Vaulot, 2019; Belevich et al., 2021).

The predominant approach in Mamiellophyceae biogeography studies is metabarcoding, which involves sequencing marker genes such as the hypervariable regions of 18S ribosomal RNA (rRNA) (Monier et al., 2016; Tragin and Vaulot, 2019; Belevich et al., 2021). Metabarcoding has inherent limitations in true quantification and suffers from biases stemming from PCR recovery, strain polymorphisms, gene copy number variations and sequencing artifacts (Monier et al., 2016), and can underestimate the diversity of microbial eukaryotes (Piganeau et al., 2011a). For instance, *Bathycoccus* 18S rRNA sequences were found to be identical in different strains, masking huge variations in other genomic regions (Leconte et al., 2020).

To address the limitations of metabarcoding, metagenome read mapping and metagenome-assembled genomes (MAGs) have emerged as valuable tools for biogeographic studies. Mapping metagenomic reads to reference genomes provides a more accurate and sensitive method for biogeographic quantification, avoiding targeted amplicon biases and gene content variations, and enabling higher strain resolution. This approach has been successfully applied to six Mamiellales genomes from the well-studied genera (*Micromonas*, *Ostreococcus* and *Bathycoccus*) using global metagenomic data from the Tara Oceans Expedition (Leconte et al., 2020). However, the lack of reference genomes from cultured strains has made achieving genome-resolved metagenomic mapping with species resolution challenging for *Mantoniella*. Although a *Mantoniella* MAG was identified in one Tara metagenomic sample from the southwestern Pacific Ocean (Delmont et al., 2022), the binning of this MAG was based on marker genes, resulting in an incomplete MAG.

Existing research on the global biogeography of Mamiellophyceae has primarily focused on regions outside the western Pacific Ocean, particularly overlooking subtropical coastal South Asia. Localised studies conducted in the West Philippine Sea (Dela Peña et al., 2021), Bohai Sea (Xu et al., 2017), South China Sea (Wu et al., 2014; Lin et al., 2017a, 2021) and East China Sea (Lin et al., 2017b, 2022) have highlighted the importance of factors like distance to the coast and depth in shaping the distribution patterns of Mamiellophyceae species. Despite these efforts, limited information exists on the occurrence of the genus *Mantoniella* in subtropical West Pacific waters, with studies indicating its presence at certain sites but without detailed species identification (Lin et al., 2017b, 2021, 2022). Notably, no cultures of *Mantoniella* have been isolated from the Pacific Ocean. Globally, only a few large-scale metabarcoding studies have investigated the biogeography of *Mantoniella* (Lovejoy et al., 2007; Tragin and Vaulot, 2019; Yau et al., 2020b).

Our study addresses research gaps on the biogeography of Mamiellophyceae, focusing specifically on the genus *Mantoniella*. We present a newly identified species, *Mantoniella tinhauana*, isolated from the subtropical coastal waters of the South China Sea. This represents the first-ever whole genome project for *Mantoniella*. By analysing the genome of this novel species and exploring its global distribution using metagenome datasets, we provide insights into its morphology, phylogeny, genome characteristics, evolutionary relationships and ecological niches. Our findings contribute to the understanding of the ecological significance and biogeography of Mamiellophyceae, furthering our knowledge of these important photosynthetic organisms in marine ecosystems.

Materials and methods

Sampling and strain isolation

Coastal surface seawater samples (2 m depth) were collected from Lau Fau Shan in the Pearl River Estuary (22°28′09.0′N 113°58′50.1′E) in June 2020. The collected samples were sequentially filtered through 50 µm mesh and 1 µm polycarbonate filters (Whatman) to remove large multicellular organisms and capture the suitable size fraction for Mamiellophyceae (Yung et al., 2022). The filtrates were grown in flasks (SPL Life Sciences) in L1 medium (Guillard and Hargraves, 1993) and cultured at room temperature (21–23°C) in a shaking incubator (100 rpm) under a 12-h light/dark cycle (30 µmol photons m^{-2} s^{-1}). After 2–3 weeks, collected algal pellets were used for 18S rRNA gene amplification (see below) to obtain initial taxonomic classification. Samples containing Mamiellophyceae were purified through serial dilution and treated with antibiotics. The novel *Mantoniella* strain obtained from this process was subcultured.

Morphology

For transmission electron microscopy (TEM), culture was centrifuged, the pellet resuspended and fixed with glutaraldehyde (2.5% in 0.2 µm-filtered seawater), rinsed with Na cacodylate buffer (0.1 $mol l^{-1}$) and fixed in OsO_4 (1%), then dehydrated with a graded series of acetone solutions. After resin embedding and polymerisation, ultrathin sections were cut using a Leica EM UC7 Ultramicrotome and stained with uranyl acetate and lead citrate. The stained samples were examined under a Hitachi HT7700 Transmission Electron

Microscope. Cell diameters were measured using the TEM images and scales as viewed on ImageJ (Collins, 2007).

Nucleic acid extraction and sequencing

For phylogenetic analysis, DNA was extracted from dense *Mantoniella* culture by centrifugation, resuspension and incubation at 98°C for 10 min, based on Saulnier et al. (2009) and Jahn et al. (2014). The 18S region was amplified following the protocol described by Hadziavdic et al. (2014) and Sanger sequenced by Tech Dragon (Hong Kong).

For whole genome sequencing, DNA was extracted from *Mantoniella* pellets using a Qiagen DNeasy Plant Pro Kit. Short-read Illumina sequencing was conducted by Novogene (Hong Kong) on the Novaseq 6,000 PE150 platform. Long-read DNA was extracted using a modified CTAB protocol (Stark et al., 2020) and sequenced on the PacBio SMRT Sequel platform by Novogene. To improve assembly contiguity, genetic material was extracted for proximity ligation (Hi-C) based on the protocol by Lafontaine et al. (2021). The chromatin was cross-linked following the instructions provided by Phase Genomics (United States) and subsequently subjected to Illumina Hi-C sequencing.

To improve gene prediction, a time-series of samples was collected from an exponentially growing culture every 3 h over a 24-h period. RNA was extracted using a Direct-zol RNA Miniprep Kit (Zymo Research) to capture the gene activity throughout the day. The RNA from the 8 timepoints was pooled and sequenced using Illumina PE150 by Novogene.

Whole genome assembly

Paired-end Illumina reads were trimmed with trimmomatic v0.39 (Bolger et al., 2014) and quality controlled with fastp v0.23.2 (Chen et al., 2018). The short Illumina reads and long PacBio reads were combined to generate an initial hybrid assembly using MaSuRCA v4.0.9 (Zimin et al., 2013). Subsequently, the assembly was refined using POLCA (Zimin and Salzberg, 2020) for calling alternatives and improving accuracy.

For contig scaffolding and misassembly correction, Hi-C reads were aligned to the draft genome assembly using bwa-mem2 v2.0 (Li and Durbin, 2009). The resulting alignments were input into SALSA2 v2.3 (with default parameters and "-e GATC --clean") (Ghurye et al., 2019).

Anvi'o v7.1 (Eren et al., 2015) was used to create a contigs database for removing extraneous sequences in the draft genome. Contigs were split into 2000 nt lengths, clustered and binned. HMM modelling and functional annotation against NCBI's COGs database (Tatusov et al., 1997) were performed. Annotated bins and GC contents were visually examined, and genome bins not belonging to eukaryotic nuclear DNA were manually removed (Delmont and Eren, 2016).

To further enhance the draft genome, the initial trimmed and quality-controlled Illumina reads were realigned to the decontaminated draft genome using Bowtie2 v2.2.5 (Langmead and Salzberg, 2012). The resulting alignment underwent gap fixing, misassembly identification, variant calling, and other improvements using Pilon v1.24 (Walker et al., 2014).

Marker gene characterisation

Mamiellophyceae 18S rRNA genes and Mamiellaceae ITS region sequences were aligned onto the novel *Mantoniella tinhauana* genome assembly using Geneious Prime v2022.2.2. The resulting 18S gene sequence obtained from this mapping approach was 1,784 bp in length and showed 100% identity to the amplicon sequencing-derived sequence, with greater completeness (deposited to GenBank: OR835992). To extract the ITS2 gene, the novel *Mantoniella* ITS region (deposited to GenBank: OR835993) was submitted to the University of Würzburg ITS2 Database (Merget et al., 2012) online platform using the Viridiplantae model and default parameters, resulting in a 253 bp-long ITS2 gene sequence.

ITS2 structure

The novel *Mantoniella* ITS2 structure was predicted using Vienna files without gaps from Yau et al. (2020b) as templates on the ITS2 Database (Merget et al., 2012). The resulting Vienna file was exported and aligned with other Mamiellophyceae ITS2 structure files (including gaps) using ClustalW v2.1 (Aiyar, 1999) in 4SALE v1.7.1 (Seibel et al., 2006) (Supplementary Table S1). The novel ITS2 structure was visualised using the ViennaRNA web service forna (Gendron et al., 2001). Each base pair in the helix structures was compared to those of other *Mantoniella* and Mamiellophyceae ITS2 using the 4SALE alignment and manually labelled. Individual RNA helix sequences were extracted using Geneious Prime and also drawn on the ViennaRNA forna platform.

Marker gene-based phylogeny

To construct the phylogenetic tree based on the 18S marker gene, the *M. tinhauana* 18S rRNA gene sequence was blasted against the NCBI nucleotide database in Geneious Prime (Supplementary Table S2). The top 10 matches, along with other complete *Mantoniella* 18S sequences (Tragin and Vaulot, 2019; Yau et al., 2020b) and representatives of other Mamiellophyceae 18S sequences were used to create the phylogenetic tree.

A total of 41 Mamiellophyceae 18S sequences, including the novel strain, were aligned using MAFFT v7.453 (Katoh and Standley, 2013). Low-quality positions containing gaps in over 50% of the sequences were removed with Goalign clean sites v0.3.5 (Lemoine and Gascuel, 2021). Maximum likelihood (ML) trees were built using IQ-TREE v2.2.0 (Nguyen et al., 2015) using the LG + F + R4 model of substitution and generating Shimodaira-Hasegawa (SH)-like approximate likelihood ratio test (aLRT) branch support values from 1,000 replicates. Markov chain Monte Carlo iterations were performed on the alignments for 1,000,000 generations sampling every 100 generations with 100,000 burn-in length using MrBayes v3.2.6 (Ronquist et al., 2012) as implemented on Geneious Prime, generating Bayesian posterior probability values for each node. The resulting tree was visualised using Interactive Tree Of Life (iTOL) v5 (Letunic and Bork, 2021).

To construct the ITS2 marker gene-based phylogenetic trees, gapped ITS2 sequences from 15 Mamiellophyceae species were aligned. ML and Bayesian trees were generated using the same methods as above.

10.3389/fmicb.2024.1358574

Genome and proteome analysis

To assess the completeness of the draft genome and Mamiellophyceae reference genomes, BUSCO v5.4.3 (Simão et al., 2015) was run against the Chlorophyta universal single-copy marker database in "genome" mode. Scaffold ends were manually examined for telomeric tandem repeats and scaffold and whole genome GC contents were computed using Geneious Prime.

The ploidy of the novel Mantoniella genome was estimated by aligning Illumina reads against the draft genome using ploidyNGS v3.1.3 (Corrêa dos Santos et al., 2017).

Transposable elements in the draft genome were identified using RepeatModeler v2.0.4 (Flynn et al., 2020), followed by masking of these elements, interspersed repeats and low complexity DNA sequences using RepeatMasker v4.1.4 (Smit et al., 2015) with RMBlast v2.13.0. Transcript reads from the transcriptome time-series were trimmed with trimmomatic, quality controlled with fastp as before, and aligned to the RepeatMasker-masked genome using STAR v2.1.10 (Dobin et al., 2013). The masked genome and the RNA-seq STAR alignment were input into BRAKER v3.0.2 (Brůna et al., 2021) for protein coding gene structure prediction in the novel genome using GeneMark and AUGUSTUS (Lukashin and Borodovsky, 1998; Keller et al., 2011), following BRAKER pipeline B.

The transcript reads were ribodepleted with SortMeRNA v4.3 (Kopylova et al., 2012) and assembled into a transcriptome with rnaSPAdes v3.15.4 (Bushmanova et al., 2019). Assembly quality was assessed using BUSCO in "transcriptome" mode against the Chlorophyta database, resulting in 94% complete BUSCOs. Open reading frames (ORFs) within the transcriptome were identified with Transdecoder v5.7.0 (Haas, 2023).

The unmasked genome, *ab initio* predictions from GeneMark and AUGUSTUS, output from BRAKER, and transcriptome ORF predictions from Transdecoder were combined in EVidenceModeler v2.0.0 (Haas et al., 2008) to generate a consensus proteome and a gene predictions file. The whole novel proteome was functionally annotated using HMMER v3.3 (Eddy, 2011) to generate Pfam (Mistry et al., 2021) domain annotations.

Gene synteny and collinearity

Mamiellophyceae proteomes (excluding *O. mediterraneus*) were obtained from NCBI. Gene synteny comparison was performed using the *M. tinhauana* gene predictions and proteome outputs from EVidenceModeler, along with those of the five other Mamiellophyceae species. The six proteomes were concatenated and subjected to all-against-all blastp analysis. MCScanX (Wang et al., 2012) was used to compare syntenic gene blocks with a minimum block size of five genes and a maximum gap size of 25 genes (Cho et al., 2023). The collinearity output was visualised using SynVisio in Multi-Level Analysis Tree View mode (Bandi et al., 2022).

The Big Outlier Chromosome (BOC), the mating type locus (MT) region within each BOC as delimited by Benites et al. (2021), and the Small Outlier Chromosome (SOC) annotated sequences were extracted from each Mamiellophyceae proteome. Gene block synteny analysis was performed using MCScanX as described above, comparing the BOC/MT/SOC regions of each Mamiellophyceae species against the entire *Mantoniella* proteome.

Orthogroup and gene expansions and contractions analysis

Orthogroups in the six proteomes were compared using Orthofinder v2.5.4 (Emms and Kelly, 2019) and visualised using UpSetR (Conway et al., 2017). Orthogroup information and the species tree produced by Orthofinder (made ultrametric) were used for gene family expansions and contractions analysis in CAFE v5 (Mendes et al., 2021) with a *p*-value cutoff of 0.05. The expansion and contraction tree was drawn using cafe5_draw_tree.py and pie charts for each tree node were added using meta-chart.com. Significantly expanded families in *M. tinhauana* were functionally annotated using eggNOG-mapper v2.1.9 (Cantalapiedra et al., 2021) with DIAMOND (Buchfink et al., 2021) and the eggNOG v5.0 database (Huerta-Cepas et al., 2019). GO enrichment analysis was performed following the published protocol (Zhou, 2022) in R and plotted using ggplot2 (Wickham, 2006).

Global distribution

Metagenomic reads from the Tara Oceans dataset were obtained from two projects (PRJEB4352-global and PRJEB9691-polar) through the European Nucleotide Archive in 2023. The samples were collected from the ocean surface at a depth of 5 m. The size fraction of interest was >0.8 µm (>0.8 µm, 0.8–5 µm or 0.8–20 µm samples were collected from different sites). In cases of site duplication, preference was given to >0.8 µm samples. A total of 124 metagenomic samples were mapped onto the full *M. tinhauana* genome and the *Micromonas pusilla* CCMP1545 genome (Worden et al., 2009) as a control using BBMap v38.96 (Bushnell, 2016) with a minimum identity of 95%. The mapping values were compiled using pileup.sh from the BBMap suite (Malfertheiner et al., 2022). To account for variations in total read numbers and genome lengths, Reads per Kilobase per Million (RPKM) values were computed as follows:

$$\mathrm{RPKM} = \mathrm{mappedReads} / \left(\mathrm{genomeLength}/1000^{*}\ \mathrm{totalReads}/1{,}000{,}000\right)$$

The coordinates and RPKM were collated. Custom code in R, along with the ggplot2 (Wickham, 2006) and scatterpie (Yu and Yu, 2018) packages, were utilised to plot the data onto world maps. Median values for environmental measurements for each sample site were downloaded (Supplementary Table S3). Spearman's rank correlation coefficients (SRCC) were calculated in R for each pair of environmental variables, and half the variables with more than 0.5 pairwise correlation were removed. The variables that were not highly collinear (only temperature, salinity and nitrate) were used for SRCC calculation with the *M. tinhauana* RPKM and plotted with ggpairs (GGally) (Schloerke et al., 2018). Some nitrate values were missing and so those samples were excluded from the nitrate-RPKM correlation study.

Results and discussion

Isolation, taxonomic classification and morphological characterisation of a novel *Mantoniella* species

In an effort to isolate *Mantoniella* species from coastal waters in the Western Pacific, a sweep of green algae from water samples were collected along the coast of Hong Kong in different seasons and subsequent purification using serial dilutions was performed. To assess their evolutionary distance compared to other cultured Mamiellophyceae, we sequenced and compared their partial 18S rRNA gene with algal sequences in GenBank. We discovered that one algal culture exhibited a remarkably high similarity to *Mantoniella squamata*, as evidenced by a 99.7% nucleotide identity.

To determine the taxonomic classification of this newly isolated alga, we constructed a phylogenetic tree based on the complete 18S rRNA gene. This analysis positioned the alga on the outer boundary of the *Mantoniella* genus, showing a close affinity to *Micromonas* (Figure 1). We named this novel species *Mantoniella tinhauana*. To aid in classification, *Mantoniella* strains were assigned to clades based on this phylogeny and previous studies (Tragin and Vaulot, 2019; Yau et al., 2020b). The novel strain had a very high shared identity (up to 99.9%) with several partial 18S sequences, for example strains assigned to clade B for which only the 18S V4 region was available (Tragin and Vaulot, 2019). As complete 18S sequences were lacking for certain strains (these were excluded), the novel *Mantoniella* could not be assigned to any known clade based on the whole 18S gene. As discussed before, relying solely on the 18S or any single marker gene for phylogenetic assessment may not be entirely reliable, especially in unicellular eukaryotes. This limitation is particularly evident in a genus like *Mantoniella*, which only has a few cultured and extensively studied species. To address this, we also examined the ITS2 marker.

The analysis of the ITS2 sequences in *M. tinhauana* revealed the presence of eukaryotic universal hallmark motifs (Mai and Coleman, 1997; Schultz et al., 2005), namely a Y-Y (U–U) mismatch in helix 2 and a YRRY (UGGU) motif in helix 3. These motifs were consistently identified in all ITS2 sequences (highlighted in yellow in Figure 2A and Supplementary Figures S1, S2). We further examined the folding patterns of their ITS2 molecules to differentiate between base differences that have structural effects and compensatory base changes shared with related Mamiellophyceae species. In helix 2 (Figure 2A), we observed that approximately half of the bases were identical in all Mamiellophyceae (white, yellow), while the other half exhibited variations that were also present in other *Mantoniella* species (blue). Additionally, two base pairs were exclusive to *M. tinhauana* and *Micromonas* or *Mamiella* species (pink). Similar differences were observed in the other three helices (Supplementary Figures S1, S2). Based on the ITS2 helix folding structures, *M. tinhauana* shares a mix of base pair variants characteristic of arctic *Mantoniella* species and *M. squamata*, placing it firmly within the *Mantoniella* genus. Interestingly, it also possesses some structural base pairs that are unique to *Micromonas* or *Mamiella* strains.

In addition to visualising and comparing the structural differences in ITS2, we constructed a phylogenetic tree based on the structurally-informed ITS2 alignments (Figure 2B). This ITS2 tree differs significantly from the phylogeny based on the 18S gene, although branch support values are predominantly low. The discrepancies between the ITS2 and 18S trees can be attributed to varying evolutionary rates and histories, hybridisation events, and selection pressures (Baldwin et al., 1995; Hershkovitz and Lewis, 1996).

We conducted transmission electron microscopy (TEM) analysis of *M. tinhauana,* revealing cells larger than typical *Ostreococcus, Bathycoccus* and *Micromonas* cells – with cell sizes increasing, respectively, from 0.6 to 3 µm, as reported in previous research (Manton and Parke, 1960; Eikrem and Throndsen, 1990; Chrétiennot-Dinet et al., 1995; Kuroiwa et al., 2004). The cells of *M. tinhauana* measured between 1.8 and 4.5 µm, with characteristic features commonly observed in cells of the *Mantoniella* genus (Figure 3). No features unique to the new species *Mantoniella tinhauana* were identified, similar to previous observations of *M. baffinensis* and *M. beaufortii* (Yau et al., 2020b). These species exhibited slight differences in size but overall resembled *M. squamata*. One exception was the radiating pattern on the spiderweb scales, which allowed differentiation of *M. beaufortii* from the other two species based on the number of radial spokes. *M. tinhauana* exhibited spiderweb-like octaradial scale symmetry just like *M. squamata* and *M. baffinensis*. In any case, morphological differences among *Mantoniella* species are minor, prompting us to investigate genetic differences as the next step in our research.

Mantoniella tinhauana exhibits double the genome size of other Mamiellophyceae species

The first-ever *Mantoniella* strain whole genome was generated using short read paired-end sequencing, PacBio SMRT sequencing, and Hi-C sequencing techniques. The completeness of the assembly was assessed using BUSCO analysis against the Chlorophyta database, which indicated a high completeness value of 97.1% (Supplementary Table S4), comparable to other Mamiellophyceae reference genomes (Table 1). The *de novo* assembly yielded a 40 Mb genome composed of 27 scaffolds, with longer scaffolds compared to other Mamiellophyceae species (Supplementary Table S5a). However, only a low percentage of *M. tinhauana* scaffolds contained telomeres. Specifically, 11 scaffolds had telomeric tandem repeats on one end [CCCTAAA or the reverse complement TTTAGGG, the same as other Mamiellophyceae and plants (Richards and Ausubel, 1988)], and only four scaffolds had telomeres on both ends. This indicates imperfect genome assembly, a common issue observed in other reference genomes such as *B. prasinos* (Table 1). Despite the larger genome size and increased number of scaffolds, ploidy prediction confirmed that *M. tinhauana* is haploid, consistent with other known Mamiellophyceae species. Repeat masking revealed that 14.9% of the genome was composed of repeat elements (Supplementary Table S6), a significantly higher proportion (double) than seen in other Mamiellophyceae (Xu et al., 2022).

Mantoniella tinhauana represents the species with the largest recorded genome size within the Mamiellophyceae class to date. This species also exhibits larger cell sizes compared to other

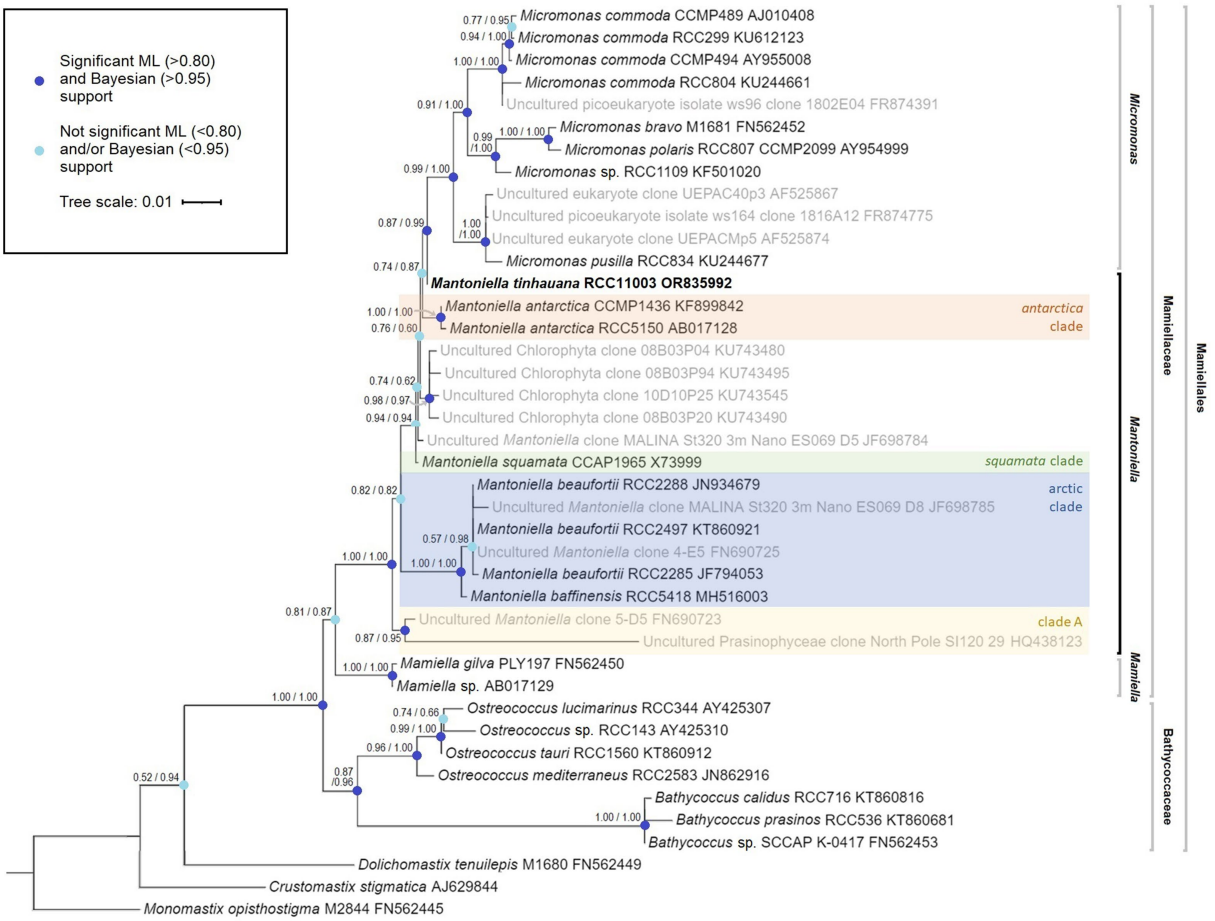

FIGURE 1
Mamiellophyceae 18S rRNA gene maximum likelihood tree, featuring species name, species code and 18S GenBank code (*Monomastix opisthostigma* as the outgroup). The numbers represent node support values, with the SH-like support values followed by the Bayesian posterior probability values. Nodes with enough support from both values (SH>0.80 and Bayes>0.95) are indicated in dark blue whereas nodes lacking sufficient support from either or both values are marked in light blue. Uncultured strains, obtained through blast search and previous studies, are depicted in grey where a complete 18S sequence was available. *Mantoniella* clades, if known, are labelled in different colours.

Mamiellales species, prompting the question of a possible correlation between genome size and cell size within the Mamiellophyceae class. Indeed, *Ostreococcus* species have the smallest cells (Chrétiennot-Dinet et al., 1995) and correspondingly small genomes. This trend continues with *Bathycoccus* species exhibiting slightly larger cells and genomes (Eikrem and Throndsen, 1990), and *Micromonas* following with even larger dimensions (Manton and Parke, 1960), as shown in Table 1. However, the number of scaffolds or chromosomes does not appear to follow a similar trend. A study contrasting the cell and genome sizes of *O. tauri* and a red algal species suggested that cell and genome sizes are not interdependent (Kuroiwa et al., 2004), but the comparison involved two phylogenetically distant species, potentially obscuring any correlation due to vastly different genomic structures and contents. To date, a systematic comparison of cell and genome sizes within Mamiellophyceae has not been undertaken. Preliminary observations hint at a significant correlation within this group. To test this hypothesis, further genomic sequencing and assembly of larger-celled Mamiellophyceae species, particularly from the genera *Mantoniella* or *Mamiella* (Alonso-González et al., 2014), would help validate this relationship between genome and cell sizes in this phylogenetic group.

Gene block synteny and chromosomal rearrangements

Pairwise gene block synteny among the different Mamiellophyceae species is depicted in Figure 4. Notably, *M. tinhauana* exhibits similar grouping and colocalisation patterns of gene blocks as those of *Micromonas* species, but with longer gene blocks, indicating gene block duplications and expansions. *O. lucimarinus* and *O. tauri* have nearly identical chromosome and gene block order. In contrast, *Micromonas commoda* and *Micromonas pusilla*, despite belonging to the same genus, display more frequent chromosomal order and gene block rearrangements, similar to those observed between *Micromonas pusilla* and *M. tinhauana*. These findings suggest that there have been more rearrangements and less consistent arrangement of syntenic blocks in the Mamiellaceae compared to the Bathycoccaceae, and

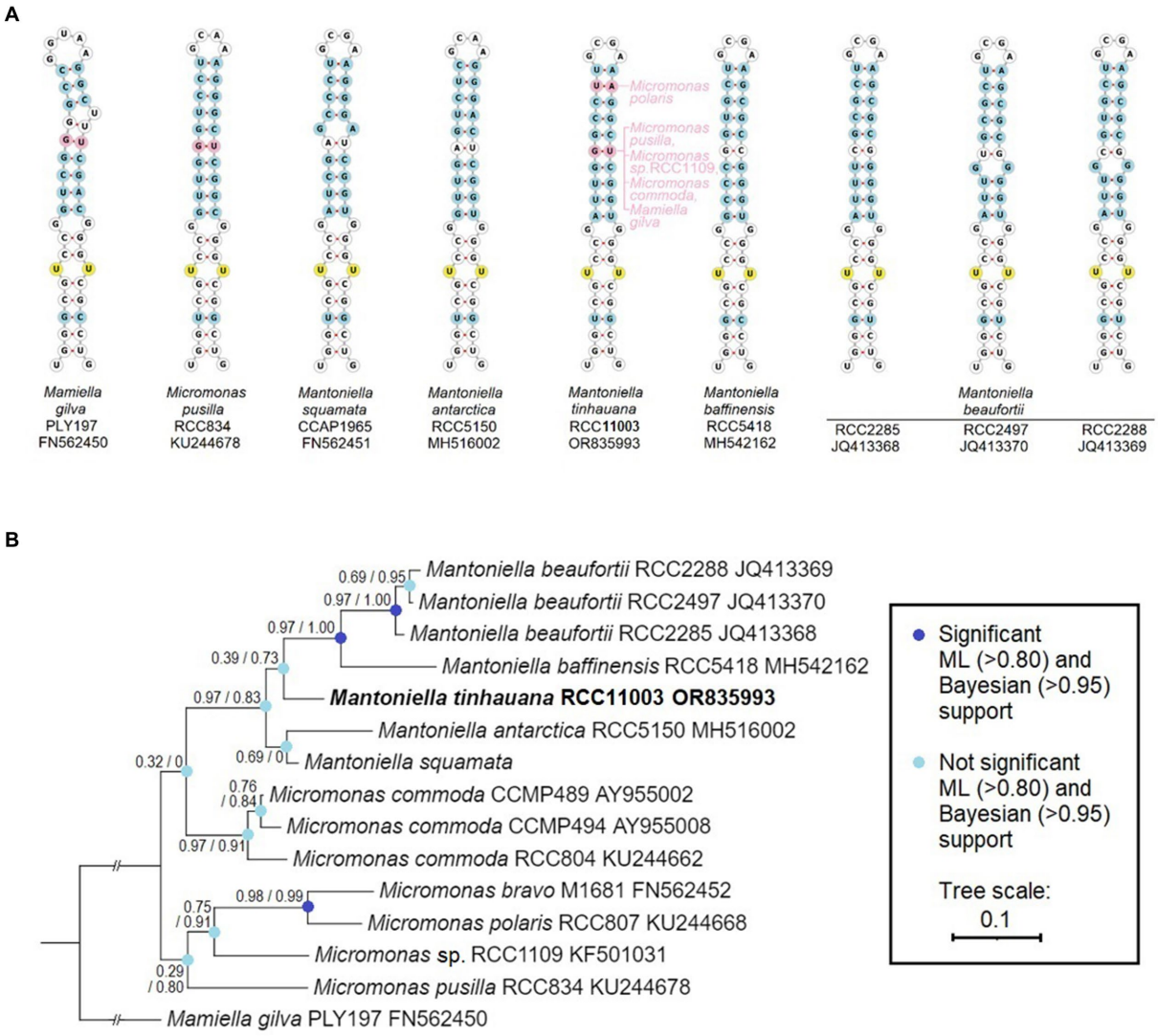

FIGURE 2
ITS2 RNA helix structural and base comparison, and phylogeny of Mamiellaceae. **(A)** ViennaRNA forna ITS2 folding structure of helix 2 (the other helices and complete ITS2 structure can be found in Supplementary Figures S1, S2), base-by-base comparison of novel *Mantoniella tinhauana* to other *Mantoniella* and Mamiellaceae strains, displayed in ITS2-based phylogenetic order. Only one representative *Micromonas* species and one *Mamiella* are shown. Yellow: universal eukaryote ITS2 motifs. Blue: site of nucleotide variant present in other *Mantoniella* species with structural effect. Pink: site of nucleotide variant absent in other *Mantoniella* species but present in other Mamiellophyceae species. **(B)** Mamiellaceae phylogenetic tree based on the structurally-informed comparison of ITS2 sequences, with branch support values as described.

M. tinhauana follows this trend. Bathycoccaceae chromosomes tend to be shorter, resulting in fewer gene blocks corresponding to different chromosomes, whereas the Mamiellaceae have longer chromosomes, increasing the likelihood of rearrangements. Given that *M. tinhauana* possesses the longest chromosomes, it is unsurprising that gene blocks from multiple chromosomes in other species correspond to syntenic blocks on a single chromosome in *M. tinhauana*, and vice versa. Importantly, 75.7% of genes across all species exhibited collinearity, which suggests that, despite the rearrangement of gene blocks among different species, there is a substantial conservation of both gene content and, to a certain extent, the order of these blocks are correctly assembled in the novel species genome. This degree of collinearity provides substantial support to the accuracy of our genome assembly. Additionally, most *M. tinhauana* scaffolds with telomeres, particularly those with telomeres at both ends, demonstrate a higher level of synteny with other Mamiellophyceae species.

Orthofinder analysis reveals species-specific characteristics of the novel *Mantoniella* proteome

In order to uncover the factors contributing to the larger genome of *M. tinhauana*, we conducted a comprehensive analysis of species orthogroups using Orthofinder. The overall and species-specific results of Orthofinder analysis can be found in Supplementary Table S7, with a graphical representation in Figure 5. The novel *Mantoniella*

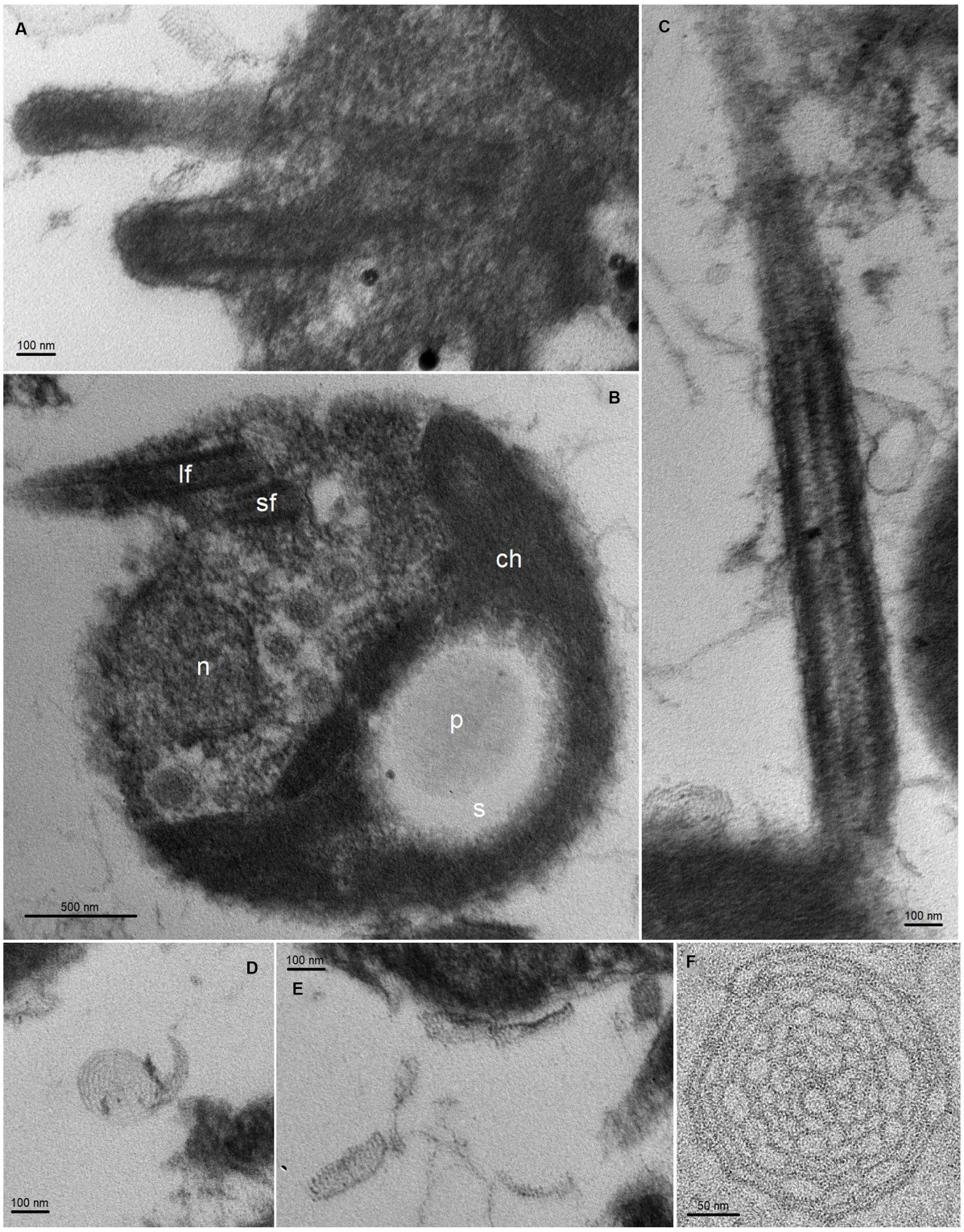

FIGURE 3
TEM thin sections of *Mantoniella tinhauana*. Cells were measured to be approximately 3 µm in diameter (10 cells measured, standard deviation 0.7 µm, min size 1.8 µm, max size 4.5 µm, median 3.1 µm), slightly smaller than but around the range of *M. squamata* (3–6.5 µm) (Manton and Parke, 1960), *M. antarctica* (2.8–5 µm) (Marchant et al., 1989), *M. beaufortii* (2.9–5 µm) and *M. baffinensis* (3.5–5.7 µm) (Yau et al., 2020b). **(A)** Bases of the long and short flagella. **(B)** Whole cell view with detail of organellar structures: n = nucleus, ch = chloroplast, s = starch granule, p = pyrenoid, lf = long flagellum, sf = short flagellum. **(C)** Detail of flagellum covered in scales (body and hair scales). **(D–F)** Body scales with octaradial spiderweb structure.

10.3389/fmicb.2024.1358574

TABLE 1 Mamiellales genomes used in this study and their characteristics.

Species	Genome size (Mb)	Chromosome / scaffold number	Genome GC (%)	% scaffold ends with telomeres	% scaffolds with two telomeres	BUSCO completeness (%)
Ostreococcus tauri RCC4221 (Blanc-Mathieu et al., 2014)	12.9	20	59.4	67.5	35.0	98.1
Ostreococcus lucimarinus CCE9901 (Palenik et al., 2007)	13.2	21	60.4	100	100	98.8
Ostreococcus mediterraneus RCC2590 (Yau et al., 2020a)	13.9	20	56.2	60.0	40.0	97.8
Bathycoccus prasinos RCC1105 (Moreau et al., 2012)	15.0	19	48.1	34.2	10.5	97.1
Micromonas commoda RCC299 (Worden et al., 2009)	21.0	17	64.0	100	100	99.1
Micromonas pusilla CCMP1545 (Worden et al., 2009)	22.0	21	65.9	90.5	90.5	98.0
Mantoniella tinhauana RCC11003	39.5	27	64.8	35.2	14.8	97.1

Except for *M. tinhauana*, marked in green, all genomes and the size and chromosome/scaffold information were obtained from NCBI.

proteome exhibited notable characteristics, including the highest level of unassigned genes (1,288 or 11.6%), species-specific orthogroups (141 or 1.8%) and genes in species-specific orthogroups (394 or 3.5%). These findings were expected, considering that *M. tinhauana* is the first proteome in its genus and a newly discovered species with a significantly larger genome. The functional annotation of genes in *Mantoniella tinhauana*-specific orthogroups (188) is listed in Supplementary Table S8, which encompass a variety of roles, including motor proteins, carbohydrate metabolism and chromosome associated proteins. We further explored these species-specific orthogroups through Gene Ontology (GO) Enrichment Analysis.

Functional significance of gene family expansions in *Mantoniella tinhauana*

To gain a comprehensive understanding of the orthogroup differences between species, particularly those with assignable functions, we performed expansions and contractions analysis. This analysis sought to elucidate the evolutionary history and relationship of *M. tinhauana* and its close relatives. Interestingly, *M. tinhauana* exhibited numerous gene family expansions, and even more contractions (Figure 6A). Additionally, GO enrichment analysis (Figure 6B) provided insights into the biological functions associated with the most significant expansions.

GO enrichment analysis revealed strong expansions in glycosylation gene families, particularly sialylation, which may be involved in the development of *M. tinhauana*'s characteristic scales and will be discussed below. It also unveiled significant expansions in Golgi associated genes, which is where sialylation takes place in the cell (Schauer and Kamerling, 2018). Expanded gene families associated with carbohydrate metabolism and cell growth (Raven and Beardall, 2003; Mathieu-Rivet et al., 2020) suggest that *M. tinhauana* is a fast-growing species well-adapted to eutrophic waters, where it was isolated.

Absence of lower GC content regions in *Mantoniella tinhauana*: implications for sexual reproduction, viral resistance and Mamiellophyceae speciation

Previously sequenced genomes of Mamiellophyceae in the genera *Micromonas, Ostreococcus* and *Bathycoccus* have a relatively high overall GC content and two lower GC content outlier chromosomes (Derelle et al., 2006; Piganeau et al., 2011b; Grimsley et al., 2015). These outlier chromosomes contain a higher proportion of transposable elements, leading to faster gene evolution and the presence of more species-specific, non-orthologous genes (Jancek et al., 2008). The BOC has distinct blocks with heterogeneous GC content, characterised by a section of lower GC flanked by normal, higher GC content. The low GC region suppresses recombination and contains one of two alternate mating type loci, which is hypothesised to predate Mamiellophyceae speciation (Blanc-Mathieu et al., 2017). In contrast, the SOC has

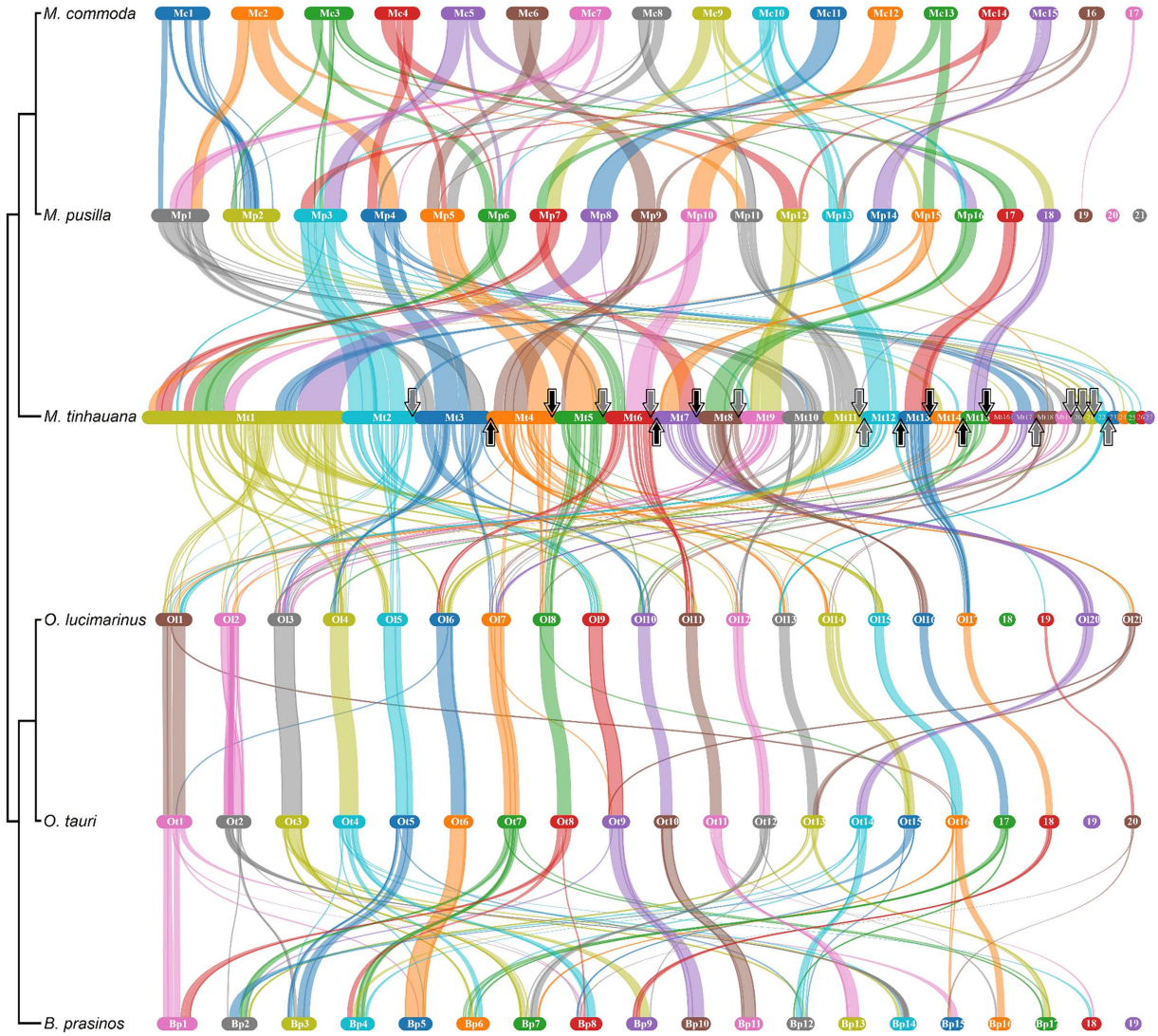

FIGURE 4
Pairwise gene block synteny of Mamiellales proteomes computed with MCScanX and visualised using SynVisio. Species are ordered by 18S-based phylogeny, with a simplified phylogenetic tree and names labelled on the left. Scaffolds or chromosomes for each species are shown in separate sections of different colours (random repeating 10 colour series), in order (largest to smallest), labelled. Collinear gene blocks between each pair of species are connected with ribbons of varying thicknesses denoting gene block lengths, in the colour corresponding to the source scaffold. For *M. tinhauana*, telomeres at the beginning (upwards arrow) or end (downwards arrow) of a scaffold are marked with arrows. The four scaffolds which have telomeres at both ends have black arrows.

low GC content throughout, and shows high variability in gene content even within the same species due to frequent duplications and internal rearrangements (Grimsley et al., 2015; Blanc-Mathieu et al., 2017). The SOC is associated with viral resistance (Moreau et al., 2012), as species possessing this variable chromosome demonstrate high viral sensitivity and the ability to rapidly develop resistance to viruses. SOC length is inversely correlated with viral susceptibility (Blanc-Mathieu et al., 2017). In unpublished experiments mentioned by Moreau et al. (2012), it was observed that two *Mamiella* and *Mantoniella* species do not exhibit the high viral sensitivity seen in the seven whole-genome sequenced species. These findings support the hypothesis that these species and potentially the entire genera may lack the SOC, although this has yet to be confirmed.

In the current study of the novel *Mantoniella* genome, no chromosomes with significantly lower GC content were identified (Supplementary Table S5b). Lower GC content is typically associated with suppressed recombination, which is a characteristic of sexual reproduction. However, no such regions were found in *M. tinhauana*, and direct observation of the process is virtually impossible. To confirm whether *M. tinhauana* undergoes sexual reproduction, we examined the presence of core meiosis genes (Derelle et al., 2006; Worden et al., 2009; Joli et al., 2017; Li et al., 2020), including the RWP-RK family of transcription factors known to be involved in gametogenesis in algae (Chardin et al., 2014). The findings demonstrate key meiosis genes are present at the expected levels in *M. tinhauana* (Supplementary Table S9), providing robust evidence supporting the existence of a sexual stage in this species.

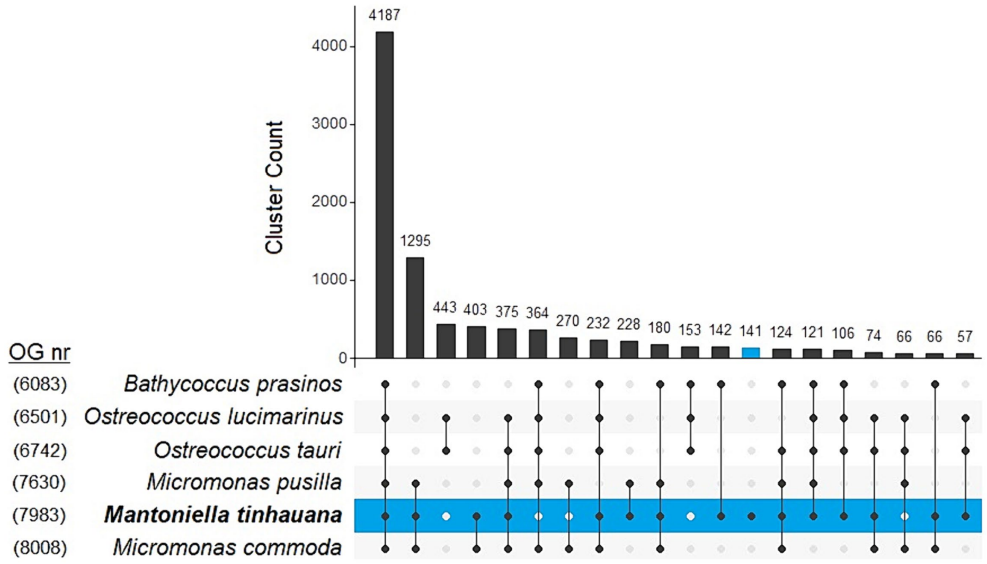

FIGURE 5
UpSet plot comparison of top 20 clustering unique and shared orthogroups in 6 Mamiellophyceae species. Number of orthogroups per species is labelled on the left.

In a study by Benites et al. (2021), the mean GC contents of coding sequences in Mamiellophyceae transcriptomes were compared to those of mating gene family coding sequences. Interestingly, some transcriptomes, including two *Mantoniella* transcriptomes, did not exhibit lower GC content in their mating gene family genes. In fact, certain species such as *Dolichomastix* even have a higher GC content in their mating genes. These findings support the possibility that earlier branching Mamiellophyceae gametologs are not confined to regions of lower GC content. It is conceivable that the genus *Mantoniella*, or at least *M. tinhauana*, never evolved to have recombination suppression in their mating gene regions, unlike *Bathycoccus, Ostreococcus* and *Micromonas* species. This could be because their mating genes are not clustered together on a single chromosome.

To investigate further, we analysed the synteny of five Mamiellophyceae BOCs in comparison to the novel *Mantoniella* scaffolds. The gene blocks did not align with a single scaffold, but with several (Figure 7A). Notably, *M. tinhauana* shares syntenic blocks with all five species BOCs, which is not the case when comparing other Mamiellaceae to Bathycoccaceae BOCs (Figure 7C). This suggests that *M. tinhauana* has gene blocks in common with both groups, further supporting its phylogenetic placement between the two. However, these syntenic blocks are located on separate scaffolds, indicating a distinct genomic organisation. The BOC has previously been identified as emerging before the speciation of Mamiellophyceae (Blanc-Mathieu et al., 2017), and thus it should be present in all Mamiellophyceae species. The absence of the BOC in the novel *Mantoniella* genome could indicate three possibilities: (a) translocation or rearrangement after the branching of the *Mantoniella* genus, (b) a more recent evolutionary origin of the BOC than previously thought, or (c) assembly errors.

To determine if the syntenic BOC blocks were associated with mating, we examined gene block synteny between the MT loci within each BOC and the *Mantoniella* proteome (Figure 7B). The analysis revealed that only a few *Micromonas* MT gene blocks were found in *M. tinhauana*, proving that the majority of syntenic blocks between Mamiellophyceae BOCs and *M. tinhauana* are unrelated to mating. When comparing BOC gene blocks among Mamiellophyceae, the syntenic blocks primarily correspond to the MT loci (Figure 7D). These findings suggest that in *M. tinhauana*, the mating loci are not clustered and have undergone rearrangements and/or genetic divergence compared to its phylogenetic relatives.

Attempts to align the distinct and variable sequences of SOC in Mamiellophyceae with the *Mantoniella* genome were unsuccessful. Consequently, the SOC can only be identified based on chromosome length and GC content. Moreau et al. (2012) proposed that *Mantoniella* may lack a SOC due to its purported lower sensitivity to viruses. The absence of the SOC in this study supports this hypothesis, although SOC-lacking species could very well interact with viruses in different ways. We are currently studying the viral susceptibility of *M. tinhauana*. Further investigations should also aim to identify virus resistance genes present in other Mamiellophyceae and determine whether the same or orthologous genes are present in the *M. tinhauana* genome, with special attention to their location if present.

Expanding gene families and scale development in *Mantoniella*

The gene family expansion analysis uncovered a significant expansion in sialylation and other glycosylation gene families in *M. tinhauana*. To investigate these expansions further, we conducted a targeted analysis on four protein families previously found to be expanded in *Bathycoccus prasinos* hypothesised to be involved in scale formation (Moreau et al., 2012). We searched for these families in the Pfam-annotated proteome of *M. tinhauana* and found similar copy number expansions in two out of the four families: glycosyltransferase family 29 and neuraminidase/sialidase

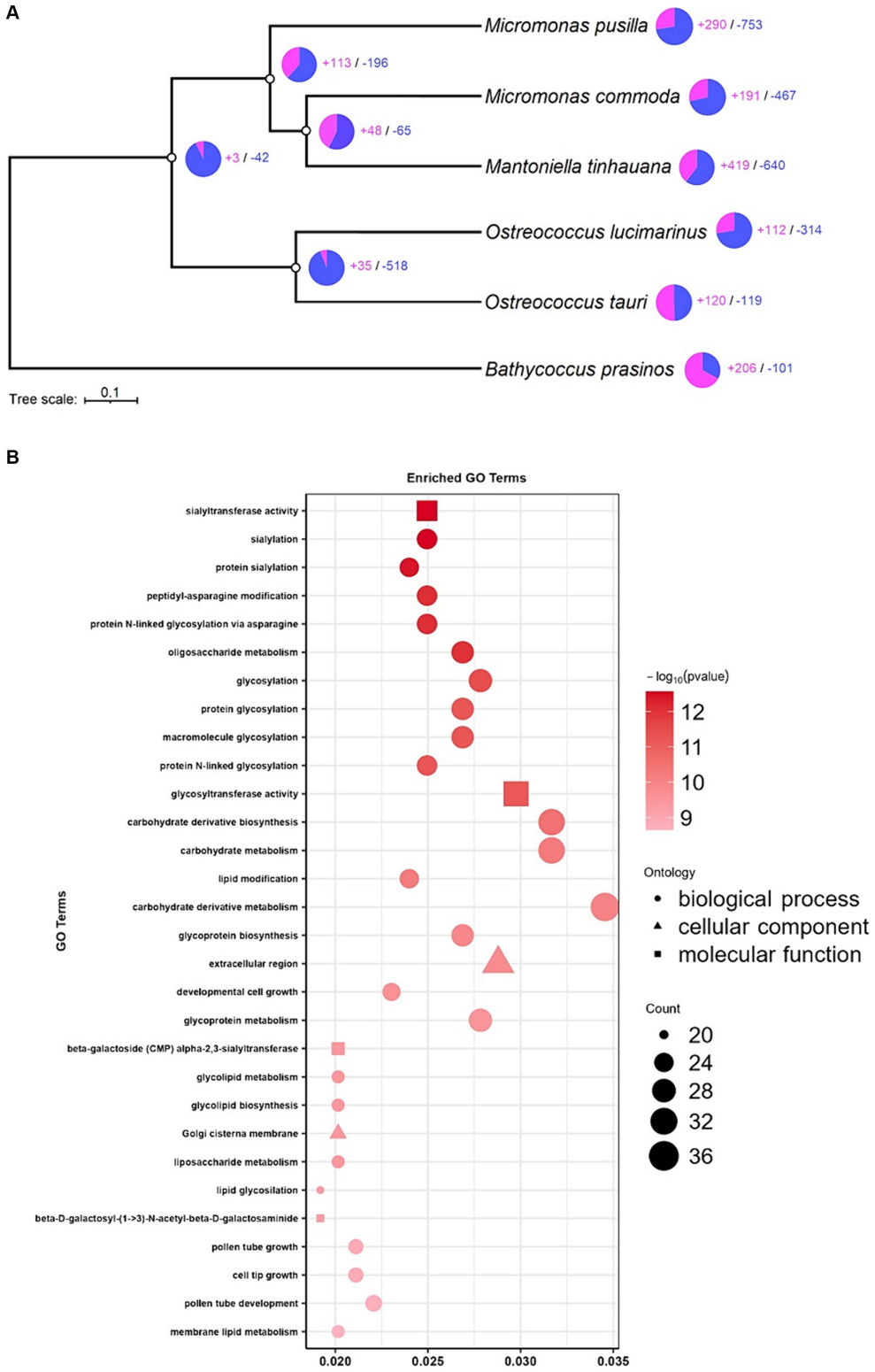

FIGURE 6
Expansion and contraction analysis and enrichment analysis. **(A)** Tree of expanded (purple) and contracted (blue) gene families. **(B)** GO enrichment analysis of significantly expanded gene families in *M. tinhauana*.

(Supplementary Table S10). Another study by van Baren et al. (2016) also identified expansions in only two out of the four families in both scaled *B. prasinos* and *D. tenuilepis* compared to non-scaled species. Our findings confirm theirs, supporting the hypothesis that glycosyltransferase family 29 and sialidases are involved in scale development.

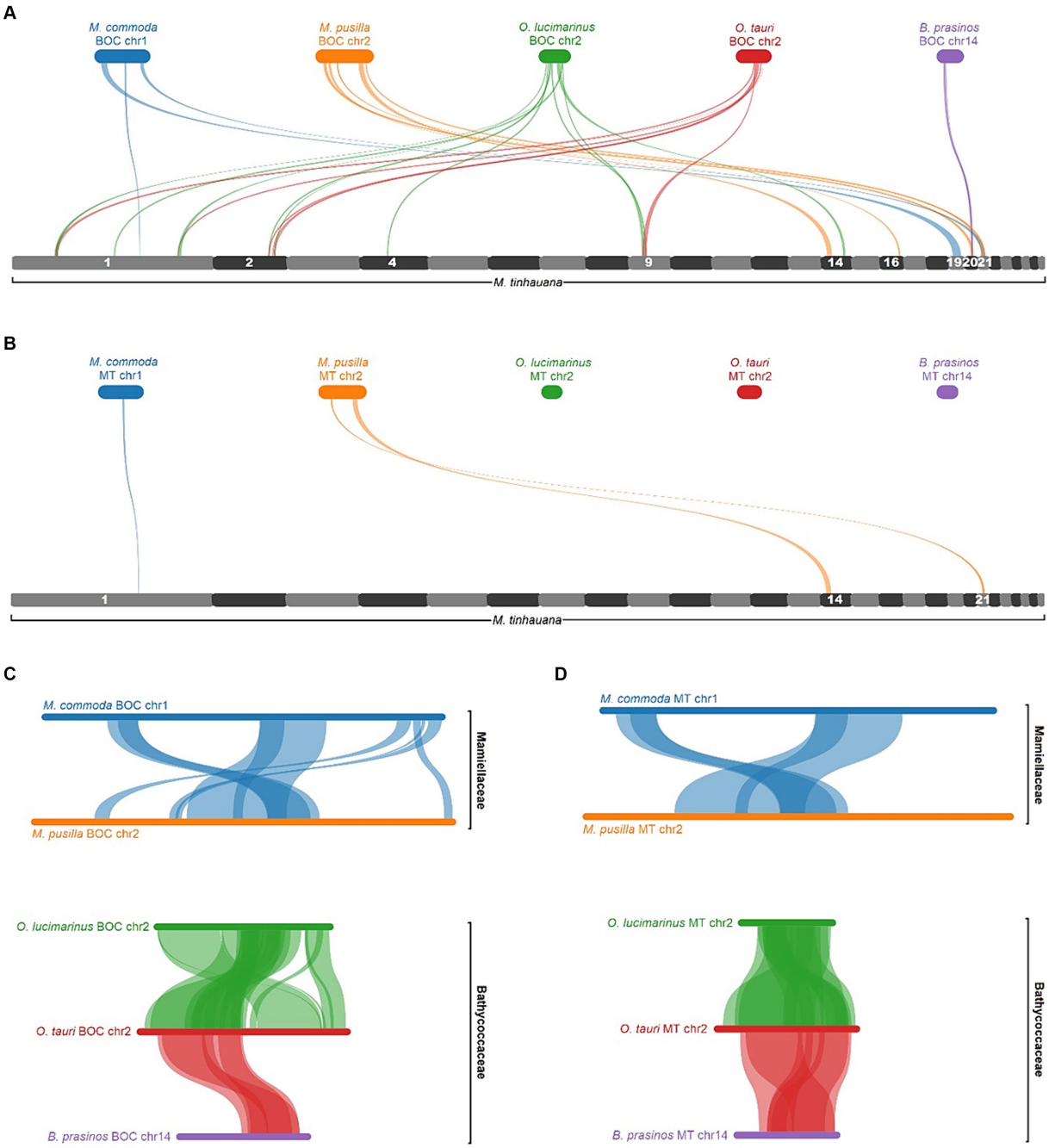

FIGURE 7
MCScanX pairwise alignment of BOCs and MTs. **(A)** BOC alignments to the full *Mantoniella tinhauana* genome. *M. tinhauana* scaffolds with syntenic blocks are numbered. **(B)** MT alignments to the *Mantoniella tinhauana* genome. **(C)** BOC alignments to one another. **(D)** MT alignments to one another. Collinear gene blocks (of at least 5 genes with a max gap of 25) are connected with ribbons of different thicknesses denoting gene block lengths, in the same colour as the source species.

Genetic basis of biflagellate phenotype in *Mantoniella*

The novel and other *Mantoniella* species possess two flagella, unlike other Mamiellophyceae genera that have one flagellum (*Micromonas*) or none (*Bathycoccus, Ostreococcus*). This difference in flagellar number should be reflected in their genomic characteristics, but gene family expansion analysis indicated no motor associated expansions. We analysed the Pfam-annotated proteome using a list of published flagella-related genes (Li et al., 2020). Comparison to other Mamiellophyceae revealed that *M. tinhauana* had higher copy numbers of certain microtubule synthesis and assembly protein domains compared to other species (Supplementary Table S11). A few cilia-, flagella- and motility-associated domains also showed a modest expansion in *M. tinhauana* compared to monoflagellated *Micromonas*. Marin and Melkonian (2010) proposed that the last common ancestor

of the Mamiellophyceae had two flagella, as monoflagellate *Monomastix* and *Micromonas* species retain two basal bodies despite having only one flagellum. The identified gene expansions could potentially explain how *M. tinhauana* retained two flagella, but further functional studies are necessary to identify the genes involved in flagellar number and length control, as well as environmentally-stimulated and synchronous flagellar beating. These areas remain largely unexplored in Mamiellophyceae. Examining the expression of key genes, and not only their copy number, would provide further insights.

Metagenomic analysis reveals the global distribution and environmental adaptation of *Mantoniella tinhauana*

Metagenomic reads obtained from the Tara Oceans Expeditions were used to investigate the presence and abundance of *M. tinhauana*. Considering the size range of *M. tinhauana* cells (>1.8 µm) and *Micromonas pusilla* cells (>1 µm) (Manton and Parke, 1960), reads from the over 0.8 µm size fraction were used. These reads were mapped onto the novel and control genomes, and the relative abundance (RPKM) was calculated (Figure 8 and Supplementary Table S3).

Our analysis revealed the widespread occurrence of *Mantoniella tinhauana* reads across the tested sites in the surface of the global ocean. The abundance of *M. tinhauana* reads was consistently low, indicating that it is a cosmopolitan species with a low-level prevalence, except for polar regions where it was higher. The mean worldwide RPKM value of the tested sites was 0.12, with a maximum of 0.43 RPKM (1.73% of reads). The mapping to the control *Micromonas pusilla* CCMP1545 genome (global mean 0.36 RPKM, maximum 1.54 RPKM or 3.38% of reads) showed similar levels as reported previously (Leconte et al., 2020) using similar methods.

To understand the environmental factors influencing the abundance of *M. tinhauana*, we examined the correlation between read abundance and various environmental variables (Figure 8C). Although statistically significant, the individual relationships were not strongly pronounced, with the most correlated factor being temperature. Nitrate showed a positive correlation with RPKM, while temperature and salinity exhibited negative correlations. These findings support the hypothesis that *M. tinhauana* is adapted to growing in diverse nutrient levels, and in environments rich in nutrients, for instance with high nitrate, it can readily thrive and proliferate. The negative correlation between the abundance of *M. tinhauana* and temperature, and its higher presence in polar regions suggest a preference for cooler habitats within this genus. All species within the genus, with the exception of *M. squamata* and *M. tinhauana*, have been isolated exclusively from polar sites. This intriguing observation presents an exciting opportunity to conduct genomic comparisons between the non-polar and polar species, with the aim of unravelling the underlying genomic traits that contribute

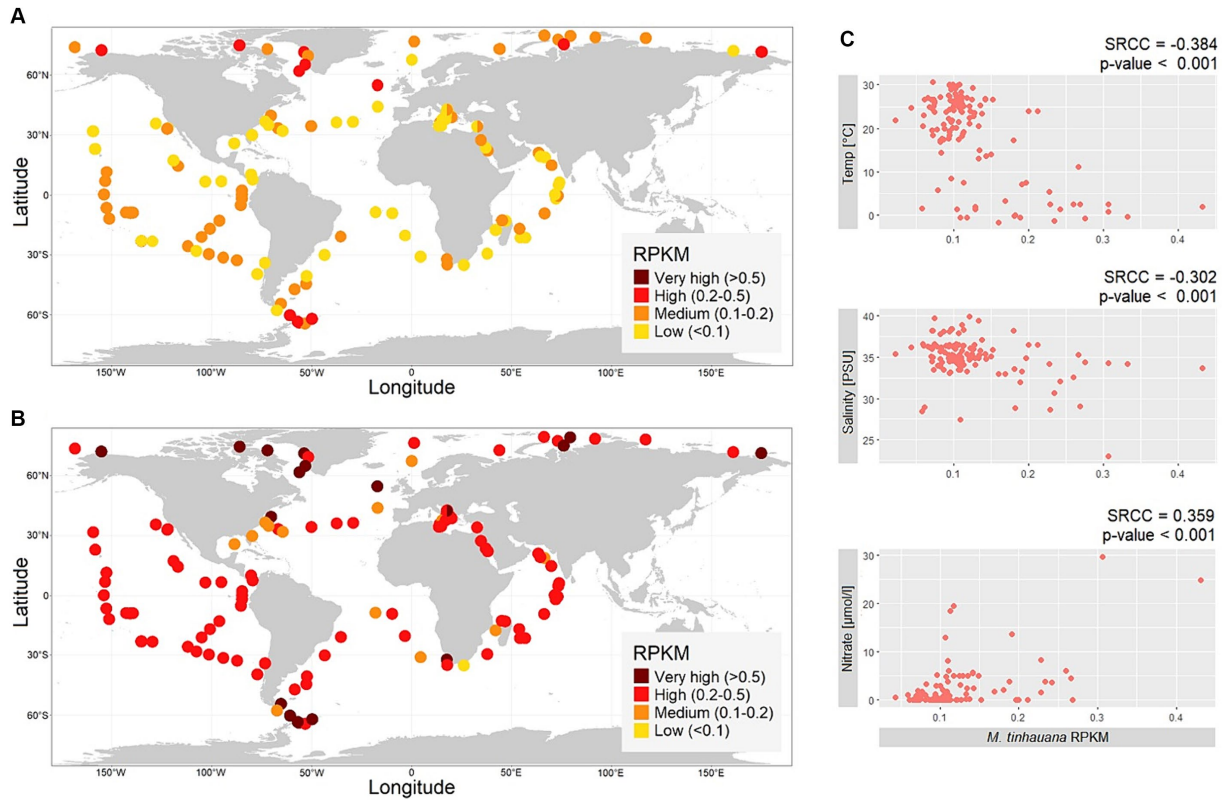

FIGURE 8
Biogeographic distribution of Mamiellophyceae. **(A,B)** Maps of global metagenomic RPKM read mapping of over 0.8 µm size fraction reads sampled at the ocean surface to **(A)** *Mantoniella tinhauana* genome, **(B)** *Micromonas pusilla* CCMP1545 genome. **(C)** Correlations between not highly collinear environmental variables and *M. tinhauana* RPKM values.

to their distinct adaptations to cold and higher temperatures, respectively.

Taxonomy

Mantoniella tinhauana RCC11003 Rey Redondo, Xu and Yung sp. nov.

Description

Illustrated in Figure 3. Round cells measuring 3 µm in diameter (standard deviation 0.7 µm, min size 1.8 µm, max 4.5 µm, median 3.1 µm), slightly smaller but around the range of other *Mantoniella* strains (Yau et al., 2020b). Biflagellate, with one long and one short flagellum. Cell body covered in octaradial spiderweb scales. One large chloroplast, occupying half the cell, with pyrenoid within starch granule. 18S and ITS2 rRNA sequences are species-specific (18S and ITS region GenBank accessions: OR835992 and OR835993, respectively).

Holotype

Isolated on the 11th June 2020 (10:30 am) from surface water (2 m depth) that was 30.5°C via peristaltic pump at the Lau Fau Shan coast of Hong Kong, in the Pacific Ocean (22°28′09.0′N 113°58′50.1′E). Culture deposited in The Roscoff Culture Collection under accession RCC11003.

Etymology

Tin Hau is the Cantonese name for the goddess of the sea revered in Hong Kong.

Habitat and ecology

Cosmopolitan species in surface water, with higher dominance in polar regions. Growth positively correlated with nitrate level and negatively correlated with temperature and salinity.

Conclusion

We have discovered a novel species of Mamiellophycean green alga, *Mantoniella tinhauana*, from coastal surface water in the Western Pacific. Morphologically, it closely resembles other *Mantoniella* species, except for its smaller cell size. Through comparison of its 18S rRNA sequence and ITS2 structure with other Mamiellophyceae, we confirmed it to be a distinct species. Phylogenetically, it falls between the genus *Micromonas* and other *Mantoniella* strains.

The genome of *M. tinhauana*, the first draft genome of a *Mantoniella* species, was assembled with high completeness and annotated. It differs significantly from other Mamiellophyceae species, with a larger genome size (concurrent with larger cell size), more repeat elements and numerous unique genes. The larger genome size of the novel strain cannot be solely explained by the observed expansions. Comparative analysis with other Mamiellophyceae genomes revealed gene block duplications, expansions, as well as regions of no synteny and known function. To gain further insights, RNAseq should be conducted to determine the functions of more actively expressed genes.

Notably, *M. tinhauana* lacks the two low-GC outlier chromosomes found in all other studied Mamiellales, which are linked to mating and viral resistance. Despite the absence of synteny with BOC and MT loci seen in other species, the presence of meiosis genes in *M. tinhauana* suggests the existence of similar mating types and sexual reproduction mechanisms. These findings pose intriguing questions regarding the ancestry and evolution of Mamiellophyceae, which can only be hypothesised with a single divergent genome. Ongoing research on the viral infection dynamics of *M. tinhauana* may shed light on the absence of SOC and viral sensitivity in this algal class.

The analysis of expanded gene families revealed high glycosylation activity involved in scale formation. This and the two flagella in *Mantoniella* prompted a comparison of targeted gene groups between the novel species and other proteomes. While some investigated genes partially explained these structural differences, further study is required to fully understand the underlying mechanisms of scale patterns, flagella production and synchronised movement. The availability of this first whole genome of a biflagellate scaled Mamiellophycean species will undoubtedly contribute to future studies in these areas and beyond.

Future efforts should be focused on assembling and analysing the whole genomes of additional Mamiellophyceae species, including other *Mantoniella* strains and members of the understudied genus *Mamiella*. The challenges encountered in assembling the divergent *de novo* genome of *M. tinhauana* highlight the need for more cultures and complete genomes to enhance assembly accuracy and efficiency. Additionally, it would be valuable to assemble the plastid (chloroplast and mitochondrial) sequences of *M. tinhauana* and compare them to those of related species.

This study represents the first exploration of the distribution of a *Mantoniella* strain using non-metabarcoding or MAG-based means. *M. tinhauana* distribution was cosmopolitan at low level and with higher prevalence at high latitudes. Temperature and salinity were negatively correlated with *M. tinhauana* RPKM values. Nitrate concentration was the most positively correlated environmental variable, although further studies on growth rate and nutrient deficiencies would be informative. To further understand Mamiellophyceae distribution, future metagenomic studies should use expanded datasets to explore depth variations, seasonality and potentially conduct a more long-term analysis of global warming. It is important to understand the precise relationship between the environment and Mamiellophyceae dominance, as these organisms play a crucial role in ocean primary productivity. Such knowledge is essential for comprehending the dynamics of the ocean as a whole and its future implications in the context of climate change.

Data availability statement

The datasets presented in this study can be found in online repositories. The names of the repository/repositories and accession number(s) can be found in the article/Supplementary material.

Author contributions

ER: Writing – original draft, Writing – review & editing. YX: Writing – original draft, Writing – review & editing. CY: Writing – original draft, Writing – review & editing.

Funding

The author(s) declare financial support was received for the research, authorship, and/or publication of this article. We gratefully acknowledge the financial support provided by the Research Grants Council of Hong Kong (Early Career scheme: 26100521).

Acknowledgments

We thank Adriana Lopes dos Santos, Sheree Yau, and Kirill Konovalov for their generous help with RNA structures, as well as Wan Siu Hei for his dedicated efforts in maintaining the algae culture, ensuring its vitality throughout the course of this study.

Conflict of interest

The authors declare that the research was conducted in the absence of any commercial or financial relationships that could be construed as a potential conflict of interest.

Publisher's note

Supplementary material

The Supplementary material for this article can be found online at: https://www.frontiersin.org/articles/10.3389/fmicb.2024.1358574/full#supplementary-material

References

Aiyar, A. (1999). "The use of CLUSTAL W and CLUSTAL X for multiple sequence alignment" in *Bioinformatics methods and protocols*. eds. S. Misener and S. A. Krawetz (Totowa, NJ: Humana Press).

Alonso-González, A., Orive, E., David, H., García-Etxebarria, K., Garrido, J. L., Laza-Martínez, A., et al. (2014). Scaly green flagellates from Spanish Atlantic coastal waters: molecular, ultrastructural and pigment analyses. *Bot. Mar.* 57, 379–402. doi: 10.1515/bot-2013-0108

Baldwin, B. G., Sanderson, M. J., Porter, J. M., Wojciechowski, M. F., Campbell, C. S., and Donoghue, M. J. (1995). The ITS region of nuclear ribosomal DNA: a valuable source of evidence on angiosperm phylogeny. *Ann. Mo. Bot. Gard.* 82, 247–277. doi: 10.2307/2399880

Balzano, S., Gourvil, P., Siano, R., Chanoine, M., Marie, D., Lessard, S., et al. (2012). Diversity of cultured photosynthetic flagellates in the north East Pacific and Arctic oceans in summer. *Biogeosci. Discuss.* 9, 4553–4571. doi: 10.5194/bgd-9-6219-2012

Bandi, V., Gutwin, C., Siri, J. N., Neufeld, E., Sharpe, A., and Parkin, I. (2022). *Visualization tools for genomic conservation*. New York, NY: Springer US.

Belevich, T. A., Milyutina, I. A., Abyzova, G. A., and Troitsky, A. V. (2021). The pico-sized Mamiellophyceae and a novel *Bathycoccus* clade from the summer plankton of Russian Arctic seas and adjacent waters. *FEMS Microbiol. Ecol.* 97:fiaa 251. doi: 10.1093/femsec/fiaa251

Benites, L. F., Bucchini, F., Sanchez-Brosseau, S., Grimsley, N., Vandepoele, K., and Piganeau, G. (2021). Evolutionary genomics of sex-related chromosomes at the base of the Green lineage. *Genome Biol. Evol.* 13:evab 216. doi: 10.1093/gbe/evab216

Blanc-Mathieu, R., Krasovec, M., Hebrard, M., Yau, S., Desgranges, E., Martin, J., et al. (2017). Population genomics of picophytoplankton unveils novel chromosome hypervariability. *Sci. Adv.* 3:e1700239. doi: 10.1126/sciadv.1700239

Blanc-Mathieu, R., Verhelst, B., Derelle, E., Rombauts, S., Bouget, F.-Y., Carré, I., et al. (2014). An improved genome of the model marine alga *Ostreococcus tauri* unfolds by assessing Illumina de novo assemblies. *BMC Genomics* 15:1103. doi: 10.1186/1471-2164-15-1103

Bolger, A. M., Lohse, M., and Usadel, B. (2014). Trimmomatic: a flexible trimmer for Illumina sequence data. *Bioinforma. Oxf. Engl.* 30, 2114–2120. doi: 10.1093/bioinformatics/btu170

Brůna, T., Hoff, K. J., Lomsadze, A., Stanke, M., and Borodovsky, M. (2021). BRAKER2: automatic eukaryotic genome annotation with gene mark-EP+ and AUGUSTUS supported by a protein database. *NAR Genomics Bioinforma.* 3:lqaa 108. doi: 10.1093/nargab/lqaa108

Buchfink, B., Reuter, K., and Drost, H.-G. (2021). Sensitive protein alignments at tree-of-life scale using DIAMOND. *Nat. Methods* 18, 366–368. doi: 10.1038/s41592-021-01101-x

Bushmanova, E., Antipov, D., Lapidus, A., and Prjibelski, A. D. (2019). rnaSPAdes: a de novo transcriptome assembler and its application to RNA-Seq data. *GigaScience* 8:giz100. doi: 10.1093/gigascience/giz100

Bushnell, B. (2016). BBMap short read aligner. 2023. Available at: http://sourceforge.net/projects/bbmap

Cantalapiedra, C. P., Hernández-Plaza, A., Letunic, I., Bork, P., and Huerta-Cepas, J. (2021). eggNOG-mapper v2: functional annotation, Orthology assignments, and domain prediction at the metagenomic scale. *Mol. Biol. Evol.* 38, 5825–5829. doi: 10.1093/molbev/msab293

Chardin, C., Girin, T., Roudier, F., Meyer, C., and Krapp, A. (2014). The plant RWP-RK transcription factors: key regulators of nitrogen responses and of gametophyte development. *J. Exp. Bot.* 65, 5577–5587. doi: 10.1093/jxb/eru261

Chen, S., Zhou, Y., Chen, Y., and Gu, J. (2018). Fastp: an ultra-fast all-in-one FASTQ preprocessor. *Bioinformatics* 34, i884–i890. doi: 10.1093/bioinformatics/bty560

Cho, C. H., Park, S. I., Huang, T.-Y., Lee, Y., Ciniglia, C., Yadavalli, H. C., et al. (2023). Genome-wide signatures of adaptation to extreme environments in red algae. *Nat. Commun.* 14:10. doi: 10.1038/s41467-022-35566-x

Chrétiennot-Dinet, M.-J., Courties, C., Vaquer, A., Neveux, J., Claustre, H., Lautier, J., et al. (1995). A new marine picoeucaryote: *Ostreococcus tauri* gen. Et sp. nov. (Chlorophyta, Prasinophyceae). *Phycologia* 34, 285–292. doi: 10.2216/i0031-8884-34-4-285.1

Collins, T. J. (2007). Image J for microscopy. *Bio. Techniques* 43, S25–S30. doi: 10.2144/000112517

Conway, J. R., Lex, A., and Gehlenborg, N. (2017). UpSetR: an R package for the visualization of intersecting sets and their properties. *Bioinformatics* 33, 2938–2940. doi: 10.1093/bioinformatics/btx364

Corrêa dos Santos, R. A., Goldman, G. H., and Riaño-Pachón, D. M. (2017). Ploidy NGS: visually exploring ploidy with next generation sequencing data. *Bioinformatics* 33, 2575–2576. doi: 10.1093/bioinformatics/btx204

Dela Peña, L., Tejada, A. J. P., Quijano, J. B., Alonzo, K. H., Gernato, E. G., Caril, A., et al. (2021). Diversity of marine eukaryotic Picophytoplankton communities with emphasis on Mamiellophyceae in northwestern Philippines. *Philipp. J. Sci.* 150, 27–42. doi: 10.56899/150.01.03

Delmont, T. O., and Eren, A. M. (2016). Identifying contamination with advanced visualization and analysis practices: metagenomic approaches for eukaryotic genome assemblies. *PeerJ* 4:e1839. doi: 10.7717/peerj.1839

Delmont, T. O., Gaia, M., Hinsinger, D. D., Frémont, P., Vanni, C., Fernandez-Guerra, A., et al. (2022). Functional repertoire convergence of distantly related eukaryotic plankton lineages abundant in the sunlit ocean. *Cell Genomics* 2:100123. doi: 10.1016/j.xgen.2022.100123

Demir-Hilton, E., Sudek, S., Cuvelier, M. L., Gentemann, C. L., Zehr, J. P., and Worden, A. Z. (2011). Global distribution patterns of distinct clades of the photosynthetic picoeukaryote *Ostreococcus*. *ISME J.* 5, 1095–1107. doi: 10.1038/ismej.2010.209

Derelle, E., Ferraz, C., Rombauts, S., Rouzé, P., Worden, A. Z., Robbens, S., et al. (2006). Genome analysis of the smallest free-living eukaryote *Ostreococcus tauri* unveils

many unique features. *Proc. Natl. Acad. Sci.* 103, 11647–11652. doi: 10.1073/pnas.0604795103

Dobin, A., Davis, C. A., Schlesinger, F., Drenkow, J., Zaleski, C., Jha, S., et al. (2013). STAR: ultrafast universal RNA-seq aligner. *Bioinforma. Oxf. Engl.* 29, 15–21. doi: 10.1093/bioinformatics/bts635

Eddy, S. R. (2011). Accelerated profile HMM searches. *PLoS Comput. Biol.* 7:e1002195. doi: 10.1371/journal.pcbi.1002195

Eikrem, W., and Throndsen, J. (1990). The ultrastructure of *Bathycoccus* gen. Nov. and *B. Prasinos* sp. nov., a non-motile picoplanktonic alga (Chlorophyta, Prasinophyceae) from the Mediterranean and Atlantic. *Phycologia* 29, 344–350. doi: 10.2216/i0031-8884-29-3-344.1

Emms, D. M., and Kelly, S. (2019). OrthoFinder: phylogenetic orthology inference for comparative genomics. *Genome Biol.* 20:238. doi: 10.1186/s13059-019-1832-y

Eren, A. M., Esen, Ö. C., Quince, C., Vineis, J. H., Morrison, H. G., Sogin, M. L., et al. (2015). Anvi'o: an advanced analysis and visualization platform for 'omics data. *PeerJ* 3:e1319. doi: 10.7717/peerj.1319

Flynn, J. M., Hubley, R., Goubert, C., Rosen, J., Clark, A. G., Feschotte, C., et al. (2020). Repeat modeler 2 for automated genomic discovery of transposable element families. *Proc. Natl. Acad. Sci.* 117, 9451–9457. doi: 10.1073/pnas.1921046117

Foulon, E., Not, F., Jalabert, F., Cariou, T., Massana, R., and Simon, N. (2008). Ecological niche partitioning in the picoplanktonic green alga *Micromonas pusilla*: evidence from environmental surveys using phylogenetic probes. *Environ. Microbiol.* 10, 2433–2443. doi: 10.1111/j.1462-2920.2008.01673.x

Gendron, P., Lemieux, S., and Major, F. (2001). Quantitative analysis of nucleic acid three-dimensional structures. *J. Mol. Biol.* 308, 919–936. doi: 10.1006/jmbi.2001.4626

Ghurye, J., Rhie, A., Walenz, B. P., Schmitt, A., Selvaraj, S., Pop, M., et al. (2019). Integrating hi-C links with assembly graphs for chromosome-scale assembly. *PLoS Comput. Biol.* 15:e1007273. doi: 10.1371/journal.pcbi.1007273

Grimsley, N., Yau, S., Piganeau, G., and Moreau, H. (2015). *Typical features of genomes in the Mamiellophyceae*. Tokyo: Springer Japan.

Guillard, R. R. L., and Hargraves, P. E. (1993). *Stichochrysis immobilis* is a diatom, not a chrysophyte. *Phycologia* 32, 234–236. doi: 10.2216/i0031-8884-32-3-234.1

Haas, B. J. (2023). Trans decoder. Available at: https://github.com/TransDecoder/TransDecoder (accessed October 3, 2023).

Haas, B. J., Salzberg, S. L., Zhu, W., Pertea, M., Allen, J. E., Orvis, J., et al. (2008). Automated eukaryotic gene structure annotation using EVidenceModeler and the program to assemble spliced alignments. *Genome Biol.* 9:R7. doi: 10.1186/gb-2008-9-1-r7

Hadziavdic, K., Lekang, K., Lanzen, A., Jonassen, I., Thompson, E. M., and Troedsson, C. (2014). Characterization of the 18S rRNA gene for designing universal eukaryote specific primers. *PLoS One* 9:e87624. doi: 10.1371/journal.pone.0087624

Hershkovitz, M. A., and Lewis, L. A. (1996). Deep-level diagnostic value of the rDNA-ITS region. *Mol. Biol. Evol.* 13, 1276–1295. doi: 10.1093/oxfordjournals.molbev.a025693

Hu, Y. O. O., Karlson, B., Charvet, S., and Andersson, A. F. (2016). Diversity of Pico- to Mesoplankton along the 2000 km salinity gradient of the Baltic Sea. *Front. Microbiol.* 7:679. doi: 10.3389/fmicb.2016.00679

Huerta-Cepas, J., Szklarczyk, D., Heller, D., Hernández-Plaza, A., Forslund, S. K., Cook, H., et al. (2019). eggNOG 5.0: a hierarchical, functionally and phylogenetically annotated orthology resource based on 5090 organisms and 2502 viruses. *Nucleic Acids Res.* 47, D309–D314. doi: 10.1093/nar/gky1085

Jahn, M. T., Schmidt, K., and Mock, T. (2014). A novel cost effective and high-throughput isolation and identification method for marine microalgae. *Plant Methods* 10:26. doi: 10.1186/1746-4811-10-26

Jancek, S., Gourbière, S., Moreau, H., and Piganeau, G. (2008). Clues about the genetic basis of adaptation emerge from comparing the proteomes of two *Ostreococcus* ecotypes (Chlorophyta, Prasinophyceae). *Mol. Biol. Evol.* 25, 2293–2300. doi: 10.1093/molbev/msn168

Joli, N., Monier, A., Logares, R., and Lovejoy, C. (2017). Seasonal patterns in Arctic prasinophytes and inferred ecology of *Bathycoccus* unveiled in an Arctic winter metagenome. *ISME J.* 11, 1372–1385. doi: 10.1038/ismej.2017.7

Katoh, K., and Standley, D. M. (2013). MAFFT multiple sequence alignment software version 7: improvements in performance and usability. *Mol. Biol. Evol.* 30, 772–780. doi: 10.1093/molbev/mst010

Keller, O., Kollmar, M., Stanke, M., and Waack, S. (2011). A novel hybrid gene prediction method employing protein multiple sequence alignments. *Bioinformatics* 27, 757–763. doi: 10.1093/bioinformatics/btr010

Kopylova, E., Noé, L., and Touzet, H. (2012). SortMeRNA: fast and accurate filtering of ribosomal RNAs in metatranscriptomic data. *Bioinformatics* 28, 3211–3217. doi: 10.1093/bioinformatics/bts611

Kuroiwa, T., Nozaki, H., Matsuzaki, M., Misumi, O., and Kuroiwa, H. (2004). Does cell size depend on the nuclear genome size in ultra-small algae such as *Cyanidioschyzon merolae* and *Ostreococcus tauri*? *Cytologia (Tokyo)* 69, 93–96. doi: 10.1508/cytologia.69.93

Lafontaine, D. L., Yang, L., Dekker, J., and Gibcus, J. H. (2021). Hi-C 3.0: improved protocol for genome-wide chromosome conformation capture. *Curr. Protoc.* 1:e198. doi: 10.1002/cpz1.198

Langmead, B., and Salzberg, S. L. (2012). Fast gapped-read alignment with bowtie 2. *Nat. Methods* 9, 357–359. doi: 10.1038/nmeth.1923

Leconte, J., Benites, L. F., Vannier, T., Wincker, P., Piganeau, G., and Jaillon, O. (2020). Genome resolved biogeography of Mamiellales. *Genes* 11:66. doi: 10.3390/genes11010066

Lemoine, F., and Gascuel, O. (2021). Gotree/Goalign: toolkit and go API to facilitate the development of phylogenetic workflows. *NAR Genomics Bioinforma.* 3:lqab 075. doi: 10.1093/nargab/lqab075

Letunic, I., and Bork, P. (2021). Interactive tree of life (iTOL) v5: an online tool for phylogenetic tree display and annotation. *Nucleic Acids Res.* 49, W293–W296. doi: 10.1093/nar/gkab301

Li, H., and Durbin, R. (2009). Fast and accurate short read alignment with burrows–wheeler transform. *Bioinformatics* 25, 1754–1760. doi: 10.1093/bioinformatics/btp324

Li, L., Wang, S., Wang, H., Sahu, S. K., Marin, B., Li, H., et al. (2020). The genome of *Prasinoderma coloniale* unveils the existence of a third phylum within green plants. *Nat. Ecol. Evol.* 4, 1220–1231. doi: 10.1038/s41559-020-1221-7

Lin, Y.-C., Chiang, K.-P., and Kang, L.-K. (2017a). Community composition of picoeukaryotes in the South China Sea during winter. *Cont. Shelf Res.* 143, 91–100. doi: 10.1016/j.csr.2017.04.009

Lin, Y.-C., Chin, C.-P., Chen, W.-T., Huang, C.-T., Gong, G.-C., Chiang, K.-P., et al. (2022). The spatial variation in chlorophyte community composition from coastal to offshore waters in a subtropical continental shelf system. *Front. Mar. Sci.* 9:865081. doi: 10.3389/fmars.2022.865081

Lin, Y.-C., Chung, C.-C., Chen, L.-Y., Gong, G.-C., Huang, C.-Y., and Chiang, K.-P. (2017b). Community composition of photosynthetic Picoeukaryotes in a subtropical coastal ecosystem, with particular emphasis on *Micromonas*. *J. Eukaryot. Microbiol.* 64, 349–359. doi: 10.1111/jeu.12370

Lin, L., Gu, H., Luo, Z., and Wang, N. (2021). Size-dependent spatio-temporal dynamics of eukaryotic plankton community near nuclear power plant in Beibu gulf, China. *J. Oceanol. Limnol.* 39, 1910–1925. doi: 10.1007/s00343-020-0248-6

Lopes dos Santos, A., Gourvil, P., Tragin, M., Noël, M.-H., Decelle, J., Romac, S., et al. (2017). Diversity and oceanic distribution of prasinophytes clade VII, the dominant group of green algae in oceanic waters. *ISME J.* 11, 512–528. doi: 10.1038/ismej.2016.120

Lovejoy, C., Vincent, W. F., Bonilla, S., Roy, S., Martineau, M.-J., Terrado, R., et al. (2007). Distribution, phylogeny, and growth of cold-adapted Picoprasinophytes in Arctic seas. *J. Phycol.* 43, 78–89. doi: 10.1111/j.1529-8817.2006.00310.x

Lukashin, A. V., and Borodovsky, M. (1998). Gene mark. Hmm: new solutions for gene finding. *Nucleic Acids Res.* 26, 1107–1115. doi: 10.1093/nar/26.4.1107

Mai, J. C., and Coleman, A. W. (1997). The internal transcribed spacer 2 exhibits a common secondary structure in Green algae and flowering plants. *J. Mol. Evol.* 44, 258–271. doi: 10.1007/PL00006143

Malfertheiner, L., Martínez-Pérez, C., Zhao, Z., Herndl, G. J., and Baltar, F. (2022). Phylogeny and metabolic potential of the candidate phylum SAR324. *Biology* 11:599. doi: 10.3390/biology11040599

Manton, I., and Parke, M. (1960). Further observations on small green flagellates with special reference to possible relatives of *Chromulina pusilla* butcher. *J. Mar. Biol. Assoc. U. K.* 39, 275–298. doi: 10.1017/S0025315400013321

Marchant, H. J., Buck, K. R., Garrison, D. L., and Thomsen, H. A. (1989). *Mantoniella* in Antarctic waters including the description of *M. antarctica* sp. nov. (Prasinophyceae). *J. Phycol.* 25, 167–174. doi: 10.1111/j.0022-3646.1989.00167.x

Marin, B., and Melkonian, M. (2010). Molecular phylogeny and classification of the Mamiellophyceae class. Nov. (Chlorophyta) based on sequence comparisons of the nuclear- and plastid-encoded rRNA operons. *Protist* 161, 304–336. doi: 10.1016/j.protis.2009.10.002

Mathieu-Rivet, E., Mati-Baouche, N., Walet-Balieu, M.-L., Lerouge, P., and Bardor, M. (2020). N- and O-glycosylation pathways in the microalgae polyphyletic group. *Front. Plant Sci.* 11:609993. doi: 10.3389/fpls.2020.609993

Mendes, F. K., Vanderpool, D., Fulton, B., and Hahn, M. W. (2021). CAFE 5 models variation in evolutionary rates among gene families. *Bioinformatics* 36, 5516–5518. doi: 10.1093/bioinformatics/btaa1022

Merget, B., Koetschan, C., Hackl, T., Förster, F., Dandekar, T., Müller, T., et al. (2012). The ITS2 database. *J. Vis. Exp. JoVE* 61:3806. doi: 10.3791/3806

Mistry, J., Chuguransky, S., Williams, L., Qureshi, M., Salazar, G. A., Sonnhammer, E. L. L., et al. (2021). Pfam: the protein families database in 2021. *Nucleic Acids Res.* 49, D412–D419. doi: 10.1093/nar/gkaa913

Monier, A., Worden, A. Z., and Richards, T. A. (2016). Phylogenetic diversity and biogeography of the Mamiellophyceae lineage of eukaryotic phytoplankton across the oceans. *Environ. Microbiol. Rep.* 8, 461–469. doi: 10.1111/1758-2229.12390

Moreau, H., Verhelst, B., Couloux, A., Derelle, E., Rombauts, S., Grimsley, N., et al. (2012). Gene functionalities and genome structure in *Bathycoccus prasinos* reflect cellular specializations at the base of the green lineage. *Genome Biol.* 13:R74. doi: 10.1186/gb-2012-13-8-r74

Nguyen, L.-T., Schmidt, H. A., Haeseler, A., and Minh, B. Q. (2015). IQ-TREE: a fast and effective stochastic algorithm for estimating maximum-likelihood phylogenies. *Mol. Biol. Evol.* 32, 268–274. doi: 10.1093/molbev/msu300

Palenik, B., Grimwood, J., Aerts, A., Rouzé, P., Salamov, A., Putnam, N., et al. (2007). The tiny eukaryote *Ostreococcus* provides genomic insights into the paradox of plankton speciation. *Proc. Natl. Acad. Sci.* 104, 7705–7710. doi: 10.1073/pnas.0611046104

Piganeau, G., Eyre-Walker, A., Grimsley, N., and Moreau, H. (2011a). How and why DNA barcodes underestimate the diversity of microbial eukaryotes. *PLoS One* 6:e16342. doi: 10.1371/journal.pone.0016342

Piganeau, G., Grimsley, N., and Moreau, H. (2011b). Genome diversity in the smallest marine photosynthetic eukaryotes. *Res. Microbiol. Genome Organ. Eukaryot. Microbes* 162, 570–577. doi: 10.1016/j.resmic.2011.04.005

Raven, J. A., and Beardall, J. (2003). "Carbohydrate metabolism and respiration in algae" in *Photosynthesis in algae*. eds. A. W. D. Larkum, S. E. Douglas and J. A. Raven (Dordrecht: Springer Netherlands).

Richards, E. J., and Ausubel, F. M. (1988). Isolation of a higher eukaryotic telomere from *Arabidopsis thaliana*. *Cell* 53, 127–136. doi: 10.1016/0092-8674(88)90494-1

Ronquist, F., Teslenko, M., Mark, P., Ayres, D. L., Darling, A., Höhna, S., et al. (2012). MrBayes 3.2: efficient Bayesian phylogenetic inference and model choice across a large model space. *Syst. Biol.* 61, 539–542. doi: 10.1093/sysbio/sys029

Saulnier, D., De Decker, S., and Haffner, P. (2009). Real-time PCR assay for rapid detection and quantification of *Vibrio aestuarianus* in oyster and seawater: a useful tool for epidemiologic studies. *J. Microbiol. Methods* 77, 191–197. doi: 10.1016/j.mimet.2009.01.021

Schauer, R., and Kamerling, J. P. (2018). "Chapter One-Exploration of the sialic acid world," in *Advances in carbohydrate chemistry and biochemistry*, ed. D. C. Baker (Academic Press Cambridge)

Schloerke, B., Cook, D., Larmarange, J., Briatte, F., Marbach, M., Thoen, E., et al. (2018). *GGally: Extension to "ggplot2."*. Geneva: Zenodo.

Schultz, J., Maisel, S., Gerlach, D., Müller, T., and Wolf, M. (2005). A common core of secondary structure of the internal transcribed spacer 2 (ITS2) throughout the Eukaryota. *RNA N. Y. N* 11, 361–364. doi: 10.1261/rna.7204505

Seibel, P. N., Müller, T., Dandekar, T., Schultz, J., and Wolf, M. (2006). 4SALE – a tool for synchronous RNA sequence and secondary structure alignment and editing. *BMC Bioinform.* 7:498. doi: 10.1186/1471-2105-7-498

Simão, F. A., Waterhouse, R. M., Ioannidis, P., Kriventseva, E. V., and Zdobnov, E. M. (2015). BUSCO: assessing genome assembly and annotation completeness with single-copy orthologs. *Bioinforma. Oxf. Engl.* 31, 3210–3212. doi: 10.1093/bioinformatics/btv351

Simmons, M. P., Sebastian, S., Adam, M., Alexander, J. L., Valeria, J., Christopher, R. P., et al. (2016). Abundance and biogeography of Picoprasinophyte ecotypes and other phytoplankton in the eastern North Pacific Ocean. *Appl. Environ. Microbiol.* 82, 1693–1705. doi: 10.1128/AEM.02730-15

Simon, N., Foulon, E., Grulois, D., Six, C., Desdevises, Y., Latimier, M., et al. (2017). Revision of the Genus *Micromonas* Manton & Parke (Chlorophyta, Mamiellophyceae), of the type Species *M. pusilla* (butcher) Manton & Parke and of the Species *M. Commoda* van Baren, Bachy and Worden and description of two new species based on the genetic and phenotypic characterization of cultured isolates. *Protist* 168, 612–635. doi: 10.1016/j.protis.2017.09.002

Smit, A., Hubley, R., and Green, P. (2015). Repeat masker. Available at: http://www.repeatmasker.org (accessed October 3, 2023).

Stark, J. R., Cardon, Z. G., and Peredo, E. L. (2020). Extraction of high-quality, high-molecular-weight DNA depends heavily on cell homogenization methods in green microalgae. *Appl. Plant Sci.* 8:e11333. doi: 10.1002/aps3.11333

Subirana, L., Péquin, B., Michely, S., Escande, M.-L., Meilland, J., Derelle, E., et al. (2013). Morphology, genome plasticity, and phylogeny in the genus *Ostreococcus* reveal a cryptic species, *O. mediterraneus* sp. nov. (Mamiellales, Mamiellophyceae). *Protist* 164, 643–659. doi: 10.1016/j.protis.2013.06.002

Tatusov, R. L., Koonin, E. V., and Lipman, D. J. (1997). A genomic perspective on protein families. *Science* 278, 631–637. doi: 10.1126/science.278.5338.631

Tragin, M., and Vaulot, D. (2018). Green microalgae in marine coastal waters: the ocean sampling day (OSD) dataset. *Sci. Rep.* 8:14020. doi: 10.1038/s41598-018-32338-w

Tragin, M., and Vaulot, D. (2019). Novel diversity within marine Mamiellophyceae (Chlorophyta) unveiled by metabarcoding. *Sci. Rep.* 9:5190. doi: 10.1038/s41598-019-41680-6

van Baren, M. J., Bachy, C., Reistetter, E. N., Purvine, S. O., Grimwood, J., Sudek, S., et al. (2016). Evidence-based green algal genomics reveals marine diversity and ancestral characteristics of land plants. *BMC Genomics* 17:267. doi: 10.1186/s12864-016-2585-6

Walker, B. J., Abeel, T., Shea, T., Priest, M., Abouelliel, A., Sakthikumar, S., et al. (2014). Pilon: an integrated tool for comprehensive microbial variant detection and genome assembly improvement. *Plo S One* 9:e112963. doi: 10.1371/journal.pone.0112963

Wang, Y., Tang, H., DeBarry, J. D., Tan, X., Li, J., Wang, X., et al. (2012). MCScanX: a toolkit for detection and evolutionary analysis of gene synteny and collinearity. *Nucleic Acids Res.* 40:e49. doi: 10.1093/nar/gkr1293

Wang, F., Xie, Y., Wu, W., Sun, P., Wang, L., and Huang, B. (2019). Picoeukaryotic diversity and activity in the northwestern Pacific Ocean based on rDNA and rRNA high-throughput sequencing. *Front. Microbiol.* 9:3259. doi: 10.3389/fmicb.2018.03259

Wickham, H. (2006). An introduction to ggplot: an implementation of the grammar of graphics in R. Statistics. Available at: https://citeseerx.ist.psu.edu/document?repid=rep1&type=pdf&doi=7f3e2207d2ef8fc0cee74069879c8adf35303a91 (accessed October 3, 2023).

Worden, A. Z., Lee, J.-H., Mock, T., Rouzé, P., Simmons, M. P., Aerts, A. L., et al. (2009). Green evolution and dynamic adaptations revealed by genomes of the marine picoeukaryotes *Micromonas*. *Science* 324, 268–272. doi: 10.1126/science.1167222

Wu, W., Huang, B., and Zhong, C. (2014). Photosynthetic picoeukaryote assemblages in the South China Sea from the Pearl River estuary to the SEATS station. *Aquat. Microb. Ecol.* 71, 271–284. doi: 10.3354/ame01681

Xu, Y., Wang, H., Sahu, S. K., Li, L., Liang, H., Günther, G., et al. (2022). Chromosome-level genome of *Pedinomonas minor* (Chlorophyta) unveils adaptations to abiotic stress in a rapidly fluctuating environment. *New Phytol.* 235, 1409–1425. doi: 10.1111/nph.18220

Xu, X., Yu, Z., Cheng, F., He, L., Cao, X., and Song, X. (2017). Molecular diversity and ecological characteristics of the eukaryotic phytoplankton community in the coastal waters of the Bohai Sea, China. *Harmful Algae* 61, 13–22. doi: 10.1016/j.hal.2016.11.005

Yau, S., Krasovec, M., Benites, L. F., Rombauts, S., Groussin, M., Vancaester, E., et al. (2020a). Virus-host coexistence in phytoplankton through the genomic lens. *Sci. Adv.* 6:eaay2587. doi: 10.1126/sciadv.aay2587

Yau, S., Santos, A. L., Eikrem, W., Ribeiro, C. G., Gourvil, P., Balzano, S., et al. (2020b). *Mantoniella beaufortii* and *Mantoniella baffinensis* sp. nov. (Mamiellales, Mamiellophyceae), two new green algal species from the high Arctic. *J. Phycol.* 56, 37–51. doi: 10.1111/jpy.12932

Yu, G., and Yu, M. G. (2018). Package "scatterpie." Available at: cran.r-project.org/web/packages/scatterpie/ (accessed October 3, 2023).

Yung, C. C. M., Rey Redondo, E., Sanchez, F., Yau, S., and Piganeau, G. (2022). Diversity and evolution of Mamiellophyceae: early-diverging Phytoplanktonic Green algae containing many cosmopolitan species. *J. Mar. Sci. Eng.* 10:240. doi: 10.3390/jmse10020240

Zhou, X. (2022). Comparative genomics analysis 3: Specific node gene family enrichment analysis (non-model species GO/KEGG enrichment analysis). Available at: https://www.jianshu.com/p/6671f3189309 (accessed October 30, 2023).

Zimin, A. V., Marçais, G., Puiu, D., Roberts, M., Salzberg, S. L., and Yorke, J. A. (2013). The MaSuRCA genome assembler. *Bioinformatics* 29, 2669–2677. doi: 10.1093/bioinformatics/btt476

Zimin, A., and Salzberg, S. (2020). The genome polishing tool POLCA makes fast and accurate corrections in genome assemblies. *PLoS Comput. Biol.* 16:e1007981. doi: 10.1371/journal.pcbi.1007981

frontiers | Frontiers in Marine Science

TYPE Original Research
PUBLISHED 08 May 2024
DOI 10.3389/fmars.2024.1374946

OPEN ACCESS

EDITED BY
Michael Rappe,
University of Hawaii at Manoa, United States

REVIEWED BY
Myrsini Chronopoulou,
Conidia Bioscience Ltd, United Kingdom
Xia Zhang,
Chinese Academy of Sciences (CAS), China

*CORRESPONDENCE
Luke DA. Walker
luke.walker3@hdr.mq.edu,.au

RECEIVED 23 January 2024
ACCEPTED 28 March 2024
PUBLISHED 08 May 2024

CITATION
Walker LD, Gribben PE, Glasby TM, Marzinelli EM, Varkey DR and Dafforn KA (2024) Above and below-ground bacterial communities shift in seagrass beds with warmer temperatures.
Front. Mar. Sci. 11:1374946.
doi: 10.3389/fmars.2024.1374946

Above and below-ground bacterial communities shift in seagrass beds with warmer temperatures

Luke DA. Walker[1,2,3]*, Paul E. Gribben[2], Tim M. Glasby[2,4], Ezequiel M. Marzinelli[3], Deepa R. Varkey[1,5] and Katherine A. Dafforn[1]

[1]School of Natural Sciences, Macquarie University, Sydney, NSW, Australia, [2]Centre for Marine Science and Innovation, School of Biological, Earth and Environmental Science, University of New South Wales, Sydney, NSW, Australia, [3]School of Life and Environmental Sciences, The University of Sydney, Sydney, NSW, Australia, [4]NSW Department of Primary Industries, Port Stephens Fisheries Institute, Taylors Beach, NSW, Australia, [5]The Australian Institute of Marine Science, Townsville, QLD, Australia

Current rates of ocean warming are predicted to exacerbate ongoing declines in seagrass populations. Above-ground responses of seagrass to increasing temperatures have been studied from a direct physiological perspective while indirect effects, including changes to microbially-mediated below-ground processes, remain poorly understood. To test potential effects of increased temperature on seagrass growth and associated microbial communities, we sampled seagrass beds experiencing ambient and elevated water temperatures at Lake Macquarie, Australia. Sites with warmer water were associated with a plume from a power station discharge channel with temperatures analogous to conditions predicted by 2100 under current rates of ocean warming (+3°C). The microbial community composition in both sediments and leaf tissues varied significantly between warm and ambient water temperatures with higher relative abundances of putative sulphate-reducing bacteria such as *Desulfocapsaceae, Desulfobulbaceae* and *Desulfosarcinaceae* in sedimentary communities in warm water. Above-ground biomass and seagrass growth rates were greater at warm sites while below-ground biomass and detrital decomposition rates showed no difference suggesting potential buffering of temperature effects below-ground. These findings suggest a 3°C rise in temperate regions is unlikely to induce mortality in seagrass however, it may shift microbial communities towards more homogenous structure and composition.

KEYWORDS

microbial community, foundation species, sediment, climate change, bacteria, microbiome, *Zostera muelleri*

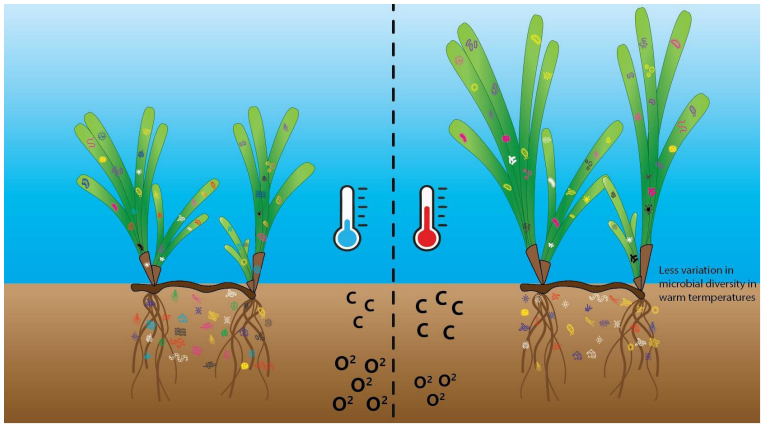

GRAPHICAL ABSTRACT

1 Introduction

The world's oceans have been warming by approximately 0.13°C decade^{-1} over the past 100 years, with mean global ocean temperatures predicted to rise 1-4°C by 2100 (Howes et al., 2015) Temperatures in shallow estuaries that have restricted water exchange with the ocean appear to be rising at a greater rate than oceanic waters, e.g. 2.16°C over the last 12 years in New South Wales, Australia (Scanes et al., 2020). This rise in temperature is having negative effects on marine and estuarine habitats including macrophytes such as seagrasses (Chefaoui et al., 2018; Babcock et al., 2019). Although slight temperature increases can in some cases enhance seagrass growth rates, once a species' thermal threshold is reached, there can be negative impacts (York et al., 2013; Anton et al., 2020; Nguyen et al., 2021). For example, prolonged marine heatwaves up to 3°C above ambient have caused seagrass mortality in temperate and subtropical regions (Marba and Duarte, 2010; Thomson et al., 2015; Serrano et al., 2021; Jung et al., 2023). While responses of some seagrasses to temperature changes have been well studied, the response of microbes and the role they play in ameliorating these environmental stressors has rarely been investigated (Garcias-Bonet et al., 2016; Fuggle et al., 2023).

Seagrasses host a wide variety of microorganisms on their leaves, rhizomes, roots, and in surrounding sediments (Weidner et al., 2000; Uku et al., 2007; Garcias-Bonet et al., 2016). Below-ground microbial processes in the plant rhizosphere govern much of the above-ground attributes of plants (Gribben et al., 2017; Wardle et al., 2004; Lugtenberg and Kamilova, 2009). Microbes can also influence growth, health, and productivity of seagrasses, and thus underpin ecosystem services such as nursery habitat, carbon sequestration, and coastal protection provided by seagrasses (Ugarelli et al., 2017; Brodersen et al., 2018). Microbes can have negative effects on plant performance through parasitism, resource competition, and pathogenesis, however, many microbes in the same physical niche can benefit host plant performance through nutrient acquisition and hormone production (Hansen et al., 2000; Mendes et al., 2013; Tarquinio et al., 2019; Tarquinio et al., 2019; Fuggle et al., 2023). Environmental stressors such as warming temperatures may disturb microbes above and below-ground which could in turn have serious implications for seagrass function (Seymour et al., 2018). Therefore, understanding how below-ground processes and microbial communities interact within seagrass meadows may be critical to our understanding of sediment function and important for the resilience and conservation of seagrasses under multiple environmental stressors.

While microbes associated with seagrass leaves, rhizosphere (i.e. root structure and sediment particles in-between and in close contact with the roots), and surrounding sediments all play important roles in the health and functioning of seagrasses, the microbes which occupy the rhizosphere and sediments in seagrass meadows are considered to be the most vital as they can influence below-ground processes in seagrass meadows (Gribben et al., 2017; Brodersen et al., 2018; Gribben et al., 2018; Martin et al., 2020). Seagrasses, commonly thrive in anoxic sediments because they can transport oxygen from their leaves to their rhizosphere (Borum et al., 2007) and their root-associated microbes can oxidise toxic sulphides (Martin et al., 2020). Further, microbes, both above and below-ground, in seagrass meadows can alter biogeochemical processes and maximise the positive metabolic responses required for seagrass to survive under stress (Lehnen et al., 2016; Crump et al., 2018). For example, bacteria provide a mechanism for sulphide oxidation, ammonium production, nitrogen fixation, and absorption of nutrients within seagrasses (Hemminga et al., 1991; Hansen et al., 2000; Cifuentes et al., 2003). In this example, seagrasses provide habitat and energy sources to hosted microbial assemblages through the exudation of nutrients while the microbes are benefiting from protection from environmental stressors (Kirchman et al., 1984; Holmer et al., 2006; Ugarelli et al., 2017). Changes in microbial communities can result in seagrasses becoming more susceptible to disease, environmental change, and competition with invasive species (Gribben et al., 2018; Tarquinio et al., 2019; Fuggle et al., 2023).

Interactions between seagrasses and their associated microbes have garnered increasing attention but little is known about the

effects of temperature on seagrass microbes and the consequences for ecosystem functions (Seymour et al., 2018). It is possible that increased water temperature will have the greatest impact on above-ground components (e.g., leaf tissue production) and processes (e.g., photosynthesis and nutrient cycling) because of direct exposure in the water column, while below-ground components may be buffered by the limited water exchange between water column and sediment bed (York et al., 2013; Sawall et al., 2021; Marbà et al., 2022).

Generally, increases in temperature lead to increases in microbial metabolism and growth, until temperatures exceed the optimal thermal range of the microbes (Pendall et al., 2004; von Lützow and Kögel-Knabner, 2009). Different species of microbes have different functions and different thermal tolerances. For example, in plant-microbial interactions, when temperatures exceed the optimal range, above-ground microbes have fewer beneficial effects on plants and can have detrimental effects, such as increased physiological costs (i.e., respiration rates) (O'Brien et al., 2020). Seagrasses can release organic compounds and exudates into the surrounding sediment, which can attract and support different microbes (Mohapatra et al., 2022). This can occur through a variety of mechanisms, including competition for resources, adaptation to environmental conditions, and interactions with other members of the microbial community (Cúcio et al., 2016; Lin et al., 2021). When certain microbial species are favoured or selected over others in a particular environment this is known as selection. As some proportion of microbial composition is selected by environmental conditions (Zhang et al., 2020), we predict that elevated temperatures may reduce variation in diversity of above and below-ground microbial communities because some thermal tolerances will be exceeded, leading to selection of a more consistent group of microbes with similar environmental functions.

The aim of this study was to investigate changes in above and below-ground microbial communities, and seagrass productivity in meadows of the seagrass *Zostera muelleri* subsp. *capricorni* (Asch.) (Hereafter referred to as *Z. muelleri*) in response to consistently elevated water temperatures (+ 3°C above ambient; ambient: 18°C in winter to 26°C in summer; warm: maximum 30°C in summer) created by a coal-fired power station. Specifically, this study determined differences in above- (seagrass leaf biomass and growth rates) and below-ground processes (root and rhizome biomass and detrital decomposition rates) and microbial communities between ambient water temperatures and elevated water temperatures. *Z. muelleri* was selected as the target species of the study because it has a wide geographical range across temperate and tropical coastal regions in the southern hemisphere (Short et al., 2007) and is susceptible to stressors associated with climate change, particularly temperature (Valle et al., 2014; Lefcheck et al., 2017). Finally, this study also examined which above and below-ground abiotic variables, independent of temperature (e.g., sediment properties and water quality), accounted for differences in seagrass productivity, detrital decomposition, and above and below-ground bacterial communities.

We hypothesised that the warm conditions would enhance seagrass productivity given the thermal optimum for *Z. muelleri* is ~27°C with negative effects not apparent until 32°C (York et al., 2013). We also predicted that detrital decomposition would be greater at warm sites because decomposition in typical anoxic sediments occurs via microbial mediation which can increase with warming temperatures (Trevathan-Tackett et al., 2017). Due to the temperature sensitive nature of many bacteria, we also predicted differences in composition of both leaf tissue and sedimentary bacterial communities between warm and ambient sites. Specifically, we predicted a reduction in variation between bacterial community assemblages in warm sites both above and below-ground in accordance with the stress gradient hypothesis which suggests that communities may tend towards higher homogeneity in stressful environmental conditions (Bertness and Callaway, 1994).

2 Methods

2.1 Survey location and sampling design

We used a thermal plume in Lake Macquarie (NSW, Australia) as analogue to future estuarine conditions under current rates of warming. Lake Macquarie is one of the largest saltwater coastal lakes in Australia, which has predominantly urbanised catchments. Lake Macquarie is a wave dominated estuary with a restricted permanent opening to the Pacific Ocean to the east, which results in limited water exchange and < 0.1 m tidal variation (Ingleton and McMinn, 2012) and freshwater inputs from Wyee Creek, Dora Creek, and Cockle Creek to the south, west and north respectively. The plume enters Myuna Bay on the western shoreline of Lake Macquarie where estuarine water used to cool Australia's largest power station has been discharged into the lake since 1980's (Figure 1).

Field surveys of *Z. muelleri* seagrass beds were conducted across seven sites (three warm and four ambient) in Lake Macquarie (Figure 1). The study sites located within this warm plume experienced an increase in water temperature of 2- 4°C above ambient (Ingleton and McMinn, 2012). Temperatures in this warm plume are analogous to IPCC predictions for global ocean temperature increases by the end of the century (Howes et al., 2015), thus it is an ideal system for investigating seagrass response to elevated water temperatures under current warming scenarios. All study sites were located on the western side of the lake at a minimum distance of 750 m apart (straight line) and were selected based on temperature profiles from previous studies (Glasby unpublished data). All sites were between 0.5-1 m water depth with large beds (extending >100 m from the shore) of *Z. muelleri.*

All sampling was conducted in the Austral summer during September 2020 and January 2021 (Supplementary Table 1). September sampling included: surveys of water and sediment quality, seagrass biomass, and the bacterial communities associated with seagrass sediments and seagrass leaf tissues while January sampling included seagrass growth rates and detrital decomposition rates. Each of these variables were collected from eight randomly selected plots (30 cm x 30 cm) at each site (total n = 56). Plots (30 cm x 30 cm) were ~2 m apart to maintain independent sampling. It is important to note the difference between warm and ambient temperatures did not change between sampling periods.

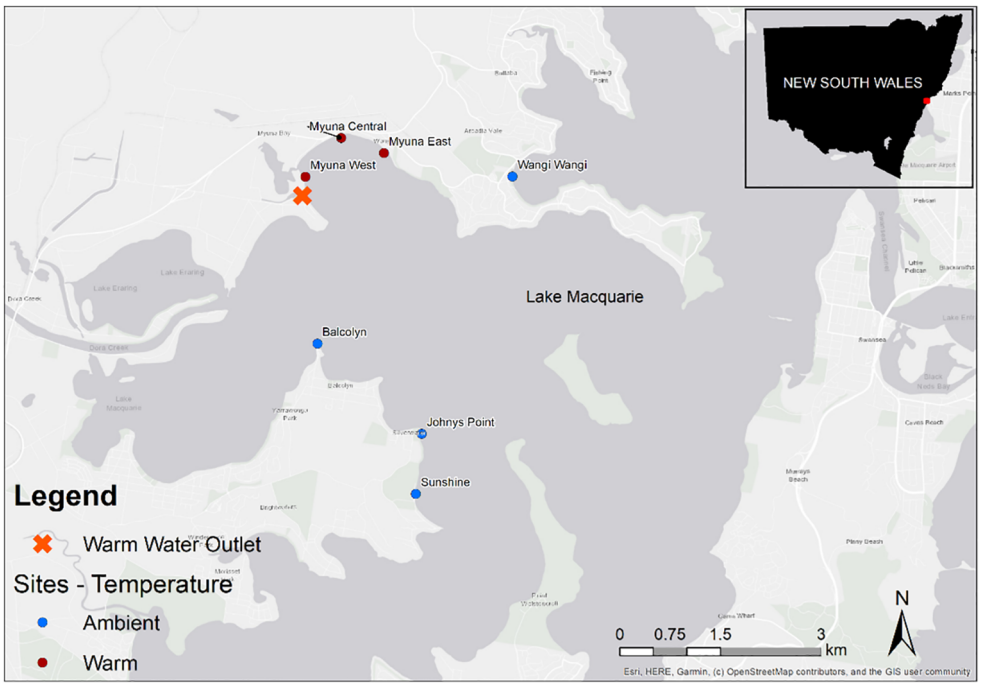

FIGURE 1
Location of study sites within Lake Macquarie, Australia. Orange cross represents the warm water outlet. Blue points represent ambient sites and brown points represent warm sites.

2.2 Environmental variables

2.2.1 Water and sediment variables

Temperature, dissolved oxygen (DO), pH and conductivity of the water were measured *in situ* at each site in September 2020 and January 2021 using a Multiparameter Water Quality Sonde (YSI, USA) deployed 0.5 m below the water surface and ~0.25 m above each replicate plot (n= 56).

Sediment pH and oxidation-reduction potential (ORP) were measured using an Orion Redox combination electrode (Thermo Fisher Scientific, USA) in each replicate plot. The probe was inserted into the sediments to a depth of 5-10 cm to sample around the seagrass rhizosphere and pH and ORP values recorded immediately (Marba et al., 2010).

Within each replicate plot, a 50 ml sediment core was collected from the top 10 cm of the seagrass bed for particle size analysis and to determine organic matter. Any visible organic matter (seagrass matter, shells, leaves, sticks etc.) and excess water was removed from the sample before storage on ice for transport to the laboratory where samples were frozen at -20°C.

2.2.2 Sediment analyses

To determine the particle size distribution at each site and to test for relationships with seagrass productivity and bacterial community measures, particle size analysis by laser diffractometry was conducted on all sediment samples following manufacturer's protocols with minor alterations (Malvern Instruments 2007). Firstly, a 30 g (wet weight) sediment sub-sample from each replicate plot was treated with hydrogen peroxide (30% H_2O_2) for at least 12 h to remove all organics. Sub-samples were stirred once for 30 s to ensure complete reaction with the hydrogen peroxide. Sub-samples were then centrifuged at 2,000 rpm for 5 min. Excess hydrogen peroxide was then removed by pouring off the top layer without losing any fine sediment particles. The remaining sediment was transferred into a new beaker. Sub-samples were then wet sieved with a 2 mm aperture sieve, transferred to a new beaker and mixed using a mechanical stirrer to ensure complete dispersion before a subsample was extracted using a pipette. Each subsample was measured in the Mastersizer 2000 laser diffraction particle size analyser (Malvern Instruments, UK) with particle refractive index of 1.54 and water refractive index of 1.33. Each sub-sample was analysed three times using a measurement time of 30 s. The average particle size distribution of the three runs was used as this is considered most representative of the true particle size distribution (Šinkovičová et al., 2017). Grain sizes were classified into two different categories: fines (0.01-62 µm) and sand (62.5-2000 µm).

Loss-on-ignition (LOI) was analysed with a Lindberg Blue box furnace to measure the organic matter (OM) of sediment sub-samples at each site and to observe relationships with seagrass productivity and bacterial community measures. Firstly, the sample was homogenised and ~3 g (wet weight) sediment was sub-sampled into a pre-weighed crucible. Sediments were then dried at 105°C for at least 12 h and weighed again to obtain dry weight. The crucible was then placed in the muffle furnace at 560°C for 12 h. The sample was then weighed immediately after being taken out of the furnace

to obtain ash dry weight. The weight before entering the furnace minus final weight equals the percentage of organic carbon loss on ignition (Wang and Wang, 2011).

2.3 Bacterial assemblage analysis

2.3.1 Above and below-ground bacterial assemblages

For assessing the above-ground microbial assemblages, seagrass leaf samples were collected aseptically from each replicate plot (same plots used for measuring seagrass biomass and environmental variables) by cutting 5-10 shoots at their base and placing them in a sterile 50 ml centrifuge tube. To assess below-ground bacterial assemblages, sediment samples were collected aseptically from each replicate plot by inserting a 50 ml centrifuge tube into the top 10 cm of sediment (the same depth as for sediment pH and ORP), ensuring minimal seagrass leaf fragments and infauna were collected. Samples were immediately put on ice and frozen at -80°C within 5 h of collection.

2.3.2 DNA extraction

For the leaf and sediment samples, genomic DNA was extracted from 0.25 g of plant tissue or sediment, using bead beating and chemical lysis with the DNeasy PowerSoil Pro Kit (QIAGEN, Germany) according to the manufacturer's standard instructions. DNA concentrations and potential contamination were evaluated using a Nanodrop-1000 spectrophotometer (Thermo Fisher Scientific, USA).

2.3.3 Bacterial community characterisation

To examine bacterial community composition, the 16S rRNA gene was amplified with the universal forward primer 27F (V1) (5′-AGAGTTTGATCMTGGCTCAG-3′) and the universal reverse primer 519R (V3) (5′-CGGTTACCTTGTTACGACTT-3′) (Weisburg et al., 1991). The V1-V3 region was polymerase chain reaction (PCR) amplified using 35 cycles at the temperatures of 94° C for 30 s, 55°C for 10 s and 72°C for 45 s. The resultant amplicons were visualised on 1% agarose gel with GelRed (1:10000). We included a positive and no template control in 60 PCR reactions.

Genomic DNA was used to prepare DNA libraries with the Illumina TruSeq DNA library preparation protocol. Sequencing was performed on the Illumina MiSeq platform at Ramaciotti Centre for Genomics (UNSW Sydney, Australia). All raw sequences and meta-data have been uploaded to NCBI Sequence Read Archive (SRA) under BioProject ID: PRJNA925291.

2.4 Seagrass productivity metrics and detrital decomposition rates

2.4.1 Above and below-ground biomass

Within each plot, a seagrass biomass sample was collected by inserting a PVC core (10 cm diameter) 15 cm into the sediments (Jacobs, 1979). The material collected above and below the sediment surface was rinsed with seawater in the field to remove excess sediment and placed in a Ziplock sample bag. All samples were placed on ice for transportation and stored at -20°C until processing.

All biomass samples were washed with tap water to remove all remaining mud, sand, shell grit and gravel. Above-ground seagrass biomass samples (all shoots and flowering shoots) were cut at the point where they intersected the rhizome (Jacobs, 1979). The separated above and below-ground materials were oven-dried at 60°C for at least 72 h to constant weight and then weighed to obtain total above and below-ground biomasses (dry weights). Total biomass was then calculated using the combined weight of the above and below-ground biomass values.

2.4.2 Growth rates

At each site, all *Z. muelleri* plants within three 5 x 5 cm plots (~2 m apart, depth 0.5-1 m) were marked using a pin prick method to assess growth rates. Specifically, two small holes were made in the sheath region of each shoot using a sharp probe to create two corresponding reference scars (Short and Duarte, 2001). One scar was on the sheath which does not grow, and the other on the leaf blades inside the sheath which continues to grow. All plants within each plot were resampled after 10-11 d using a trowel for collection and were placed on ice for transport and stored at 4°C until analysis.

Plants were rinsed in the laboratory to remove all sediment and the below-ground components of the plants were discarded leaving only the marked shoots. The entirety of each marked shoot was then cut at the bottom of each shoot's lowest corresponding reference scar and above the highest reference scar (Short and Duarte, 2001). The remaining plant tissue between the reference scars is the new growth which developed between the time of marking and time of sampling. The combined new leaf tissue for the five shoots was oven dried at 60°C for at least 72 h and weighed to obtain an average value of new growth per shoot per day between shoot marking and collection (Short and Duarte, 2001).

2.4.3 Detrital decomposition rates

A detrital decomposition experiment was conducted to examine the rate at which seagrass detritus decomposed within seagrass sediments. Three sample bags (~2 L each) of wet *Z. muelleri* detritus were collected from each site to prepare litter bags. All detritus was mixed and dried for at least 72 h at 60°C.

For the decomposition experiment, green, senescent *Z. muelleri* leaf detritus was added to 1.0 mm nylon mesh litter bags (whole leaf detritus ~10 g dry weight in 15 cm × 15 cm bag: nylon mesh from Allied Filter Fabrics Pty Ltd., NSW, Australia). Litter bags enable tracking of seagrass biomass loss and have been used previously in decomposition studies (Harrison, 1989; Mateo and Romero, 1996; Trevathan-Tackett et al., 2020b). To replicate natural decomposition conditions, litter bags were secured to the sediments using metal stakes. Three litter bags per site were secured 10-20 m from shore at a depth of 0.5-1 m, central to the meadow and left 13 - 14 d before being collected. Each bag was then washed thoroughly to remove any sediment from the bags taking care to ensure that no detrital matter was lost. Litter bags were then

dried in an oven at 60°C for at least 72 h and then the detritus was weighed. Dry weight after decomposition was then compared to dry weight before decomposition to determine the percentage of detritus that had decomposed.

2.5 Statistical analyses

2.5.1 Bioinformatics

FASTQ files were quality trimmed [maximum truncation lengths of 290 bps (forward) and 260 bps (reverse; maximum expected error of 2 (forward) and 6 (reverse)]. Sample inference was made using the core DADA2 denoising algorithm to reconstruct exact Amplicon Sequence Variants (ASVs) and filter rare ASVs and chimera sequences. After denoising, paired reads were merged to unique sequences and ASV taxonomic classifications were obtained using the SILVA reference database (v. 138). Quality of sampling and processing was also assessed through the calculation of Good's coverage and rarefaction curves. From this table, chimera removal was done through a consensus method and with a conservative approach (Callahan et al., 2016). Chloroplast, archaea and mitochondria were removed from the ASV table prior to statistical analysis. All steps of this pipeline were done using the dada2 package (Callahan et al., 2016) in R Studio (V.3.6 R Core Team 2017).

2.5.2 Bacterial community

ASVs from sedimentary and leaf tissue bacterial datasets were removed if their total abundance was <0.01% of the total dataset. Each dataset was then standardised for sequencing depth by dividing each cell by total reads per sample.

Sedimentary and leaf surface tissue bacterial community data were compared between temperature category (fixed, two levels: warm versus ambient) and sites (random, 3 levels for warm and 4 levels for ambient) using PERMANOVA (Anderson, 2005) in the PERMANOVA+ add-on for primer V7 (PRIMER-E, UK) (Clarke and Gorley, 2006). Bray–Curtis similarity matrices were generated using square root-transformed relative abundance (community structure) of ASVs or ASV presence/absence (community composition), using 999 permutations of residuals under a reduced model. Bacterial diversity within temperature categories (alpha diversity) was estimated using, Shannon and Chao1 diversity indices on rarefied ASV data.

PERMANOVA was also used to generate estimates of components of variation for fixed and random effects to compare the relative importance of each factor in explaining total variation in the model (Underwood and Chapman, 1996; Anderson, 2007). Multivariate patterns in bacterial assemblages were visualised using non-metric multidimensional scaling (nMDS) derived from Bray–Curtis similarity matrices (PRIMER-E).

Relationships between environmental variables and bacterial community structure and composition were identified using multivariate multiple regression (DISTLM) within the PERMANOVA+ add-on (Clarke and Gorley, 2006). Where two or more environmental variables were strongly correlated ($R^2 > 0.9$), just one variable was retained in the model to represent the correlated variables while the others were excluded from the model. Analyses of these relationships used Akaike Information Criterion (AIC) and a stepwise selection procedure to select the best explanatory model.

Differences in the abundances of ASVs between warm and ambient temperatures were identified using the ANCOMBC package (Lin and Peddada, 2020) in R Studio using default parameters (version 3.5.4; R Core Team 2017).

2.5.3 Seagrass and environmental variables

All analyses were performed on untransformed data after first checking data for homogeneity of variance using Shapiro-Wilk test and Levene's test. All statistical analyses were conducted using R Studio (version 3.5.4; R Core Team 2017) with the lme4 (Bates et al., 2014), and vegan packages (version 2.5–2) (Oksanen et al., 2013).

To determine differences in seagrass response variables (above and below-ground biomass, growth rates and detrital decomposition) between temperature categories (fixed factor with two levels: warm, ambient), a linear mixed-effects models (LMM) was fitted, including site as a random factor nested in temperature.

To examine the relationship between each seagrass response variable and all water and sediment variables, a stepwise model selection procedure and the AIC was used to select the best model. Before fitting models, each abiotic covariate was plotted against each seagrass response variable to check for linearity. No transformations were required as all relationships were linear.

Pearson correlation coefficient was used to determine relationships between highly correlated variables (P>0.8). ORP and sediment pH were the only covariates with a Pearson's correlation coefficient (R > 0.8) (Supplementary Table 2). Model selection was performed for each seagrass response variable with both ORP, and sediment pH included, and also with one excluding the other. As the model with only ORP included had the lowest AIC value, sediment pH was removed from each stepwise model selection. All remaining covariates were normalised using the formula, X-mean/SD, before the model selection was run.

3 Results

3.1 Water and sediment variables

Water temperatures were consistently higher (~3°C) at warm sites than ambient sites ($F_{1,5} = 33.1$, $p < 0.05$) at both sampling times ($F_{1,103} = 0.01$, p (interaction) = 0.93). Temperatures were higher in January (warm mean 29.4°C) compared to September (warm mean 21.5°C) ($F_{1,103} = 7800$, $p < 0.05$; Figure 2). The maximum water temperature recorded in summer was 29.96°C.

The above-ground abiotic variables (dissolved oxygen (DO), conductivity, and pH of the water column) did not differ significantly between warm and ambient sites (Supplementary Table 3). However, the below-ground variables organic matter (OM) and sediment pH were greater, and sediments were finer (smaller grain size) at warmer sites, and ORP was greater in ambient sites (Supplementary Table 3).

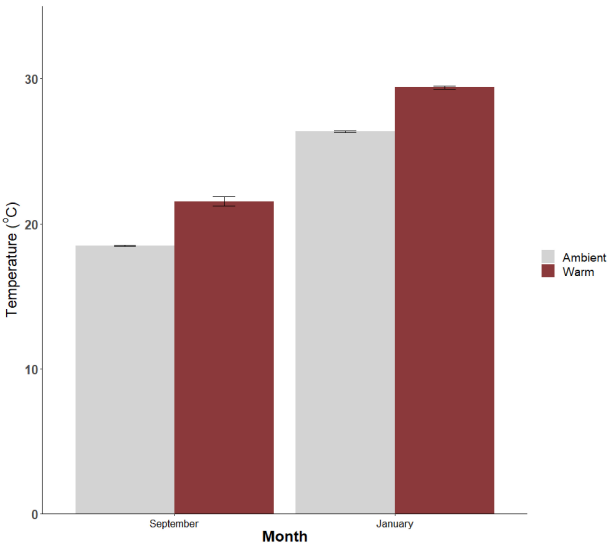

FIGURE 2
Mean (± SE) water temperature recorded at warm and ambient seagrass sites in Lake Macquarie, Australia during each sampling period (September 2020 and January 2021; N=56).

3.2 Bacterial communities and alpha diversity

3.2.1 Bacterial community structure and composition

Overall, 1135 ASVs were obtained from leaf tissues and 1907 ASVs from sediments. Bacterial community structure (relative abundance of individual ASVs) in leaf tissues and sediments differed between warm and ambient sites (leaf: $F_{1,34}$ = 3.29, p = 0.02, sediments: $F_{1,34}$ = 2.42, p = 0.04; Figures 3A, B; Supplementary Table 4). A similar trend was observed for leaf tissue and sedimentary bacterial community composition (presence/absence of ASVs) between warm and ambient sites, although this was not significant (leaf: $F_{1,34}$ = 2.54, p = 0.05, sediments: $F_{1,34}$ = 1.98, p = 0.085; Figures 3C, D; Supplementary Table 4).

Leaf tissue and sedimentary bacterial community structure had less dispersion among replicate samples in warm sites compared to ambient sites (leaf: $F_{1,34}$ = 18.11, p = 0.0001, sediments: $F_{1,34}$ = 6.6, p= 0.0001, Figures 3A, B). This was similar to community composition (leaf: $F_{1,34}$ = 16.71, p = 0.0001, sediments: $F_{1,34}$ = 6.6, p = 0.0001, Figures 3C, D).

3.2.2 Bacterial diversity

Neither of the alpha diversity measures for leaf bacterial communities differed between warm and ambient sites (Shannon diversity: p = 0.2154; Figure 4A, Chao1 diversity: p = 0.7718; Figure 4B).

Of the two alpha diversity analyses for sedimentary communities, one showed no differences between warm and ambient sites (Shannon diversity: p > 0.05; Figure 4C), while the other (Chao1, p < 0.05; Figure 4D) showed warm sites had significantly higher alpha diversity than ambient sites.

3.2.3 Environmental influences

The stepwise model selection for leaf tissue bacterial community structure found that pH (10.4%), DO (5.4%), conductivity (15.9%), ORP (3%), and OM (17.7%) were significant explanatory variables accounting for 52.4% of the variance among replicates (Figure 5A; Supplementary Table 5). Bacterial community composition variation on leaves between warm and ambient communities was partitioned along decreasing OM (18.2%), pH (6.8%), and DO (4.7%) and increasing conductivity (15.7%) and ORP (3.5%) (Figure 5B).

The stepwise model selection for sedimentary bacterial community structure explained 42% of variance (R^2 = 0.42) and included water quality variables – pH (16.5%), conductivity (12%), and DO (4%), and a sediment variable - OM (8.5%) (Figure 5C; Supplementary Table 5). Variation in sedimentary bacterial community composition was explained by the same variables except DO (R^2 = 0.36). The dissimilarity of warm and ambient community composition was also along increasing pH (15%), and OM (9%) and decreasing conductivity (12%) (Figure 5D).

3.2.4 Bacterial assemblage changes

A total of 353 bacterial ASVs (31%) on leaf tissue differed significantly in abundance between warm and ambient sites. The following taxa were relatively more abundant at warm sites *Aliikangiella* (g), *Aquimarina* (g), *Bdellovibrionaceae OM27 clade* (g), *Candidatus Amoebophilus* (g), *Coxiella* (g), *Flavobacteriaceae* (f), *Folkiniaceae MD3-55* (g), *Lacinutrix* (g), *Microtrichaceae* (f), *Nannocystaceae* (f), *Planctomycetota OM190* (cl), *Planktomarina* (g), *Rhodobacteraceae* (f), *Sandaracinaceae* (f), *Ulvibacter* (g), *Woeseia* (g), and *Yoonia-Loktanella* (g). In contrast, *Robiginitalea* (g), *Schizothrix LEGE 07164* (g), and *Sagittlula* (g) were relatively more abundant at ambient temperatures (Supplementary Figure 1).

Most bacterial ASVs within the top 25 ASVs that were differentially abundant in leaf tissue between warm and ambient sites were from aerobic bacteria [Flavobacteriaceae (f), Coxiella (g), Planktomarina (g)] (Supplementary Figure 1). The top 25 differentially abundant ASVs also included a mix of heterotrophs [Ulvibacter (g)] and chemotrophs [Sandaracinaceae (f), Robiginitalea (g)] related to various functions including nutrient cycling, and toxin defence [Aquimarina (g)] (Supplementary Figure 1).

In sedimentary bacterial communities the relative abundance of 337 ASVs (18%) differed significantly between warm and ambient temperatures. ASVs with the highest increase in relative abundance in sediments at warm sites belonged to the following taxa: *Bacteroidales SB-5* (f), *BD2-2* (f), *Desulfocapsaceae* (f), *Desulfobulbaceae* (f), *Desulfosarcinaceae* (f), *Sva0081 sediment group* (g), *Woeseia* (g), *Gammaproteobacteria Incertae Sedis* (o), *Robiginitalea* (g), *Sva0485* (p), *Thiogranum* (g), and *Thiotrichaceae* (f). At ambient sites, ASVs with the highest increase relative abundance belonged to the following taxa: *Bacteroidales* (o), BD2-2 (f), *Candidatus Amoebophilus* (g), *Desulfobulbaceae* (f), *Desulfosarcinaceae* (f), *LCP-80* (g), *SEEP-SRB1*

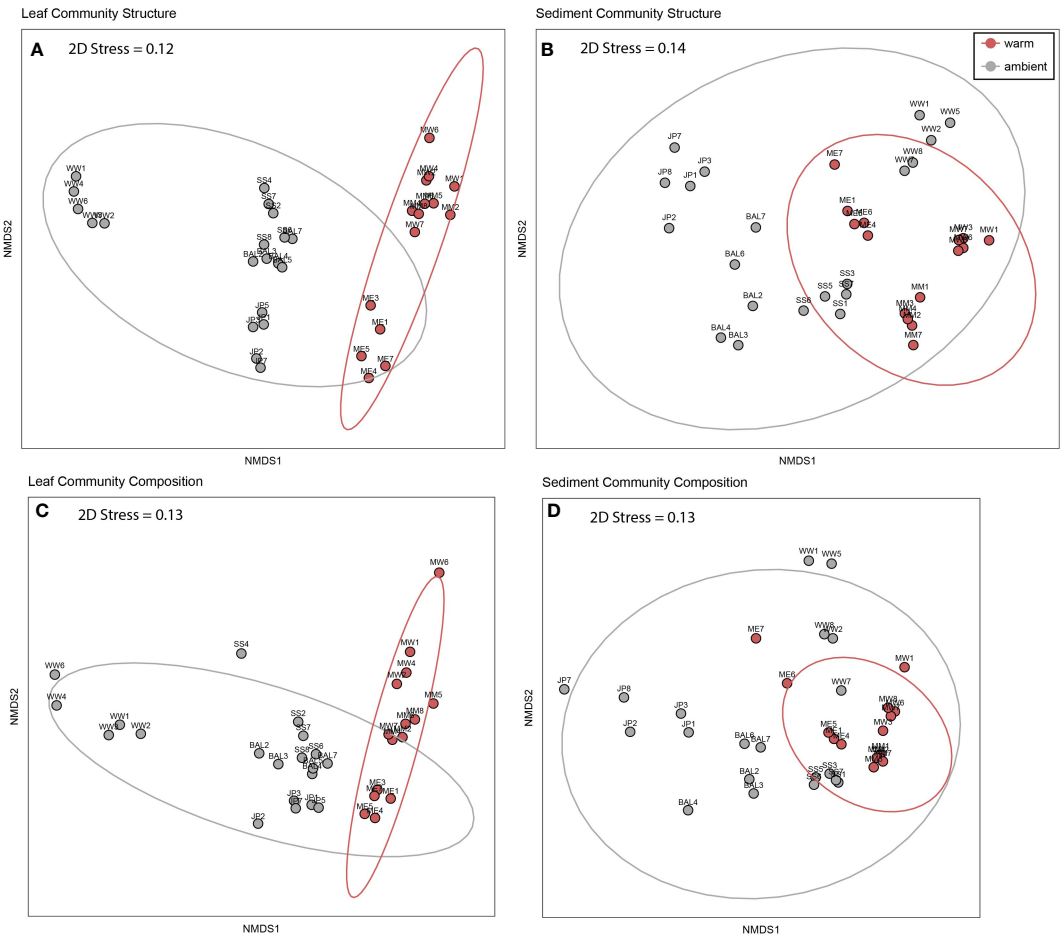

FIGURE 3
Non-metric multidimensional scaling (nMDS) of leaf tissue and sedimentary bacterial assemblages in warm and ambient sites sampled from seagrass meadows in Lake Macquarie (N=35). **(A)** Structure of leaf tissue communities (square root transformed) **(B)** Structure of sedimentary communities **(C)** Composition of leaf tissue communities **(D)** Composition of sedimentary communities. Data was standardised by total ASV abundances and then nMDS plots were constructed with Bray-Curtis dissimilarity matrices.

(g), *Gammaproteobacteria* (cl), *Woeseia* (g), *Halioglobus* (g), and *Gammaproteobacteria HOC36* (o) (Supplementary Figure 3).

Among the 25 bacterial ASVs most significantly different in sedimentary communities between warm and ambient sites, there was a mix of aerobes [*Halioglobus* (g), *Thiogranum* (g)] and anaerobes [*Desulfocapsaceae*, *Desulfosarcinaceae* (f)] (Supplementary Figure 3) which are related to various functions such as nitrogen fixing, sulfur oxidation, and pathogen defence that were more abundant in warm sites. ASVs which were more abundant in ambient sites were chemotrophs associated with sulfur cycling [*Desulfocapsaceae* (f)] (Supplementary Figure 3).

3.3 Seagrass biomass, growth rates & decomposition rates

Above-ground seagrass biomass ($F_{1,55} = 22.2$, $p < 0.001$; sampled in September; Figure 6A) and growth rates ($F_{1,55} = 15.9$, $p < 0.001$; sampled in January; Figure 6B; Supplementary Table 6) were both over 1.5 times greater at warm sites compared to ambient sites.

Stepwise model selection indicated that above-ground seagrass tissue biomass was best predicted by sediment organic matter (31%), with the two being positively associated (AIC = 95.09; Supplementary Figure 2A; Supplementary Table 7).

Seagrass leaf growth rates were positively correlated with increased pH (11.2%), increased water conductivity (7.2%), and increased water temperature (27.1%) and negatively correlated with increasing sediment ORP (10%) (AIC = 4.67; Supplementary Tables 4, 7; Supplementary Figures 2B–E).

Considering conductivity ranged from 49.6-50.9 S/m across all sites, we believe this proportion of variation to be biologically insignificant.

Below-ground biomass of seagrass (sampled in September) and detrital decomposition rates (sampled in January) did not differ between warm and ambient sites but tended to be greater at warm compared to ambient sites ($F_{1,34} = 1.08$, $p > 0.05$ and $F_{1,20} = 4.0$, $p > 0.05$, respectively; Supplementary Table 6; Figure 7).

Variation in below-ground biomass was best explained by sediment organic matter (35%) and temperature (5%), where below-ground biomass increased with increasing sediment organic matter and

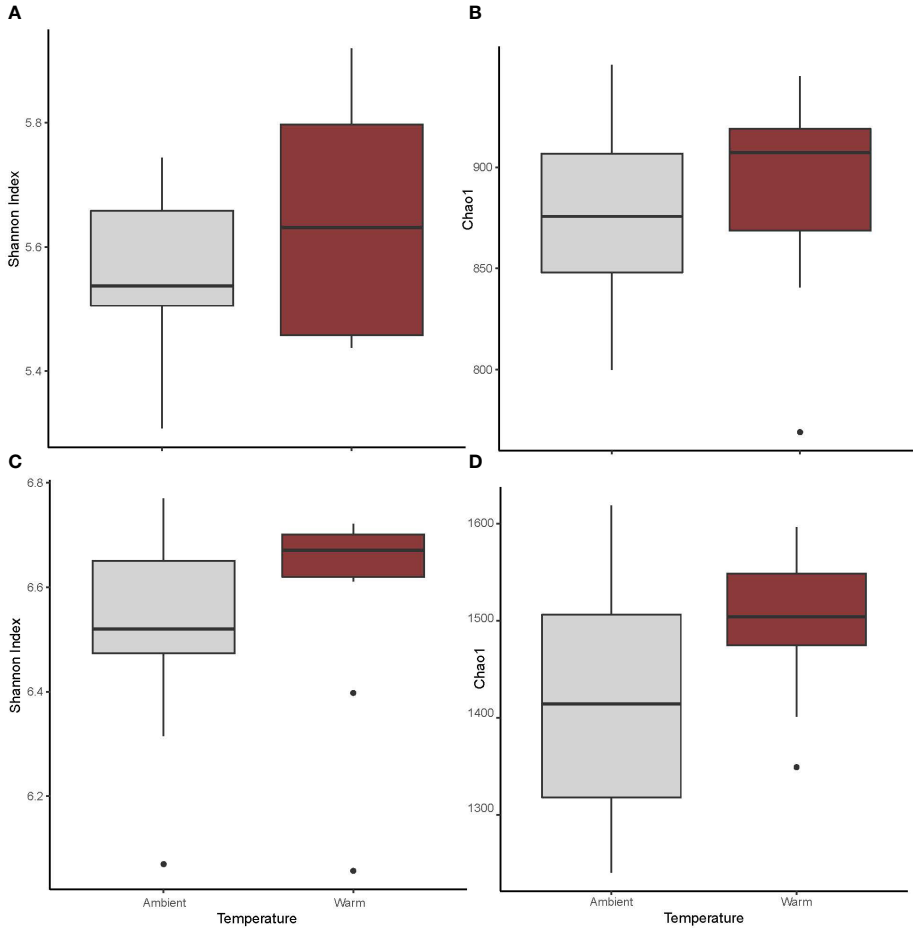

FIGURE 4
Alpha diversity of microbial communities associated with Z. muelleri leaves and sediments at warm and ambient sites within Lake Macquarie. Mean species richness estimated as **(A)** Leaf-Shannon index, and **(B)** leaf-Chao1, and as **(C)** sediment-Shannon index, and **(D)** sediment-Chao1. Mean species richness estimated, n = 25.

slightly increased with increasing temperature (AIC = 218.24; Supplementary Figures 4A, B; Supplementary Table 7).

Rates of detrital decomposition decreased as sediment ORP (0.57) increased but were not correlated to any other environmental variable (AIC = 163.64; Supplementary Figure 4C; Supplementary Table 7).

4 Discussion

In this study, a warm plume from a power station discharge channel in Lake Macquarie, Australia provided a thermal plume ~3°C above ambient lake temperatures which was used to investigate *in situ* differences in above and below-ground microbial communities, and seagrass productivity, in response to long term exposure to elevated water temperatures. Overall, we observed stronger changes in above-ground than below-ground bacterial communities and productivity with increased temperatures which support our hypothesis that the effects of water temperature are stronger above-ground and processes occurring below-ground may be buffered from increases in water temperature.

4.1 Microbial community response to temperature

Bacterial community composition in both sediment and leaf tissue was more homogeneous (i.e. less variable) in warm sites compared to ambient temperature sites. This result aligns with the Stress Gradient Hypothesis (SGH) which posits that environments under stress will have lower community richness where the remaining species occupy niches that directly affect the function of plants (Bertness and Callaway, 1994; Callaway, 2007). In this case under increased temperatures, facilitative interactions between bacteria and seagrass should be stronger compared with ambient/benign conditions where facilitative interactions are weaker (Bertness and Callaway, 1994). Interestingly, above-ground bacterial communities were more homogeneous than below-ground communities in both warm and ambient sites. This result suggests above-ground communities may have greater responses to elevated temperatures than the adjacent below-ground communities potentially due to thermal buffering provided by the top layer of sediments in seagrass meadows. The lower variation in microbial communities under elevated temperatures might indicate

10.3389/fmars.2024.1374946

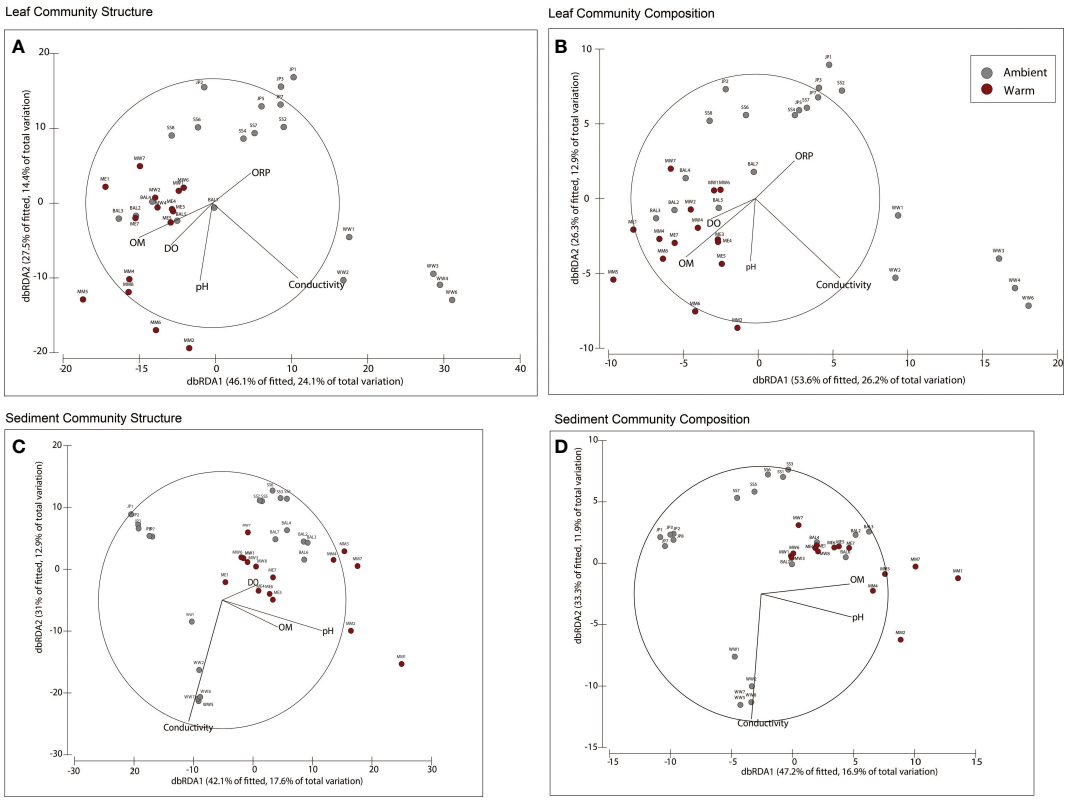

FIGURE 5
Distance-based redundancy analyses with vectors overlayed for variables selected by model selection for **(A)** Leaf tissue bacterial community structure, and **(B)** Leaf tissue bacterial community composition. **(C)** Sedimentary bacterial community structure, and **(D)** Sedimentary bacterial community composition. OM, Organic matter; DO, Dissolved oxygen; ORP, Oxidation-Reduction Potential.

a stronger relationship between seagrass and their microbes under stressful conditions. A lower variation in microbial community structure signifies a consistent diversity across samples which suggests little environmental fluctuation which ensures consistent uniform nutrient availability, disease suppression, and overall plant performance through beneficial relationships between microbes and plants (Waymouth et al., 2020). The increase in community homogeneity may also be due to a more consistent assemblage of

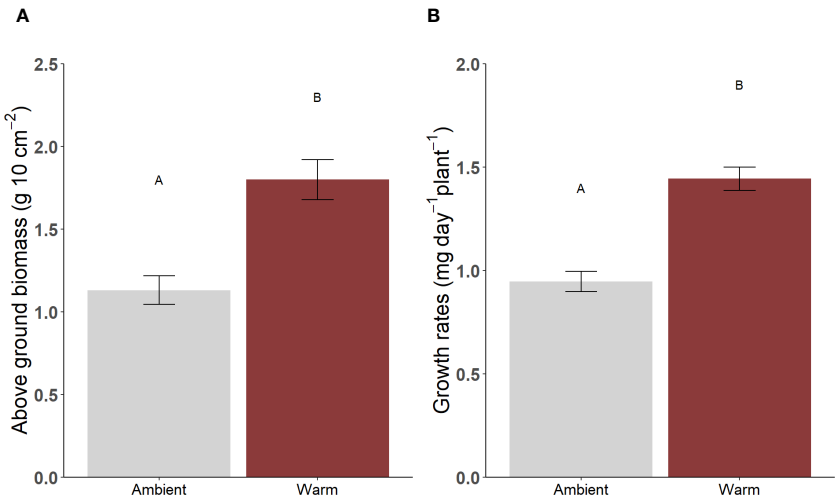

FIGURE 6
Mean (± SE) **(A)** Above-ground biomass, **(B)** Seagrass leaf tissue growth rates, at ambient and warm sites in Lake Macquarie. Sampling was conducted in September for **(A)** and January for **(B)**. AB used to indicate statistical significance between temperature categories (AB used to indicate statistical significance between temperature categories; N=56).

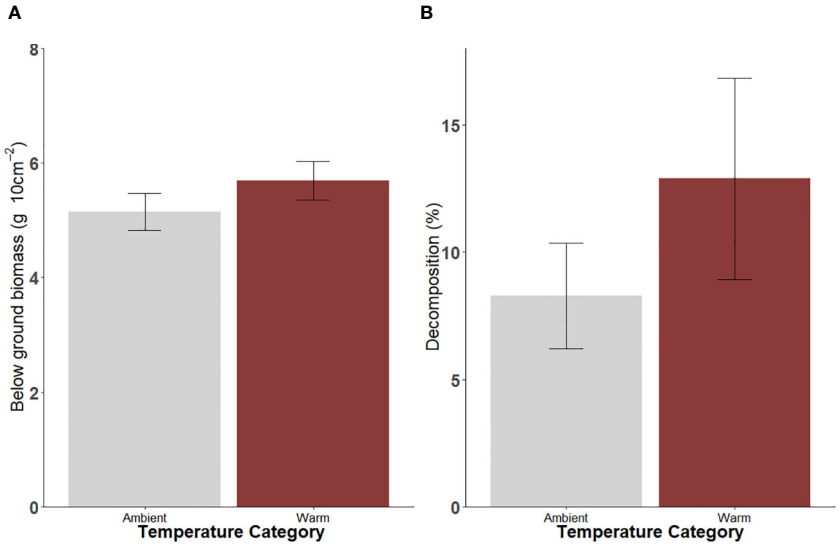

FIGURE 7
Mean (± SE) **(A)** below-ground biomass **(B)** detrital decomposition at ambient and warm sites in Lake Macquarie. Sampling was conducted in September for **(A)** and January for **(B)**. AB used to indicate statistical significance between temperature categories (n=56).

bacterial groups which can tolerate higher temperature (ASV's pertaining to thermally tolerant bacteria are discussed later in this section).

An alternative cause of the differences in microbial communities to environmental selection is the selection of preferential bacterial species by plants to aid plant performance under less favourable conditions may be facilitated through the exudation of organic compounds such as sugars, amino acids, and volatile organic compounds into the surrounding water (Naylor et al., 2017; Sasse et al., 2018; Jones et al., 2019). These compounds can function as chemoattractants, attracting certain bacterial species to the area around the plant's roots. As these exudates occur in response to external environmental forcing on the plants, the change in bacterial communities recorded in this study in warm and ambient temperatures may be related to seagrass nutrient exudation, but this was beyond the scope of testing in the current study.

We also cannot discount the possibility that the increased variability among ambient sites is due to the larger spatial separation across all four ambient sites relative to the three warm sites. The environmental conditions and terrestrial inputs may be more similar between the warm sites which leads to more similar microbial communities (Stadler and del Giorgio, 2022). However, between all sites a spatial separation of at least 750m was maintained, and all sites had a similar neighbouring land use (vegetated parkland) to control for these variables. A key knowledge gap to be determined, is whether differences in microbial communities under environmental stressors are linked to direct environmental selection of microbes or a case of plants selecting the microbes for their own benefits. Three of the four alpha diversity results indicate no changes in diversity between ambient and warm sites however, all show a non-significant trend towards increased diversity in warm sites. This indicates warmer water may select for a slightly wider range of microbes without removing any taxa which may already be present at ambient sites, but overall, warm communities were more homogenous than ambient sites.

Leaf tissue bacterial communities at warm sites contained greater relative abundances of bacteria related to nutrient cycling functions are known to be thermally tolerant [e.g., *Woeseia (g)* (Hoffmann et al., 2020)]. Of the ASVs which varied most significantly between warm and ambient temperatures, ASV3170 (belonging to family *Rhodobacteraceae*) was the most abundant in warm temperatures. This result of *Rhodobacteraceae* tolerating increased temperatures has been shown in multiple studies before (Elifantz et al., 2013; Pootakham et al., 2019; Miyamoto et al., 2023). *Rhodobacteraceae* spp. can have mutualistic relationships with eukaryotes such as micro- and macroalgae (Bischoff et al., 2021). Additionally, some *Rhodobacteraceae* spp. are capable of harvesting light to increase biomass yields under stressed environmental conditions, which may explain its presence in warm sites. It can also breakdown antagonistic bacterial pathogens which may protect the seagrass host in this case (Zhang et al., 2016). This pattern has also been shown in other marine systems by Pootakham et al. (2019), which found that various *Rhodobacteraceae* spp. in coral species *Porites lutea* are indicator species of thermal stress. Stratil et al. (2013) and Qiu et al. (2019) found that warming caused a shift in epiphytic bacterial communities on brown macroalgae Fucus vesiculosus and Ecklonia radiata. In both cases diversity decreased under warmer temperature treatments where bacteria such as Rhodobacteraceae, Thalassomonas and Alteromonadaceae were more abundant in warmer temperatures. The results of this present study found no differences in bacteria belonging to Thalassomonas or Alteromonadaceae; however, bacteria belonging to Rhodobacteraceae were relatively more abundant in warm sites. As previously mentioned, some Rhodobacteraceae

species are regarded as extremophiles due to the stressed marine environments they can survive in which may account for their higher relative abundance in warm conditions (Pujalte et al., 2014). As such, there is potential that this bacterial family may have the same applicability as an indicator species of thermal stress in seagrass meadows.

The leaf tissue ASVs with higher relative abundances in ambient sites were mostly aerobes with functions associated with nutrient and carbon cycling [*Robiginitalea, Sagittula* (Egan et al., 2013; Tarquinio et al., 2021)]. Interestingly, *Sagittula* spp. can mineralise aromatic compounds from marine vascular plants, which results in the sequestration of inorganic carbon (Gulvik and Buchan, 2013). In the context of seagrass meadows, *Sagittula* spp. could influence carbon storage potential. As this bacterium has an optimum temperature of 25°C and was relatively less abundant in warm temperatures, further temperature increases could have consequences for the storage of inorganic carbon in seagrass sediments (Lee et al., 2013).

Sedimentary bacterial communities within seagrass meadows can provide specific functions within typically anoxic and organic enriched sediments (Lugtenberg and Kamilova, 2009; Trevathan-Tackett et al., 2017; Tarquinio et al., 2019; Martin et al., 2020). The interactions between seagrasses and their associated bacterial communities are key to survival in the anoxic marine sediments (Fraser et al., 2018). Although few studies have focussed on the effects of warming on bacterial communities in seagrass sediments, Hicks et al. (2018) found bacterial communities from intertidal mud flats were significantly affected by increases in temperature with bacteria belonging to *Proteobacteria* phylum increasing significantly between temperatures. This phylum contains a diverse range of functional groups ranging from sulphide-oxidisers to nitrogen cyclers (Seymour et al., 2018; Zhang et al., 2020; Tarquinio et al., 2021). In the present study, nine of the 25 ASVs most differentially abundant in sedimentary communities between warm and ambient sites belonged to the *Proteobacteria* phylum. In general, sedimentary bacterial communities in warm sites had higher relative abundances of sulphide reducing bacteria [e.g., *Bacteroidetes BD2-2 (f), Desulfocapsaceae (f), Desulfosarcinaceae (f)*] commonly found in sulphide rich environments (Holmer et al., 2006; Trevathan-Tackett et al., 2017; Martin et al., 2020). This suggests warm sites are richer in sulphide than ambient sites, which is supported by the results of lower ORP (commonly associated with sulphide rich conditions) in warm sites and high organic matter in warm sites (Martin et al., 2020). Sedimentary bacteria with higher relative abundances in the ambient sites included *Halioglobus* and other chemotrophs with a broad range of associated functions including nitrogen cycling, ferric iron reduction, and other nutrient cycling capabilities (Park et al., 2012; Lehnen et al., 2016; Szitenberg et al., 2022). More oxygenated conditions likely support more diverse and variable microbial communities and decrease the reliance of seagrass on facilitative interactions with sediment bacterial communities.

Variation in leaf tissue bacterial community structure and composition between warm and ambient sites was best explained by increasing pH and increasing organic matter (variables not colinear to temperature). While precise effects of elevated water temperature on epiphytic bacterial communities in seagrasses is still unclear, this interaction has been examined in habitat-forming macroalgae (Stratil et al., 2013). Increasing pH and organic matter also explained the most variation in sedimentary bacterial community structure and composition between warm and ambient sites. The greater separation of warm and ambient bacterial communities with increased organic matter is supported by the higher abundances of bacteria which are found in more anoxic, sulphide rich sediments commonly associated with high organic matter such as *Desulfocapsaceae* and Sva0081 sediment group (Waite et al., 2020; Jantharadej et al., 2021). The separation of bacterial communities due to variability in pH has important implications similar to temperature, as climate change is predicted to enhance the effects of ocean acidification in many marine ecosystems. Su et al. (2021) found changes in pH levels significantly altered sedimentary bacterial community composition which supports the findings of this study. None of the genera among the 20 most significantly different between warm and ambient sites in this study were identified as pH-sensitive or pH-tolerant by Su et al. (2021). However, five pH-sensitive genera did belong to *Proteobacteria* phylum which was commonly found in both warm and ambient sites.

4.2 Seagrass response to elevated temperatures

The above-ground biomass production of *Z. muelleri* was elevated by 11% (± 0.18) on average at warm sites with water temperatures ~3°C above ambient, suggesting a potential increase in seagrass metabolism and photosynthesis under warmer conditions. The same patterns between temperature, seagrass metabolism, and photosynthesis have been previously observed at Lake Macquarie (Cams Wharf; York et al., 2013) and elsewhere [Great Barrier Reef; Collier et al. (2017); Red Sea, Anton et al. (2020)]. York et al. (2013) found 27°C led to the highest seagrass biomass while 32°C resulted in 100% mortality of seagrass within 42 days. Collier et al. (2017) found 31°C led to the highest seagrass biomass while temperatures exceeding 35°C negatively affected growth of *Z. muelleri*. It is important to note that the Collier et al. (2017) study was conducted in tropical waters with much warmer ambient temperatures compared to Lake Macquarie. Differences in optimal temperatures found in these previous studies and the higher above-ground biomass at warm sites (long-term thermal exposure) recorded in the present study may therefore indicate that this species is able to adapt to local conditions over time. Additionally, an increase in the ratio of above to below-ground partitioning of resources has previously been recorded as a physiological response to environmental stress and may indicate poor survival outlook (Nixon et al., 2001).

Contrary to our predictions, below-ground biomass production in this study was not significantly related to warmer temperatures. This result is similar to those of Kaldy and Dunton (2000) who found no seasonal differences in seagrass below-ground biomass, while identifying a peak in above-ground biomass and biomass production in warmer months. Similarly, detrital decomposition

rates did not differ between ambient and warm temperatures, despite an increase in anoxic sediment conditions, and potentially sulphide production (as evidenced through changes in microbial composition). However, previous studies found that increased temperatures increase detrital decomposition rates (Trevathan-Tackett et al., 2017; Trevathan-Tackett et al., 2020a). The non-significant trend in this study may be a result of different deployment intervals, daily temperature pulses, or differences in anoxic vs aerobic decay. The aforementioned studies were conducted under lab conditions for 30 and 80 d while this decomposition component was conducted over 12 d in the field with temperatures fluctuating based on time of day, hence greater deployment times may be required in future experiments.

5 Conclusions

Under current rates of warming, seagrass ecosystems are likely to experience a shift in bacterial communities both above-ground in plant tissue and below-ground in surrounding sediments, as well as an increase in above-ground plant productivity. Our results suggest that sedimentary processes may receive some physical thermal buffering from the rising temperatures, however, these increased temperatures may cause decoupling of processes that contribute to nutrient cycling above and below-ground. This study provided further evidence that increased temperature of ~3°C may increase above-ground biomass production in seagrasses in temperate regions (York et al., 2013; Collier et al., 2017), with changes observed in above-ground productivity of plants, potentially as a response to environmental conditions. This study also advances our understanding of seagrass-temperature interactions and explores associated changes in above and below-ground bacterial communities that might lead to changes in ecosystem functions of seagrass meadows. Future research direction on this topic should involve examining the effects of seasonal variation on seagrass-associated microbial communities and should also integrate manipulative experiments to examine the extent to which temperature, among other environmental changes in estuaries, impacts the interactions between seagrass and associated above and below-ground bacterial communities to determine the importance of these interactions to the resilience of seagrass in the face of warming temperatures.

Data availability statement

The original contributions presented in the study are publicly available. This data can be found here: https://www.ncbi.nlm.nih.gov/bioproject/PRJNA925291/.

Author contributions

LW: Conceptualization, Data curation, Formal analysis, Investigation, Methodology, Project administration, Writing – original draft, Writing – review & editing. PG: Conceptualization, Formal analysis, Funding acquisition, Supervision, Writing – review & editing. TG: Conceptualization, Methodology, Project administration, Supervision, Validation, Writing – review & editing. EM: Formal analysis, Methodology, Software, Supervision, Writing – review & editing. DV: Formal analysis, Supervision, Writing – review & editing. KD: Conceptualization, Funding acquisition, Investigation, Methodology, Project administration, Supervision, Validation, Writing – review & editing.

Funding

The author(s) declare financial support was received for the research, authorship, and/or publication of this article. This research was supported by funding from the Australian Research Council (LP200200220 awarded to PG) and Macquarie University HDR funding (awarded to LW).

Acknowledgments

We acknowledge the provision of laboratory space and equipment from Sydney institute of Marine Science and Macquarie Geoanalytical. And support in DNA sequencing from Ramaccioti centre for Genomics. The authors would like to thank all students, volunteers, and colleagues for their significant contribution to the various stages of this study, in particular Amy MacIntosh and Sebastian Vadillo. We also thank the reviewers who have improved this manuscript through their insightful comments.

Conflict of interest

The authors declare that the research was conducted in the absence of any commercial or financial relationships that could be construed as a potential conflict of interest.

The author(s) declared that they were an editorial board member of Frontiers, at the time of submission. This had no impact on the peer review process and the final decision.

Publisher's note

Supplementary material

The Supplementary Material for this article can be found online at: https://www.frontiersin.org/articles/10.3389/fmars.2024.1374946/full#supplementary-material

References

Anderson, M. J. (2005). *Permutational multivariate analysis of variance* Vol. 26 (Auckland: Department of Statistics, University of Auckland), 32–46.

Anderson, D. R. (2007). *Model based inference in the life sciences: a primer on evidence* (Springer Science & Business Media).

Anton, A., Baldry, K., Coker, D. J., and Duarte, C. M. (2020). Drivers of the low metabolic rates of seagrass meadows in the Red Sea. *Front. Mar. Sci.* 7, 69. doi: 10.3389/fmars.2020.00069

Babcock, R. C., Bustamante, R. H., Fulton, E. A., Fulton, D. J., Haywood, M. D. E., Hobday, A. J., et al. (2019). Severe continental-scale impacts of climate change are happening now: extreme climate events impact marine habitat forming communities along 45% of Australia's coast. *Front. Mar. Sci.* 6. doi: 10.3389/fmars.2019.00411

Bates, D., Mächler, M., Bolker, B., and Walker, S. (2014). Fitting linear mixed-effects models using lme4. *J. Stat. Softw.* 67 (1), 1–48. doi: 10.18637/jss.v067.i01

Bertness, M. D., and Callaway, R. (1994). Positive interactions in communities. *Trends Ecol. Evol.* 9, 191–193. doi: 10.1016/0169-5347(94)90088-4

Bischoff, V., Zucker, F., and Moraru, C. (2021). "Marine bacteriophages," in *Encyclopedia of Virology*, *4th ed*. Eds. D. H. Bamford and M. Zuckerman (Academic Press, Oxford), 322–341. doi: 10.1016/B978-0-12-809633-8.20988-6

Borum, J., Sand-Jensen, K., Binzer, T., Pedersen, O., and Greve, T. (2007). *Oxygen movement in seagrasses, seagrasses: biology, ecology and conservation* (Netherlands: Springer), 255–270.

Brodersen, K. E., Siboni, N., Nielsen, D. A., Pernice, M., Ralph, P. J., Seymour, J., et al. (2018). Seagrass rhizosphere microenvironment alters plant-associated microbial community composition. *Environ. Microbiol.* 20 (8), 2854–2864. doi: 10.1111/1462-2920.14245

Callahan, B. J., McMurdie, P. J., Rosen, M. J., Han, A. W., Johnson, A. J. A., and Holmes, S. P. (2016). DADA2: high-resolution sample inference from Illumina amplicon data. *Nat. Methods* 13, 581–583. doi: 10.1038/nmeth.3869

Callaway, R. M. (2007). *Positive interactions and interdependence in plant communities* (Springer Science & Business Media).

Chefaoui, R. M., Duarte, C. M., and Serrão, E. A. (2018). Dramatic loss of seagrass habitat under projected climate change in the Mediterranean Sea. *Global Change Biol.* 24, 4919–4928. doi: 10.1111/gcb.14401

Cifuentes, A., Antón, J., De Wit, R., and Rodríguez-Valera, F. (2003). Diversity of bacteria and Archaea in sulphate-reducing enrichment cultures inoculated from serial dilution of *Zostera noltii* rhizosphere samples. *Environ. Microbiol.* 5, 754–764. doi: 10.1046/j.1470-2920.2003.00470.x

Clarke, K., and Gorley, R. (2006). *PRIMER version 6: user manual*. Plymouth, England: Tutorial, E-PRIMER.

Collier, C. J., Ow, Y. X., Langlois, L., Uthicke, S., Johansson, C. L., O'Brien, K. R., et al. (2017). Optimum temperatures for net primary productivity of three tropical seagrass species. *Front. Plant Sci.* 8, 1446.

Crump, B. C., Wojahn, J. M., Tomas, F., and Mueller, R. S. (2018). Metatranscriptomics and amplicon sequencing reveal mutualisms in seagrass microbiomes. *Front. Microbiol.* 9, 388. doi: 10.3389/fmicb.2018.00388

Cúcio, C., Engelen, A. H., Costa, R., and Muyzer, G. (2016). Rhizosphere microbiomes of European seagrasses are selected by the plant, but are not species specific. *Front. Microbiol.* 7. doi: 10.3389/fmicb.2016.00440

Egan, S., Harder, T., Burke, C., Steinberg, P., Kjelleberg, S., and Thomas, T. (2013). The seaweed holobiont: understanding seaweed–bacteria interactions. *FEMS Microbiol. Rev.* 37, 462–476. doi: 10.1111/1574-6976.12011

Elifantz, H., Horn, G., Ayon, M., Cohen, Y., and Minz, D. (2013). Rhodobacteraceae are the key members of the microbial community of the initial biofilm formed in Eastern Mediterranean coastal seawater. *FEMS Microbiol. Ecol.* 85 (2), 348–357. doi: 10.1111/1574-6941.12122

Fraser, M. W., Gleeson, D. B., Grierson, P. F., Laverock, B., and Kendrick, G. A. (2018). Metagenomic evidence of microbial community responsiveness to phosphorus and salinity gradients in seagrass sediments. *Front. Microbiol.* 9, 1703. doi: 10.3389/fmicb.2018.01703

Fuggle, R. E., Gribben, P. E., and Marzinelli, E. M. (2023). Experimental evidence root-associated microbes mediate seagrass response to environmental stress. *J. Ecol.* 111, 1079–1093. doi: 10.1111/1365-2745.14081

Garcias-Bonet, N., Arrieta, J. M., Duarte, C. M., and Marba, N. (2016). Nitrogen-fixing bacteria in Mediterranean seagrass (Posidonia oceanica) roots. *Aquat. Bot.* 131, 57–60. doi: 10.1016/j.aquabot.2016.03.002

Gribben, P. E., Thomas, T., Pusceddu, A., Bonechi, L., Bianchelli, S., Buschi, E., et al. (2018). Below-ground processes control the success of an invasive seaweed. *J. Ecol.* 106, 2082–2095. doi: 10.1111/1365-2745.12966

Gribben, P. E., Nielsen, S., Seymour, J. R., Bradley, D. J., West, M. N., and Thomas, T. (2017). Microbial communities in marine sediments modify success of an invasive macrophyte. *Sci. Rep.* 7, 9845. doi: 10.1038/s41598-017-10231-2

Gulvik, C. A., and Buchan, A. (2013). Simultaneous catabolism of plant-derived aromatic compounds results in enhanced growth for members of the roseobacter lineage. *Appl. Environ. Microbiol.* 79, 3716–3723. doi: 10.1128/AEM.00405-13

Hansen, J. W., Udy, J. W., Perry, C. J., Dennison, W. C., and Lomstein, B. A. (2000). Effect of the seagrass *Zostera capricorni* on sediment microbial processes. *Mar. Ecol. Prog. Ser.* 199, 83–96. doi: 10.3354/meps199083

Harrison, P. G. (1989). Detrital processing in seagrass systems: a review of factors affecting decay rates, remineralization and detritivory. *Aquat. Bot.* 35, 263–288. doi: 10.1016/0304-3770(89)90002-8

Hemminga, M. A., Harrison, P. G., and Van Lent, F. (1991). The balance of nutrient losses and gains in seagrass meadows. *Mar. Ecol. Prog. Ser.*, 85–96. doi: 10.3354/meps071085

Hicks, N., Liu, X., Gregory, R., Kenny, J., Lucaci, A., Lenzi, L., et al. (2018). Temperature driven changes in benthic bacterial diversity influences biogeochemical cycling in coastal sediments. *Front. Microbiol.* 9, 1730.

Hoffmann, K., Bienhold, C., Buttigieg, P. L., Knittel, K., Laso-Pérez, R., Rapp, J. Z., et al. (2020). Diversity and metabolism of Woeseiales bacteria, global members of marine sediment communities. *ISME J.* 14, 1042–1056. doi: 10.1038/s41396-020-0588-4

Holmer, M., Pedersen, O., and Ikejima, K. (2006). Sulfur cycling and sulfide intrusion in mixed Southeast Asian tropical seagrass meadows. *Botanica Marina* 49, 91–102. doi: 10.1515/BOT.2006.013

Howes, E. L., Joos, F., Eakin, M., and Gattuso, J.-P. (2015). An updated synthesis of the observed and projected impacts of climate change on the chemical, physical and biological processes in the oceans. *Front. Mar. Sci.* 2, 36. doi: 10.3389/fmars.2015.00036

Ingleton, T., and McMinn, A. (2012). Thermal plume effects: A multi-disciplinary approach for assessing effects of thermal pollution on estuaries using benthic diatoms and satellite imagery. *Estuar. Coast. Shelf Sci.* 99, 132–144. doi: 10.1016/j.ecss.2011.12.024

Jacobs, R. (1979). Distribution and aspects of the production and biomass of eelgrass, *Zostera marina L.*, at Roscoff, France. *Aquat. Bot.* 7, 151–172. doi: 10.1016/0304-3770(79)90019-6

Jantharadej, K., Limpiyakorn, T., Kongprajug, A., Mongkolsuk, S., Sirikanchana, K., and Suwannasilp, B. B. (2021). Microbial community compositions and sulfate-reducing bacterial profiles in malodorous urban canal sediments. *Arch. Microbiol.* 203, 1981–1993. doi: 10.1007/s00203-020-02157-7

Jones, P., Garcia, B. J., Furches, A., Tuskan, G. A., and Jacobson, D. (2019). Plant host-associated mechanisms for microbial selection. *Front. Plant Sci.* 10, 862. doi: 10.3389/fpls.2019.00862

Jung, E. M. U., Abdul Majeed, N. A. B., Booth, M. W., Austin, R., Sinclair, E. A., Fraser, M. W., et al. (2023). Marine heatwave and reduced light scenarios cause species-specific metabolomic changes in seagrasses under ocean warming. *New Phytol.* 239 (5), 1692–1706. doi: 10.1111/nph.19092

Kaldy, J., and Dunton, K. (2000). Above and below-ground production, biomass and reproductive ecology of Thalassia testudinum (turtle grass) in a subtropical coastal lagoon. *Mar. Ecol. Prog. Ser.* 193, 271–283. doi: 10.3354/meps193271

Kirchman, D. L., Mazzella, L., Alberte, R. S., and Mitchell, R. (1984). Epiphytic bacterial production on Zostera marina. Marine ecology progress series. *Oldendorf* 15, 117–123. doi: 10.3354/meps015117

Lee, D.-H., Cho, S. J., Kim, S. M., and Lee, S. B. (2013). Sagittula marina sp. nov., isolated from seawater and emended description of the genus Sagittula. *Int. J. Sys. Evolutionary Microbiol.* 63, 2101–2107. doi: 10.1099/ijs.0.040766-0

Lefcheck, J. S., Wilcox, D. J., Murphy, R. R., Marion, S. R., and Orth, R. J. (2017). Multiple stressors threaten the imperilled coastal foundation species eelgrass (Zostera marina) in Chesapeake Bay, USA. *Global Change Biol.* 23, 3474–3483. doi: 10.1111/gcb.13623

Lehnen, N., Marchant, H. K., Schwedt, A., Milucka, J., Lott, C., Weber, M., et al. (2016). High rates of microbial dinitrogen fixation and sulfate reduction associated with the Mediterranean seagrass Posidonia oceanica. *Sys. Appl. Microbiol.* 39, 476–483. doi: 10.1016/j.syapm.2016.08.004

Lin, H., and Peddada, S. D. (2020). Analysis of compositions of microbiomes with bias correction. *Nat. Commun.* 11, 3514. doi: 10.1038/s41467-020-17041-7

Lin, X., Wang, S., Zhang, X., Hsieh, T.-H., Sun, Z., and Xu, T. (2021). Near-field route optimization-supported polar ice navigation via maritime radar videos. *J. Advanced Transportation* 2021, 2798351. doi: 10.1155/2021/2798351

Lugtenberg, B., and Kamilova, F. (2009). Plant-growth-promoting rhizobacteria. *Annu. Rev. Microbiol.* 63, 541–556. doi: 10.1146/annurev.micro.62.081307.162918

Marba, N., and Duarte, C. M. (2010). Mediterranean warming triggers seagrass (Posidonia oceanica) shoot mortality. *Global Change Biol.* 16, 2366–2375. doi: 10.1111/j.1365-2486.2009.02130.x

Marba, N., Duarte, C., Terrados, J., Halun, Z., Gacia, E., and Fortes, M. (2010). Effects of seagrass rhizospheres on sediment redox conditions in SE Asian coastal ecosystems. *Estuaries Coasts* 33, 107–117. doi: 10.1007/s12237-009-9250-0

Marbà, N., Jordà, G., Bennett, S., and Duarte, C. M. (2022). Seagrass thermal limits and vulnerability to future warming. *Front. Mar. Sci.* 9. doi: 10.3389/fmars.2022.860826

Martin, B. C., Alarcon, M. S., Gleeson, D., Middleton, J. A., Fraser, M. W., Ryan, M. H., et al. (2020). Root microbiomes as indicators of seagrass health. *FEMS Microbiol. Ecol.* 96, fiz201. doi: 10.1093/femsec/fiz201

Mateo, M., and Romero, J. (1996). Evaluating seagrass leaf litter decomposition: an experimental comparison between litter-bag and oxygen-uptake methods. *J. Exp. Mar. Biol. Ecol.* 202, 97–106. doi: 10.1016/0022-0981(96)00019-6

Mendes, R., Garbeva, P., and Raaijmakers, J. M. (2013). The rhizosphere microbiome: significance of plant beneficial, plant pathogenic, and human pathogenic microorganisms. *FEMS Microbiol. Rev.* 37 (5), 634–663.

Miyamoto, H., Kawachi, N., Kurotani, A., Moriya, S., Suda, W., Suzuki, K., et al. (2023). Computational estimation of sediment symbiotic bacterial structures of seagrasses overgrowing downstream of onshore aquaculture. *Environ. Res.* 219, 115130. doi: 10.1016/j.envres.2022.115130

Mohapatra, M., Manu, S., Dash, S. P., and Rastogi, G. (2022). Seagrasses and local environment control the bacterial community structure and carbon substrate utilization in brackish sediments. *J. Environ. Manage.* 314, 115013. doi: 10.1016/j.jenvman.2022.115013

Naylor, D., DeGraaf, S., Purdom, E., and Coleman-Derr, D. (2017). Drought and host selection influence bacterial community dynamics in the grass root microbiome. *ISME J.* 11, 2691–2704. doi: 10.1038/ismej.2017.118

Nguyen, H. M., Ralph, P. J., Marín-Guirao, L., Pernice, M., and Procaccini, G. (2021). Seagrasses in an era of ocean warming: a review. *Biol. Rev.* 96, 2009–2030. doi: 10.1111/brv.12736

Nixon, S., Buckley, B., Granger, S., and Bintz, J. (2001). Responses of very shallow marine ecosystems to nutrient enrichment. *Hum. Ecol. Risk Assess.: Int. J.* 7 (5), 1457–1481.

O'Brien, A. L., Dafforn, K., Chariton, A., Airoldi, L., Schäfer, R. B., and Mayer-Pinto, M. (2023). Multiple stressors. In *Marine pollution–monitoring, management and mitigation* (Cham: Springer Nature Switzerland) pp. 305–315. doi: 10.1101/2020.05.19.105098

Oksanen, J., Blanchet, F. G., Kindt, R., Legendre, P., Minchin, P. R., O'hara, R., et al. (2013). *Package 'vegan' Community ecology package, version*. 2 (9), 1–295.

Park, S., Yoshizawa, S., Inomata, K., Kogure, K., and Yokota, A. (2012). Halioglobus japonicus gen. nov., sp. nov. and Halioglobus pacificus sp. nov., members of the class Gammaproteobacteria isolated from seawater. *Int. J. Syst. Evol. Microbiol.* 62, 1784–1789. doi: 10.1099/ijs.0.031443-0

Pendall, E., Bridgham, S., Hanson, P. J., Hungate, B., Kicklighter, D. W., Johnson, D. W., et al. (2004). Below-ground process responses to elevated CO2 and temperature: a discussion of observations, measurement methods, and models. *New Phytol.* 162, 311–322. doi: 10.1111/j.1469-8137.2004.01053.x

Pootakham, W., Mhuantong, W., Yoocha, T., Putchim, L., Jomchai, N., Sonthirod, C., et al. (2019). Heat-induced shift in coral microbiome reveals several members of the Rhodobacteraceae family as indicator species for thermal stress in Porites lutea. *MicrobiologyOpen* 8, e935. doi: 10.1002/mbo3.935

Pujalte, M. J., Lucena, T., Ruvira, M. A., Arahal, D. R., and Macián, M. C. (2014). "The family rhodobacteraceae," in *The Prokaryotes: Alphaproteobacteria and Betaproteobacteria*. Eds. E. Rosenberg, E. F. DeLong, S. Lory, E. Stackebrandt and F. Thompson (Springer Berlin Heidelberg, Berlin, Heidelberg), 439–512. doi: 10.1007/978-3-642-30197-1_377

Qiu, Z., Coleman, M. A., Provost, E., Campbell, A. H., Kelaher, B. P., Dalton, S. J., et al. (2019). Future climate change is predicted to affect the microbiome and condition of habitat-forming kelp. *Proc. R. Soc. B: Biol. Sci.* 286, 20181887. doi: 10.1098/rspb.2018.1887

R Core Team (2017). *R: A language and environment for statistical computing* (Vienna: R Foundation for Statistical Computing). Available at: https://www.R-project.org/.

Sasse, J., Martinoia, E., and Northen, T. (2018). Feed your friends: do plant exudates shape the root microbiome? *Trends Plant Sci.* 23, 25–41. doi: 10.1016/j.tplants.2017.09.003

Sawall, Y., Ito, M., and Pansch, C. (2021). Chronically elevated sea surface temperatures revealed high susceptibility of the eelgrass Zostera marina to winter and spring warming. *Limnol. Oceanogr.* 66, 4112–4124. doi: 10.1002/lno.11947

Scanes, E., Scanes, P., and Ross, P. M. (2020). Climate change rapidly warms and acidifies Australian estuaries. *Nat. Commun.* 11, 1803. doi: 10.1038/s41467-020-15550-z

Serrano, O., Arias-Ortiz, A., Duarte, C. M., Kendrick, G. A., and Lavery, P. S. (2021). "Impact of marine heatwaves on seagrass ecosystems," in *Ecosystem Collapse and Climate Change*. Eds. J. G. Canadell and R. B. Jackson (Springer International Publishing, Cham), 345–364. doi: 10.1007/978-3-030-71330-0_13

Seymour, J. R., Laverock, B., Nielsen, D. A., Trevathan-Tackett, S. M., and Macreadie, P. I. (2018). "The microbiology of seagrasses," in *Seagrasses of Australia: Structure, Ecology and Conservation*. Eds. A. W. D. Larkum, G. A. Kendrick and P. J. Ralph (Springer International Publishing, Cham), 343–392. doi: 10.1007/978-3-319-71354-0_12

Short, F. T., and Duarte, C. M. (2001). Methods for the measurement of seagrass growth and production. *Global Seagrass Res. Methods* 2001, 155–198. doi: 10.1016/B978-044450891-1/50009-8

Short, F., Carruthers, T., Dennison, W., and Waycott, M. (2007). Global seagrass distribution and diversity: a bioregional model. *J. Exp. Mar. Biol. Ecol.* 350 (1–2), 3–20.

Šinkovičová, M., Igaz, D., Aydın, E., and Jarošová, M. (2017). Soil particle size analysis by laser diffractometry: result comparison with pipette method. *IOP Conf. Series: Mater. Sci. Eng.* 245, 072025. doi: 10.1088/1757-899X/245/7/072025

Stadler, M., and del Giorgio, P. A. (2022). Terrestrial connectivity, upstream aquatic history and seasonality shape bacterial community assembly within a large boreal aquatic network. *ISME J.* 16, 937–947. doi: 10.1038/s41396-021-01146-y

Stratil, S. B., Neulinger, S. C., Knecht, H., Friedrichs, A. K., and Wahl, M. (2013). Temperature-driven shifts in the epibiotic bacterial community composition of the brown macroalga *Fucus vesiculosus*. *MicrobiologyOpen* 2, 338–349. doi: 10.1002/mbo3.79

Su, X., Yang, X., Li, H., Wang, H., Wang, Y., Xu, J., et al. (2021). Bacterial communities are more sensitive to ocean acidification than fungal communities in estuarine sediments. *FEMS Microbiol. Ecol.* 97 (5), fiab058. doi: 10.1093/femsec/fiab058

Szitenberg, A., Beca-Carretero, P., Azcárate-García, T., Yergaliyev, T., Alexander-Shani, R., and Winters, G. (2022). Teasing apart the host-related, nutrient-related and temperature-related effects shaping the phenology and microbiome of the tropical seagrass *Halophila stipulacea*. *Environ. Microbiome* 17, 1–17. doi: 10.1186/s40793-022-00412-6

Tarquinio, F., Attlan, O., Vanderklift, M. A., Berry, O., and Bissett, A. (2021). Distinct endophytic bacterial communities inhabiting seagrass seeds. *Front. Microbiol.* 12. doi: 10.3389/fmicb.2021.703014

Tarquinio, F., Hyndes, G. A., Laverock, B., Koenders, A., and Säwström, C. (2019). The seagrass holobiont: understanding seagrass-bacteria interactions and their role in seagrass ecosystem functioning. *FEMS Microbiol. Lett.* 366 (6), fnz057. doi: 10.1093/femsle/fnz057

Thomson, J. A., Burkholder, D. A., Heithaus, M. R., Fourqurean, J. W., Fraser, M. W., Statton, J., et al. (2015). Extreme temperatures, foundation species, and abrupt ecosystem change: an example from an iconic seagrass ecosystem. *Global Change Biol.* 21, 1463–1474. doi: 10.1111/gcb.12694

Trevathan-Tackett, S. M., Brodersen, K. E., and Macreadie, P. I. (2020a). Effects of elevated temperature on microbial breakdown of seagrass leaf and tea litter biomass. *Biogeochemistry* 151, 171–185. doi: 10.1007/s10533-020-00715-1

Trevathan-Tackett, S. M., Jeffries, T. C., Macreadie, P. I., Manojlovic, B., and Ralph, P. (2020b). Long-term decomposition captures key steps in microbial breakdown of seagrass litter. *Sci. Total Environ.* 705, 135806. doi: 10.1016/j.scitotenv.2019.135806

Trevathan-Tackett, S. M., Seymour, J. R., Nielsen, D. A., Macreadie, P. I., Jeffries, T. C., Sanderman, J., et al. (2017). Sediment anoxia limits microbial-driven seagrass carbon remineralization under warming conditions. *FEMS Microbiol. Ecol.* 93 (6), fix033. doi: 10.1093/femsec/fix033

Ugarelli, K., Chakrabarti, S., Laas, P., and Stingl, U. (2017). The seagrass holobiont and its microbiome. *Microorganisms* 5, 81. doi: 10.3390/microorganisms5040081

Uku, J., Björk, M., Bergman, B., and Díez, B. (2007). Characterization and comparison of prokaryotic epiphytes associated with three East African seagrasses. *J. Phycol.* 43 (4), 768–779. doi: 10.1111/j.1529-8817.2007.00371.x

Underwood, A. J., and Chapman, M. G. (1996). Scales of spatial patterns of distribution of intertidal invertebrates. *Oecologia* 107, 212–224. doi: 10.1007/BF00327905

Valle, M., Chust, G., del Campo, A., Wisz, M. S., Olsen, S. M., Garmendia, J. M., et al. (2014). Projecting future distribution of the seagrass Zostera noltii under global warming and sea level rise. *Biol. Conserv.* 170, 74–85. doi: 10.1016/j.biocon.2013.12.017

von Lützow, M., and Kögel-Knabner, I. (2009). Temperature sensitivity of soil organic matter decomposition—what do we know? *Biol. Fertil. Soils* 46, 1–15. doi: 10.1007/s00374-009-0413-8

Waite, D. W., ChuvoChina, M., Pelikan, C., Parks, D. H., Yilmaz, P., Wagner, M., et al. (2020). Proposal to reclassify the proteobacterial classes Deltaproteobacteria and Oligoflexia, and the phylum Thermodesulfobacteria into four phyla reflecting major functional capabilities. *Int. J. Sys. Evolutionary Microbiol.* 70, 5972–6016. doi: 10.1099/ijsem.0.004213

Wang, Q., and Wang, Y. (2011). Optimizing the weight loss-on-ignition methodology to quantify organic and carbonate carbon of sediments from diverse sources. *Environ. Monit. Assess.* 174, 241–257. doi: 10.1007/s10661-010-1454-z

Wardle, D., Bardgett, R., Klironomos, J., Setälä, H., Putten, W., and Wall, D. (2004). Ecological linkages between aboveground and belowground biota. *Sci. (New York N.Y.)* 304, 1629–1633. doi: 10.1126/science.1094875

Waymouth, V., Miller, R. E., Ede, F., Bissett, A., and Aponte, C. (2020). Variation in soil microbial communities: elucidating relationships with vegetation and soil properties, and testing sampling effectiveness. *Plant Ecol.* 221 (9), 837–851. doi: 10.1007/s11258-020-01029-w

Weidner, S., Arnold, W., Stackebrandt, E., and Pühler, A. (2000). Phylogenetic analysis of bacterial communities associated with leaves of the seagrass Halophila stipulacea by a culture-independent small-subunit rRNA gene approach. *Microbial Ecol.* 39, 22–31. doi: 10.1007/s002489900194

Weisburg, W. G., Barns, S. M., Pelletier, D. A., and Lane, D. J. (1991). 16S ribosomal DNA amplification for phylogenetic study. *J. Bacteriol.* 173 (2), 697–703.

York, P. H., Gruber, R. K., Hill, R., Ralph, P. J., Booth, D. J., and Macreadie, P. I. (2013). Physiological and morphological responses of the temperate seagrass Zostera muelleri to multiple stressors: investigating the interactive effects of light and temperature. *PloS One* 8 (10), e76377. doi: 10.1371/journal.pone.0076377

Zhang, Y., Sun, Y., Jiao, N., Stepanauskas, R., and Luo, H. (2016). Ecological genomics of the uncultivated marine roseobacter lineage CHAB-I-5. *Appl. Environ. Microbiol.* 82, 2100–2111. doi: 10.1128/AEM.03678-15

Zhang, X., Zhao, C., Yu, S., Jiang, Z., Liu, S., Wu, Y., et al. (2020). Rhizosphere microbial community structure is selected by habitat but not plant species in two tropical seagrass beds. *Front. Microbiol.* 11. doi: 10.3389/fmicb.2020.00161

frontiers | Frontiers in Microbiology

TYPE Original Research
PUBLISHED 19 June 2024
DOI 10.3389/fmicb.2024.1400343

OPEN ACCESS

EDITED BY
Jin Zhou,
Tsinghua University, China

REVIEWED BY
Guangtao Zhang,
Binzhou Medical University, China
Eun Young Yoon,
Seoul National University, Republic of Korea

*CORRESPONDENCE
Yeong Du Yoo
ydyoo77@kunsan.ac.kr

RECEIVED 13 March 2024
ACCEPTED 10 June 2024
PUBLISHED 19 June 2024

CITATION
Lee MJ, Hwang YJ, Choi YB and Yoo YD (2024) Grazing impact of the calanoid copepods *Acartia* spp. on the toxic dinoflagellate *Alexandrium pseudogonyaulax* in the western coastal waters of Korea. *Front. Microbiol.* 15:1400343. doi: 10.3389/fmicb.2024.1400343

Grazing impact of the calanoid copepods *Acartia* spp. on the toxic dinoflagellate *Alexandrium pseudogonyaulax* in the western coastal waters of Korea

Moo Joon Lee[1], Yeong Jong Hwang[2], Yong Bum Choi[3] and Yeong Du Yoo[3]*

[1]Department of Marine Biotechnology, Anyang University, Incheon, Republic of Korea, [2]School of Earth and Environmental Sciences, College of Natural Sciences, Seoul National University, Seoul, Republic of Korea, [3]Department of Ocenogaphy, College of Ocean Sciences, Kunsan National University, Kunsan, Republic of Korea

Marine dinoflagellate species in the genus *Alexandrium* are well known to produce paralytic shellfish poison as well as common coastal species with cosmopolitan distribution. However, few studies on the feeding of copepods on *Alexandrium* species have been conducted. The toxic dinoflagellate *Alexandrium pseudogonyaulax* contains goniodomin A and causes red tides in many countries. To investigate the relationship between the toxic dinoflagellate *A. pseudogonyaulax* and the calanoid copepods *Acartia* spp., we quantified the ingestion rates of *Acartia* spp. feeding on *A. pseudogonyaulax* as a function of prey concentration. Additionally, we estimated grazing coefficients by integrating data from field observations of *Acartia* spp. and coexisting *A. pseudogonyaulax* with laboratory measurements of ingestion rates obtained during this investigation. Furthermore, we compared the ingestion rates of *Acartia* spp. and other predators feeding on *Alexandrium* species as previously reported. The ingestion rates of *Acartia* spp. on *A. pseudogonyaulax* increased continuously with increasing mean prey concentration. The highest values among the ingestion rate of *Acartia* spp. feeding on *A. pseudogonyaulax* was 3,407 cells predator^{-1} d^{-1} (4,872 ng C predator^{-1} d^{-1}) at the given prey concentration. The calculated grazing coefficients for *Acartia* spp. on *A. pseudogonyaulax* in Shiwha Bay, Korea, were up to 0.073 d^{-1}. The results of this study suggest that *A. pseudogonyaulax* may decrease or maintain the population of *Acartia* spp. in marine food webs.

KEYWORDS

ingestion, food web, metazooplankton, predator, ecology

1 Introduction

Marine dinoflagellates and copepods are important components of aquatic environments (Calbet et al., 2003; Jeong et al., 2010, 2021; Turner et al., 2012; Kim et al., 2013). Marine dinoflagellates are ubiquitous species that can dominate the biomass and density of the marine environment (Jeong et al., 2010, 2013, 2021; Hansen, 2011; Nagarkar et al., 2018; Goswami et al., 2020; Telesh et al., 2021). Copepods are major zooplankton in marine food webs and are

effective grazers of protist prey species and sometimes control dinoflagellate populations (Watras et al., 1985; Campbell et al., 2005; Jeong et al., 2010; Kim et al., 2013). Therefore, to understand the roles and population dynamics of dinoflagellates in marine communities, growth and mortality due to zooplankton predation must be explored.

Marine dinoflagellate species of the genus *Alexandrium* are widely distributed and sometimes cause red tides or harmful algal blooms (Anderson, 1997; Cembella et al., 2000; Grattan et al., 2016; Kremp et al., 2019; Shin et al., 2021). Several species of *Alexandrium* have been well–studied for their physiological and ecological properties, such as toxin profiles, growth rates, distributions, and predation, because they often cause large-scale shellfish mortality and human illnesses due to the toxins they produce (Parkhill and Cembella, 1999; Cembella et al., 2000, 2002; Navarro et al., 2006; Etheridge, 2010; Bill et al., 2016; Grattan et al., 2016; Kim et al., 2016; Kang et al., 2018). Many *Alexandrium* species produce toxins, such as paralytic shellfish poisoning (PSP) and other allelochemicals, which are potentially transferred to marine organisms in higher trophic levels (Cembella et al., 2000; Turner et al., 2005; Sephton et al., 2007; Ma et al., 2011; Anderson et al., 2012; Tillmann et al., 2016). Therefore, they are of interest to government officials, fish consumers, and marine scientists (Alcala et al., 1988; Anderson et al., 2012). Thus, understanding the interactions between dinoflagellates and their consumers is important for understanding the diversity of red tides and harmful algal species (Turner et al., 2006; Jeong et al., 2010; Kim et al., 2013; Yoo et al., 2013; Kang et al., 2018).

In this study, we isolated and established a clonal culture of *Alexandrium pseudogonyaulax* from the coastal waters of Korea (Yoo et al., 2023). In many countries, this species produces goniodomin A, which cause red tides (Matsuoka and Fukuyo, 2003; Bravo et al., 2006; Kremp et al., 2019). Previously, *A. pseudogonyaulax* has been shown to be a phototrophic dinoflagellate. However, this species is a mixotrophic dinoflagellate (Blossom et al., 2012). Several studies have been performed on the taxonomy, ecology, physiology, distribution, bioinformatics, and cysts of this species (Montresor and Marino, 1996; Matsuoka and Fukuyo, 2003; Blossom et al., 2012; Triki et al., 2016; Yoo et al., 2023). However, few studies have been conducted on the mortality of *A. pseudogonyaulax* caused by grazers. Grazing can play an important role in dinoflagellate population dynamics (Watras et al., 1985; Turner et al., 2006; Jeong et al., 2010; Yoo et al., 2013). Copepods are effective grazers of several dinoflagellates (Watras et al., 1985; Jeong et al., 2010; Kim et al., 2013). Thus, to understand the roles and population dynamics of *A. pseudogonyaulax*, the predator–prey relationships between *A. pseudogonyaulax* and copepods was investigated. Additionally, we compared the ingestion rates of *Acartia* spp. in the present study with those of other *Alexandrium* species and dinoflagellates reported in the literature. The results of this study provide a basis for understanding the interactions between *A. pseudogonyaulax* and *Acartia* spp. and their population dynamics in marine planktonic food webs.

2 Materials and methods

2.1 Preparation of experimental organisms

For isolation and culture of *Alexandrium pseudogonyaulax*, plankton samples collected with Niskin sampler were taken from Shiwha Bay, Korea when the water temperature and salinity were 25.4°C and 23.9, respectively (Table 1). These samples were screened through a 202–Nitex mesh and placed in 6–well tissue culture plates (SPL lifesciences, Gyeonggido, Korea). A clonal culture of *A. pseudogonyaulax* was established by performing two serial single–cell isolations. As the concentration of *A. pseudogonyaulax* increased, this species was subsequently transferred to 50–mL and 500–mL polycarbonate (PC) bottles containing fresh f/2–Si medium (Guillard and Ryther, 1962). Freshly filtered seawater was used to fill bottles containing the f/2-Si medium and *A. pseudogonyaulax*. The capped bottles were then incubated at 20°C under illumination of 20 µmol photons m^{-2} s^{-1} of cool white fluorescent light on a 14:10 h light:dark cycle. Once dense cultures of *A. pseudogonyaulax* were obtained, the cells were transferred to new 2–L PC bottles containing fresh f/2-Si medium approximately 3 weeks before the feeding experiments were conducted at a temperature of 15°C.

Copepods were collected Shiwha Bay, Korea, using a 303 µm mesh net when water temperature and salinity were 7.3°C and 27.2, respectively (Table 1). The copepods were acclimatized in a 15°C room in the presence of *Prorocentrum cordatum* for 10 days. Adult female *Acartia* spp. (*A. hongi* and *A. omorii*) were used in the experiments. *A. hongi* and *A. omorii* which co-occur in the western coastal waters of Korea, are very similar and it is impossible to distinguish between these two species when they are alive (Soh and Suh, 2000).

The mean equivalent spherical diameter (ESD) of live *A. pseudogonyaulax* was measured using an electron–particle counter (Coulter Multisizer II; Coulter Corporation, Miami, Florida, United States). The carbon content of this species was estimated based on the cell volume according to Menden-Deuer and Lessard (2000).

2.2 Swimming speed

A dense culture (*ca.* 1,500 cells mL^{-1}) of *A. pseudogonyaulax*, which grew photosynthetically under a 14:10 h light:dark cycle at 20 µmol photons m^{-2} s^{-1} in f/2–Si medium was transferred to a 250–mL PC bottle. Subsequently, an aliquot from the bottle was transferred to a 50–mL cell culture flask and allowed to acclimate for 30 min. The observations were conducted at 20°C using a video analyzing system (SV-C660, Samsung) and a CCD camera (KP-D20BU, Hitachi). The video camera was focused on a field of view within the cell culture flask and observed as a single field under a dissecting microscope at 50× magnification. The mean and maximum swimming velocities of all *A. pseudogonyaulax* cells in motion within the first 10 min were recorded and analyzed. The linear displacement of the cells within a single–frame playback was measured to calculate the average swimming speed. The swimming velocities of 30 cells were assessed.

2.3 Ingestion rates of *Acartia* spp. on *Alexandrium pseudogonyaulax*

This experiment was designed to measure the ingestion and clearance rates of *Acartia* spp. on *A. pseudogonyaulax* as a function of prey concentration (Table 2). Adult female *Acartia* spp. (a combination of *A. hongi* and *A. omorii*) were used in the present study.

TABLE 1 Isolation and maintenance conditions of the experimental organisms.

Organisms	Location	Temp (°C)	Sal	ESD (μm)	Prey species	Concentration (cells mL^{-1})
Alexandrium pseudogonyaulax	Shiwha Bay, Korea	25.4	23.9	24.8		
Acartia spp. (*A. hongi* and *A. omorii*)	Shiwha Bay, Korea	7.3	27.2		*Prorocentrum cordatum*	12,000

ESD, equivalent spherical diameter.

TABLE 2 Experimental design for feeding by the copepods *Acartia* spp. on *Alexandrium pseudogonyaulax*.

Abundance of *Alexandrium pseudogonyaulax*	Abundance of *Acartia* spp. (*A. hongi* and *A. omorii*)
0	20
25 (36)	20
63 (91)	20
132 (189)	20
265 (379)	20
688 (983)	20
1,429 (2,044)	20

The numbers are the initial abundances (cells mL^{-1} for *A. pseudogonyaulax* and inds. L^{-1} for *Acartia* spp.) of *A. pseudogonyaulax* and *Acartia* spp. Values in the parentheses in *A. pseudogonyaulax* are the abundances in ng C mL^{-1}.

For the feeding experiment, the initial concentrations of *A. pseudogonyaulax* were dertermined using an autopipette to deliver predetermined volumes of known cell concentrations to the bottles and those of *Acartia* spp. were obtained by individually transferring *Acartia* spp. using a pasteur pipette. Triplicate 500–mL PC bottles (mixtures of predator and prey) and triplicate control bottles (*A. pseudogonyaulax* prey only) were set up for each predator–prey combination. In order to maintain consistent water conditions, the water from the predator culture was passed through a 0.7 μm GF/F filter before being added to the prey control bottles. The volume of the filtered predator culture added to the experimental bottles for each predator–prey combination was matched with an equal amount of filtered water added to the prey control bottles. All the bottles were filled to capacity with freshly filtered seawater and capped. To determine the initial predator and prey densities, a 10–mL sample was extracted from each bottle and fixed with 1% Lugol's solution for fixation. The fixed sample were examined using a light microscope to determine the abundance of predator and prey species. The cells in three 1–mL Sedgwick-Rafter chambers (SRCs) were counted to determine the actual densities of predator and prey species. The bottles were refilled to capacity with freshly filtered seawater, capped, and placed on rotating wheels at a temperature of 15°C, following the conditions outlined earlier. We considered any dilution of the cultures associated with refilling the bottles when determining the clearance rate. A 10–mL aliquot was taken from each bottle after 24 and 48–h incubation periods and fixed with 1% Lugol's solution. The abundance of prey species was determined by counting all or > 200 cells in three 1–mL SRCs. Following sub–sampling, the bottles were filled with freshly filtered seawater and placed back on rotating wheels. After incubation for 48 h, the *Acartia* spp. were counted. The mortality of *Acartia* spp. occurred until the end of the incubation period. The ingestion and clearance rates were calculated using the equations of Frost (1972).

2.4 Grazing impact

We calculated the grazing coefficients attributable to *Acartia* spp. on *A. pseudogonyaulax* by combining field data on the abundances of *Acartia* spp. and *A. pseudogonyaulax* with the ingestion rates of *Acartia* spp. on *A. pseudogonyaulax* obtained in the present study. Data on the abundance of *Acartia* spp. and co-occurring *A. pseudogonyaulax* used in this estimation were obtained from water samples from Shiwha Bay, Korea using real-time PCR for *A. pseudogonyaulax* and cell counting for *Acartia* spp.

The grazing coefficients (g, d^{-1}) were calculated as follows:

$$g = \mathrm{CR} \times \mathrm{GC} \times 24 \quad (1)$$

where CR is the clearance rate (mL predator^{-1} h^{-1}) of a *Acartia* spp. on *A. pseudogonyaulax* at a given prey concentration and GC is the predator concentration (cells mL^{-1}). The CR values were calculated as follows:

$$\mathrm{CR} = \mathrm{IR} / X \quad (2)$$

where IR is the ingestion rate (cells predator^{-1} h^{-1}) of the predator on the prey and X is the prey concentration (cells mL^{-1}).

2.5 Species-specific primer and probe design and specificity analysis

We developed species-specific primer and probe set for *A. pseudogonyaulax* and obtained the sequences of the internal transcribed spacer region of ribosomal DNA (ITS rDNA) of *A. pseudogonyaulax* and other dinoflagellate species belonging to the *Alexandrium* genus and related dinoflagellate species from GenBank. These sequences were aligned using MEGA v.11. *A. pseudogonyaulax* specific primers and probe were developed by searching the arrangement for unique portions of the ITS rDNA sequences for *A. pseudogonyaulax*. Primer and probe sequences were analyzed using Primer 4 (Whitehead Institute for Biomedical Research, Cambridge, MA, United States) and Oligo Calc: Oligonucleotide Properties Calculator (Kibbe, 2007) to investigate the optimal melting temperature and secondary structure, respectively. Primers and probe were synthesized by Bioneer (Table 3). The probe was dual labeled with the fluorescent dyes FAM and BHQ1 at the 5′ and 3′ ends.

Specificity analysis of the primer and probe sets for *A. pseudogonyaulax* was performed using DNA extracts of *A. pseudogonyaulax* and related dinoflagellate species in the Family Pyrocystaceae. The qPCR reaction mixture contained 1 μL of DNA template, 0.2 μM of specific forward and reverse primers, 0.15 μM of the specific probe, 5 μL of qPCRBIO Probe Separate-ROX (Genepole, Gwangmyeong, Korea), and deionized sterilized water (DDW; Bioneer), with a final total volume of 10 μL. The qPCR assay was conducted using the Rotor-Gene Q (Qiagen, Hilden, Germany). The

TABLE 3 Sequences of the primers and probe for *Alexandrium pseudogonyaulax* used in this study.

Target gene	Analysis	Primer name		Primer sequence (5′ – 3′)	References
ITS rDNA	PCR	ITSF2	Forward	TACGTCCCTGCCCTTTGTAC	Litaker et al. (2003)
		LSU500R	Reverse	CCCTCATGGTACTTGTTTGC	Litaker et al. (2003)
	qPCR	Apsudo_F	Forward	GAAGGTGTGCTTGATCCAATGTAA	This study
		Apseudo_R	Reverse	CACACACAATGGCAAACCTTTCAC	This study
		Apseudo_P	Probe	TGCTTATGGGCTTCTG	This study

ITS, Internal transcribed spacer; PCR, polymerase chain reaction; qPCR, quantitative real-time PCR.

cycling conditions were initialized with a denaturation step at 95°C for 3 min, followed by 40 cycles of 10 s at 95°C for 10 s, and 58°C for 40 s.

2.6 Standard curve construction

A standard curve for exploring the abundance of *A. pseudogonyaulax* was constructed using a qPCR. DNA was extracted from the culture of *A. pseudogonyaulax* (4,200 cells mL^{-1}) in the growth phase using the AccuPrep Genomic DNA Extraction Kit (Bioneer), targeting 1, 10, 100, 1,000, 2,000, and 4,000 *A. pseudogonyaulax* cells. The qPCR assay was performed using the reaction mentioned above under the following thermal cycling conditions: 95°C for 3 min, followed by 45 cycles of 10 s at 95°C for 10 s, and 58°C for 40 s.

2.7 Quantification using qPCR

We developed species-specific primer and probe set for *A. pseudogonyaulax*, and obtained the sequences of the internal transcribed spacer region of ribosomal DNA (ITS rDNA) of *A. pseudogonyaulax* and related dinoflagellates.

The previously mentioned qPCR assay conditions were used to analyse the abundance of *A. pseudogonyaulax* in field samples. The DNA from each sample was amplified four times to ensure the accuracy of results. The sample using DDW as the template was used as a negative control, whereas the one used to construct a standard curve was used as positive and standard control.

3 Results

3.1 Ingestion rates of *Acartia* spp. on *Alexandrium pseudogonyaulax*

The ingestion rate of *Acartia* spp. on *A. pseudogonyaulax* continuously increased with increasing prey concentration (Figure 1). The highest ingestion and clearance rates of *Acartia* spp. on *A. pseudogonyaulax* at the given prey concentration was 3,407 cells *Acartia*$^{-1}$ d^{-1} (4,872 ng C *Acartia*$^{-1}$ d^{-1}) and 192 mL *Acartia*$^{-1}$ h^{-1}, respectively.

3.2 Grazing impact

The grazing coefficients attributable to *Acartia* spp. on co-occurring *A. pseudogonyaulax* in Shiwha Bay, Korea were affected by the abundance of *Acartia* predators (Figure 2). The abundance of *Acartia* spp. and *A. pseudogonyaulax* were 1.5–126.0 cells mL^{-1} and

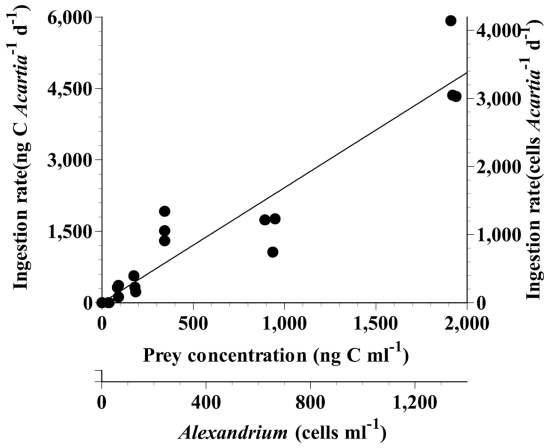

FIGURE 1
Ingestion rates (IR) of *Acartia* spp. (*A. hongi* and *A. omorii*) feeding on *Alexandrium pseudogonyaulax* as a function of mean prey concentration (x). Symbols represent treatment means ± 1 SE. The curves were fitted using the linear regression equation. IR (ng C *Acartia*$^{-1}$ d^{-1}) = 2.42×(x), r^2 = 0.938.

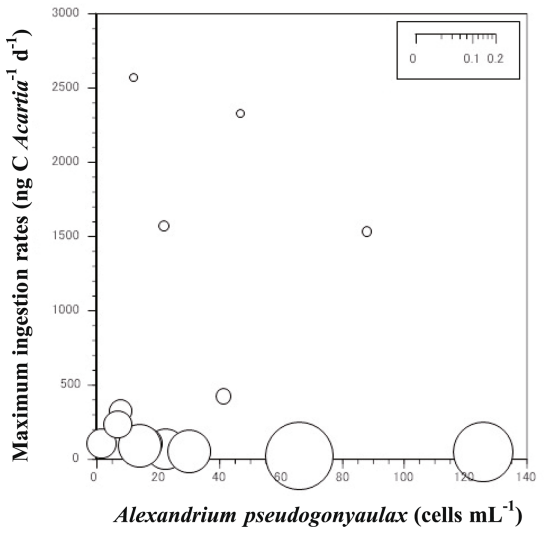

FIGURE 2
Calculated grazing coefficients (g, d^{-1}) of the *Acartia* spp. (*A. hongi* and *A. omorii*) in relation to the population of co-occurring *Alexandrium pseudogonyaulax* in the western coastal waters of Korea.

2–2,570 ind. m^{-3}, respectively. The grazing coefficients attributable to *Acartia* spp. on co-occurring *A. pseudogonyaulax* were 0.001 to 0.073 d^{-1} (i.e., up to 7% of *A. pseudogonyaulax* population could be removed by the copepod *Acartia* spp. in a day).

4 Discussion

The calanoid copepod *Acartia* is a major components metazooplankton in marine environments (Kim et al., 2013; Rice et al., 2015; Lee et al., 2017). Several *Acartia* species such as *Acartia bifilosa*, *Acartia grani*, *Acartia hudsonica,* and *Acartia tonsa* feed on *Alexandrium* spp., including toxic strains of *Alexandrium fundyense, Alexandrium minutum, Aleandrium ostenfeldii,* and *Alexandrium tamarense* and non-toxic strain of *A. tamarense* (Teegarden, 1999; Colin and Dam, 2002, 2003, 2007; da Costa and Fernández, 2002; Teegarden et al., 2003, 2008; da Costa et al., 2008; Sopanen et al., 2011). Among the maximum ingestion rates (MIRs) of *Acartia* grazers on *Alexandrium* prey species, the MIRs were not significantly correlated with the prey (19–28 μm of equivalent spherical diameter) and predator sizes (Figure 3). *Acartia* spp. (*A. hongi* and *A. omorii*) were significantly larger than *A. grani* and *A. tonsa* (Table 4).

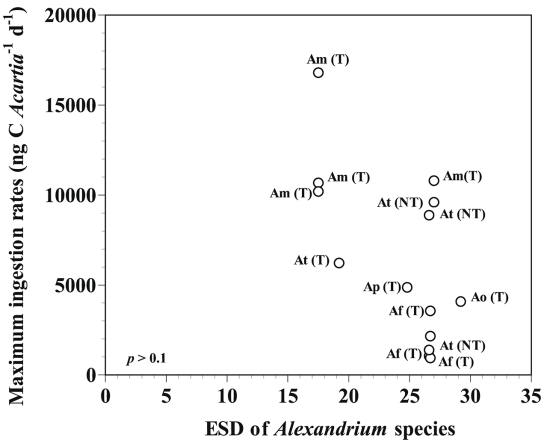

FIGURE 3
Maximum ingestion rates of *Acartia* spp. feeding on *Alexandrium* prey species as a function of prey size (ESD: equivalent spherical diameter, μm). The *p*-value was $p > 0.1$ (linear regression ANOVA). Af (T): toxic strain of *A. fundyense*; Am (T): toxic strain of *A. minutum*; Ao (T): toxic strain of *A. ostenfeldii*; Ap (T): toxic strain of *A. pseudogonyaulax*; At (T): toxic strain of *A. tamarense*; At (NT): non-toxic strain of *A. tamarense*. The data were obtained from Calbet et al. (2003), Colin and Dam (2002, 2003, 2007), da Costa and Fernández (2002), da Costa et al. (2008), Sopanen et al. (2011), Teegarden (1999), and Teegarden et al. (2003, 2008).

Among the MIRs of *Acartia* grazers on *Alexandrium* prey species, the MIR of *A. hudsonica* on the toxic of *A. tamarense* strain was higher than that on the non-toxic strain of *A. tamarense* (Colin and Dam, 2007; Teegarden et al., 2008). Additionally, the MIR of *A. tonsa* on the toxic of *A. fundyense* strain was lower than that on the non-toxic strain of *A. tamarense* (Teegarden, 1999). Thus, the toxicity of *Alexandrium* prey species probably did not affect the MIRs of *Acartia* grazers.

Among the MIRs of *Acartia* grazers on *Alexandrium* prey species, the MIR of *Acartia* spp. on *A. pseudogonyaulax* was higher than *A. bifilosa* on *A. ostenfeldii*, but lower than that of *A. grani* on *A. minutum* (da Costa and Fernández, 2002; da Costa et al., 2008). Many *Alexandrium* species contain PSP toxins; however, the subgenus *Gessnerium* does not produce PSP toxins (Balech, 1995). *A. pseudogonyaulax* belonging to the subgenus *Gessnerium* may not produce PSP toxins, but may produce goniodomin A (Balech, 1995; Matsuoka and Fukuyo, 2003; Bravo et al., 2006). Furthermore, *A. pseudogonyaulax* is a mixotrophic species when mucus traps are used to immobilize prey cells prior to ingestion (Blossom et al., 2012). Therefore, the mucus trap excreted by *A. pseudogonyaulax* may not only function to effectively accumulate toxins but also be used to avoid encounters and ingestion by potential predators.

The motility of dinoflagellates is not only relevant to potential predators but is also important for resource availability (Buskey, 1997; Tillmann and Reckermann, 2002; Jeong et al., 2015, 2017). The

TABLE 4 Comparison of maximum ingestion rates of *Acartia* species on *Alexandrium* species.

Prey species	Temp	Predator species	MIR	References
Alexandrium pseudogonyaulax (T)	20.0	*Acartia* spp. (*A. hongi* and *A. omorii*)	4,872	This study
Alexandrium fundyense (T)	12.0	*Acartia hudsonica*	10,800	Teegarden et al. (2008)
Alexandrium fundyense (T)	14.0	*Acartia hudsonica*	1,060	Colin and Dam (2002)
Alexandrium fundyense (T)	14.0	*Acartia hudsonica*	3,563	Colin and Dam (2003)
Alexandrium fundyense (T)	17.0	*Acartia hudsonica*	948	Teegarden et al. (2003)
Alexandrium fundyense (T)	19.0	*Acartia tonsa*	2,160	Teegarden (1999)
Alexandrium mimutum (T)	15.5	*Acartia grani*	10,680	Calbet et al. (2003)
Alexandrium mimutum (T)	17.5	*Acartia grani*	10,200	da Costa and Fernández (2002)
Alexandrium mimutum (T)	17.5	*Acartia grani*	16,800	da Costa et al. (2008)
Alexandrium osfeldii (T)	11.0	*Acartia bifilosa*	4,080	Sopanen et al. (2011)
Alexandrium tamarense (T)	14.0	*Acartia hudsonica*	6,220	Colin and Dam (2007)
Alexandrium tamarense (NT)	14.0	*Acartia hudsonica*	1,390	Colin and Dam (2002)
Alexandrium tamarense (NT)	14.0	*Acartia hudsonica*	9,600	Teegarden et al. (2008)
Alexandrium tamarense (NT)	19.0	*Acartia tonsa*	8,880	Teegarden (1999)

ESD, equivalent spherical diameter (μm); Temp, temperature (°C); MIR, maximum ingestion rate (ng C Acartia^{-1} d^{-1}); T, toxic strain; NT, non-toxic strain.

swimming speed of *A. pseudogonyaulax* ($n = 30$) was 263–512 μm s^{-1}. The average (±standard error) swimming speed of *A. pseudogonyaulax* was 372 (±12) μm s^{-1}. The maximum swimming speed of *A. pseudogonyaulax* was faster than that of *A. minutum* but slower than that of *A. tamarense* (Kang et al., 2018). Thus, the swimming speed of *Alexandrium* prey species probably did not affect the MIRs of *Acartia* grazers. Other properties, such as the biochemical factors of *Alexandrium* species, may affect the ingestion of *Acartia* grazers more than their physical and behavior properties.

Grazing impacts calculated by using field observation data of *Acartia* spp. and coexisting *A. pseudogonyaulax* with laboratory measurements of ingestion rates suggest that up to 7% of *A. pseudogonyaulax* populations may be eliminated in a day by the copepods *Acartia* spp. Therefore, the copepod *Acartia* species could have a considerable potential grazing impact on *Alexandrium* populations in Shiwha Bay.

Few studies have been conducted on the grazing effects of copepods on *Alexandrium* species in the field. The grazing effect of *A. hudsonica* on *Alexandrium* spp. was 0.8 d^{-1} at Cundy's Harbor (Campbell et al., 2005). In Cape Cod embayment, the grazing pressure of *A. hudsonica* feeding on *A. tamarense* was less than 1% (Turner and Anderson, 1983). Additionally, the grazing coefficients of the copepods such as *Acartia granii* and *Oithona davisae* on *A. minutum* were 0.00003–0.00007 d^{-1} (i.e., up to 0.007% of *Alexandrium* populations could be removed by the copepod populations in a day) in the Arenys de Mar harbor (Calbet et al., 2003). Thus, the copepod *Acartia* species sometimes have a considerable potential grazing impact on populations of *Alexandrium*.

5 Conclusion

The present study investigated the grazing by calanoid copepods *Acartia* spp. on the toxic dinoflagellate *Alexandrium pseudogonyaulax*. The grazing of *Acartia* spp. can affect the abundance of *Alexandrium* populations in many countries. A total of 34 *Alexandrium* species have been reported, but there have been few studies on grazing by metazooplankton on *Alexandrium* spp. (Calbet et al., 2003; Campbell et al., 2005; Guiry and Guiry, 2020). Therefore, constant investigation of feeding by dominant copepods on *Alexandrium* species would be worthwhile to enhance our understanding of the interactions and population dynamics between the copepods and dinoflagellates in natural marine ecosystems.

Data availability statement

The datasets presented in this study can be found in online repositories. The names of the repository/repositories and accession number(s) can be found in the article/supplementary material.

Author contributions

ML: Conceptualization, Investigation, Writing – original draft. YH: Investigation, Writing – original draft. YC: Conceptualization, Investigation, Writing – review & editing. YY: Conceptualization, Investigation, Writing – original draft, Writing – review & editing.

Funding

The author(s) declare that financial support was received for the research, authorship, and/or publication of this article. This research was supported by the National Research Foundation (NRF) of Korea (NRF-2021M3I6A1091272 and NRF-2022R1A2C1004906) and the Korea Institute of Marine Science & Technology Promotion (KIMST) funded by the Ministry of Oceans and Fisheries (KIMST-20220526, KIMST- 20220163 and RS-2023-00256330).

Conflict of interest

The authors declare that the research was conducted in the absence of any commercial or financial relationships that could be construed as a potential conflict of interest.

The author(s) declared that they were an editorial board member of Frontiers, at the time of submission. This had no impact on the peer review process and the final decision.

Publisher's note

References

Alcala, A. C., Alcala, L. C., Garth, J. S., Yasumura, D., and Yasumoto, T. (1988). Human fatality due to ingestion of the crab *Demania reynaudii* that contained a palytoxin-like toxin. *Toxicon* 26, 105–107. doi: 10.1016/0041-0101(88)90142-0

Anderson, D. M. (1997). Bloom dynamics of toxic *Alexandrium* species in the northeastern US. *Limnol. Oceanogr.* 42, 1009–1022. doi: 10.4319/lo.1997.42.5_part_2.1009

Anderson, D. M., Alpermann, T. J., Cembella, A. D., Collos, Y., Masseret, E., and Montresor, M. (2012). The globally distributed genus Alexandrium: multifaceted roles in marine ecosystems and impacts on human health. *Harmful Algae* 14, 10–35. doi: 10.1016/j.hal.2011.10.012

Balech, E. (1995). *The genus Alexandrium Halim (Dinoflagellata). Publ Sherkin is Mar Station*. Cork: Sherkin Island, Co.

Bill, B. D., Moore, S. K., Hay, L. R., Anderson, D. M., and Trainer, V. L. (2016). Effects of temperature and salinity on the growth of *Alexandrium* (Dinophyceae) isolates from the Salish Sea. *J. Phycol.* 52, 230–238. doi: 10.1111/jpy.12386

Blossom, H., Daugbjerg, N., and Hansen, P. J. (2012). Toxic mucus traps: a novel mechanism that mediates prey uptake in the mixotrophic dinoflagellate *Alexandrium pseudogonyaulax*. *Harmful Algae* 17, 40–53. doi: 10.1016/j.hal.2012.02.010

Bravo, I., Garcés, E., Diogène, J., Fraga, S., Sampedro, N., and Figueroa, R. I. (2006). Resting cysts of the toxigenic dinoflagellate genus *Alexandrium* in recent sediments from the Western Mediterranean coast, including the first description of cysts of *A. kutnerae* and *A. peruvianum*. *Eur. J. Phycol.* 41, 293–302. doi: 10.1080/09670260600810360

Buskey, E. J. (1997). Behavioral components of feeding selectivity of the heterotrophic dinoflagellate *Protoperidinium pellucidum*. *Mar. Ecol. Prog. Ser.* 153, 77–89. doi: 10.3354/meps153077

Calbet, A., Vaqué, D., Felipe, J., Vila, M., Sala, M. M., Alcaraz, M., et al. (2003). Relative grazing impact of microzooplankton and mesozooplankton on a bloom of the toxic dinoflagellate *Alexandrium minutum*. *Mar. Ecol. Prog. Ser.* 259, 303–309. doi: 10.3354/meps259303

Campbell, R. G., Teegarden, G. J., Cembella, A. D., and Durbin, E. G. (2005). Zooplankton grazing impacts on *Alexandrium* spp. in the nearshore environment of the Gulf of Maine. *Deep Sea Res. II Top. Stud. Oceanogr.* 52, 2817–2833. doi: 10.1016/j.dsr2.2005.06.008

Cembella, A. D., Lewis, N. I., and Quilliam, M. A. (2000). The marine dinoflagellate *Alexandrium ostenfeldii* (Dinophyceae) as the causative organism of spirolide shellfish toxins. *Phycologia* 39, 67–74. doi: 10.2216/i0031-8884-39-1-67.1

Cembella, A. D., Quilliam, M. A., Lewis, N. I., Bauder, A. G., Dell'Aversano, C., Thomas, K., et al. (2002). The toxigenic marine *dinoflagellate Alexandrium tamarense* as the probable cause of mortality of caged salmon in Nova Scotia. *Harmful Algae* 1, 313–325. doi: 10.1016/S1568-9883(02)00048-3

Colin, S. P., and Dam, H. G. (2002). Latitudinal differentiation in the effects of the toxic dinoflagellate *Alexandrium* spp. on the feeding and reproduction of populations of the copepod *Acartia hudsonica*. *Harmful Algae* 1, 113–125. doi: 10.1016/S1568-9883(02)00007-0

Colin, S. P., and Dam, H. G. (2003). Effects of the toxic dinoflagellate *Alexandrium fundyense* on the copepod *Acartia hudsonica*: a test of the mechanisms that reduce ingestion rates. *Mar. Ecol. Prog. Ser.* 248, 55–65. doi: 10.3354/meps248055

Colin, S. P., and Dam, H. G. (2007). Comparison of the functional and numerical responses of resistant versus non-resistant populations of the copepod *Acartia hudsonica* fed the toxic dinoflagellate *Alexandrium tamarense*. *Harmful Algae* 6, 875–882. doi: 10.1016/j.hal.2007.05.003

da Costa, R. M., and Fernández, F. (2002). Feeding and survival rates of the *copepods Euterpina acutifrons* Dana and *Acartia grani* Sars on the dinoflagellates *Alexandrium minutum* Balech and *Gyrodinium corsicum* Paulmier and the Chryptophyta *Rhodomonas baltica* Karsten. *J. Exp. Mar. Biol. Ecol.* 273, 131–142. doi: 10.1016/S0022-0981(02)00132-6

da Costa, R. M., Pereira, L. C. C., and Fernández, F. (2008). Effects of toxic *Alexandrium minutum* strains on the feeding and survival rates of pelagic marine copepods *Acartia grani* and *Euterpina acutifrons*. *Hydrobiologia* 614, 55–63. doi: 10.1007/s10750-008-9536-4

Etheridge, S. M. (2010). Paralytic shellfish poisoning: seafood safety and human health perspectives. *Toxicon* 56, 108–122. doi: 10.1016/j.toxicon.2009.12.013

Frost, B. W. (1972). Effects of size and concentration of food particles on the feeding behavior of the marine planktonic copepod *Calanus pacificus*. *Limnol. Oceanogr.* 17, 805–815. doi: 10.4319/lo.1972.17.6.0805

Goswami, P., Gupta, S., Das, A. K., Vinithkumar, N. V., Dharani, G., and Kirubagaran, R. (2020). Impact of a dinoflagellate bloom on the marine plankton community structure of Port Blair Bay, Andaman Island. *Reg. Stud. Mar. Sci.* 37:101320. doi: 10.1016/j.rsma.2020.101320

Grattan, L. M., Holobaugh, S., and Morris, J. G. Jr. (2016). Harmful algal blooms and public health. *Harmful Algae* 57, 2–8. doi: 10.1016/j.hal.2016.05.003

Guillard, R. R. L., and Ryther, J. H. (1962). Studies of marine planktonic diatoms. I. *Cyclotella nana* Hustedt and *Detonula confervacea* (Cleve) gran. *Can. J. Microbiol.* 8, 229–239. doi: 10.1139/m62-029

Guiry, M. D., and Guiry, G. M. (2020). *Algae Base*. Galway: World-wide Electronic Publication, National University of Ireland.

Hansen, P. J. (2011). The role of photosynthesis and food uptake for the growth of marine mixotrophic dinoflagellates. *J. Eukaryot. Microbiol.* 58, 203–214. doi: 10.1111/j.1550-7408.2011.00537.x

Jeong, H. J., Kang, H. C., Lim, A. S., Jang, S. H., Lee, K., Lee, S. Y., et al. (2021). Feeding diverse prey as an excellent strategy of mixotrophic dinoflagellates for global dominance. *Sci. Adv.* 7:eabe4214. doi: 10.1126/sciadv.abe4214

Jeong, H. J., Kim, J. S., Lee, K. H., Seong, K. A., Yoo, Y. D., Kang, N. S., et al. (2017). Differential interactions between the nematocyst-bearing mixotrophic dinoflagellate *Paragymnodinium shiwhaense* and common heterotrophic protists and copepods: killer or prey. *Harmful Algae* 62, 37–51. doi: 10.1016/j.hal.2016.12.005

Jeong, H. J., Lim, A. S., Franks, P. J. S., Lee, K. H., Kim, J. H., Kang, N. S., et al. (2015). A hierarchy of conceptual models of red-tide generation: nutrition, behavior, and biological interactions. *Harmful Algae* 47, 97–115. doi: 10.1016/j.hal.2015.06.004

Jeong, H. J., Yoo, Y. D., Kim, J. S., Seong, K. A., Kang, N. S., and Kim, T. H. (2010). Growth, feeding and ecological roles of the mixotrophic and heterotrophic dinoflagellates in marine planktonic food webs. *Ocean Sci. J.* 45, 65–91. doi: 10.1007/s12601-010-0007-2

Jeong, H. J., Yoo, Y. D., Kim, T. H., Seong, K. A., Kang, N. S., Lee, K. H., et al. (2013). Red tides in Masan Bay, Korea in 2004-2005: I. Daily variations in the abundance of red-tide organisms and environmental factors. *Harmful Algae* 30S, S75–S88. doi: 10.1016/j.hal.2013.10.008

Kang, H. C., Jeong, H. J., Kim, S. J., You, J. H., and Ok, J. H. (2018). Differential feeding by common heterotrophic protists on 12 different *Alexandrium* species. *Harmful Algae* 78, 106–117. doi: 10.1016/j.hal.2018.08.005

Kibbe, W. A. (2007). OligoCalc: an online oligonucleotide properties calculator. *Nucleic Acids Res.* 35, W43–W46. doi: 10.1093/nar/gkm234

Kim, J. H., Jeong, H. J., Lim, A. S., Rho, J. R., and Lee, S. B. (2016). Killing potential protest predators as a survival strategy of the newly described dinoflagellate *Alexandrium pohangense*. *Harmful Algae* 55, 41–55. doi: 10.1016/j.hal.2016.01.009

Kim, J. S., Jeong, H. J., Yoo, Y. D., Kang, N. S., Kim, S. K., Song, J. Y., et al. (2013). Red tides in Masan Bay, Korea, in 2004-2005: III. Daily variations in the abundance of metazooplankton and their grazing impacts on red-tides organisms. *Harmful Algae* 30, S102–S113. doi: 10.1016/j.hal.2013.10.010

Kremp, A., Hansen, P. J., Tillmann, U., Savela, H., Suikkanen, S., Voß, D., et al. (2019). Distributions of three *Alexandrium* species and their toxins across a salinity gradient suggest an increasing impact of GDA producing *a. pseudogonyaulax* in shallow brackish waters of northern Europe. *Harmful Algae* 87:101622. doi: 10.1016/j.hal.2019.101622

Lee, M. J., Jeong, H. J., Kim, J. S., Jang, K. K., Kang, N. S., Jang, S. H., et al. (2017). Ichthyotoxic *Cochlodinium polykrikoides* red tides offshore in the South Sea, Korea in 2014: III. Metazooplankton and their grazing impacts on red-tide organisms and heterotrophic protists. *Algae* 32, 285–308. doi: 10.4490/algae.2017.32.11.28

Litaker, R. W., Vandersea, M. W., Kibler, S. R., Reece, K. S., Stokes, N. A., Steidinger, K. A., et al. (2003). Identification of *Pfiesteria piscicida* (Dinophyceae) and *Pfiesteria*-like organisms using internal transcribed spacer-specific PCR assays. *J. Phycol.* 39, 754–761. doi: 10.1046/j.1529-8817.2003.02112.x

Ma, H., Krock, B., Tillmann, U., Bickmeyer, U., Graeve, M., and Cembella, A. (2011). Mode of action of membrane-disruptive lytic compounds from the marine dinoflagellate *Alexandrium tamarense*. *Toxicon* 58, 247–258. doi: 10.1016/j.toxicon.2011.06.004

Matsuoka, K., and Fukuyo, Y. (2003). "Taxonomy of cysts" in *Manual on Harmful Marine Microalgae* (Paris: UNESCO), 563–592.

Menden-Deuer, S., and Lessard, E. J. (2000). Carbon to volume relationships for dinoflagellates, diatoms, and other protist plankton. *Limnol. Oceanogr.* 45, 569–579. doi: 10.4319/lo.2000.45.3.0569

Montresor, M., and Marino, D. (1996). Modulating effect of cold-dark storage on excystment in *Alexandrium pseudogonyaulax* (Dinophycea). *Mar. Biol.* 127, 55–60. doi: 10.1007/BF00993643

Nagarkar, M., Countway, P. D., Yoo, Y. D., Daniels, E., Poulton, N. J., and Palenik, B. (2018). Temporal dynamics of eukaryotic microbial diversity at a coastal Pacific site. *ISME J.* 12, 2278–2291. doi: 10.1038/s41396-018-0172-3

Navarro, J. M., Muñoz, M. G., and Contreras, A. M. (2006). Temperature as a factor regulating growth and toxin content in the dinoflagellate *Alexandrium catenella*. *Harmful Algae* 5, 762–769. doi: 10.1016/j.hal.2006.04.001

Parkhill, J. P., and Cembella, A. D. (1999). Effects of salinity, light and inorganic nitrogen on growth and toxigenicity of the marine dinoflagellate *Alexandrium tamarense* from northeastern *Canada*. *J. Plankton Res.* 21, 939–955. doi: 10.1093/plankt/21.5.939

Rice, E., Dam, H. G., and Stewart, G. (2015). Impact of climate change on estuarine zooplankton: surface water warming in Long Island sound is associated with changes in copepod size and community structure. *Estuar. Coasts* 38, 13–23. doi: 10.1007/s12237-014-9770-0

Sephton, D. H., Haya, K., Martin, J. L., LeGresley, M. M., and Page, F. H. (2007). Paralytic shellfish toxins in zooplankton, mussels, lobsters and caged Atlantic salmon, *Salmo salar*, during a bloom of *Alexandrium fundyense* off grand Manan Island, in the bay of Fundy. *Harmful Algae* 6, 745–758. doi: 10.1016/j.hal.2007.03.002

Shin, H. H., Li, Z., Kim, H. J., Park, B. S., Lee, J., Shin, A. Y., et al. (2021). *Alexandrium catenella* (group I) and *A. pacificum* (group IV) cyst germination, distribution, and toxicity in Jinhae-Masan Bay, Korea. *Harmful Algae* 110:102122. doi: 10.1016/j.hal.2021.102122

Soh, H. Y., and Suh, H. L. (2000). A new species of *Acartia* (Copepoda, Calanoida) from the Yellow Sea. *J. Plankton Res.* 22, 321–337. doi: 10.1093/plankt/22.2.321

Sopanen, S., Setälä, O., Piiparinen, J., Erler, K., and Kremp, A. (2011). The toxic dinoflagellate *Alexandrium ostenfeldii* promotes incapacitation of the calanoid copepods *Eurytemora affinis* and *Acartia bifilosa* from the northern Baltic Sea. *J. Plankton Res.* 33, 1564–1573. doi: 10.1093/plankt/fbr052

Teegarden, G. J. (1999). Copepod grazing selection and particle discrimination on the basis of PSP toxin content. *Mar. Ecol. Prog. Ser.* 181, 163–176. doi: 10.3354/meps181163

Teegarden, G., Campbell, R. G., Anson, D. T., Ouellett, A., Westman, B. A., and Durbin, E. G. (2008). Copepod feeding response to varying *Alexandrium* spp. cellular toxicity and cell concentration among natural plankton samples. *Harmful Algae* 7, 33–44. doi: 10.1016/j.hal.2007.05.010

Teegarden, G. J., Cembella, A. D., Capuano, C. L., Barron, S. H., and Durbin, E. G. (2003). Phycotoxin accumulation in zooplankton feeding on *Alexandrium fundyense*–vector or sink? *J. Plankton Res.* 25, 429–443. doi: 10.1093/plankt/25.4.429

Telesh, I., Schubert, H., and Skarlato, S. (2021). Abiotic stability promotes dinoflagellate blooms in marine coastal ecosystems. *Estuar. Coast. Shelf Sci.* 251:107239. doi: 10.1016/j.ecss.2021.107239

Tillmann, U., Krock, B., Alpermann, T. J., and Cembella, A. (2016). Bioactive compounds of marine dinoflagellate isolates from western Greenland and their phylogenetic association within the genus *Alexandrium*. *Harmful Algae* 51, 67–80. doi: 10.1016/j.hal.2015.11.004

Tillmann, U., and Reckermann, M. (2002). Dinoflagellate grazing on the raphidophyte *Fibrocapsa japonica*. *Aquat. Microb. Ecol.* 26, 247–257. doi: 10.3354/ame026247

Triki, H. Z., Laabir, M., Moeller, P., Chomérat, N., and Daly-Yahia, O. K. (2016). First report of goniodomin a production by the dinoflagellate *Alexandrium pseudogonyaulax*

developing in southern Mediterranean (Bizerte lagoon, Tunisia). *Toxicon* 111, 91–99. doi: 10.1016/j.toxicon.2015.12.018

Turner, J. T., and Anderson, D. M. (1983). Zooplankton grazing during dinoflagellate blooms in a Cape Cod embayment, with observations of predation upon tintinnids by copepods. *Mar. Ecol.* 4, 359–374. doi: 10.1111/j.1439-0485.1983.tb00119.x

Turner, J. T., Borkman, D. G., and Hunt, C. D. (2006). Zooplankton of Massachusetts Bay, USA, 1992–2003: relationships between the copepod *Calanus finmarchicus* and the North Atlantic oscillation. *Mar. Ecol. Prog. Ser.* 311, 115–124. doi: 10.3354/meps311115

Turner, J. T., Doucette, G. J., Keafer, B. A., and Anderson, D. M. (2005). Trophic accumulation of PSP toxins in zooplankton during *Alexandrium fundyense* blooms in Casco bay, gulf of Maine, April–June 1998. II: zooplankton abundance and size-fractionated community composition. *Deep Sea Res. II Top. Stud. Oceanogr.* 52, 2784–2800. doi: 10.1016/j.dsr2.2005.06.012

Turner, J. T., Roncalli, V., Ciminiello, P., Dell'Aversano, C., Fattorusso, E., Tartaglione, L., et al. (2012). Biogeographic effects of the Gulf of Mexico red tide dinoflagellate *Karenia brevis* on Mediterranean copepods. *Harmful Algae* 16, 63–73. doi: 10.1016/j.hal.2012.01.006

Watras, C. J., Garcon, V. C., Olson, R. J., Chishom, S. W., and Anderson, D. M. (1985). The effect of zooplankton grazing on estuarine blooms of the toxic dinoflagellate *Gonyaulax tamarensis*. *J. Plankton Res.* 7, 891–908. doi: 10.1093/plankt/7.6.891

Yoo, Y. D., Hwang, Y. J., and Lee, M. J. (2023). Morphological and molecular characterization of the toxic dinoflagellate *Alexandrium pseudogonyaulax* in Korea. *Kor. J. Hydrogr. Mar. Spat. Informat* 12, 47–55.

Yoo, Y. D., Jeong, H. J., Kim, J. S., Kim, T. H., Kim, J. H., Seong, K. A., et al. (2013). Red tides in Masan Bay, Korea in 2004–2005: II. Daily variations in the abundance of heterotrophic protists and their grazing impact on red-tide organisms. *Harmful Algae* 30S, S89–S101. doi: 10.1016/j.hal.2013.10.009

frontiers | Frontiers in Microbiology

TYPE Original Research
PUBLISHED 19 August 2024
DOI 10.3389/fmicb.2024.1417651

OPEN ACCESS

EDITED BY
Jin Zhou,
Tsinghua University, China

REVIEWED BY
Chad Larson,
Washington State Department of Ecology, United States
Guntram Weithoff,
University of Potsdam, Germany

*CORRESPONDENCE
Lijuan Ren
✉ lijuanren@jnu.edu.cn

†These authors have contributed equally to this work

RECEIVED 15 April 2024
ACCEPTED 31 July 2024
PUBLISHED 19 August 2024

CITATION
Peng Y, Wu C, Ma G, Chen H, Wu QL, He D, Jeppesen E and Ren L (2024) Insight into diversity change, variability and co-occurrence patterns of phytoplankton assemblage in headwater streams: a study of the Xijiang River basin, South China. *Front. Microbiol.* 15:1417651. doi: 10.3389/fmicb.2024.1417651

Insight into diversity change, variability and co-occurrence patterns of phytoplankton assemblage in headwater streams: a study of the Xijiang River basin, South China

Yuyang Peng[1†], Chuangfeng Wu[1†], Guibin Ma[1], Haiming Chen[1], Qinglong L. Wu[2,3], Dan He[2], Erik Jeppesen[4,5,6,7] and Lijuan Ren[1*]

[1]Department of Ecology and Institute of Hydrobiology, Jinan University, Guangzhou, China, [2]Center for Evolution and Conservation Biology, Southern Marine Sciences and Engineering Guangdong Laboratory, Guangzhou, China, [3]State Key Laboratory of Lake Science and Environment, Nanjing Institute of Geography and Limnology, Chinese Academy of Sciences, Nanjing, China, [4]Sino-Danish Centre for Education and Research, University of Chinese Academy of Sciences, Beijing, China, [5]Department of Ecoscience, Aarhus University, Aarhus, Denmark, [6]Limnology Laboratory, Department of Biological Sciences and Centre for Ecosystem Research and Implementation, Middle East Technical University, Ankara, Türkiye, [7]Institute for Ecological Research and Pollution Control of Plateau Lakes, School of Ecology and Environmental Science, Yunnan University, Kunming, China

Phytoplankton has been used as a paradigm for studies of coexistence of species since the publication of the "paradox of the plankton." Although there are a wealth of studies about phytoplankton assemblages of lakes, reservoirs and rivers, our knowledge about phytoplankton biodiversity and its underlying mechanisms in mountain headwater stream ecosystems is limited, especially across regional scales with broad environmental gradients. In this study, we collected 144 phytoplankton samples from the Xijiang headwater streams of the Pearl River across low altitude (< 1,000 m) located in Guangxi province, intermediate altitude (1,000 m < altitude <2,000 m) in Guizhou province and high altitude (> 2,000 m) in Yunnan province of China. Our study revealed high phytoplankton diversity in these streams. Freshwater phytoplankton, including cyanobacteria, Bacillariophyta, Chlorophyta, Rhodophyta, Chrysophyta, Euglenophyta, Glaucophyta, Phaeophyta and Cryptophyta, were all detected. However, phytoplankton alpha diversity exhibited a monotonic decreasing relationship with increasing altitude. High altitudes amplified the "isolated island" effect of headwater streams on phytoplankton assemblages, which were characterized by lower homogeneous selection and higher dispersal limitation. Variability and network vulnerability of phytoplankton assemblages increased with increasing altitudes. Our findings demonstrated diversity, variability and co-occurrence patterns of phytoplankton assemblages linked to environmental factors co-varying with altitude across regional scales.

KEYWORDS

headwater streams, phytoplankton diversity, region-scale biogeography, assembly processes, variability and vulnerability

1 Introduction

Since the publication of the "paradox of the plankton" (Hutchinson, 1961), phytoplankton has been considered a useful paradigm system for exploring the mechanisms maintaining high biodiversity. Environmental factors such as temperature and nutrient availability have been demonstrated to influence phytoplankton biodiversity (Irigoien et al., 2004; Morán et al., 2010; Vallina et al., 2014; Verbeek et al., 2018; Chang et al., 2022). Although there is wealth of scientific information about freshwater phytoplankton assemblages of lakes, reservoirs and rivers (Caputo et al., 2008; Naselli-Flores, 2014; Lu and Gan, 2015; Hu et al., 2017; Yu et al., 2023; Stanković et al., 2024), our knowledge about phytoplankton biodiversity and its underlying mechanisms in mountain stream ecosystems is limited (Wang et al., 2016, 2021; de Oliveira et al., 2020; Fodelianakis et al., 2022). Biodiversity of mountains have been studied intensively for more than 250 years, originating with Linnaeus (1781) and Von Humboldt (1849). However, uncovering the mechanisms underlying the extraordinary biodiversity in mountain areas remains a great challenge (Rahbek et al., 2019a; Trew and Maclean, 2021). It is unclear whether the general high abundance, small size, fast population growth and long-range dispersal of algae is sufficient to avoid altitude constrains in mountain stream ecosystems.

Mountain stream ecosystems, including headwater streams, are downstream sources for new propagules, which play an important role in maintaining region-scale aquatic phytoplankton biodiversity and ecosystem services (Sharma et al., 2016; de Oliveira et al., 2020; Zeng et al., 2023), but many are under threat due to ongoing environmental changes, such as habitat loss, pollution, mine drainage, and global warming (Trew and Maclean, 2021; Schmeller et al., 2022). Understanding the altitudinal patterns of phytoplankton assemblages and their underlying mechanisms in such ecosystems is, therefore, essential to predict their response to future environmental changes and to develop water management policies to mitigate the pressures of environmental changes on biodiversity loss (Cardinale et al., 2012; Trew and Maclean, 2021; Schmeller et al., 2022). In the Pearl River Basin of China, headwater streams cover a broad altitudinal gradient, spanning from approximately 320 to 2,220 m (Liu and Han, 2021b), thus providing an ideal altitudinal gradient for a study of phytoplankton biodiversity patterns. In the largest branch of the Pearl River Basin, the Xijiang River area, mountains or hills may contribute to local coexistence of diverse phytoplankton in its headwater ecosystems in three different ways: (i) by creating heterogeneous climatic habitats for phytoplankton within narrow geographical ranges; (ii) by functioning as dispersal barriers to neighboring "isolated island" headwater streams; (iii) by being a modifier of environmental, hydrological and mineralogical conditions (Vetaas et al., 2019; Rahbek et al., 2019b). Climatic, environmental, hydrological and mineralogical fluctuations across altitudinal gradients might result in diverse non-equilibrium dynamics of phytoplankton in local headwater streams (Naselli-Flores et al., 2003a,b). The diversity of phytoplankton in headwater streams of the Xijiang River area might thus expectedly be characterized by higher coexistence at lower altitudes, where environmental filtering and dispersal barriers may be weaker than any other altitudinal areas (Stomp et al., 2011; Vetaas et al., 2019). In addition, the heterogeneous climatic, environmental, hydrological and mineralogical conditions along the altitudinal gradients may alter the influence of the four key processes that control the biodiversity of phytoplankton on mountains or hills: speciation, dispersal, selection and drift (Rahbek et al., 2019b; Wang et al., 2021, 2022; Pritsch et al., 2023). For instance, seasonal changes in environmental variables at higher altitudes may lead to the loss of phytoplankton species by selecting phytoplankton taxa with a broad range of environmental tolerance (Currie et al., 2004). Temperature, which has direct linkages with altitude, might also impact phytoplankton biodiversity through impacting their physiological metabolisms (Brown et al., 2004; Allen and Gillooly, 2007; Gillooly and Allen, 2007; Stomp et al., 2011). In addition, as precipitation is lower at higher altitudes in the Xijiang River area (Zeng and Han, 2020a,b), the dispersal rates of phytoplankton by atmospheric water circulation might be limited, resulting in an enhanced "isolated island" effect of mountain headwater streams on phytoplankton assemblages. Phytoplankton assemblages in headwater streams might thus exhibit higher variability at higher altitudes. Diversity loss and increased variability of phytoplankton assemblage at higher altitudes might furthermore cause higher network vulnerability of the co-occurrence of phytoplankton to climatic, environmental, hydrological and mineralogical fluctuations. In a co-occurrence network, vulnerability is a measure of the relative contribution of the phytoplankton taxa to the global efficiency. It is accompanied by various network indices, including node or link quantity, network components and heterogeneity, keystone species and modularity (Dunne et al., 2002; Grilli et al., 2016; Yuan et al., 2021). Network vulnerability is an important index that can provide information on how fast the consequence of environmental/ecological fluctuations traverse to parts or the entire co-occurrence network (Yuan et al., 2021).

To explore species coexistence of phytoplankton, we constructed a community assembly framework (Ning et al., 2020) and co-occurrence networks (Yuan et al., 2021) in headwater streams to elucidate the biodiversity patterns of phytoplankton along an altitudinal gradient (Figure 1). Prior research shows that dispersal limitation, homogenizing dispersal, homogeneous and heterogeneous selection, and drift play different roles in controlling regional-scale biodiversity and co-occurrence patterns of phytoplankton (Guelzow et al., 2017; Klais et al., 2017; Kruk et al., 2021). More substantial seasonal changes, lower temperatures, and higher UV radiation at higher altitudes may impose stronger homogeneous or heterogeneous selection on phytoplankton assemblages. Conversely, lower immigration rates at higher altitudes potentially result in stronger dispersal limitation of phytoplankton among headwater streams. Changed balance of community assembly processes along altitude gradient may have influences on the patterns of diversity, variability and network vulnerability of phytoplankton in headwater streams. Therefore, we hypothesized that in headwater streams in the Xijiang River area: (1) "isolated island" effect of mountain headwater streams on phytoplankton assemblage might be enhanced by altitudes; (2) coexistences of diverse phytoplankton would occur at low altitudes, with lower variability and lower vulnerability of the co-occurrence phytoplankton taxa at lower altitudes; (3) the phytoplankton assemblage along the altitude gradient would be shaped by the balance of selection, dispersal and stochastic drift. To test these three hypotheses, we used high-throughput sequencing to study 144 phytoplankton samples collected in the Xijiang headwater streams of the Pearl River in southern China. The locations covered a broad gradient of altitude, spanning from approximately 320 to 2,220 m

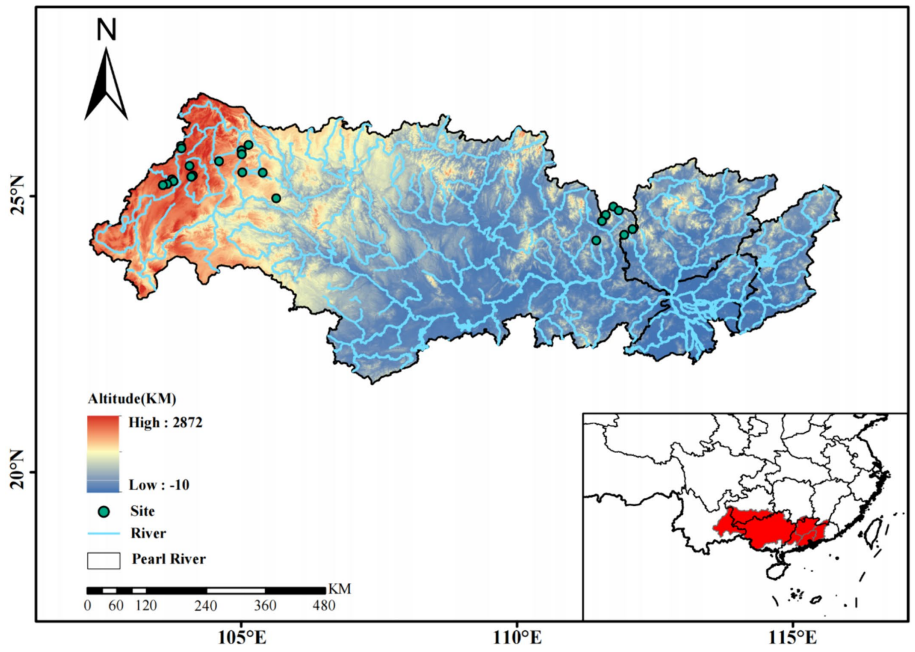

FIGURE 1
The location of sampling sites in headwater streams in the Xijiang River basin, South China.

(Zeng and Han, 2020a; Liu and Han, 2021a), which provides an ideal altitudinal gradient for the study of phytoplankton biodiversity patterns.

2 Materials and methods

2.1 Study area at the Xijiang River

The Zhujiang River (Pearl River), located in South-East China, is the second largest river by discharge or the third largest river by length (approximately 2,300 km) in China (Zeng and Han, 2020a,b). Among the four parts of the Pearl River (the Xijiang River, the Beijiang River, the Dongjiang River, and the Zhujiang delta water system), the Xijiang River is the largest tributary of the Pearl River and is famous for its karst landform (Liu and Han, 2021b). The Xijiang River originates in the Yunnan-Guizhou plateau (Maxiong mountain) and then flows through Yunnan, Guizhou, Guangxi and Guangdong Provinces and discharges into the South China Sea (Liu and Han, 2021a,b). There are mountains and hills with altitudes ranging from approximately 300 to 2,300 m in the Xijiang River area. The soil in the region, consists Precambrian metamorphic rocks and Quaternary fluvial sediments (Liu and Han, 2021a; Liu et al., 2022). Permian and Triassic carbonate bedrocks dominate in the upper headwater of the Xijiang River basin, and these Karst geomorphologic phenomena are well developed (Li et al., 2020). The lower headwater of the river basin is primarily characterized by siliceous sedimentary rocks and magmatic and metamorphic rocks (Liu and Han, 2021b). The river is affected by the sub-tropic monsoon climate, with an annual mean temperature ranging from 14°C to 22°C and the annual mean rainfall between 1,200 and 2,200 mm/year (Zeng and Han, 2020b; Liu and Han, 2021b). Precipitation is concentrated in the wet season (April to September temporally) and decreases spatially toward the west (Zeng and Han, 2020a,b).

2.2 Sample collection and analysis

From November 2020 to January 2021, 144 phytoplankton samples were collected at 24 stations along the headwater streams (54 samples in Yunnan province, 42 samples in Guizhou province, 48 samples in Guangxi province) (Figure 1). These headwater streams are the source streams at the initiation points of all Xijiang River networks. These headwater streams have small size with an average depth of 0.28 m and an average flow velocity of 0.045 $m \cdot s^{-1}$. At each station, phytoplankton samples (1 to 2 L water, 3 replicates) were collected from surface waters. We separated the samples into cell size >3 μm (primarily micro- and nanophytoplankton) and sizes ranging from 0.2 to 3 μm (primarily picophytoplankton) by filtering the samples through 3-μm-pore-size Isopore filters (Millipore, Billerica, MA, United States), followed by filtration through 0.2-μm-pore-size Isopore filters (Millipore, Billerica, MA, United States). The filters were stored at −80°C for further analyses.

Dissolved oxygen (DO), pH, conductivity and oxidation–reduction potential (ORP) were measured *in situ* using a YSI multiparameter probe (YSI Proplus, Yellow Springs, OH, United States). Depth of the stream (depth) and flow velocity (velocity) were also measured *in situ*. Monthly mean temperature (MMT) was obtained by extracting layer information using ArcGIS. Ammonium (NH_4^+), nitrate (NO_3^-), nitrite (NO_2^-), total nitrogen (TN), total phosphorus (TP), phosphate (PO_4^{3-}), silicate (SiO_3^{2-}), total content of Fe^{3+} (Fe^{3+}), total content of Mn^{2+} (Mn^{2+}), total content of Ca^{2+} (Ca^{2+}), total content of Mg^{2+} (Mg^{2+}), total organic carbon (TOC) and chlorophyll *a* (Chla) were measured in the laboratory according to standard methods (Greenberg et al., 1992).

2.3 DNA extraction, amplification, sequencing and data processing

Genomic DNA was extracted using the DNeasy PowerWater DNA Isolation Kit (QIAGEN, Hilden, Germany). The V4 hyper-variable region of the 16S rRNA genes was amplified with primers 515F- (5′- GTGCCAGCMGCCGCGGTAA−3′) and 806R (3′-GGACTACHVGGGTWTCTAAT−5′). To distinguish the samples in one Illumina sequencing run, specific 12-mer tag was added to the 5′ end of each primer of each DNA sample. Three replicates of each sample were PCR amplified in a 50 μL reaction mixture containing 25 μL 2x PCR Premix Taq, 10 mM of each primer, 60 ng of genomic DNA and 20 μL of nuclease-free water. The cycling conditions of PCR included 94°C for 5 min, followed by 30 cycles of denaturation at 94°C for 30 s, annealing at 52°C for 30 s, extension at 72°C for 30 s and a final extension at 72°C for 10 min. Positive amplicons were quantified using the PicoGreen dsDNA assay kit (Invitrogen Corporation, Carlsbad, CA, United States) and purified with Zymo's Genomic DNA Clean and Concentrator kit (Zymo Research Corporation, Irvine, CA, United States). Finally, the amplicons were sequenced using the Illumina HiSeq PE250 platform at Novogene Bioinformatics Technology Co., Ltd. (Beijing, China).

Raw reads of the 16S rRNA gene sequences were analyzed using QIIME 2 (Bolyen et al., 2019). Briefly, (1) demultiplexed samples were imported and exported as a single QIIME 2 artefact file; (2) the sequences were trimmed with cutadapt implemented in QIIME2; (3) dada2 was used to filter, de-replicate, detect reference-free chimera, merge paired-end reads and to cluster the combined sequences to ASV (Amplicon Sequence Variant) table (Callahan et al., 2017); (4) all 16S ASVs identified as chloroplast were picked out from the overall ASV table; (5) chloroplast 16S ASVs were then taxonomically assigned at 90% nucleotide identity against the QIIME 2 classify-sklearn plugin (Decelle et al., 2015; Duerschlag et al., 2022); (6) to reduce errors in the sequencing process, ASVs present in less than three samples were discarded in the subsequent analyses (Needham et al., 2018).

2.4 Null model analysis and co-occurrence network construction

To assess the community assembly, the framework of community assembly mechanisms by phylogenetic-bin-based null model analysis (iCAMP) was performed over the whole phytoplankton sample set, including 144 samples, using iCAMP in the R statistical computing environment (Ning et al., 2020).[1] We then got the relative importance of heterogeneous selection, homogeneous selection, dispersal limitation, homogenizing dispersal and drift, and other fractions for each sample.

A co-occurrence network was constructed where we filtered out the low abundance (relative abundance <0.005) and low frequency (presence <3 samples) taxa before calculating correlation coefficients between any pairwise ASVs. Further, the network adjacency matrix was obtained with a Spearman's correlation coefficient (r) higher than 0.7 and significance (p) < 0.05. The network adjacency matrix was visualized in Gephi (version 0.9.2). The nodes of each network were classified into different topological roles according to within-module connectivity (Zi) and among-module connectivity (Pi) values, including module hubs (highly connected nodes within modules, Zi ≥ 2.5, Pi <0.62), network hubs (highly connected nodes within entire network, Zi ≥ 2.5, Pi ≥0.62), connectors (nodes that connect modules, Zi < 2.5, Pi ≥0.62) and peripherals (nodes connected in modules with few outside connections, Zi < 2.5, Pi <0.62) (Kougioumoutzis et al., 2014). To assess network stability, we calculated network vulnerability based on the codes proposed by Yuan et al. (2021). The network vulnerability means the relative contribution of the node to the global efficiency. The vulnerability of a network is indicated by the maximal vulnerability of nodes in the network. In ecological networks, it can provide information on how fast the consequence of biological/ecological events traverse to parts or the entire network (Yuan et al., 2021).

2.5 Statistical analyses

The diversity indexes including alpha diversity (ASV richness), beta diversity (Bray-Curtis's dissimilarity within each group) and gamma diversity (ASV richness), were calculated using vegan in R. Pearson correlations and principal component analysis (PCA) were performed to depict the relationships among all investigated environmental variables using corrgram (Friendly, 2002) and vegan (Oksanen et al., 2017) in R, respectively. The phytoplankton structure based on Bray-Curtis's distance was visualized using non-metric multidimensional scaling (NMDS). To test for significant differences between phytoplankton structure in various altitudinal groups, permutational multivariate analysis of variance using distance matrices (PERMANOVA) was carried out based on Bray-Curtis's dissimilarity using vegan in R. To analyze the taxa-location relationships, a venn network was constructed in R using the data on phytoplankton taxa and the location groups. Significant differences in phytoplankton beta diversity (i.e., phytoplankton variability) among the different groups were tested by permutation test and Tukey multiple comparisons for homogeneity of multivariate dispersions using vegan in R. A permutation multivariate analysis of variance (permutation MANOVA), followed by a pairwise permutation t test, was performed to analyze the significant differences of community assembly processes in groups of altitudes using the RVAideMemoire package in R (Hervé, 2021). Relationships between phytoplankton composition and investigated environmental variables were assessed by Mantel statistics with 999 permutations and canonical correlation analysis (CCA) with an automatic stepwise model using permutation tests in vegan in R. Multiple regression on distance matrices (MRM) was conducted to investigate the relationships of phytoplankton composition with environmental (E.) and spatial (S.) factors and their mixed effect (Mix.). The sampling maps were generated based on an open-access Google satellite map using ArcGIS (version 10.8).

3 Results

3.1 Environmental properties in the headwater streams

Principal component analysis (PCA) revealed that the environmental properties could be reduced to two principal components (PC1 and PC2) that explained 25.1 and 18.9% of the variation, respectively (Supplementary Figure S1). Altitude had the

1 https://www.R-project.org

highest correlation with PC1, followed by monthly mean temperature (MMT) (Supplementary Figure S1). The altitude of the sampling sites ranged from 320 to 2,220 m, whereas the MMT of the sampling sites varied between 9.8 and 17.2°C. According to the altitude, the 72 sampling sites were categorized into three groups, including low altitude (LA, altitude <1,000 m) located in Guangxi province, intermediate altitude (MA, 1,000 m < altitude <2,000 m) in Guizhou province and high altitude (HA: altitude >2,000 m) in Yunnan province.

Altitude was negatively correlated with MMT, water velocity and the aquatic concentration of PO_4^{3-} and Chla (Pearson correlation: $r > -0.25$, $p < 0.05$, Supplementary Figure S2) and positively linked to the concentration of Ca^{2+}, Mg^{2+}, conductivity, TN and NO_3^- (Pearson correlation: $r > 0.34$, $p < 0.05$, Supplementary Figure S2). Significant positive correlations were also observed among Ca^{2+}, Mg^{2+}, Fe^{3+}, Mn^{2+}, conductivity, NO_2^- and NH_4^+ (Pearson correlation: $r > 0.60$, $p < 0.05$, Supplementary Figures S1, S2). The concentration of Chla was positively linked to the concentrations of TP, PO_4^{3-} and MMT (Pearson correlation: $r > 0.28$, $p < 0.05$, Supplementary Figure S2) and marginally correlated with the concentration of Fe^{3+} (Pearson correlation: $r = 0.21$, $p < 0.1$, Supplementary Figure S2).

3.2 The alpha and gamma patterns of phytoplankton assemblages in the Xijiang headwater streams

In total, we obtained 413 ASVs in the streams, belonging to nine phyla: cyanobacteria, Bacillariophyta, Chlorophyta, Rhodophyta, Chrysophyta, Euglenophyta, Glaucophyta, Phaeophyta and Cryptophyta (Supplementary Figure S3). However, the nine phyla were found for both cell sizes (Supplementary Figure S3). Micro- and nanophytoplankton were primarily composed of *Microcoleus* and *Bacillariophyceae*, whereas picophytoplankton mainly included *Microcoleus*, *Pseudanabaena* and *Chamaesiphon* (Supplementary Figure S3). Compared with picophytoplankton, a significantly higher alpha diversity was observed for micro- and nanophytoplankton (t test: $t = -5.667$, $p < 0.001$). When relating alpha diversity to altitude, we found that the alpha diversity of both picophytoplankton and micro- and nanophytoplankton's decreased gradually with increasing altitudes (picophytoplankton: $R^2 = 0.144$, $p < 0.01$; micro- and nanophytoplankton: $R^2 = 0.316$, $p < 0.01$) at a rate of 9 ASV per km for picophytoplankton and 25 ASV per km for micro- and nanophytoplankton (Figures 2C,D). In three altitude groups, including low altitude (LA, altitude <1,000 m), intermediate altitude (MA, 1000 m < altitude <2000 m) and high altitude (HA: altitude >2000 m), higher alpha diversity was observed at lower altitudes for both picophytoplankton (ANOVA test: $F = 7.551$, $p < 0.01$) and micro- and nanophytoplankton (ANOVA test: $F = 21.93$, $p < 0.01$) (Figures 2A,B).

The highest gamma diversity was also observed for the lowest altitudinal group (Figures 2E,F). The bipartite association network analysis revealed that of the detected 362 picophytoplankton ASVs, only 84 ASVs were present in all three altitudinal groups. Meanwhile, among the 411 micro- and nanophytoplankton ASVs, there were 200 ASVs in all three altitudinal groups (Figure 3). Compared with lower altitudinal groups, a much lower number of unique picophytoplankton ASVs were found in higher altitudinal groups (Figure 3A). Moreover, much lower shared picophytoplankton ASVs were observed between HA and LA as well as between HA and MA than between MA and LA (Figure 3A). For the micro- and nanophytoplankton, the highest unique ASVs were also found in the lowest altitudinal group (Figure 3B).

3.3 The variability of phytoplankton assemblages in the Xijiang headwater streams

In contrast to alpha diversity, phytoplankton beta diversity was significantly higher in the higher altitudinal groups for the overall picophytoplankton (permutation test of multivariate homogeneity of group dispersions: $F = 3.905$, $p < 0.05$; Figures 4A,C) as well as for micro- and nanophytoplankton (permutation test of multivariate homogeneity of group dispersions: $F = 9.358$, $p < 0.01$; Figures 4B,D). For the dominant phytoplankton taxa, including *Bacillariophyceae* of Bacillariophyta, *Cryptomonadaceae* of Cryptophyta, *Microcoleus*, *Pseudanabaena*, *Chamaesiphon*, *Phormidium* and *Leptolyngbya* of cyanobacteria and *Euglenaceae* of Euglenophyta, only *Chamaesiphon* in the picophytoplankton exhibited a similar beta diversity pattern to the overall phytoplankton pattern with higher beta diversity in the higher altitudinal groups (Supplementary Figure S5), while the beta diversity of the micro- and nanophytoplankton, including *Bacillariophyceae*, *Microcoleus* and *Chamaesiphon*, all being significantly higher in the higher altitudinal groups (Supplementary Figure S6).

Significant differences in overall phytoplankton structure were observed across the three altitudinal groups for both the overall picophytoplankton (permutation MANOVA: $F = 2.552$, $p < 0.05$; Table 1) and the overall micro- and nanophytoplankton (permutation MANOVA: $F = 2.976$, $p < 0.01$; Table 1). Between the pairwise altitudinal groups, the overall picophytoplankton and overall micro- and nanophytoplankton structure also exhibited significant differences (pairwise permutation MANOVA: $F = 2.007$, $p < 0.05$; Table 1). Of the three altitudinal groups, there were also significant structure differences in specific picophytoplankton clades, such as *Microcoleus*, *Chamaesiphon*, *Phormidium* and *Leptolyngbya* (permutation MANOVA: $F > 1.633$, $p < 0.05$; Supplementary Table S1), and in specific micro- and nanophytoplankton clades, including *Bacillariophyceae*, *Cryptomonadaceae*, *Microcoleus*, *Chamaesiphon*, *Phormidium* and *Leptolyngbya* (permutation MANOVA: $F > 1.661$, $p < 0.05$; Supplementary Table S1).

3.4 The assembly processes of phytoplankton in the streams

Among the deterministic and stochastic assembly processes (homogeneous and heterogeneous selection, dispersal limitations, homogenizing dispersal and the drift and other fractions), the drift and other fractions were found to contribute the largest fraction to the community assembly of both picophytoplankton and micro- and nanophytoplankton, followed by dispersal limitations and homogeneous selection (Figure 5). For both the picophytoplankton and the micro- and nanophytoplankton, a lower relative importance of homogeneous selection was detected for higher altitudinal groups (Figure 5), indicating that the relative importance of deterministic processes in

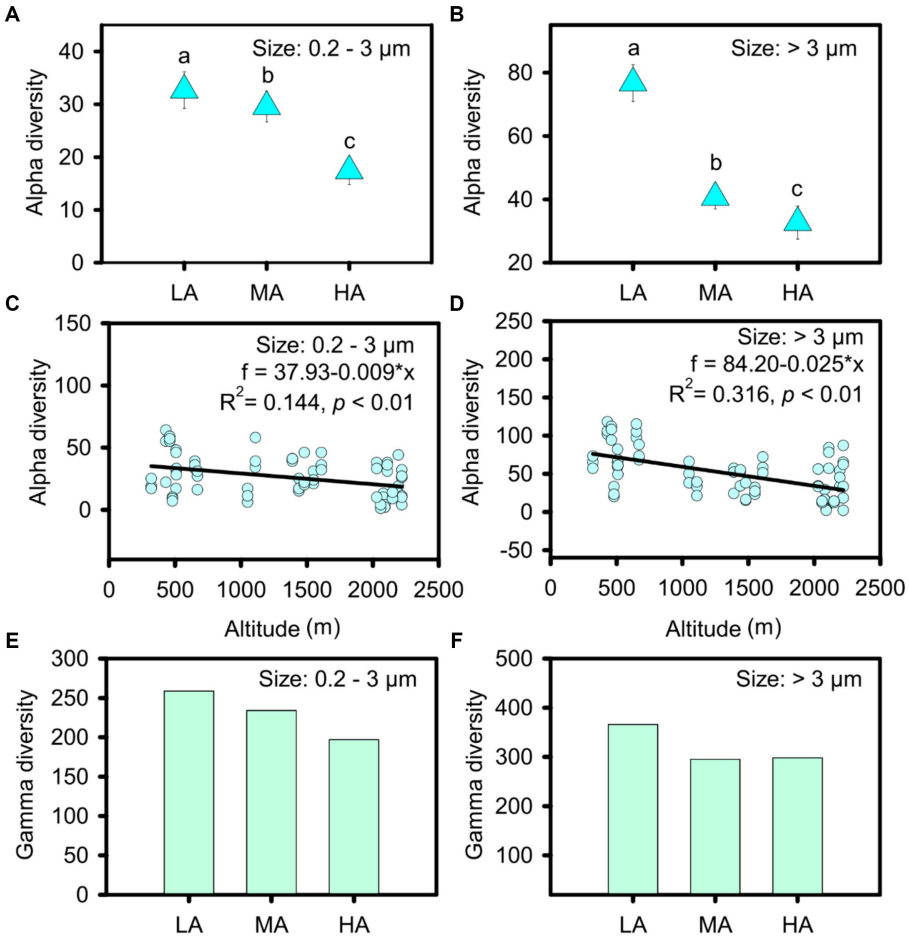

FIGURE 2
Alpha diversity **(A–D)** and gamma diversity **(E,F)** of the picophytoplankton (size: 0.2–3 μm) and micro- and nanophytoplankton (size >3 μm) communities in the three altitude groups. LA, altitude <1,000 m; MA, 1,000 m < altitude <2,000 m; HA, altitude >2,000 m. Significant differences ($p < 0.05$) among groups are indicated by different alphabetic letters above the bars.

shaping the phytoplankton assemblages significantly decreased in higher altitudinal groups. However, the processes of dispersal limitations increased in relative importance in shaping the micro- and nanophytoplankton assemblages in higher altitudinal groups (Figure 5).

When relating environmental variables to phytoplankton structure, we found, among the investigated 19 environmental factors, that the picophytoplankton composition was significantly related to stream altitude, ORP and SiO_3^{2-} concentrations, while the composition of the micro- and nanophytoplankton was significantly related to stream altitude, stream depth and ORP (Supplementary Figure S7). However, in the different altitudinal groups, both the picophytoplankton and the micro- and nanoplankton community structure was significantly related to different combinations of environmental variables (Supplementary Figure S8). Furthermore, multiple regressions on distance matrices (MRM) using permutation tests (Table 2) revealed that the pure effect of environmental variables in explaining both the picophytoplankton and the micro- and nanophytoplankton structure remarkably decreased in the higher altitude groups, while the pure effects of spatial factors increased in the higher altitudinal groups (Table 2). The largest fraction of both the picophytoplankton and the micro- and nanophytoplankton structure could not be explained by the investigated environmental variables or the spatial factors (Table 2).

3.5 The vulnerability of phytoplankton assemblages in the streams

Co-occurrence networks were performed to examine the coexistence of diverse phytoplankton in the streams in the different altitudinal groups (Table 3; Supplementary Figure S9). In a co-occurrence network, the phytoplankton ASVs are referred to nodes, while the connections between the nodes are called edges. In the picophytoplankton network, there were 92 nodes and 479 links for the LA, 64 nodes and 252 links for the MA and 50 nodes and 300 links for the HA (Table 3; Supplementary Figure S9). However, in each altitudinal group, more nodes and links were observed in the micro- and nanophytoplankton than for picophytoplankton. Thus, we observed a network of 196 nodes and 803 links for LA, a network of 113 nodes and 344 links for MA and a network of 112 nodes and 663 links for HA in the micro- and nanophytoplankton (Table 3; Supplementary Figure S9). As for the three altitudinal groups, we found that the co-occurrence networks in the higher altitudinal groups tended to have fewer nodes, fewer links and fewer positive correlations. Both picophytoplankton and micro- and nanophytoplankton co-occurrence networks had a lower diameter, a lower network radius, a lower characteristic path length, a lower network heterogeneity, lower connected components and lower modularity (i.e.,

10.3389/fmicb.2024.1417651

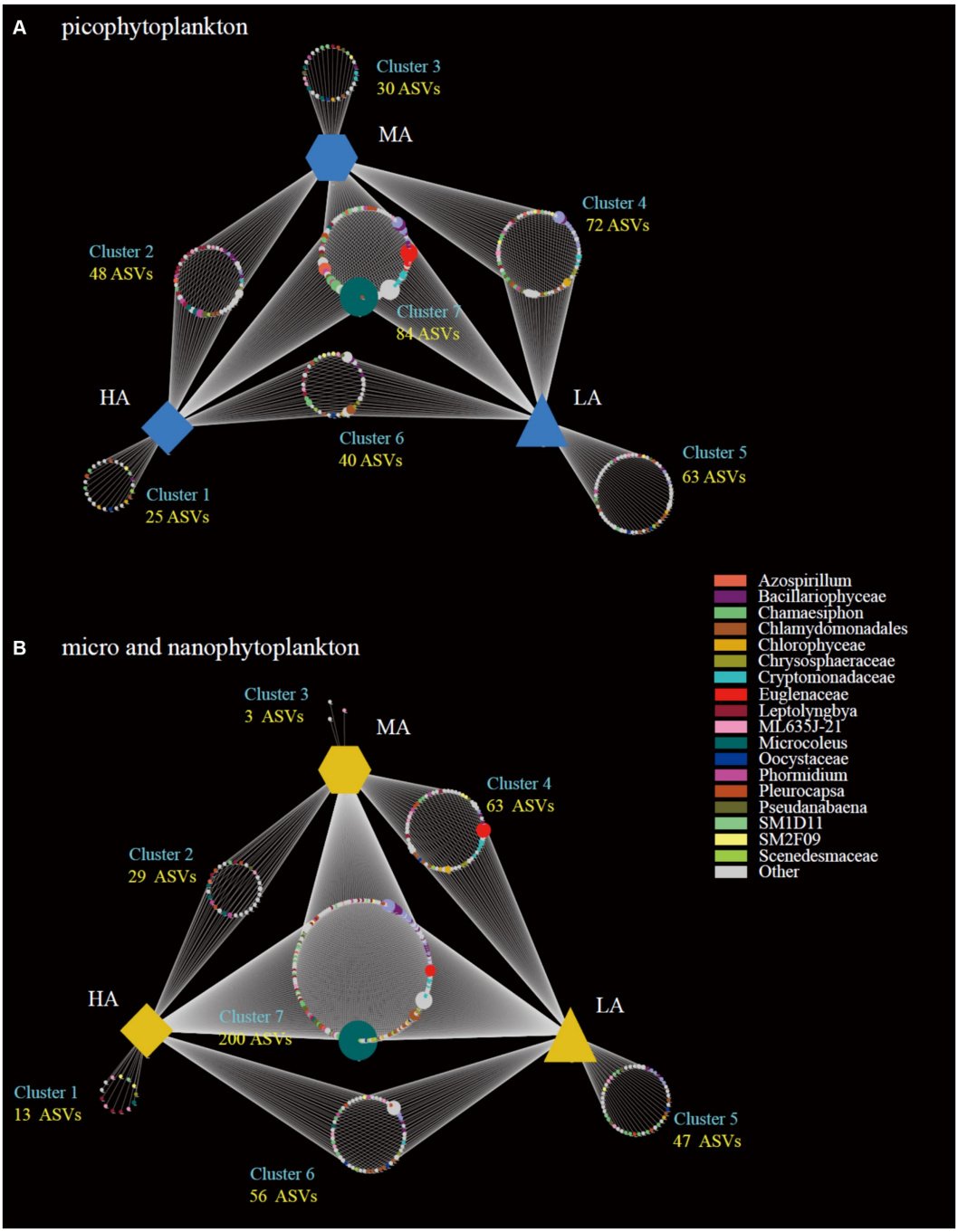

FIGURE 3
Bipartite association networks showing the associations between the three altitude groups and the significantly associated ASVs of the picophytoplankton (size: 0.2–3 μm; **A**) and micro- and nanophytoplankton (size >3 μm; **B**) communities, respectively. LA, altitude <1,000 m; MA, 1,000 m < altitude <2,000 m; HA, altitude >2,000 m.

the degree that a network can be divided into communities or modules) in the higher altitudinal groups than in the other two groups (Table 3).

In both the picophytoplankton and the micro- and nanophytoplankton, the majority of ASVs were nodes connected in modules with few outside, called peripheral (picophytoplankton: 77.2% for LA, 79.7% for MA, and 80.0% for HA; micro- and nanophytoplankton: 71.9% for LA, 62.0% for MA and 77.7% for HA, Figures 6A,B). Among these peripherals, all ASVs had links inside their modules. In the picophytoplankton networks, connectors (i.e., nodes that connect modules) occupied 22.8% ASVs for LA, 20.3% ASVs for MA and 20.0% ASVs for HA, respectively. In the micro- and nanophytoplankton networks, connectors occupied 27.4% ASVs for LA, 38.1% ASVs for MA and 22.3% ASVs for HA, respectively. In the micro- and nanophytoplankton network, the ASV2324 (belonging to cyanobacteria, Figure 6B) was identified as module hubs, having particularly strong associations with most of nodes in the module. We further observed that

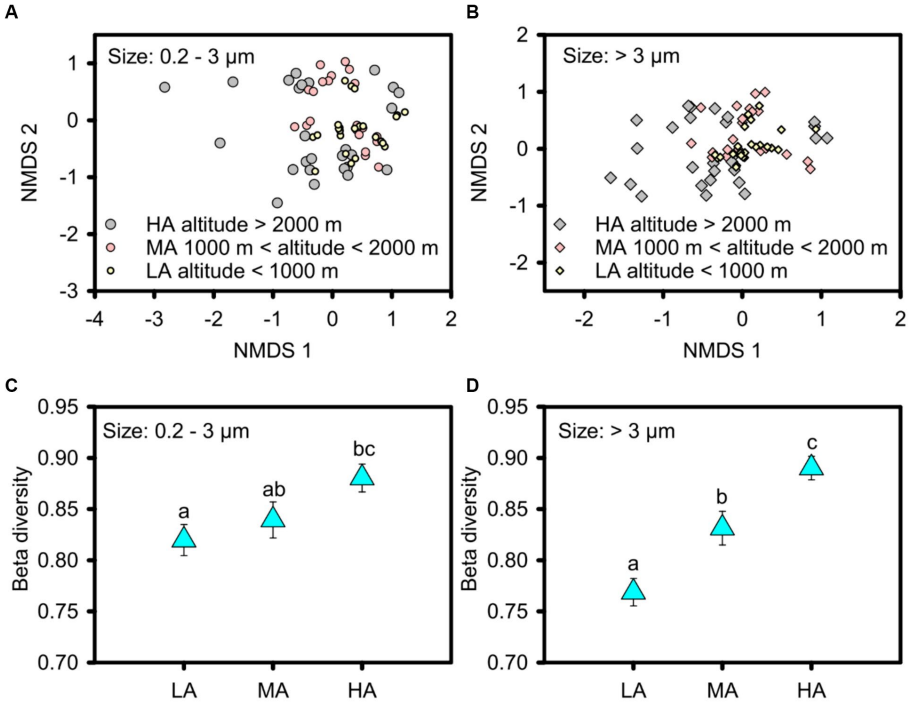

FIGURE 4
Non-metric multidimensional scaling (NMDS) ordinations showing the beta diversity of the picophytoplankton [size: 0.2–3 μm, **(A,C)**] and micro- and nanophytoplankton [size >3 μm, **(B,D)**] communities in the three altitude groups. Significant differences in beta diversity in the three altitude groups were tested by multivariate homogeneity of group dispersions (variances). LA, altitude <1,000 m; MA, 1000 m < altitude <2000 m; HA, altitude >2000 m. Significant differences ($p < 0.05$) among groups are indicated by different alphabetic letters above the bars.

TABLE 1 Pairwise permanova of picophytoplankton (size: 0.2–3 μm) and micro- and nanophytoplankton (size >3 μm) community structure based on Bray–Curtis dissimilarity.

Groups	Picophytoplankton		Micro- and nanophytoplankton	
	F	*p*	F	*p*
Whole	2.552	0.001**	2.976	0.001**
LA vs. MA	2.007	0.028*	3.153	0.003**
LA vs. HA	2.862	0.001**	3.387	0.003**
MA vs. HA	2.718	0.001**	2.427	0.006**

*$p < 0.05$; **$p < 0.01$.
LA, altitudes <1,000 m; MA, 1,000 m < altitudes <2,000 m; HA, altitudes >2,000 m.

for both picophytoplankton and micro- and nanophytoplankton, the number of keystone taxa decreased with increasing altitude (picophytoplankton: 21 for LA, 13 for MA and 10 for HA, respectively; micro- and nanophytoplankton: 57 for LA, 43 for MA and 25 for HA, respectively). Moreover, for both the picophytoplankton and the micro- and nanophytoplankton networks, the highest network vulnerability was observed in the HA groups, indicating that HA phytoplankton networks were less stable than those of LA and MA (Figures 6C,D).

4 Discussion

Phytoplankton is a polyphyletic group, which has been used as a paradigm system for studying species coexistence since the publication of Hutchinson's "The Paradox of the Plankton" (Hutchinson, 1961). We found high phytoplankton diversity in the headwater streams of Xijiang River basin. Common freshwater phytoplankton, including cyanobacteria, Bacillariophyta, Chlorophyta, Rhodophyta, Chrysophyta, Euglenophyta, Glaucophyta, Phaeophyta and Cryptophyta, were all detected in both picophytoplankton and micro- and nanophytoplankton. The regional coexistences of diverse phytoplankton communities in mountain streams might be explained by climatic variation, niche diversification, and the recruitment of phytoplankton from the local benthic habitats (Naselli-Flores et al., 2003b; Becker et al., 2008; Rahbek et al., 2019b; Trew and Maclean, 2021). In the Xijiang River basin, headwater stream habitats cover a broad altitudinal gradient spanning from approximately 320 to 2,220 m. Within narrow spatial ranges and across regional-scale habitats, there are not only heterogeneous climatic habitats for phytoplankton assemblage, but also heterogeneity in environmental,

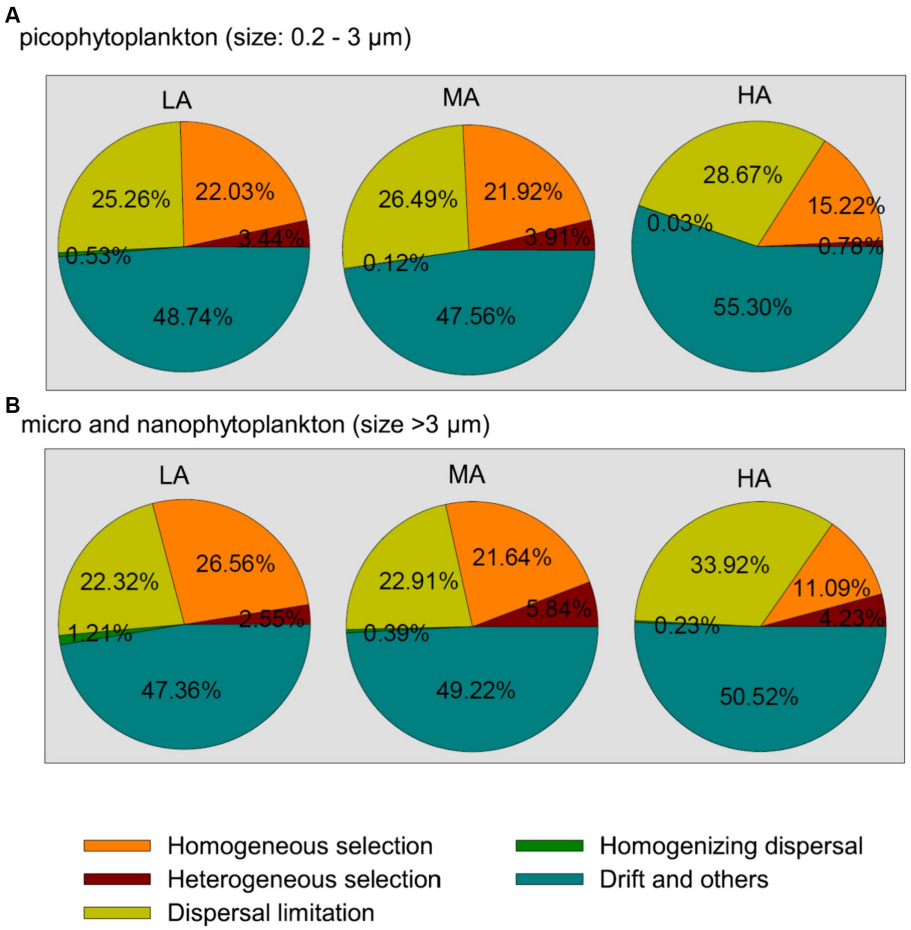

FIGURE 5
The community assembly processes of the picophytoplankton [size: 0.2–3 μm, **(A)**] and micro- and nanophytoplankton [size >3 μm, **(B)**] communities in the three altitude groups. LA, altitude <1,000 m; MA, 1,000 m < altitude <2,000 m; HA, altitude >2,000 m.

TABLE 2 **Multiple regression on distance matrices (MRM) using permutation tests of picophytoplankton (size: 0.2–3 μm) and micro- and nanophytoplankton (size >3 μm) community structure by environmental (E.) and spatial (S.) factors and their mixed effect (Mix.).**

Index	Picophytoplankton			Micro- and nanophytoplankton		
	LA	MA	HA	LA	MA	HA
Pure E.	2.28	8.12	0.14	33.12	16.39	0.87
Pure S.	0.96	8.16	21.68	2.5	8.47	17.41
Mix.	7.95	5.11	4.31	1.7	7.43	6.42
Residuals	88.81	78.61	73.87	62.68	67.71	75.3

hydrological, and mineralogical conditions (Supplementary Figure S1). The differentiation of environmental conditions might benefit the aggregations of diverse phytoplankton in both local and regional scales (Naselli-Flores et al., 2003b; Rahbek et al., 2019a,b). These diverse centers of endemism among headwater streams might support the coexistences of diverse phytoplankton across regional scale habitats (Naselli-Flores et al., 2003a; Stomp et al., 2011; Vallina et al., 2014).

Headwater streams as ours may not only have rapid speciation of taxa but also act as environmental filters (areas with especially high rates of emigration or extinction) (Rahbek et al., 2019b; Brighenti et al., 2021; Chang et al., 2021). We found that phytoplankton diversity decreased monotonically with increasing altitude at a rate of 9 ASV per km for picophytoplankton, and 25 ASV per km for micro- and nanophytoplankton. Headwater streams at higher altitudes served as a filter for microbes, as they had lower alpha and gamma diversity and less unique phytoplankton taxa. Monotonically decreasing altitudinal patterns of microorganisms have also been observed in previous studies, examples being the species diversity of cyanobacterial communities in subarctic ponds in Finland and Norway (Teittinen et al., 2017), biofilm bacterial diversity in streams throughout New Zealand (Lear et al., 2013) and sediment bacterial diversity in subtropical lakes in China (Zeng et al., 2016).

TABLE 3 Major topological properties of the observed picophytoplankton (pico) and micro- and nanophytoplankton (micro- and nano) co-occurrence networks in the headwater streams of Xijiang River for three altitudinal groups and their associated random networks.

Sample	Pico observed networks			Pico random networks			Micro- and nano observed networks			Micro- and nano random networks		
	LA	MA	HA	LA	MA	HA	LA	MA	HA	LA	MA	HA
No. of ASVs	413	413	413	413	413	413	413	413	413	413	413	413
No. of nodes	92	64	50	92	64	50	196	113	112	196	113	112
No. of edges	479	252	300	479	252	300	803	344	663	803	344	663
Average number of neighbors	17.63	8.76	18.78	10.41	7.875	12.00	8.79	8.23	10.37	8.19	6.08	11.84
Network diameter	5	4	2	3	4	3	11	11	7	5	6	4
Network radius	3	2	1	3	3	2	6	6	4	3	4	3
Average path length	1.725	1.969	1.304	2.148	2.207	1.792	4.41	4.137	2.582	2.72	2.788	2.152
Clustering coefficient	0.719	0.606	0.843	0.104	0.132	0.239	0.528	0.548	0.728	0.041	0.033	0.109
Network density	0.477	0.351	0.696	0.114	0.125	0.245	0.078	0.161	0.221	0.042	0.054	0.107
Network heterogeneity	0.557	0.57	0.304	0.277	0.295	0.236	0.667	0.723	0.712	0.339	0.386	0.278
Network centralization	0.324	0.357	0.328	0.085	0.084	0.128	0.146	0.199	0.28	0.035	0.054	0.084
Connected components	9	7	6	1	1	1	8	10	6	1	1	1
Modularity	0.493	0.675	0.225				0.762	0.746	0.519			

LA, low altitudes (altitudes <1,000 m); MA, intermediate altitudes (1,000 m < altitudes <2,000 m); HA, high altitudes (altitudes >2,000 m).

We found key variables that likely co-varied with altitude in explaining the altitude effects on phytoplankton (Supplementary Figure S1). For instance, temperature, which has direct linkages with altitude, is the key factor in the metabolic theory of ecology (Brown et al., 2004; Allen and Gillooly, 2007; Gillooly and Allen, 2007). Thus, metabolic processes influence microbial growth and intraspecific and interspecific competition, and they probably enhance the rate of speciation (Brown et al., 2004). Positive correlation between temperature and diversity has been found for both freshwater and marine phytoplankton in large-scale research investigations (Segura et al., 2015; Righetti et al., 2019). Reduced dispersal might be another mechanism by which phytoplankton diversity may decrease at higher altitudes (Verreydt et al., 2012; Xing and Ree, 2017; Rahbek et al., 2019b). Mountains between headwater streams constitute natural geographical barriers that reduce dispersal for microbes (Chang et al., 2021; Schmeller et al., 2022). Thus, microbial communities in mountain streams have low immigration rates, especially in areas with low precipitation (Schmeller et al., 2022). In our study area, precipitation decreases with increasing altitude (Zeng and Han, 2020b), potentially resulting in weaker microbial dispersal among headwater streams and lower species diversity at higher altitudes. Meanwhile, microorganisms with small cell size are expected to disperse more widely than the larger ones (Gaston et al., 2000). Therefore, compared with picophytoplankton, the larger-sized micro- and nanophytoplankton may have a higher dispersal limitation, explaining the higher slope of linear decreasing relationships between micro- and nanophytoplankton alpha diversity and altitudes than we found for picophytoplankton. In addition, the species diversity of phytoplankton might also be reduced by a shorter growing season at higher altitudes by excluding species appearing during the seasonal succession (Klausmeier, 2010). Moreover, at higher altitudes, the seasonal changes in environmental variables increase, potentially leading to loss of phytoplankton species by filtering of sensitive taxa with a narrow range of environmental tolerance (Currie et al., 2004). Finally, the high UV radiation at higher altitudes may threaten UV-sensitive species of phytoplankton, thus reducing its diversity (Callieri et al., 2001).

The altitudinal diversity pattern of phytoplankton was found to be related to the changes in the balance between homogeneous and heterogeneous selection, dispersal limitations, homogenizing dispersal and stochastic drift (Rahbek et al., 2019b; Wang et al., 2021, 2022; Pritsch et al., 2023). Drift was found to dominate community assembly of both picophytoplankton and micro- and nanophytoplankton in our headwater streams, suggesting that stochastic drift contributes to the non-equilibrium nature of the phytoplankton, thus supporting a high phytoplankton diversity in headwater streams. Moreover, we found that the relative importance of homogeneous selection decreased in shaping both the picophytoplankton and the micro- and nanophytoplankton assemblages at higher altitudes, whereas dispersal limitations increased in the importance for micro- and nanophytoplankton assemblages at higher altitudes. The decreased homogeneous selection at higher altitudes might be due to the complex terrain, high climatic unpredictability as well as increased heterogeneity of environmental variables as shown in the Supplementary Figure S1 and in previous

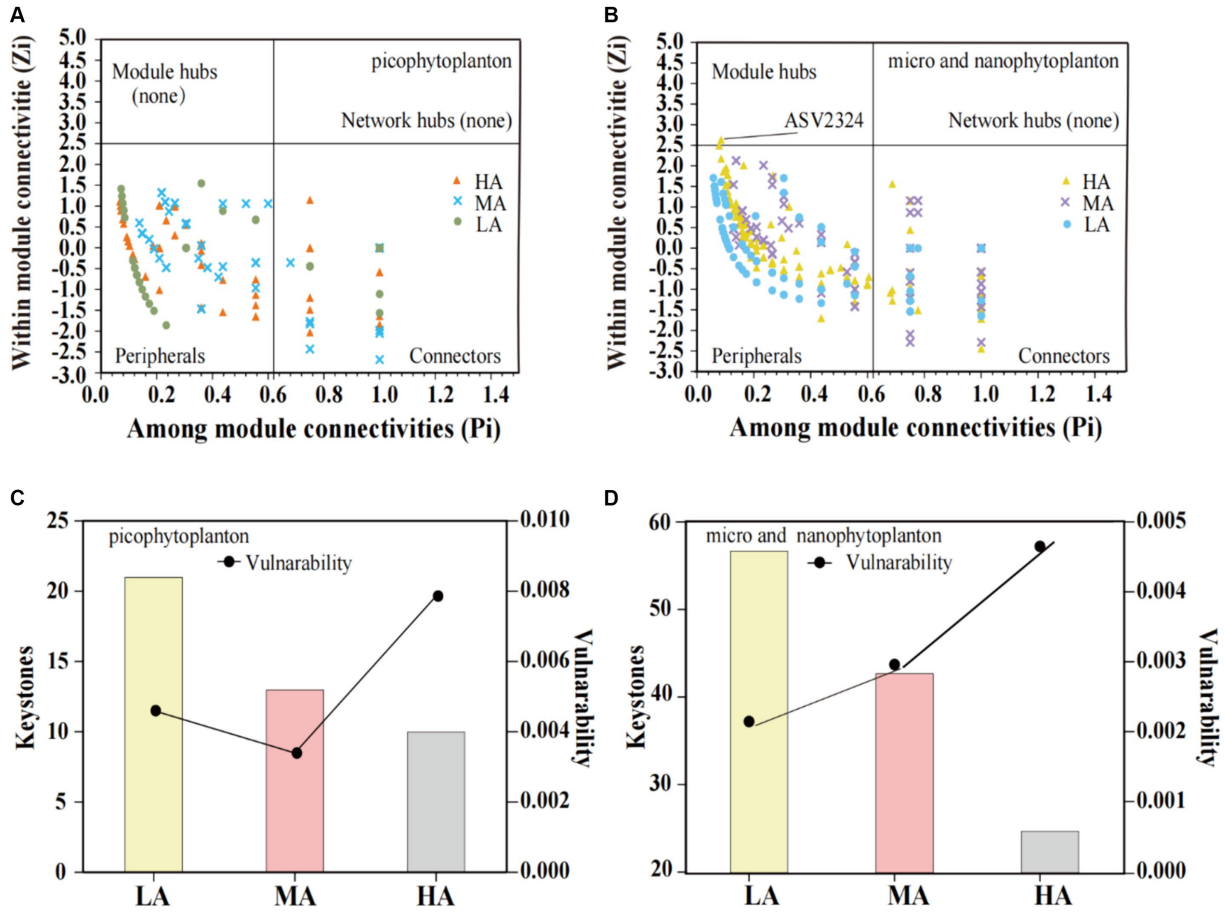

FIGURE 6
Scatter plot of within-module connectivity (Zi) and among-module connectivity (Pi) showing the distribution of the picophytoplankton [size: 0.2–3 μm, **(A)**] and micro- and nanophytoplankton [size >3 μm, **(B)**] based on their topological roles. The number of keystone taxa and vulnerability of the picophytoplankton [size: 0.2–3 μm, **(C)**] and micro- and nanophytoplankton [size >3 μm, **(D)**] networks in the three altitude groups. LA, altitude <1,000 m; MA, 1,000 m < altitude <2,000 m; HA, altitude >2,000 m.

studies (Maloufi et al., 2016; Teittinen and Virta, 2021). The increased dispersal limitations for micro- and nanophytoplankton assemblages at higher altitudes may be ascribed to the enhanced "isolated island" effect of mountain headwater streams and the lower precipitation at higher altitudes at the Xijiang River (Zeng and Han, 2020a,b). The biodiversity of headwater stream phytoplankton was thus characterized by higher variability (both picophytoplankton and micro- and nanophytoplankton) at higher altitudes, where lower homogeneous selection was found than at lower altitudes (Stomp et al., 2011). In addition, more phytoplankton clades showed higher variability at higher altitudes for micro- and nanophytoplankton (i.e., *Bacillariophyceae* and *Microcoleus*) than for picophytoplankton (i.e., only *Chamaesiphon*). This might be explained by higher dispersal limitation and lower homogeneous selection of micro- and nanophytoplankton than of picophytoplankton at higher altitudes (Figure 5).

Besides higher variability, we also found a higher vulnerability of the phytoplankton network structure at higher altitudes, indicating that the decreased homogeneous selection at higher altitudes also resulted in decreased stability of coexisting phytoplankton taxa. Moreover, the higher vulnerability of the coexisting phytoplankton taxa was found to be accompanied by various indices of lower network complexity, such as fewer node and link numbers, lower network heterogeneity, fewer connected components, fewer keystone species and lower modularity. Previous studies have revealed ecological importance of node and link numbers, keystone species, modularity and connectance in maintaining network stability and vulnerability in response to disruptions (Dunne et al., 2002; Grilli et al., 2016; Yuan et al., 2021). These results may reflect that complexity of communities begets its stability (MacArthur, 1955).

5 Conclusion

We found high phytoplankton diversity in the studied headwater streams. However, the general high abundance, small size, fast population growth and long-range dispersal of phytoplankton was not sufficient to avoid altitudinal constrains in phytoplankton assemblages. Phytoplankton alpha diversity exhibited a monotonic decreasing relationship with altitude. Such a diversity pattern across the altitudinal gradient is shaped by the balance of selection, dispersal and stochastic drift fractions. High altitudes amplified the "isolated island" effect of the headwater streams, and both the picophytoplankton and the micro- and nanophytoplankton assemblages at higher altitudes was composed of taxa influenced by lower homogeneous selection and higher dispersal limitation. Therefore, the phytoplankton assemblages at higher altitudes exhibited higher variability and vulnerability. These findings are essential

for increasing our understanding of aquatic biodiversity in headwater streams, and we encourage long-term and large-scale biodiversity surveys to be conducted to better explore the impacts of environmental changes, such as climate warming, on aquatic biodiversity.

Data availability statement

The obtained sequencing data in this study were deposited into the Sequence Read Archive (SRA) of the National Center for Biotechnology Information (https://www.ncbi.nlm.nih.gov/) database under accession number PRJNA1003967 (TaxID: 1169740). Other data that support the findings of this study will be made available from the corresponding author on reasonable request.

Author contributions

YP: Data curation, Formal analysis, Investigation, Methodology, Writing – original draft. CW: Data curation, Formal analysis, Investigation, Methodology, Writing – original draft. GM: Data curation, Formal analysis, Investigation, Writing – original draft. HC: Formal analysis, Writing – review & editing. QW: Funding acquisition, Writing – review & editing. DH: Formal analysis, Writing – review & editing. EJ: Conceptualization, Funding acquisition, Writing – review & editing. LR: Conceptualization, Funding acquisition, Project administration, Supervision, Visualization, Writing – original draft, Writing – review & editing.

Funding

The author(s) declare that financial support was received for the research, authorship, and/or publication of this article. This work was supported by the Second Tibetan Plateau Scintific Expedition and Research (STEP) program (2019QZKK0503), National Natural Science Foundation of China (32171517), Project of Southern Marine Science and Engineering Guangdong Laboratory (Guanzhou) (GML20220017), and the TÜBITAK program BIDEB22232 (118C250).

Acknowledgments

We are grateful to Lu Wang and Jian Liao for their assistance with the experimental sampling and Anne Mette Poulsen for English language assistance.

Conflict of interest

The authors declare that the research was conducted in the absence of any commercial or financial relationships that could be construed as a potential conflict of interest.

Publisher's note

Supplementary material

The Supplementary material for this article can be found online at: https://www.frontiersin.org/articles/10.3389/fmicb.2024.1417651/full#supplementary-material

References

Allen, A. P., and Gillooly, J. F. (2007). The mechanistic basis of the metabolic theory of ecology. *Oikos* 116, 1073–1077. doi: 10.1111/j.2007.0030-1299.16079.x

Becker, V., Huszar, V. L. M., Naselli-Flores, L., and Padisák, J. (2008). Phytoplankton equilibrium phases during thermal stratification in a deep subtropical reservoir. *Freshw. Biol.* 53, 952–963. doi: 10.1111/j.1365-2427.2008.01957.x

Bolyen, E., Rideout, J. R., Dillon, M. R., Bokulich, N. A., Abnet, C. C., Al-Ghalith, G. A., et al. (2019). Reproducible, interactive, scalable and extensible microbiome data science using QIIME 2. *Nat. Biotechnol.* 37, 852–857. doi: 10.1038/s41587-019-0209-9

Brighenti, S., Hotaling, S., Finn, D. S., Fountain, A. G., Hayashi, M., Herbst, D., et al. (2021). Rock glaciers and related cold rocky landforms: overlooked climate refugia for mountain biodiversity. *Glob. Chang. Biol.* 27, 1504–1517. doi: 10.1111/gcb.15510

Brown, J. H., Gillooly, J. F., Allen, A. P., Savage, V. M., and West, G. B. (2004). Toward a metabolic theory of ecology. *Ecology* 85, 1771–1789. doi: 10.1890/03-9000

Callahan, B. J., McMurdie, P. J., and Holmes, S. P. (2017). Exact sequence variants should replace operational taxonomic units in marker-gene data analysis. *ISME J.* 11, 2639–2643. doi: 10.1038/ismej.2017.119

Callieri, C., Morabito, G., Huot, Y., Neale, P. J., and Litchman, E. (2001). Photosynthetic response of pico-and nanoplanktonic algae to UVB, UVA and PAR in a high mountain lake. *Aquat. Sci.* 63, 286–293. doi: 10.1007/PL00001355

Caputo, L., Naselli-Flores, L., Ordoñez, J., and Armengol, J. (2008). Phytoplankton distribution along trophic gradients within and among reservoirs in Catalonia (Spain). *Freshw. Biol.* 53, 2543–2556. doi: 10.1111/j.1365-2427.2008.02082.x

Cardinale, B. J., Duffy, J. E., Gonzalez, A., Hooper, D. U., Perrings, C., Venail, P., et al. (2012). Biodiversity loss and its impact on humanity. *Nature* 486, 59–67. doi: 10.1038/nature11148

Chang, C., Gao, L., Wei, J., Ma, N., He, Q., Pan, B., et al. (2021). Spatial and environmental factors contributing to phytoplankton biogeography and biodiversity in mountain ponds across a large geographic area. *Aquat. Ecol.* 55, 721–735. doi: 10.1007/s10452-021-09857-2

Chang, C. W., Miki, T., Ye, H., Souissi, S., Adrian, R., Anneville, O., et al. (2022). Causal networks of phytoplankton diversity and biomass are modulated by environmental context. *Nat. Commun.* 13:1140. doi: 10.1038/s41467-022-28761-3

Currie, D. J., Mittelbach, G. G., Cornell, H. V., Field, R., Guégan, J. F., Hawkins, B. A., et al. (2004). Predictions and tests of climate-based hypotheses of broad-scale variation in taxonomic richness. *Ecol. Lett.* 7, 1121–1134. doi: 10.1111/j.1461-0248.2004.00671.x

de Oliveira, P. H. F., Machado, K. B., Teresa, F. B., Heino, J., and Nabout, J. C. (2020). Spatial processes determine planktonic diatom metacommunity structure of headwater streams. *Limnologica* 84:125813. doi: 10.1016/j.limno.2020.125813

Decelle, J., Romac, S., Stern, R. F., Bendif, E. M., Zingone, A., Audic, S., et al. (2015). PhytoREF: a reference database of the plastidial 16S rRNA gene of photosynthetic eukaryotes with curated taxonomy. *Mol. Ecol. Resour.* 15, 1435–1445. doi: 10.1111/1755-0998.12401

Duerschlag, J., Mohr, W., Ferdelman, T. G., LaRoche, J., Desai, D., Croot, P. L., et al. (2022). Niche partitioning by photosynthetic plankton as a driver of CO_2-fixation across the oligotrophic South Pacific Subtropical Ocean. *ISME J.* 16, 465–476. doi: 10.1038/s41396-021-01072-z

Dunne, J. A., Williams, R. J., and Martinez, N. D. (2002). Network structure and biodiversity loss in food webs: robustness increases with connectance. *Ecol. Lett.* 5, 558–567. doi: 10.1046/j.1461-0248.2002.00354.x

Fodelianakis, S., Washburne, A. D., Bourquin, M., Pramateftaki, P., Kohler, T. J., Styllas, M., et al. (2022). Microdiversity characterizes prevalent phylogenetic clades in

the glacier-fed stream microbiome. *ISME J.* 16, 666–675. doi: 10.1038/s41396-021-01106-6

Friendly, M. (2002). Corrgrams: exploratory displays for correlation matrices. *Am. Stat.* 56, 316–324. doi: 10.1198/000313002533

Gaston, K. J., Blackburn, T. M., Greenwood, J. J. D., Gregory, R. D., Quinn, R. M., and Lawton, J. H. (2000). Abundance-occupancy relationships. *J. Appl. Ecol.* 37, 39–59. doi: 10.1046/j.1365-2664.2000.00485.x

Gillooly, J. F., and Allen, A. P. (2007). Linking global patterns in biodiversity to evolutionary dynamics using metabolic theory. *Ecology* 88, 1890–1894. doi: 10.1890/06-1935.1

Greenberg, A. E., Clesceri, L. S., and Eaton, A. D. (1992). Standard methods for the examination of water and wastewater. *18th* Edn. Washington DC: American Public Health Association.

Grilli, J., Rogers, T., and Allesina, S. (2016). Modularity and stability in ecological communities. *Nat. Commun.* 7:12031. doi: 10.1038/ncomms12031

Guelzow, N., Muijsers, F., Ptacnik, R., and Hillebrand, H. (2017). Functional and structural stability are linked in phytoplankton metacommunities of different connectivity. *Ecography* 40, 719–732. doi: 10.1111/ecog.02458

Hervé, M. (2021). RVAideMemoire: testing and plotting procedures for biostatistics. R package version. Available at: https://CRAN.R-project.org/package=RVAideMemoire

Hu, R., Duan, X., Peng, L., Han, B., and Naselli-Flores, L. (2017). Phytoplankton assemblages in a complex system of interconnected reservoirs: the role of water transport in dispersal. *Hydrobiologia* 800, 17–30. doi: 10.1007/s10750-017-3146-y

Hutchinson, G. E. (1961). The paradox of the plankton. *Am. Nat.* 95, 137–145. doi: 10.1086/282171

Irigoien, X., Hulsman, J., and Harris, R. P. (2004). Global biodiversity patterns of marine phytoplankton and zooplankton. *Nature* 429, 863–867. doi: 10.1038/nature02593

Klais, R., Norros, V., Lehtinen, S., Tamminen, T., and Olli, K. (2017). Community assembly and drivers of phytoplankton functional structure. *Funct. Ecol.* 31, 760–767. doi: 10.1111/1365-2435.12784

Klausmeier, C. A. (2010). Successional state dynamics: a novel approach to modeling nonequilibrium foodweb dynamics. *J. Theor. Biol.* 262, 584–595. doi: 10.1016/j.jtbi.2009.10.018

Kougioumoutzis, K., Simaiakis, S. M., and Tiniakou, A. (2014). Network biogeographical analysis of the Central Aegean archipelago. *J. Biogeogr.* 41, 1848–1858. doi: 10.1111/jbi.12342

Kruk, C., Piccini, C., Devercelli, M., Nogueira, L., Accattatis, V., Sampognaro, L., et al. (2021). A trait-based approach predicting community assembly and dominance of microbial invasive species. *Oikos* 130, 571–586. doi: 10.1111/oik.07694

Lear, G., Washington, V., Neale, M., Case, B., Buckley, H., and Lewis, G. (2013). The biogeography of stream bacteria. *Glob. Ecol. Biogeogr.* 22, 544–554. doi: 10.1111/geb.12046

Li, S. L., Xu, S., Wang, T. J., Yue, F. J., Peng, T., Zhong, J., et al. (2020). Effects of agricultural activities coupled with karst structures on riverine biogeochemical cycles and environmental quality in the karst region. *Agric. Ecosyst. Environ.* 303:107120. doi: 10.1016/j.agee.2020.107120

Linnaeus, C.. (1781). Select dissertations from the Amoenitates Academicae. (Translator, F. J. Brand); London, UK: G. Robinson J. Robson.

Liu, J., and Han, G. (2021a). Tracing riverine particulate black carbon sources in Xijiang River basin: insight from stable isotopic composition and bayesian mixing model. *Water Res.* 194:116932. doi: 10.1016/j.watres.2021.116932

Liu, J., and Han, G. (2021b). Controlling factors of riverine CO_2 partial pressure and CO_2 outgassing in a large karst river under base flow condition. *J. Hydrol.* 593:125638. doi: 10.1016/j.jhydrol.2020.125638

Liu, Q., Lai, Z., Wang, C., Ni, J., and Gao, Y. (2022). Seasonal variation significantly affected bacterioplankton and eukaryoplankton community composition in Xijiang River, China. *Environ. Monit. Assess.* 194:55. doi: 10.1007/s10661-021-09712-9

Lu, Z., and Gan, J. (2015). Controls of seasonal variability of phytoplankton blooms in the Pearl River estuary. *Deep Sea res. II Top Stud. Oceanogr.* 117, 86–96. doi: 10.1016/j.dsr2.2013.12.011

MacArthur, R. (1955). Fluctuations of animal populations and a measure of community stability. *Ecology* 36, 533–536. doi: 10.2307/1929601

Maloufi, S., Catherine, A., Mouillot, D., Louvard, C., Couté, A., Bernard, C., et al. (2016). Environmental heterogeneity among lakes promotes hyper β-diversity across phytoplankton communities. *Freshw. Biol.* 61, 633–645. doi: 10.1111/fwb.12731

Morán, X. A. G., López-Urrutia, Á., Calvo-Díaz, A., and Li, W. K. W. (2010). Increasing importance of small phytoplankton in a warmer ocean. *Glob. Chang. Biol.* 16, 1137–1144. doi: 10.1111/j.1365-2486.2009.01960.x

Naselli-Flores, L. (2014). Morphological analysis of phytoplankton as a tool to assess ecological state of aquatic ecosystems: the case of Lake Arancio, Sicily, Italy. *Inland Waters* 4, 15–26. doi: 10.5268/IW-4.1.686

Naselli-Flores, L., Padisák, J., and Dokulil, M. T. (Eds.) (2003a). Phytoplankton and equilibrium concept: the ecology of steady-state assemblages. Dordrecht: Springer Netherlands.

Naselli-Flores, L., Padisák, J., Dokulil, M. T., and Chorus, I. (2003b). "Equilibrium/steady-state concept in phytoplankton ecology" in Phytoplankton and equilibrium concept: The ecology of steady-state assemblages. Developments in hydrobiology. eds. L. Naselli-Flores, J. Padisák and M. T. Dokulil (Dordrecht: Springer).

Needham, D. M., Fichot, E. B., Wang, E., Berdjeb, L., Cram, J. A., Fichot, C. G., et al. (2018). Dynamics and interactions of highly resolved marine plankton via automated high-frequency sampling. *ISME J.* 12, 2417–2432. doi: 10.1038/s41396-018-0169-y

Ning, D., Yuan, M., Wu, L., Zhang, Y., Guo, X., Zhou, X., et al. (2020). A quantitative framework reveals ecological drivers of grassland microbial community assembly in response to warming. *Nat. Commun.* 11:4717. doi: 10.1038/s41467-020-18560-z

Oksanen, J., Blanchet, F. G., Kindt, R., Legendre, P., Minchin, P. R., O'hara, R. B., et al. (2017) Vegan: community ecology package. R package Version 2.4–3. Available at: https://CRAN.R-project.org/package=vegan

Pritsch, H., Schirpke, U., Jersabek, C. D., and Kurmayer, R. (2023). Plankton community composition in mountain lakes and consequences for ecosystem services. *Ecol. Indic.* 154:110532. doi: 10.1016/j.ecolind.2023.110532

Rahbek, C., Borregaard, M. K., Antonelli, A., Colwell, R. K., Holt, B. G., Nogues-Bravo, D., et al. (2019a). Building mountain biodiversity: geological and evolutionary processes. *Science* 365, 1114–1119. doi: 10.1126/science.aax0151

Rahbek, C., Borregaard, M. K., Colwell, R. K., Dalsgaard, B., Holt, B. G., Morueta-Holme, N., et al. (2019b). Humboldt's enigma: what causes global patterns of mountain biodiversity? *Science* 365, 1108–1113. doi: 10.1126/science.aax0149

Righetti, D., Vogt, M., Gruber, N., Psomas, A., and Zimmermann, N. E. (2019). Global pattern of phytoplankton diversity driven by temperature and environmental variability. *Sci. Adv.* 5:eaau6253. doi: 10.1126/sciadv.aau6253

Schmeller, D. S., Urbach, D., Bates, K., Catalan, J., Cogălniceanu, D., Fisher, M. C., et al. (2022). Scientists' warning of threats to mountains. *Sci. Total Environ.* 853:158611. doi: 10.1016/j.scitotenv.2022.158611

Segura, A. M., Calliari, D., Kruk, C., Fort, H., Izaguirre, I., Saad, J. F., et al. (2015). Metabolic dependence of phytoplankton species richness. *Glob. Ecol. Biogeogr.* 24, 472–482. doi: 10.1111/geb.12258

Sharma, R. C., Singh, N., and Chauhan, A. (2016). The influence of physico-chemical parameters on phytoplankton distribution in a head water stream of Garhwal Himalayas: a case study. *Egypt. J. Aquat. Res.* 42, 11–21. doi: 10.1016/j.ejar.2015.11.004

Stanković, I., Gligora Udovič, M., Žutinić, P., Hanžek, N., and Plenković-Moraj, A. (2024). Is salinity a driving factor for the phytoplankton community structure of a brackish shallow Mediterranean lake? *Hydrobiologia* 851, 999–1013. doi: 10.1007/s10750-023-05300-9

Stomp, M., Huisman, J., Mittelbach, G. G., Litchman, E., and Klausmeier, C. A. (2011). Large-scale biodiversity patterns in freshwater phytoplankton. *Ecology* 92, 2096–2107. doi: 10.1890/10-1023.1

Teittinen, A., and Virta, L. (2021). Exploring multiple aspects of taxonomic and functional diversity in microphytobenthic communities: effects of environmental gradients and temporal changes. *Front. Microbiol.* 12:668993. doi: 10.3389/fmicb.2021.668993

Teittinen, A., Wang, J., Strömgård, S., and Soininen, J. (2017). Local and geographical factors jointly drive elevational patterns in three microbial groups across subarctic ponds. *Glob. Ecol. Biogeogr.* 26, 973–982. doi: 10.1111/geb.12607

Trew, B. T., and Maclean, I. M. D. (2021). Vulnerability of global biodiversity hotspots to climate change. *Glob. Ecol. Biogeogr.* 30, 768–783. doi: 10.1111/geb.13272

Vallina, S. M., Follows, M. J., Dutkiewicz, S., Montoya, J. M., Cermeno, P., and Loreau, M. (2014). Global relationship between phytoplankton diversity and productivity in the ocean. *Nat. Commun.* 5:4299. doi: 10.1038/ncomms5299

Von Humboldt, A. (1849). Aspects of nature, in different lands and different climates; with scientific elucidations. (Lea and Blanchard).

Verbeek, L., Gall, A., Hillebrand, H., and Striebel, M. (2018). Warming and oligotrophication cause shifts in freshwater phytoplankton communities. *Glob. Chang. Biol.* 24, 4532–4543. doi: 10.1111/gcb.14337

Verreydt, D., De Meester, L., Decaestecker, E., Villena, M. J., Van Der Gucht, K., Vannormelingen, P., et al. (2012). Dispersal-mediated trophic interactions can generate apparent patterns of dispersal limitation in aquatic metacommunities. *Ecol. Lett.* 15, 218–226. doi: 10.1111/j.1461-0248.2011.01728.x

Vetaas, O. R., Paudel, K. P., and Christensen, M. (2019). Principal factors controlling biodiversity along an elevation gradient: water, energy and their interaction. *J. Biogeogr.* 46, 1652–1663. doi: 10.1111/jbi.13564

Wang, J., Hu, A., Meng, F., Zhao, W., Yang, Y., Soininen, J., et al. (2022). Embracing mountain microbiome and ecosystem functions under global change. *New Phytol.* 234, 1987–2002. doi: 10.1111/nph.18051

Wang, J., Pan, F., Soininen, J., Heino, J., and Shen, J. (2016). Nutrient enrichment modifies temperature-biodiversity relationships in large-scale field experiments. *Nat. Commun.* 7:13960. doi: 10.1038/ncomms13960

Wang, J., Soininen, J., and Heino, J. (2021). Ecological indicators for aquatic biodiversity, ecosystem functions, human activities and climate change. *Ecol. Indic.* 132:108250. doi: 10.1016/j.ecolind.2021.108250

Xing, Y., and Ree, R. H. (2017). Uplift-driven diversification in the Hengduan Mountains, a temperate biodiversity hotspot. *Proc. Natl. Acad. Sci. USA* 114, E3444–E3451. doi: 10.1073/pnas.1616063114

Yu, S., Ren, Z., Yang, Y., Zhang, C., Ma, K., Xie, Y., et al. (2023). Spatial heterogeneity in summer phytoplankton communities shaped by anthropogenic and natural effects in typical coastal bay-river systems in South China. *Ecol. Indic.* 154:110602. doi: 10.1016/j.ecolind.2023.110602

Yuan, M. M., Guo, X., Wu, L., Zhang, Y., Xiao, N., Ning, D., et al. (2021). Climate warming enhances microbial network complexity and stability. *Nat. Clim. Chang.* 11, 343–348. doi: 10.1038/s41558-021-00989-9

Zeng, J., and Han, G. (2020a). Tracing zinc sources with Zn isotope of fluvial suspended particulate matter in Zhujiang River, Southwest China. *Ecol. Indic.* 118:106723. doi: 10.1016/j.ecolind.2020.106723

Zeng, J., and Han, G. (2020b). Preliminary copper isotope study on particulate matter in Zhujiang River, Southwest China: application for source identification. *Ecotoxicol. Environ. Saf.* 198:110663. doi: 10.1016/j.ecoenv.2020.110663

Zeng, C., Xing, R., Huang, B., Cheng, X., Shi, W., and Liu, S. (2023). Phytoplankton in headwater streams: spatiotemporal patterns and underlying mechanisms. *Front. Plant Sci.* 14:1276289. doi: 10.3389/fpls.2023.1276289

Zeng, J., Zhao, D., Li, H., Huang, R., Wang, J., and Wu, Q. L. (2016). A monotonically declining elevational pattern of bacterial diversity in freshwater lake sediments. *Environ. Microbiol.* 18, 5175–5186. doi: 10.1111/1462-2920.13526

Frontiers in Microbiology

Explores the habitable world and the potential of microbial life

The largest and most cited microbiology journal which advances our understanding of the role microbes play in addressing global challenges such as healthcare, food security, and climate change.

Discover the latest Research Topics

See more →

Frontiers

Avenue du Tribunal-Fédéral 34
1005 Lausanne, Switzerland
frontiersin.org

Contact us

+41 (0)21 510 17 00
frontiersin.org/about/contact